Transcription-replication conflict resolution by nuclear RNAi

A dissertation presented

By

King Hei (Teri) Cheng

to

The Cold Spring Harbor Laboratory School of Biological Sciences

at

Cold Spring Harbor Laboratory

in Partial Fulfillment of the Requirements

for the Degree of

Doctor of Philosophy

in

Biological Sciences

Cold Spring Harbor Laboratory

Feb 2024

Table of Contents

Acknowledgement

First and foremost, I would like to thank my mentor, Rob Martienssen. Thank you for your advice and insight throughout my PhD, while also allowing the intellectual freedom to investigate scientific questions in my own way. I am incredibly lucky to be able to train to become an independent scientist under your guidance. I would also like to thank my thesis committee – Leemor Joshua-Tor, Bruce Stillman, and Adrian Krainer – for their advice and suggestions. Thank you also to Robin Allshire for generously taking the time to serve as the external examiner for this thesis.

I can only say I am privileged to be working with the wondering people at Martienssen lab, and I would like to express my profound gratitude to you all. Thank you to Cris, Jon (for training me into a highly competent maize geneticist), Evan, Hyun Soo, Jason, Cristian, Uma, Michael R, Joe, Josh, Ben B, Ben R, Seung Cho, Sonali, Sami, and Liam for all of the help, discussions, and fun times. The patio hangouts, city outings, backyard barbecues, (weird) lab DJ parties, will forever be some of my fondest memories. Shoutout to Joshua Steinberg, my office and lab mate, and co-owner of our stereo HomePod Mini pair, for not only bringing fun and energy to my PhD study, but also for our scientific discussions. I want to especially thank Hyun Soo and Benjamin Roche, the Pombe gurus, for not only teaching me how to work with the species and sharing reagents, but also innumerable insightful scientific exchanges that helped develop my project. Thank you, Benjamin, for your guidance especially in the early years. Your enthusiasm to science is infectious, and I treasure every morning coffee chat we had.

I am also very grateful to everyone working in CSHL who has created a fantastic environment to conduct research. Special thanks to Michele Murrell and Jeremy Patino for keeping the building stocked and for making my sometimes-complicated media plates. Thanks to all the Delbruckians for your help and for creating best department on campus to work in. Huge shoutout to everyone at the school – Zach Lippman, Alex Gann, Monn Monn Myat, Alyson Kass-Eisler, Brianna Campmier, Kim

Creteur, Catherine Perez, Kim Graham – for taking care of everything behind the scene and be available to help whenever needed. I know I have a crazily busy thesis committee – thank you for making sure the meeting can happen twice a year.

I am also thankful to have met my fellow classmates – Dani, Marie, Ilgin, Connor, Asad, Mo, Alexa, Jenelys, Amritha, Jonathan – and become good friends. It has been reassuring and comforting to share the ups and downs together through our PhD journeys. Shoutout to Alexa Pagliaro – who made plain, unseasoned oatmeal my first meal in the US; to Asad Lakhani – with whom I shared an apartment with over five years; and to Danielle Ciren and Jenelys Ruiz – the 'mall crew' – for all the fun times we had (even in Japan!). I cannot wait to see your success in the future.

Pursuing a PhD at the other side of the globe would not have been possible without my friends and family, who have supported me since day one. Thank you to Dr. Christine Yu, for making biology special to me as a high school student. Special shoutout to Ted Leung, for being supportive throughout all the years, and for all the fun activities and travel we have had. Lastly, I would like to express my deepest gratitude to my parents, Mabel and Terence. Thank you, for your unconditional love and support.

Summary

RNA interference (RNAi) plays important roles in the nucleus in addition to its well-known function in post-transcriptional gene silencing. In the fission yeast *Schizosaccharomyces pombe*, these roles include transcriptional silencing of heterochromatin, chromosome segregation, and release of RNA polymerase II (Pol II) from highly transcribed genes. Emerging evidence in recent years suggest that nuclear RNAi has additional roles in maintaining genome stability beyond centromere function, but a mechanistic insight is still lacking. Here, I show that Dicer (Dcr1) terminates promoter-proximally paused Pol II in the presence of R-loops, thereby reducing transcription-replication conflicts (TRCs). We found that *dcr1*Δ became hypersensitive to replication stress when R-loops accumulated. Using classical genetic and genomic approaches, we showed that this was due to mis-regulated nascent transcription dynamics. We discovered sRNA mapping to transcription start sites (TSSs) and termination sites (TTSs), whose biogenesis depended on both Dcr1 and RNase H. Argonaute (Ago1) was implicated in *dcr1*Δ-induced genome instability, as its deletion suppressed the genotoxic stress phenotype of *dcr1*Δ.

We further characterized how Dcr1 limits TRCs, and discovered this was in part mediated by a novel function of the helicase/ATPase domain of Dcr1. In the absence of Dcr1, DNA breaks accumulated around TSSs, and replication progressed more slowly genome-wide. At highly transcribed regions, we found that *dcr1*Δ accumulated more extensive fork resection, suggesting frequent occurrence of fork stalling and reversal, and in head-on collisions, we observed a significant decrease in replication speed. Overall, the results support the novel function of Dcr1 in terminating promoter-proximal Pol II, thereby leaving way for DNA polymerase during replication. We hypothesize this represents one of the ancient roles of Dicer before the emergence of silencing function via the RNAi pathway.

List of abbreviations

2DGE	Bi-dimensional gel electrophoresis
5-FOA	5-Fluoroorotic acid
5mC	5-methylcytosine
AsAgo	Asgard Argonaute
ASO	Antisense oligonucleotide
BLM	Bloom syndrome protein
bp	Base pair
BrdU	5-Bromo-2'-deoxyuridine
CD	Codirectional
Cdc45	Cell division cycle 45
cDNA	Coplementary DNA
CENP-A	Centromere protein A
CFS	Common fragile site
CGI	CpG island
ChIP	Chromatin immunoprecipitation
CHX	Cycloheximide
CI	Termination index
CLRC	Cryptic loci regulator complex
CMG	Cdc45/Mcm2-7/GINS
CPS	Cleavage and polyadenylation site
CPT	Camptothecin
CRISPR	Clustered regularly interspersed short palindromic repeat
CTD	C-terminal domain
CTGS	Co-transcriptional gene silencing
CtIP	CTBP-interacting protein
DDR	DNA damage response
DDRNA	DNA damage response RNA
DdRP	DNA-dependent RNA polymerase
dilncRNA	Damage-induced long non-coding RNA
diRNA	DSB-induced small RNA
DNAP	DNA polymerase
dNTP	Deoxyribonucleotide
DPBB	Double-psi β-barrel
DSB	Double-strand break
dsDNA	Double-stranded DNA
DSIF	DRB sensitivity-inducing factor
dsRBD	Double-stranded RNA binding doain
dsRNA	Double-stranded RNA
DUF283	Domain of unknown function 283
eAgo	Eukaryotic Argonaute
EDTA	Ethylenediainetetraacetic acid
EMM	Edinburgh minimal medium
EMS	Ethyl methanesulfonate
EMSA	Electrophoretic mobility shift assay
ERα	Estrogen receptor α
eRdRP	Eukaryotic RdRP
ESP	Eukaryotic signature protein
FA	Fanconi anemia

FANCJ	Fanconi anemia protein J
FANCM	Fanconi anemia protein M
FISH	Fluorescence *in situ* hybridization
FuDR	5-fluoro-2'-deoxyuridine
G4	G quadruplex
Gb	Gigabase
gDNA	Genomic DNA
GFP	Green fluorescent protein
GINS	Go-ichi-ni-san
GLOE-seq	Genome-wide ligation of 3'-hydroxy ends followed by sequencing
gRNA	Guide RNA
GTF	General transcription factor
H3K4	Histone H3 lysine 4
H3K9	Histone H3 lysine 9
H3K9ac	Histone H3 lysine 9 acetylation
H3K9me2	Histone H3 lysine 9 dimethylation
H3K9me3	Histone H3 lysine 9 trimethylation
H3K14ac	Histone H3 lysine 14 acetylation
H3K27	Histone H3 lysine 27
H3K36me3	Histone H3 lysine 36 trimethylation
H4K20me1	Histone H4 lysine 20 monomethylation
HhH	Helix-hairpin-helix
hmwDNA	High molecular weight DNA
HO	Head-on
HP1	Heterochromatin protein 1
HR	Homologous repair
HU	Hydroxyurea
Indel	Insertion-deletion mutation
ICL	Interstrand crosslink
IES	Internal eliminated sequence
IP-MS	Immunoprecipitation-mass spectrometry
ITC	Initially transcribing complex
LECA	Last eukaryotic common ancestor
lncRNA	Long non-coding RNA
LUCA	Last universal common ancestor
Mcm	Minichromosome maintenance
ME	Malt extract
MEF	Mouse embryonic fibroblast
mESC	Mouse embryonic stem cell
miDAS	Mitotic DNA synthesis
miRNA	microRNA
MMS	Methyl methanesulfonate
MRN	Mre11-Rad50-Nbs1
mRNA	Messenger RNA
MST	Microscale thermophoresis
NAD	Nicotinamide adenine dinucleotide
NDR	Nucleosome-depleted region
NELF	Negative elongation factor
NER	Nucleotide excision repair
NHEJ	Non-hoologous end joining
nt	Nucleotide

NTP	Ribonucleotide
NTS	Non-transcribed strand
pAgo	Prokaryotic Argonaute
PAZ	Piwi/Argonaute/Zwille
PCR	Polymerase chain reaction
PI	Pausing index
PIC	Preinitiation complex
piRNA	Piwi-interacting RNA
PNUTS	PP1-nuclear targeting subunit
Pol I	RNA polymerase I
Pol II	RNA polymerase II
Pol III	RNA polymerase III
Pol V	RNA polymerase V
PolD	Family D DNA polymerase
PP1	Protein phosphatase 1
priRNA	Primal RNA
PRO-seq	Precision run-on sequencing
pS2	Phosphorylation on serine 2
pS5	Phosphorylation on serine 5
PTGS	Post-transcription gene silencing
qiRNA	QDE-2-interacting sRNA
RdDM	RNA-dependent DNA methylation
rDNA	Ribosomal DNA
rasiRNA	Repeat-associated small interfering RNA
RDR	Recombination dependent replication
RdRP	RNA-dependent RNA polymerase
RER	Ribonucleotide excision repair
RFB	Replication fork barrier
RFD	Replication fork directionality
RISC	RNA-induced silencing complex
risiRNA	ribosomal siRNA
RITS	RNA-induced transcriptional silencing
RLR	RIG-I-like receptor
RNAi	RNA interference
RNAP	RNA polymerase
RNase A	Ribonuclease A
RNase III	Ribonuclease III
RNase H	Ribonuclease H
RNA-seq	RNA sequencing
rNMP	Ribonucleotide monophosphate
RNR	Ribonucleotide reductase
ROS	Reactive oxygen species
RPA	Relication protein A
RRM	RNA-recognition motif
rRNA	Ribosomal RNA
RsAgo	*Rhodobacter sphaeroides* Argonaute
RS	Replication slippage
RTEL	Regulator of telomere elongation
RT-qPCR	Reverse transcription-quantitative polymerase chain reaction
scnRNA	Scan RNA
SDS	Sodium dodecyl sulfate

SF2	Superfamily 2
SiAgo	*Sulfolobus islandicus* pAgo
SIR	Silent information regulator
siRNA	Small interfering RNA
SMC	Structural maintenance of chromosome
SNP	Single nucleotide polymorphism
sRNA	Small RNA
sRNA-seq	Small RNA sequencing
SSB	Single-strand break
ssDNA	Single-stranded DNA
Su[Ste]	*Suppressor of Stellate*
TAM	Transcription-associated mutagenesis
TAR	Transcription-associated recombination
TBP	TATA-binding protein
TBZ	Thiabendazole
TC-NER	Transcription-coupled nucleotide excision repair
TCR	Transcription-coupled repair
TE	Transposable element
TERRA	Telomeric repeat-containing RNA
TEV	Tobacco etch virus
TF	Transcription factor
TGS	Transcription gene silencing
TLS	Translesion synthesis
TMP	Trimethyl psoralen
Top1	Topoisomerase I
Top1cc	Top1 cleavage complex
tracrRNA	Trans-activating CRISPR RNA
TRC	Transcription-replication conflict
TS	Transcribed strand
TSS	Transcription start site
UTR	Untranslated region
UV	Ultraviolet
vRdRP	Viral RdRP
WAGO	Worm-specific Argonaute
WRN	Werner syndrome helicase
WT	Wild type
XPF	Xeroderma pigmentosum, complementation group F
XPG	Xeroderma pigmentosum, complementation group G
YES	Yeast extract with supplement
γH2A.X	Gamma H2A.X

List of figures and tables

Chapter 1: Introduction

1.1 Overview

RNA interference (RNAi) is an ancient pathway that co-evolved with DNA and RNA metabolic pathways across the evolutionary timescale. In this chapter, I will briefly describe the evolutionary origin of RNAi, highlighting how individual components of the core RNAi pathway have a distinct origin and therefore ancestral functions that are likely independent of its silencing function. Next, I will provide an overview of the known roles of RNAi factors in maintaining genome stability, ranging from promoting faithful chromosome segregation to coordinating responses to DNA damage. In cycling cells, transcriptional activity is a significant source of genome instability, and the nature, sources, and resolution of genome instability will be discussed. In the last section, I will describe the transcription regulatory function of RNAi at the chromatin level, and, given its functions in maintaining genome stability, a potential connection to limiting transcription-replication conflicts, which forms the basis of my dissertation research.

1.2 The evolutionary origin of RNA interference

RNAi is the phenomenon that an RNA acts in a sequence-specific manner to suppress the expression of a genetic element. Works in the past decades have tremendously expanded our understanding of the mechanism of RNAi, and have delineated the core RNAi machinery as containing a Dicer, Argonaute, and an RNA-dependent RNA polymerase (RdRP). Although gene silencing and genome defense are the primary functions attributed to the RNAi machinery, it has a long, ancient evolutionary history that predates its 'canonical' silencing function.

The last eukaryotic common ancestor (LECA) is believed to possess an intact RNAi pathway, as RNAi genes are encoded in species spanning the eukaryotic tree of life (Cerutti and Casas-Mollano 2006; Shabalina and Koonin 2008). Research on RNAi had been focused on miRNA, owing to its

important roles in development and clinical relevance in human diseases (Ha and Kim 2014); however, the siRNA pathway is more ancestral for at least two reasons. First, the plant and animal miRNA pathways differ fundamentally in their biogenesis and function, and are thought to be exapted from a functional proto-RNAi machinery (Axtell, Westholm, and Lai 2011; Shabalina and Koonin 2008). Second, LECA possessed an RdRP, which was involved in the siRNA, but not the miRNA pathway. The ancestral function of RNAi, therefore, had long been attributed to innate immune defense against viruses and transposable elements (TEs). In recent years, however, new phylogenetic and evolutionary findings have challenged this view – instead of RNAi evolved to defend the genome, it was proposed that the presence of RNAi permitted the expansion of genomic parasites (Torri et al. 2022). What then, could be the ancestral function(s) of RNAi? Below, I describe the current understanding on the evolutionary origin of Dicer, Argonaute, and RdRP, highlighting their newly discovered functions in bacteria and archaea.

Argonuate was discovered in eukaryotes – it was named after the octopus *Argonauta argo* because mutant *Arabidopsis thaliana* had curly leaves that resembled squid tentacles (Bohmert et al. 1998; Fagard et al. 2000). Soon prokaryotic homologs were identified (Cerutti, Mian, and Bateman 2000), and are now known to be present in all domains of life, although only in ~9% and ~32% of bacteria and archaea respectively. Phylogenetic analyses suggested extensive horizontal gene transfer in prokaryotes (Swarts, Makarova, et al. 2014). Prokaryotic Argonautes (pAgos) are highly diverse compared to those in eukaryotes (eAgos). Notably, pAgos have diverse guide and substrate preferences: whereas eAgos use RNA guide to target RNA, pAgos use also DNA-mediated DNA/RNA-targeting and RNA-mediated DNA-targeting (Doxzen and Doudna 2017; Lisitskaya et al. 2022; Ma et al. 2005:5; Swarts, Jore, et al. 2014). Most ascribed functions to pAgos are related to defense against viral/plasmid infections, agreeing with observation that many pAgo genes are encoded within the genomic 'defense islands' – clusters of genes related to defense (Makarova et al. 2009, 2011), although the majority of pAgos remain poorly characterized.

pAgos are classified into long pAgos and short pAgos, of which the former is better characterized. Long pAgos carry all the domains in eAgos, but unlike eAgos, the majority of long pAgos are catalytically inactive (Swarts, Makarova, et al. 2014). To date, most studies focused on catalytically active long pAgos, and they were implicated in genome defense via DNA guide-mediated cleavage of foreign DNA (Kuzmenko et al. 2020). Long pAgo in *Thermus thermophilus* has also been shown to facilitate replication termination and disentanglement of the circular chromosome, via its DNA-guided DNA nuclease activity (Jolly et al. 2020). Inactive long pAgos are poorly characterized, but when one such pAgo from *Rhodobacter sphaeroides* (RsAgo) was expressed in *Escherichia coli*, it led to a decrease in transformation efficiency (Olovnikov et al. 2013); one hypothesis could be that RsAgo bound directly to the plasmid DNA to mediate transcriptional silencing, or to recruit other factors.

Short pAgos are predominantly (~94%) bacterial; they lack the N-terminal and PAZ domains, and their PIWI domain is catalytically inactive as well (Koopal, Mutte, and Swarts 2023). Their biological roles are only beginning to be unraveled, but most short pAgos studied so far are either fused to a catalytic domain, or stably interacting with an effector protein, thereby exerting enzymatic activity after target recognition. pAgos appear to mediate population-immunity by triggering cell death when foreign DNA is recognized. This is done via diverse mechanisms. For example, short pAgos from clade S1A are fused to a SIR2 domain, which depletes the cellular nicotinamide adenine dinucleotide (NAD) pool upon target recognition (Zaremba et al. 2022). *Sulfolobus islandicus* pAgo (SiAgo), on the other hand, activates a membrane protein Aga2 to disrupt membrane polarity upon viral infection (Zeng et al. 2022).

Metagenomic and phylogenetic studies had illuminated the evolutionary history of Argonautes. In 2017, multiple archaeal species were discovered from metagenomic sequencing, which formed a

monophyletic clade called Asgard (Zaremba-Niedzwiedzka et al. 2017). Notably, the study confidently placed eukaryotes as descendants of Asgard archaea, supporting the two-domain hypothesis of eukaryotic origin (Williams et al. 2013). Asgard archaea were found to encode diverse sets of proteins previously thought of as eukaryotic signature protein (ESPs) (Liu et al. 2021; Zaremba-Niedzwiedzka et al. 2017), and indeed, recent analyses suggested Asgard Argonautes (asAgo) as the ancestor of both eukaryotic and bacterial long pAgos (Leão et al. 2023). The ancient asAgo was inferred to possess a highly conserved PIWI domain, but with a mutated catalytic tetrad (DEDX) and was therefore likely to be inactive. This suggests that the slicer activity, and by extension, its role as the effector of the RNA-induced silencing complex (RISC), was likely a derived trait.

Dicer, on the other hand, is a eukaryote-specific fusion protein with domains of bacterial and archaeal origins (Shabalina and Koonin 2008). As in Argonautes, the ancestral functions of these protein domains appeared very different. The C-terminus of Dicer contains two RNase III domains, which are involved in cleaving double stranded RNA (dsRNA) and are almost exclusively found in bacteria (Nicholson 2014). The primary function of bacterial RNase III is ribosomal RNA (rRNA) processing, in which the stem-loop structures in the pre-rRNA are cleaved to promote efficient maturation (Bubunenko et al. 2013). Beyond that, bacterial RNase III also recognizes a multitude of dsRNA (Court et al. 2013). For example, RNase III targets the stem-loop structures formed at the 5' and 3' untranslated regions (UTRs) of many mRNA genes. Depending on the UTRs, this can either activate or inhibit gene expression. In some cases it destabilizes the mRNA by making it available for exonucleases (Régnier and Grunberg-Manago 1990), but in others it promotes ribosome binding by removing the occluding stem-loops (Aristarkhov et al. 1996). Bacterial RNase III also recognizes dsRNA formed when sRNA pairs with another RNA in *trans*. This is best illustrated in the clustered regularly interspersed short palindromic repeat (CRISPR) system. Here, a sRNA called tracrRNA base pairs with spacer sequence between each guide RNA (gRNA); RNase III contributes to gRNA maturation by processing the tracrRNA:spacer duplex (Deltcheva et al. 2011).

The N-terminus of Dicer is a helicase, and its closest homolog is that of an archaeal protein, Hef (Koonin 2017; Nishino et al. 2005; Shabalina and Koonin 2008; Sinha et al. 2018). Both belong to the RIG-I-like subfamily of the superfamily 2 (SF2) helicase (Byrd and Raney 2012). Additionally, Hef belongs to the XPF/Mus81/FANCM protein family, all containing a C-terminal ERCC4-like nuclease domain and a tandem helix-hairpin-helix $(HhH)_2$ domain (Ciccia, McDonald, and West 2008). Supporting a common evolutionary origin, the helicase domains of Dicer, Hef, and FANCM all carry an additional lobe (domain 2; Hel2i in Dicer) on top of the canonical two RecA-like folds found in all SF2 helicases (Byrd and Raney 2012; Nishino et al. 2005; Sinha et al. 2018; Whitby 2010; Zapletal et al. 2022). Hef is structurally most similar to the eukaryotic protein XPF, involved in nucleotide excision repair (NER) and interstrand crosslink (ICL) repair (Ciccia et al. 2008), but is functionally more closely related to Mus81 (Lestini, Duan, and Allers 2010), which participates in resolving stalled replication fork (Munoz-Galvan et al. 2012; Roseaulin et al. 2008). Accordingly, the helicase of Hef has a clear preference of binding branched DNA over linear double-stranded DNA (dsDNA) (Komori et al. 2002, 2004). Although orthologues of Hef are present in Asgard archaea (White and Allers 2018), it is unclear whether the ancestor of Dicer's helicase was capable of DNA metabolism. In fact, the primary sequence of Dicer helicase and Hef are highly divergent, especially domain 2, which is thought to confer substrate specificity to SF2 helicases (Nishino et al. 2005).

Lastly, despite phylogenetic analyses strongly suggesting eukaryotic RdRP (eRdRP) is found in LECA (Cerutti and Casas-Mollano 2006), homologs are very rare in bacteria and archaea (Shabalina and Koonin 2008). Intriguingly, RdRPs are common in RNA viruses (vRdRP), but structural studies suggested the two were unrelated: whereas the catalytic core of vRdRP carried the RNA-recognition motif (RRM) domain (Krupovic, Dolja, and Koonin 2019), that of eRdRP was a double-psi β-barrel (DPBB) domain instead (Salgado et al. 2006). DPBB domain is an ancient fold – possibly predates the last universal common ancestor (LUCA) – that is found in the multi-subunit DNA-dependent RNA

polymerases (DdRP) in all three domains of life, as well as in the family D DNA polymerase (PolD) in Archaea (Koonin et al. 2020). Indeed, the closest identified homologs of eRdRP were DdRPs from bacteriophages, and it was therefore hypothesized that eRdRP originated from a phage that infected the proto-mitochondrial α-proteobacterium (Drobysheva et al. 2021; Iyer, Koonin, and Aravind 2003).

In summary, although identified as an integrated silencing machinery, the ancestral RNAi proteins appeared to have evolved independently before being acquired – again, independently over a long evolutionary timescale – by a proto-eukaryote. Given the context, it is therefore not surprising that in recent years, RNAi proteins are ascribed functions outside of canonical RNAi, and sometimes in pathways independent of each other. This might reflect their ancestral roles before a functional RNAi pathway was formed. Below, I describe the functions of nuclear RNAi that are independent of its silencing abilities.

1.3 Nuclear RNAi and its role in genome maintenance

Studies of TGS in *S. pombe* and RNA-dependent DNA methylation (RdDM) in plants (Chan et al. 2004; Volpe et al. 2002) had shown that RNAi played an important role in the nucleus. Nuclear RNAi is now known to be widespread in nature, conserved from kinetoplastids to vertebrates, and participates in diverse physiological processes. The topic has recently been reviewed in depth (Gutbrod and Martienssen 2020); here, I focus on the specific role of nuclear RNAi on genome stability, which forms the basis of my studies.

1.3.1 Centromere function

The centromere is the location on a chromosome that serves as the assembly site of the kinetochore, a protein complex that ensures proper segregation of genetic material (Mellone and Fachinetti 2021). Despite performing a highly conserved function, centromeric DNA repeats are among

the most rapidly evolving sequences, an observation known as the 'centromere paradox' (Henikoff, Ahmad, and Malik 2001). Because of this, centromeres are remarkably diverse across taxa, and there are very few, if any, generalizable principles applicable to all species (Talbert and Henikoff 2020). In fact, centromeres in most species are epigenetically defined, marked by the presence of nucleosomes containing the histone H3 variant centromere protein A (CENP-A) (Van Hooser et al. 2001); specific DNA sequences are neither necessary nor sufficient for the specification of centromeres. Nevertheless, most centromeres harbor repetitive sequences, and are themselves flanked by other repetitive sequences, known as pericentromeric repeats, that are compacted into heterochromatin. The role of these pericentromeric heterochromatin is not entirely clear, but it is frequently enriched with cohesin and other SMC complexes (Eckert, Gravdahl, and Megee 2007), critical for ensuring proper cohesion of sister chromatids during mitosis (Uhlmann 2016). An additional, non-mutually exclusive proposal is that pericentromeric heterochromatin acts as a mechanical tension buffer to absorb and communicate the pulling force from microtubules (Bloom 2014). Regardless, in many species, disrupting pericentromeric heterochromatin leads to segregation defects, arguing for its role in facilitating centromere function. For example, in *S. pombe*, deletion of Swi6, the heterochromatin protein HP1 homolog, specifically disrupts Rad21 cohesin recruitment at the centromere, but not along the chromosome arm (Bernard et al. 2001).

In many species, disrupting the RNAi machinery leads to chromosome segregation defects. For *S. pombe*, which carries one each of Dicer (Dcr1), Argonaute (Ago1), and RdRP (Rdp1), disrupting any of the three causes lagging chromosomes and segregation defects (Volpe et al. 2003). Additionally, these RNAi mutants become susceptible to microtubule poisons, such as thiabendazole (TBZ) (Hall, Noma, and Grewal 2003; Provost et al. 2002; Volpe et al. 2003). This is also documented in other unicellular eukaryotes across diverse taxa. In *Trypanosoma brucei*, a parasitic unicellular kinetoplastid, disrupting its Argonaute led to chromosome segregation defects (Durand-Dubief and Bastin 2003). Similarly, in the ciliate *Tetrahymena thermophila*, deleting its Dicer homolog Dcl1 led to mitotic

phenotypes such as lagging chromosomes and sensitivity to microtubule poison (Mochizuki and Gorovsky 2005).

Studying the chromosomal function of RNAi in higher eukaryotes is often more difficult for at least two reasons. First, RNAi is involved in miRNA biogenesis; disruption of which often leads to early embryonic lethality (Bernstein et al. 2003), although this has also been speculated to be caused by unresolved DNA damage in rapidly dividing cells (Swahari, Nakamura, and Deshmukh 2016). Second, higher eukaryotes – especially in plants – often harbor multiple copies of RNAi, and they regularly perform overlapping functions (Borges and Martienssen 2015). Nevertheless, emerging evidence supports the segregation function of RNAi is also conserved in higher eukaryotes. In arthropods, Dcr-2 and AGO2 are specialized for the endogenous siRNA pathways (Aderounmu et al. 2023; Lee et al. 2004; Mukherjee, Campos, and Kolaczkowski 2013), and their disruption leads to chromosomal defects (Pek and Kai 2011), as well as heterochromatin defects (Deshpande, Calhoun, and Schedl 2005). Similarly, in vertebrates, chromosome mis-segregation, bridging chromosomes, among other segregation defects have been observed in human RPE-1 cells (Huang et al. 2015), HeLa cells (Pek and Kai 2011), mouse fibroblast (Harfe et al. 2005), as well as mouse embryonic stem cells (mESCs) (Gutbrod et al. 2022). Notably, knocking out DGCR8, a subunit of the microprocessor complex involved in the generation of miRNA, does not lead to lethality, suggesting that the segregation defect of Dicer knockout is independent of the loss of miRNA (Gutbrod et al. 2022; Huang et al. 2015).

Mechanistically how RNAi ensures proper chromosome segregation function is not fully understood, but in *S. pombe*, this is done by promoting the formation of pericentromeric heterochromatin. In a process called co-transcriptional gene silencing (CTGS), small interfering RNA (siRNA) is generated from transcripts originating in the pericentromeric regions (Bühler and Moazed 2007; Bühler, Verdel, and Moazed 2006; Volpe et al. 2002). In this model, nascent pericentromeric

transcripts recruit the RNA-induced transcriptional silencing (RITS) complex via siRNA-loaded Ago1 (Verdel et al. 2004). RITS physically interacts with the RDRC complex (Motamedi et al. 2004), which contains Rdp1, thereby generating dsRNA to make more siRNA. RITS also recruits the cryptic loci regulator complex (CLRC) (Bayne et al. 2010) containing Clr4, the only H3K9 methyltransferase in *S. pombe*, therefore inducing heterochromatin formation. On top of the recruitment of Swi6 and therefore cohesin described above, pericentromeric heterochromatin also promotes *de novo* Cnp1 (CENP-A homolog) deposition in *S. pombe* (Folco et al. 2008), directly influencing centromere establishment.

It has not been established whether RNAi in other species promotes chromosomal functions also via pericentromeric heterochromatin regulation, but many observations point to such possibility. TEs play an important role in shaping centromere evolution. Many centromeres are comprised primarily of TEs (Gao et al. 2015), and centromeric satellite repeats often bear sequence similarity with, and are proposed to have originated from, TEs (Gong et al. 2012; Shang et al. 2010; A. Sharma, Wolfgruber, and Presting 2013; Talbert and Henikoff 2020). Centromeres are almost universally transcribed at a low level (Lopes et al. 2023; Talbert and Henikoff 2018), albeit elevated expression is usually harmful (Bouzinba-Segard, Guais, and Francastel 2006; Ohkuni and Kitagawa 2011). In *S. pombe*, it is this transcription that initiates CTGS to promote heterochromatin assembly (see above); a similar mechanism could therefore operate in other species. Centromeric transcripts accumulate in *Dicer1*$^{-/-}$ knockout mESCs, although H3K9me3 level did not decrease (Gutbrod et al. 2022). On the other hand, mutant *A. thaliana* defective in DNA methylation requires RNAi to establish pericentromeric H3K9 methylation (Shimada et al. 2023), promoting centromere function in a way similar to that in *S. pombe*. In any case, whenever repetitive sequences comprise pericentromeric heterochromatin, the targeting activity of RNAi seems to become critical in ensuring proper segregation function. Further supporting this observation, the loss of RNAi in some *Cryptococcus sp.* is correlated with shorter centromeres (Yadav et al. 2018), and in *Trypanosoma cruzi*, which, unlike *T. brucei*, has lost a functional RNAi pathway (Lye et al. 2010), its centromeres lack repetitive sequences (Obado et al. 2007). In the most

striking case of the budding yeast *Saccharomyces cerevisiae*, the loss of the entire RNAi pathway is correlated with the presence of a genetically defined point centromere. Therefore, although RNAi itself is not strictly necessary for centromere function, its presence correlates with the accumulation of repetitive elements, entailing its co-option into regulating the centromeric process.

1.3.2 Regulation of DNA metabolism

On top of its prominent role in centromere function, RNAi has additional roles in DNA metabolism, including programmed DNA elimination, copy number maintenance, and regulation of DNA repair. These processes not only ensure genome integrity, but could also alter gene expression through DNA changes.

Programmed DNA elimination refers to the selective removal of genetic material during the somatic development of an organism. It ranges from the removal of select regions along a chromosome in nematodes to the elimination of an entire set of paternal genome in certain arthropods, and is found in diverse species, from unicellular ciliates to angiosperms and vertebrates (Dedukh and Krasikova 2022). The mechanism of DNA elimination is relatively well understood in ciliates, and involves the use of RNAi machinery (Gao et al. 2023; Noto and Mochizuki 2017).

Ciliates are unicellular eukaryotes that possess a transcriptionally active, polyploid macronucleus and a transcriptionally inert diploid micronucleus. During sexual reproduction, the micronucleus produces new micronuclei and macronuclei, and the parental macronucleus is destroyed (Noto and Mochizuki 2017). The development of new macronuclei requires programmed DNA elimination, of which sequences called internal eliminated sequences (IESs) are removed. In *T. thermophila* this amounts to ~30% of the genome, and the process starts with the production of sRNAs called ‘scan RNAs’ (scnRNAs) by the Dicer homolog Dcl1p, with bidirectional transcripts generated in the IESs as substrates. The scnRNAs are then loaded onto the Argonaute Twi1p and travel into the

parental macronucleus. There, long noncoding RNA (lncRNA) is generated and scnRNAs that bind complementarily to nascent lncRNA from the macronuclear genome are degraded. The surviving scnRNAs then travel to the newly developing macronucleus and guide heterochromatin formation, triggering H3K9 and H3K27 methylation. The heterochromatin then recruits the HP1 homolog Pdd1p and IESs are excised by the transposase Tpb2p (Rzeszutek, Maurer-Alcalá, and Nowacki 2020). Via this negative selection mechanism, sequences that have been preserved in the parental macronucleus would not be eliminated in daughter macronuclei. scnRNA-based DNA elimination is found in other ciliates such as *Paramecium* and *Oxytricha*, though there are subtle mechanistic differences (Gao et al. 2023).

DNA elimination is also observed in nematodes, copepods, lampreys and hagfishes (Smith, Timoshevskiy, and Saraceno 2021), but whether a ncRNA- and RNAi-based mechanism is involved remains unclear. In all species it is mostly the repetitive, TE-derived sequences that are removed, although a recent genome assembly study of the hagfish *Eptatretus atami* shows that ~1,600 genes are removed during early embryo development (Marlétaz et al. 2024). In the worm *Ascaris*, certain worm-specific Argonautes (WAGOs) have biased distribution on chromatin, binding to sequences that are removed (Estrem and Wang 2023), and in sea lampreys (*Petromyzon marinus*), the regions to be eliminated are also tagged with heterochromatic marks (Timoshevskiy et al. 2016). The case of copepods is more extreme. In *Mesocyclops edax*, TEs proliferate uncontrollably during germline development, resulting a genome size of ~15 Gb compared to ~3 Gb in somatic genome; instead of epigenetically silencing the TEs they were excised during embryogenesis (Sun et al. 2014). An RNAi-based mechanism similar to that in ciliates was proposed, although it remained to be verified.

The role of RNAi in genome stability extends beyond heterochromatin-based mechanisms; for example, a prominent role for RNAi has been found in ribosomal DNA (rDNA) copy number maintenance. Most organisms carry multiple copies (100s to 1000s) of rDNA, often in tandem repeats

on a few rDNA loci. The copy number varies drastically between species, individuals, and even between cells in a single organism (Nelson et al. 2019). Nevertheless, being critical for cellular viability, rDNA copy number is tightly regulated to be within a homeostatic range, and in many species disrupting the RNAi machinery leads to rDNA repeat instability.

In *S. pombe*, Dcr1 deletion leads to a reduction of rDNA copy number, both under mitotic growth as well as over meiotic generations. rRNA is normally transcribed by RNA polymerase I (Pol I), but surprisingly, RNA polymerase II (Pol II) accumulates at the rDNA loci in *dcr1*Δ, and is accompanied with the enrichment of DNA damage marks such as Rad52 and Crb2 on the chromatin (Castel et al. 2014). Such effect is not observed in *dcr1-5* mutant, of which the two RNase III domains are catalytically inactivated, nor in *ago1*Δ cells (Castel et al. 2014), suggesting Dcr1 acts in a way independent of canonical RNAi. As rRNA comprises up to ~80% of cellular RNA, rDNA loci are highly transcriptionally active. This makes rDNA loci into hotspots of transcription-replication conflicts (TRCs) (Achar and Foiani 2017), which, if left unchecked, can cause DNA damage and copy number variation (Helmrich et al. 2013). A possible role of Dcr1, therefore, could be to promote transcription termination to limit replication stress. Supporting this, negative epistatic interactions have been observed between *dcr1*Δ and DNA replication factors such as *mrc1*Δ, and *dcr1*Δ exacerbates replication fork stalling at the centromeric repeats (Zaratiegui et al. 2011), another difficult-to-replicate region (Barra and Fachinetti 2018). Under physiological condition, only a subset of rDNA copies are transcriptionally active, and the rest are heterochromatinized (Srivastava, Srivastava, and Ahn 2016). In *dcr1*Δ, sRNAs mapping to rDNA loci are lost, but there is little change to the H3K9me2 level, further highlighting a role independent of RNAi-directed heterochromatin formation (Castel et al. 2014).

In other organisms a sRNA-based mechanism seems to be involved too. In *N. crassa*, rDNA copy instability is observed in the *quelling-deficient-2* (*qde-2*) Argonaute mutant, and QDE2-loaded siRNA mapping to rDNA loci can be detected in wild type (WT) (Cecere and Cogoni 2009). Whereas

in *S. pombe* there is no change to H3K9me level, in *D. melanogaster* a loss of H3K9me2 across the whole rDNA gene is observed in *dcr-2*, and both Argonaute (Ago2) and Dicer (Dcr2) are important for nucleolar organization (Peng and Karpen 2007). In *C. elegans*, disruption of the piRNA pathway causes infertility only after 17 generations, and it is proposed to be caused by an upregulation of ribosomal siRNA (risiRNA) concomitant with a progressive decrease in rDNA copy number, disrupting cellular physiology in late generations. Interestingly, mutating the RNAi machinery restores fertility and is correlated with an increase in rDNA copies (Wahba, Hansen, and Fire 2021). A notable exception is Dcr-1, which, when mutated, restores fertility without restoring rDNA copies.

1.3.3 DNA damage checkpoint, response, and repair

There is accumulating evidence that nuclear RNAi is intimately linked with the DNA damage checkpoint response, and DNA repair. In the presence of DNA damage, an evolutionarily conserved DNA damage response (DDR) pathway is activated, which propagates the signal from the site of damage to induce cell cycle arrest, allowing extra time for repair (Ciccia and Elledge 2010). Some of the earliest responses include the phosphorylation and activation of ATM – which is a kinase itself and phosphorylates ATR, as well as the histone H2A-variant H2A.X (Giglia-Mari, Zotter, and Vermeulen 2011). Activated ATM, ATR and phosphorylated H2A.X (γH2A.X) further amplify the signal, recruiting secondary factors to facilitate repair.

When RNAi is disrupted, cells accumulate endogenous DNA damage, DDR activation is frequently impaired, and the cell cycle progresses despite unresolved DNA damage. In *S. pombe*, *dcr1*Δ leads to elevated level of Rad52 foci marking DNA damage, most prominent during S-phase – suggesting a role in preventing replication-induced damage – but also persist until G2 phase (Zaratiegui et al. 2011). In response to hydroxyurea (HU), a genotoxic drug that induces replication stress by depleting the cellular deoxyribonucleotide (dNTP) pool (Singh and Xu 2016), the cyclin-dependent kinase Cdc2 (Cdc28 in *S. cerevisiae*) is hyperphosphorylated to arrest cells at the S-M checkpoint

(Rhind, Furnari, and Russell 1997). In *dcr1*Δ and *ago1*Δ cells, Cdc2 fails to be properly activated and cells are not properly arrested (Carmichael et al. 2004). Notably, these phenotypes are much milder, or even absent in *rdp1*Δ cells, suggesting a role independent to canonical RNAi. In *T. thermophila*, an RNAi pathway distinct from that involved in DNA elimination (see above) limits the accumulation of DNA damage, as its disruption leads to elevated expression of DNA repair genes, and cells accumulate nuclear Rad51 and γH2A.X foci suggesting persistent damage (S. R. Lee et al. 2021).

Impairment of DDR activation in RNAi mutants is also documented in mammals. In a study of mouse cerebellar development, conditional deletion of either Dicer or Drosha in neuronal precursors – which undergo rapid cell division associated with replicative stress (Y. Lee, Katyal, et al. 2012; Y. Lee, Shull, et al. 2012) – triggers the accumulation of γH2A.X foci, as well as DNA breaks (Swahari, Nakamura, Baran-Gale, et al. 2016). Similar phenotypes are also observed in human HEK293T cells when Dicer is knocked down (Tang et al. 2008). In addition to limiting endogenous stress, RNAi factors have also been shown to actively respond to exogenous damage. When HEK293 cells and mouse embryonic fibroblasts (MEFs) are treated with damaging agents such as etoposide or γ-irradiation, Dicer becomes phosphorylated and localizes into the nucleus (Burger et al. 2017; Burger and Gullerova 2018). In fact, Dicer phosphorylation – and by extension, its subcellular localization – is tightly regulated; its mis-regulation is observed in tumor samples and is implicated in cancer progression, potentially by altering its interaction with the DDR pathway (Reyes-Castro et al. 2023; Swahari, Nakamura, and Deshmukh 2016). Consequently, disruption of cellular Dicer or Drosha level in both human fibroblasts and zebrafish larvae leads to impaired accumulation of DDR foci (e.g. phosphorylated ATM) when the cells were exposed to ionizing radiation (Francia et al. 2012). No effect was observed when downstream miRNA effectors such as TNRC6A/B/C were knocked down, suggesting a miRNA-independent mechanism.

In recent years, transcription activity and RNA have emerged as important players in DDR (Long, Liu, and Gullerova 2021), and RNAi is likely closely tied to this phenomenon. In *S. pombe*, Pol II has been detected at an artificially induced DSB, and plays a role in facilitating efficient repair (Ohle et al. 2016). Whether the transcript is processed into sRNA was not tested in this example, but that appears to be the case in *A. thaliana* and in mammalian systems (Burger et al. 2017; Francia et al. 2012, 2016; Miki et al. 2017; Wei et al. 2012). In *A. thaliana*, the sRNA population is known as DSB-induced small RNAs (diRNA); their biogenesis and functions are still poorly understood, but in two cases using transgenic reporter systems, parts of the RdDM machinery appear to be involved. DCL4, RDR6, and potentially DCL2 are required for diRNA production, and efficient repair of damage requires NRPD1 and NRPD2, the largest subunits of RNA Pol IV and Pol V respectively (Miki et al. 2017; Wei et al. 2012). Crucially, AGO4 and DRM1/2, key effector proteins of the RdDM pathway, are not required, arguing against the utilization of canonical RdDM pathway. How repair is promoted by the RdDM pathway machinery remains unresolved, but given that active transcription – in the experiment, by Pol II – proximal to the induced DSB site is required (Miki et al. 2017), one can speculate Pol IV and V might functionally substitute Pol II to initiate diRNA generation and therefore DDR activation.

In mammalian systems, nuclear RNAi factors – specifically Dicer and Drosha – have been shown to localize to DSBs to process the damage-induced lncRNA (dilncRNA) (Burger et al. 2017), generating sRNA termed DNA damage response RNAs (DDRNAs). sRNA mapping to the vicinity of an induced DSB is also detected in *D. melanogaster* (Michalik, Böttcher, and Förstemann 2012). The recruitment of RNAi factors appears to be tightly coordinated with that of Pol II. A critical player in DSB repair is the Mre11-Rad50-Nbs1 (MRN) complex, which acts as a DSB sensor and transmits the information via activating ATM, amongst additional roles (Lamarche, Orazio, and Weitzman 2010). The MRN complex has been shown to recruit both Pol II (Michelini et al. 2017) and Drosha (Cabrini et al. 2021), although in different cell lines – mouse NIH2/4 and human U2OS respectively. At DSB, active Pol II recruited by the MRN complex initiates bi-directional transcription to and from the break

site, generating dilncRNA that base-interacts with one another to form dsRNA. These dsRNA are processed by Drosha and Dicer, forming DDRNAs (Michelini et al. 2017). It should be noted, however, that DDRNAs are not always produced at DSBs, and its production is likely influenced by the underlying sequence complexity, as well as transcriptional activity (Lu et al. 2018).

The downstream functions of damage-localized RNAi factors and the damage-induced RNAs are less clear, partly owing to differences in experimental designs and because different kinds of DNA damage elicit distinct repair pathway choices (Ait Saada, Lambert, and Carr 2018; Ceccaldi, Rondinelli, and D'Andrea 2016; Ciccia and Elledge 2010; Scully et al. 2019). At the very least, RNAi is required for proper DNA damage tolerance and efficient damage repair. In *S. pombe*, *dcr1*Δ and *ago1*Δ are sensitive to HU (Carmichael et al. 2004). *Dcr1*Δ and *ago1*Δ also negatively interacts with *mrc1*Δ and *swi3*Δ (Zaratiegui et al. 2011), parts of the fork protection complex Mrc1/Swi1/Swi3 that promotes replication stress tolerance by stabilizing stalled forks (Shimmoto et al. 2009). In *A. thaliana*, deleting either DCL2/3/4 reduces DSB repair efficiency, along with a reduction of diRNA level (Wei et al. 2012). The diRNA potentially exerts its function via Argonaute as an effector protein, as AGO2, but not AGO4/6, is required for its production as well as efficient repair (Miki et al. 2017; Wei et al. 2012) The function of diRNA remains controversial, as *RDR2*$^{-/-}$ and *RDR6*$^{-/-}$ mutants, despite having only ~10-20% of WT level of diRNA, remain as efficient as WT in repairing DSB.

In mammals, where the effects are studied in more details, both the RNAi factors themselves and the accompanying DDRNAs appear to be important. siRNA inhibition of Dicer or Drosha reduces both HR and non-homologous end joining (NHEJ) efficiency (Lu et al. 2018), although Drosha has been documented to preferentially promote the NHEJ pathway (Cabrini et al. 2021). Dicer and Drosha are important for the recruitment of 53BP1 and MDC1 (Burger, Schlackow, and Gullerova 2019; Francia et al. 2016), two downstream response factors that coordinate with γH2A.X and influence repair pathway choices (Ciccia and Elledge 2010). In the human A549 cancer cell line, when Dicer or Drosha

is inhibited by siRNA and cells treated with γ-irradiation, 53BP1 – but not γH2A.X – foci formation is impaired (Lu et al. 2018). 53BP1 is inhibited by TIRR (Dai et al. 2018; Drané et al. 2017), and lncRNA generated from DSB has been shown to separate TIRR from 53BP1, leading to its activation, in a manner that is dependent on the activity of Dicer and Drosha (Ketley et al. 2022). The ability of Dicer and Drosha to activate DDR depends on DDRNAs generated by Dicer, as RNase A treatment of permeabilized NIH2/4 cells leads to impaired DDR foci formation after irradiation, and is restored when the cells are incubated with site-specific synthetic sRNA (Francia et al. 2012). Base-pairing interaction with dilncRNA is required for these sRNA to recruit 53BP1, and it can be prevented by the addition of antisense oligonucleotides (ASOs) disrupting their interactions (Michelini et al. 2017). Similar to *A. thaliana*, the Argonaute Ago2 has been shown to act as an effector protein, promoting Rad51 recruitment to DSB and facilitating HR-based repair (Gao et al. 2014).

Based on studies in diverse species, RNAi likely assists in the initial recognition of DNA damage, in pathway distinct to that of canonical miRNA and siRNA. There exists a complex coordination between the RNAi machinery and DNA repair factors, which responds dynamically depending on the underlying sequence as well as its transcriptional activity. This is illustrated in the case of *N. crassa*, where sRNA production appears to be triggered in response to DNA damage. Here, histidine treatment – which inhibits DNA replication and induces DNA damage – triggers the production of 20 – 21 nt long QDE-2-interacting sRNA (qiRNA) that originates from the rDNA loci (Lee et al. 2009). In parallel, DNA damage proximal to tandem repeats appears to be the trigger for quelling, and in the process siRNA is produced (Yang, Ye, and Liu 2015). Notably, the production of these damage-induced sRNA depends not only on Dicer homologues DCL-1 and DCL-2, the Argonaute QDE-2, and QDE-1 – an enzyme with both DdRP and RdRP activities, but also on QDE-3, a RecQ DNA helicase, as well as the HR machinery such as Rad51 and Rad54 (Lee et al. 2010; Zhang et al. 2013). In the case of quelling, therefore, sRNA is only generated when DNA damage occurs at tandem repeats, by the combined action of RNAi and HR factors. In fact, DNA repair factors have also been

implicated in silencing, suggesting a reciprocal interaction between DNA repair and RNAi. In *S. pombe*, *dcr1*Δ and *ago1*Δ negatively interact with *rad51*Δ (Zaratiegui et al. 2011), a highly conserved protein involved in HR based DNA repair (Bonilla et al. 2020), Interestingly, the knockouts *rad51*Δ and *rad54*Δ – also an HR factor, partially lose centromeric silencing (Onaka et al. 2016), and the Rad54 homolog DRD1 is required for silencing in *A. thaliana* (Kanno et al. 2004).

1.4 Transcription-replication conflict: sources and resolution

DNA repair, recombination, and replication occur on the very same substrate that undergoes transcription. It is therefore of no surprise that there exist complex interactions between the machineries. For example, when an RNA polymerase (RNAP) encounters a DNA lesion, the blocked RNAP acts as a sensor to stimulate DNA repair, in a process known as transcription-coupled repair (TCR) (Selby et al. 2023). Exogenous DNA damage also downregulates transcriptional activity, and is proposed as a way to limit the transcription machinery from interfering with DNA repair (Machour and Ayoub 2020). On the other hand, transcription-replication conflicts (TRCs) occur when the replisome progression is influenced by the transcription machinery. Its potential to induce genome instability has been known for a long time, but recent advances have revealed the mechanism to be far more complex than previously appreciated. In this section, I first describe the individual connection of transcription and replication to genome stability, followed by a discussion on the mechanisms in place to coordinate the two processes simultaneously.

1.4.1 Transcription and genome stability

The phenomenon of transcription-associated mutagenesis (TAM) was first noted in bacteria in the early 1970s, when exogenous mutagens were more effective when the reporter gene was transcriptionally active (Herman and Dworkin 1971; Savić and Kanazir 1972). In eukaryotes, it was first demonstrated in *S. cerevisiae*, using an inducible promoter system and a frameshifted *lys2* allele

(Datta and Jinks-Robertson 1995). In higher eukaryotes, TAM was demonstrated using a hypermutating mouse cell line harboring a doxycycline-inducible GFP transgene gene with a premature stop codon, in which the frequency of GFP^+ reversion correlated transcription (Bachl et al. 2001). On top of TAM, transcription is also known to stimulate recombination, in a process called transcription-associated recombination (TAR). This was first observed in *E. coli* deficient in *recA*, the prokaryotic ortholog of Rad51 (Shinohara, Ogawa, and Ogawa 1992), that RNAP activity promoted recombination between two mutant λ phage (Ikeda and Kobayashi 1977). In *S. cerevisiae*, inter- and intra-chromosomal recombination was stimulated when a Pol I promoter-containing sequence, *HOT1*, was placed at an ectopic location (Keil and Shirleen Roeder 1984; Voelkel-Meiman, Keil, and Roeder 1987). In *S. pombe* too, replacing the native *ade6* promoter with a strong constitutive *adh1* promoter stimulated both mitotic and meiotic recombination (Grimm et al. 1991).

Transcription destabilizes DNA in multiple ways, causing different mutational and recombinatorial consequences (Aguilera 2002; Gaillard and Aguilera 2016; Jinks-Robertson and Bhagwat 2014; Kim and Jinks-Robertson 2012). In replication-independent events, transcriptional activity alone increases the frequency of most, if not all, kinds of mutation (Lippert et al. 2004), but leaves a particular mutational signature, the most prominent being that the non-transcribed strand (NTS) mutates more frequently than the transcribed strand (TS) (Beletskii and Bhagwat 1996; Green et al. 2003; Mugal, von Grünberg, and Peifer 2009). Definitive explanation is still lacking, but evidence suggests this is due to both the NTS being more susceptible to DNA damage during transcription, and the lesions occurring at TS being more efficiently repaired. Preferential DNA repair via nucleotide excision repair (NER) is observed in both prokaryotes and eukaryotes, a phenomena known as transcription-coupled NER (TC-NER) (Gaillard and Aguilera 2013; Hanawalt and Spivak 2008; Selby et al. 2023), and presumably, this is due to the fact that stalled Pol II is the trigger of TC-NER (Li et al. 2014), which is more efficiently induced by lesions at the TS.

Single-stranded DNA (ssDNA) is more chemically reactive and prone to DNA damage (Lindahl 1993). It is therefore hypothesized that NTS is more susceptible to TAM by being more frequently in the ssDNA state: an active, elongating Pol II has a transcription bubble of ~10 nt, with accompanying NTS potentially exposed as ssDNA (Gnatt et al. 2001). Additionally, transcription induces positive and negative supercoiling ahead and behind the RNAP respectively (Liu and Wang 1987). Negative supercoiling unwinds DNA, favoring the formation of non-B DNA structures. In particular, the nascent RNA is prone to stably base-pairing with the TS, forming a three-stranded structure known as R-loop (see below). This exposes the NTS as ssDNA, rendering it more susceptible to DNA damage. Any processes favoring the formation of R-loop would therefore potentially contribute to the NTS-TS bias. Agreeing with this hypothesis, when the human cytosine deaminase (AID), which preferentially acts on ssDNA, is expressed in *S. cerevisiae*, mutating the THO/TREX complex to promote R-loop formation (Huertas and Aguilera 2003) leads to elevated targeting of AID to NTS (Gómez-González and Aguilera 2007). Additionally, synonymous mutations that promote RNA folding, and therefore reducing the likelihood of R-loop formation, have been shown to reduce TAM frequency (Chen, Yang, and Zhang 2016).

On top of the NTS-TS bias, TAM is also enriched (up to 50% of all mutations) in 2- to 5-bp deletions (Lippert et al. 2004), and genetic studies have pointed to abortive topoisomerase I (Top1) as the main source of TAM, contributing to the observed mutational signature (Lippert et al. 2011; Takahashi et al. 2011). Transcription-induced negative supercoiling is primarily resolved by Top1 (Brill and Sternglanz 1988), which relieves torsional stress by creating a single strand nick, allowing controlled rotation of the duplex DNA. In the reaction intermediate, Top1 is covalently linked with the 3'-end of the nick; when the 5'-hydroxyl group is displaced – by existing DNA damage (Pourquier et al. 1997), or underlying tandem repeats – Top1 could be trapped, forming the Top1 cleavage complex (Top1cc). Repairing such trapped Top1cc is error prone, generating short deletions.

Recombination requires the generation of a stretch of ssDNA, called presynaptic filament, capable of homology search (Heyer, Ehmsen, and Liu 2010); therefore, it is widely assumed that TAR is caused by the induction of DNA breaks by transcription. In support of this, genetic data suggested transcription initiated a response similar to that of DSB induction, rather than a specific pathway of HR events (González-Barrera, García-Rubio, and Aguilera 2002). Here, replication is a major player, and TRC constitutes the primary source of transcription-dependent breaks, which will be discussed in subsequent sections. Nevertheless, prolonged exposure of ssDNA, by topological constraints, or by transcribing through regions prone to non-B DNA formation, can subject the DNA to various damaging agents, creating breaks that are recombinogenic (Gaillard and Aguilera 2016). This is supported by the fact that *top1/top2* mutant in *S. cerevisiae* displayed a hyper-recombination phenotype at the rDNA repeats (Christman, Dietrich, and Fink 1988). Additionally, transcription can promote the expansion of GAA repeats independent of replication in human cells (Ditch et al. 2009; Lin, Dion, and Wilson 2006), and in *S. cerevisiae*, the same repeat stimulates mitotic recombination outside of S phase (Tang et al. 2011), further highlighting how transcription through difficult templates can be inherently recombinogenic. Finally, the recombinogenic potential of DNA damage agents such as UV irradiation and methyl methanesulfonate (MMS) is synergistically increased when transcription is active (García-Rubio et al. 2003; Hendriks et al. 2008), suggesting that recombination is stimulated when transcription progression is impeded.

1.4.2 Characteristics and sources of TRCs

Collisions between the replisome and the transcription machinery can occur codirectionally (CD) or head-on (HO). In bacteria, where replisomes move much faster than RNAPs (Brewer 1988), replisome rear-ending the RNAP represents the majority of CD-TRC, whereas in eukaryotes, replisomes and RNAPs move at comparable speed (Muniz, Nicolas, and Trouche 2021; Técher et al. 2013), making the alternative scenario – RNAP rear-ending the replisome – equally likely. HO-TRCs have a more severe consequence, even at a low level of transcription. In fact, *in vitro* experiments in

Bacteria show that a single RNAP can lead to prolonged stalling of the replisome, and even dislodge the replisome altogether (Liu and Alberts 1995; Pomerantz and O'Donnell 2010). HO-TRCs have also been shown to slow or completely stall the replisome *in vivo* in *E. coli* and *Bacillus subtilis* (French 1992; Lang et al. 2017; Mirkin and Mirkin 2005). In *B. subtilis*, a reporter gene placed HO induces 60% more overall mutation than when placed CD (Sankar et al. 2016). In this system, HO- and CD-TRCs generate distinct mutational spectra – for example, HO-TRCs generate more mutation at the 3' end of the reporter gene, consistent with the location when such encounter occurs.

Engineered constructs are also used to study TRC in eukaryotes *in vivo*. In *S. cerevisiae*, HO-TRC triggers recombination between introduced direct repeats more frequently, and is dependent on S-phase transcription (Prado and Aguilera 2005). As described above, TAM is characterized by a mutational signature of 2-5 bp deletions, and its occurrence is dependent on replication (Kim et al. 2007). Similar to that in *B. subtilis*, distinct mutational spectra are observed between HO- and CD-TRC, with CD-TRC generating the 2-5 bp deletion more frequently, while HO-TRC tends to generate more complex indels. Studying TRC in higher eukaryotes with reporter assay is more challenging, but using a plasmid system in HEK293 cells, HO-TRC was shown to induce plasmid instability and to activate distinct DDR than CD-TRC (Hamperl et al. 2017). Therefore, TRC, at least when artificially engineered at a high level, causes genome instability in both prokaryotes and eukaryotes.

Given the mutagenic potential of TRC, cells employ multiple methods to limit its occurrence. This is most prominent in prokaryotes, where aligning genes co-directional to the single replication origin is selectively advantageous over evolutionary time. As such, the most highly transcribed genes – those encoding rRNA and ribosomal proteins – are almost always co-directional across many species (McLean, Wolfe, and Devine 1998). This is also observed for essential genes, presumably to reduce the rate of mutagenesis caused by HO-TRC (Rocha and Danchin 2003; Zheng et al. 2015). On the other hand, orienting genes associated with environmental stress and pathogen defense head-on to replication,

and thereby increasing its mutagenic potential, appears to promote adaptive evolution (Lang et al. 2017; Merrikh and Merrikh 2018; Paul et al. 2013). In eukaryotes, the effect is less pronounced, although in *S. cerevisiae* a strong preference for tRNA genes to align co-directionally with origins is observed (Osmundson et al. 2017). Additionally, within rDNA repeats, sequences that act as replication fork barrier (RFB) have been found from yeast to mammals; they block replication from one direction and thereby promoting replisome progression co-directionally with rRNA genes (Gadaleta and Noguchi 2017).

Spatiotemporal separation between transcription and replication has been proposed as a mechanism to reduce TRC in eukaryotes. Early imaging studies showed conflicting results on whether the two machineries are spatially separated (Hassan et al. 1994; Wansink et al. 1994; Wei et al. 1998), but this is supported by recent sequencing and microscopy analyses (Meryet-Figuiere et al. 2014; Uchino et al. 2021). Nevertheless, TRCs are inevitable for several reasons. First, transcription remains active in S phase – in fact, certain classes of genes such as histones and cyclin/cyclin-dependent kinases (CDKs) are upregulated specifically in S phase (Bertoli, Skotheim, and de Bruin 2013). Second, in higher eukaryotes some of the longest genes take longer than one cell cycle to transcribe, making encounters inevitable (Helmrich, Ballarino, and Tora 2011). Lastly, both transcription and replication activity appear to correlate with a similar set of epigenetic signals (Prioleau and MacAlpine 2016). In the broadest sense, transcriptionally active euchromatin, marked by histone marks such as H3K4 methylation and H3K36me3, generally replicates early, whereas heterochromatin marked by H3K9me2 replicates late (Marchal, Sima, and Gilbert 2019). At a smaller scale, the most efficient origins colocalize with transcription start sites (TSSs) (Chen et al. 2019; Huvet et al. 2007; Petryk et al. 2016). This is also in agreement with the fact that genomic and epigenomic features associated with origins are often shared with TSSs. For example, origins tend to locate in GC-rich DNA and G quadruplexes (G4s) (Besnard et al. 2012; Cayrou et al. 2011; Langley et al. 2016), features frequently found in CpG islands (CGIs) around eukaryotic promoters (Deaton and Bird 2011). Marks associated with open

chromatin, including H4K20me1 and H3K9ac, are enriched amongst the most efficient, constitutive, and early-replication origins (Picard et al. 2014). Naturally, this would align replication to transcription, minimizing HO-TRC; however, transcription appears to play an active role in shaping replication initiation that confounds this simple deduction. In G1 phase, origin recognition complex (ORC) is loaded onto the origin, which serves to recruit the Mcm2-7 replicative helicase as a double hexamer, responsible for initiating bidirectional replication in S phase (Bell and Stillman 1992; Evrin et al. 2009). Multiple Mcm2-7 double hexamers can be loaded iteratively by a single ORC (Bowers et al. 2004), which could then translocate away from ORC and distribute throughout the genome (Remus et al. 2009). RNAPs can actively push the Mcm2-7 complex (Gros et al. 2015; Scherr et al. 2022), and G1 transcription clears intragenic Mcm2-7 (Akerman et al. 2020). In cancer cells, perturbing such processes by activating G1-shortening oncogenes causes replication stress within active genes (Macheret and Halazonetis 2018). While this mechanism limits initiation within actively transcribing genes, an unavoidable consequence is that Mcm2-7 becomes enriched downstream of genes, at transcription termination sites (TTSs) (Chen et al. 2019; Koyanagi et al. 2022). In this respect, TRC is likely to occur frequently despite multiple mechanisms to reduce its abundance and severity.

TRCs impeding replication are observed in physiological conditions, and are especially enriched at certain hotspots. In *B. subtilis*, chromatin immunoprecipitation (ChIP) revealed that replication restart factors such as DnaB and DnaD accumulate at rRNA genes (Smits et al. 2011), suggesting the necessity for replication restart at highly transcribed loci. Single molecule studies showed that the replicative helicase, DnaC, frequently stalls and this can be ameliorated by inhibiting transcription with rifampicin (Mangiameli et al. 2017). In *S. cerevisiae*, tRNA genes have been shown to frequently arrest the replisome, and the effect is more severe when aligned HO to origins (Claussin, Vazquez, and Whitehouse 2022; Deshpande and Newlon 1996; Osmundson et al. 2017). In higher eukaryotes, TRCs have been implicated as contributing to genome instability at regions known as common fragile sites (CFSs). CFSs are loci that exhibit an elevated level of DNA gaps and breaks,

recurrently causing chromosome segregation defects (Durkin and Glover 2007). CFSs are enriched with sequences prone to form non-B DNA structures, and are expected to be difficult to replicate. Indeed, mild DNA checkpoint defects are sufficient to induce breaks at CFSs without any additional exogenous replication stress (Casper et al. 2002). CFSs are frequently located within highly transcribed and long genes (Barlow et al. 2013; Helmrich et al. 2006; Wilson et al. 2015), and therefore TRC has been implicated as the underlying trigger for instability. An alternative explanation posits that transcriptional activity limits zones of replication (see above), creating origin-poor regions around CFS; this causes the region to be replicated late in S phase, potentially well into mitosis, an observation known as mitotic DNA synthesis (MiDAS) (Brison et al. 2019; Macheret et al. 2020). It is possible that both mechanisms contribute to genome instability at CFSs.

It is not entirely clear how transcription stalls replication; collision events are likely very heterogeneous in nature, and its outcome and resolution depend on the state the two machineries are in during the encounter. In principle, any DNA-bound protein, including RNAP, transcription factors (TFs) and general transcription factors (GTFs), has the potential to blcok replication, and so are promoter-bound and actively elongating RNAPs. In fact, a recent study suggests the ability of tRNA genes to unidirectionally block replication depends on the asymmetrical binding of TFIIIB, an essential TF, onto the promoter, rather than Pol III per se (Yeung and Smith 2020). Nevertheless, most transcriptional events do not appear to impact replication in any significant way, at least when only the RNAP holoenzyme is concerned. In *in vitro* studies using bacteriophage replication systems such as T4 and ϕ29 phages, the DNA polymerase (DNAP) can co-directionally bypass a transcriptionally competent RNAP from *E. coli* after a brief slowing down (Elías-Arnanz and Salas 1997; Liu et al. 1993; Liu, Wong, and Alberts 1994; Liu and Alberts 1995). In HO collision, the further addition of a replicative helicase permits the T4 DNAP to efficiently bypass *E. coli* RNAP (Liu and Alberts 1995). In these circumstances, the bacterial RNAP remains bound to the DNA and can resume RNA synthesis, using the daughter DNA strand as the new template. In studies using *E. coli* replisomes, however, RNAP

displacement appears to be necessary for the resumption of replication (Pomerantz and O'Donnell 2008, 2010). Here, CO-TRC terminates leading strand synthesis, but surprisingly, after RNAP eviction, replication at the leading strand is resumed using the nascent RNA transcript as a primer (Pomerantz and O'Donnell 2008). In eukaryotes, it is therefore assumed that replisome progression requires RNAP eviction. This suggests premature transcription termination is evitable, but recent studies suggest that RNAP, along with its associated nascent transcript, is held proximal to the replisome and is reloaded rapidly post-replication to resume RNA synthesis (Bruno, Coronel-Guisado, and González-Aguilera 2024; Fenstermaker et al. 2023; Werner and Hamperl 2024). This is done via direct interaction with the constitutive replisome component proliferating cell nuclear antigen (PCNA) (Fenstermaker et al. 2023), a DNA clamp that promotes replication processivity (Bell and Labib 2016). This suggests that in eukaryotes also, the replisome is not necessarily stalled by RNAP, though further study is required to address how frequent such RNAP bypass occurs.

Transcription is a tightly regulated process, and RNAP is frequently paused and stalled within the transcription cycle (Shandilya and Roberts 2012). This can serve as a point of regulation, as exemplified by promoter-proximal pausing, where Pol II is actively held in check by protein factors and requires 'licensing' before entering productive elongation (Core and Adelman 2019; Welsh and Gardini 2023). During elongation, protein obstacles, specific DNA sequences, and DNA lesions also frequently cause RNAP stalling. Stalled RNAP promotes the formation of R-loops – implicated in genome instability (see next section) – by lengthening the time window that nascent RNA can re-anneal to upstream DNA unwound by negative supercoiling. Additionally, stalled RNAP can undergo backtracking, in which the RNAP reverse translocates, displacing the 3' RNA from the active site, leading to RNAP arrest (Noe Gonzalez, Blears, and Svejstrup 2021; Wang et al. 2009).

It is these aberrant states of RNAP that present a greater threat to TRC-induced genome instability. In an *E. coli* plasmid system to study collision *in vivo*, TRC does not lead to DSB formation

unless transcription elongation is further inhibited with a phage protein (Dutta et al. 2011). Backtracked RNAP is resolved by GreA and GreB, homologs of the eukaryotic GTF TFIIS, which act by stimulating RNA cleavage to generate new, re-aligned 3' ends (Nudler 2009). When GreA or GreB is deleted, even CO-TRC leads to DSB formation (Dutta et al. 2011; Tehranchi et al. 2010), highlighting the potency of arrested RNAP in obstructing replisome progression. In mammalian cells too, a dominant-negative TFIIS mutant that stabilizes backtracked Pol II leads to a genome instability phenotype (Sheridan et al. 2019; Zatreanu et al. 2019), and in human cells, the RecQ family DNA helicase RECQL5 has been shown to promote transcription elongation, the absence of which causes Pol II backtracking and leads to replication stress (Saponaro et al. 2014; Urban et al. 2016). Similarly, proper termination of RNAP prevents excessive TRC. In bacteria, transcription termination relies on Rho and accessory factors NusA and NusG (Hao, Svetlov, and Nudler 2021), and defects in this pathway trigger the formation of replication-dependent DSBs (Washburn and Gottesman 2011). Importantly, this phenotype can be suppressed by a mutation in the RNAP which reduces its stability, strongly suggesting that the RNAP enzyme contributes directly to TRC-induced DNA damage. Agreeing with this finding, in *S. cerevisiae*, a Pol II mutant that promotes tighter association with chromatin worsens the genome instability phenotype caused by TRC (Felipe-Abrio et al. 2014). The CTD of Pol II contains multiple tandem repeats of the heptapeptide YSPTSPS, and dynamic post-translational modification of the heptapeptide has been known to regulates the transcription cycle of Pol II (Eick and Geyer 2013). In particular, phosphorylation on serine 5 (pS5) has been associated with promoter-proximally paused Pol II. A study in HeLa cell has found that inhibition of pS5 phosphatases protein phosphatase 1 (PP1), PP1-nuclear targeting subunit (PNUTS), and a PNUTS binding partner WDR82 leads to Pol II stabilization, which triggers replication stress (Landsverk et al. 2020).

In addition to RNAP and its associated factors, transcription also generates topological constraints and alters the chromatin environment that contributes to stalling the replisome. In mammalian cells, siRNA-mediated knockdown of Top1 leads to a global decrease in replication speed

and increase in S-phase DNA breaks, which can be alleviated by inhibiting transcription with cordycepin (Tuduri et al. 2009). In another study, Top1 knockdown has been shown to preferentially induce DSB and γH2A.X at TTSs when a downstream origin is present, potentially triggering HO-TRC (Promonet et al. 2020). Additionally, transcriptional activity drastically modifies the chromatin landscape, in part due to co-transcriptional recruitment of histone modifying enzymes (Henikoff and Shilatifard 2011; Millán-Zambrano et al. 2022). Interestingly, a recent study proposes that co-transcriptionally deposited H3K4 methylation acts as a "molecular speed bump" that slows down the replication fork to reduce the severity of potential TRC at sites of high transcriptional activity (Chong et al. 2020). Nonetheless, it remains to be determined how prevalent co-transcriptional modification of chromatin environment causes replication stress.

1.4.3 R-loops as a source of genome instability

The R-loop is a non-B, three-stranded DNA structure consisting of a DNA:RNA hybrid and a displaced ssDNA (Brickner, Garzon, and Cimprich 2022; Castillo-Guzman and Chédin 2021; García-Muse and Aguilera 2019; Petermann, Lan, and Zou 2022). Some of the most abundant R-loops are generated co-transcriptionally, formed when the nascent RNA re-anneals upstream with the template strand, although evidence exists that during Pol II backtracking, anterior R-loops ahead of the polymerase can form (Zatreanu et al. 2019). Besides forming co-transcriptionally, R-loops or DNA:RNA hybrids can also arise through other means. Another abundant source of DNA:RNA hybrids is the RNA primer generated by the DNA primase at Okazaki fragments during lagging strand synthesis, and are efficiently removed during normal replication (Bell and Labib 2016). Telomeric repeats, despite being characterized by epigenetic modification linked to heterochromatin, are transcribed into lncRNA called telomeric repeat-containing RNA (TERRA) (Toubiana and Selig 2018). TERRA is shown to interact with telomeric proteins and base-pair with the DNA repeats to form R-loops, and is important for proper telomere maintenance. It is believed that telomeric R-loops form *in cis* through co-transcriptional activities, although *in vitro* study shows that telomeric proteins can stimulate TERRA

invasion, suggesting the potential for telomeric R-loops to form *in trans* (Lee et al. 2018). Lastly, sRNA and lncRNA generated at DSB, described in a previous section, are also reported to form DNA:RNA hybrids (Cohen et al. 2018; Francia et al. 2012; Ohle et al. 2016; Wei et al. 2012). Indeed, R-loops forming at DSBs have been proposed as a mechanism to promote RNA-templated DNA repair (Chandramouly et al. 2021; Mazina et al. 2017; McDevitt et al. 2018; Meers et al. 2020).

Given that, at least under physiological conditions, most R-loops are co-transcriptional by-products, their characteristics naturally vary and depend on the condition of the associated RNAP. It has been proposed that Pol II-associated R-loops can be classified into two classes, one that is associated with promoter-proximally paused RNAP, and one with elongating RNAP (Castillo-Guzman and Chédin 2021). In particular, R-loops associated with paused Pol II are predicted to arise more frequently and to be more harmful, given their close association with paused Pol II and associated GTFs. It needs to be emphasized, however, that R-loops by themselves do not necessary cause replication stress; it is their frequent association with pathological transcription intermediates that connects R-loops to genome instability. In fact, *in vitro,* bacterial replisomes easily bypass naked R-loops on either strand (Brüning and Marians 2020). Naked R-loops can temporarily stall the replisome in *S. cerevisiae* (Kumar et al. 2021), but this is likely insufficient to induce DNA breaks, and genetic analyses have uncovered histone mutants that accumulate R-loops but do not display any genome instability phenotype (García-Pichardo et al. 2017). Indeed, physiological R-loops can have beneficial functions, for example guiding transcription factor binding and promoting immunoglobulin class-switching (García-Muse and Aguilera 2019). Nevertheless, DNA:RNA hybrid is thermodynamically more stable than dsDNA (Lesnik and Freier 1995). In this respect, R-loops, once formed, could exacerbate a paused or arrested RNAP, rendering its removal more difficult.

While R-loops can stimulate mutation by exposing one strand of DNA to genotoxic agents, numerous studies strongly suggest that the major mechanism of R-loop-induced genome instability

depends on replication. In *B. subtilis*, R-loops accumulate preferentially at HO-TRC, and are actively removed by RNase HIII (Lang et al. 2017), one of the RNases in the RNase H family that degrades ribonucleotides from DNA:RNA hybrid (Hyjek, Figiel, and Nowotny 2019). Deleting RNase HIII and inducing the expression of a head-on construct (lacZ) trigger cell death, suggesting that R-loop accumulation enhances the severity of TRC events (Lang et al. 2017). In *E. coli* too, inducing transcription of a plasmid-borne mouse Ig gene Sγ3 region, which is prone to R-loop formation, triggers plasmid loss and DDR, which can be alleviated by overexpressing RNase H1 (Gan et al. 2011). In *S. cerevisiae*, defects in the THO/TREX complex lead to a global accumulation of R-loops and an increase in recombination frequency, and can be suppressed by overexpressing RNase H1 (Huertas and Aguilera 2003). Using a direct repeat system described above (Prado and Aguilera 2005), it has also been shown that recombination caused by HO-TRC can be alleviated by overexpressing RNase H1 (García-Rubio et al. 2018). Notably, when Yra1 – a protein that stably binds to DNA:RNA hybrid – is overexpressed instead, recombination frequency is enhanced in both CO- and HO-TRC contexts, highlighting that R-loops by themselves are not necessary recombinogenic, but depend highly on their status and how they are resolved. Consistent with this idea, the genome instability phenotype caused by overexpressing a dominant-negative TFIIS allele in mammalian cells can be suppressed by further overexpressing RNase H1 (Zatreanu et al. 2019).

The importance of limiting excessive R-loop formation can be appreciated by the numerous amount of enzymes dedicated to its removal or prevention (Brickner et al. 2022; Petermann et al. 2022). As described above, topoisomerase plays an essential function in limiting transcription-induced negative supercoiling, which promotes R-loop formation (Drolet 2006). In *E. coli*, *topA* topoisomerase I null mutants fail to produce full-length mRNA, which can be suppressed by overexpressing RNase H (Baaklini et al. 2004). In *S. cerevisiae* too, the topoisomerase 1 and 2 double mutant has been shown to accumulate R-loops at the rDNA loci, and is defective in rRNA synthesis (Hage et al. 2010). The genome instability phenotype in mammalian cells with Top1 knockdown, described above, is also R-

loop-dependent and is suppressible by overexpressing RNase H1 (Promonet et al. 2020; Tuduri et al. 2009).

On top of RNase H, multiple nucleases are also involved in R-loop processing that contribute to both replication-dependent or independent genome instability. This includes XRN2, a 5'-3' exoribonuclease, which is recruited to sites of DNA damage to resolve R-loops (Dang and Morales 2020; Morales et al. 2016; Skourti-Stathaki, Proudfoot, and Gromak 2011), as well as the nuclear exosome, a multi-subunit 3'-5' exoribonuclease (Papadopoulos et al. 2022). Interestingly, certain DNA repair factors such as CTBP-interacting protein (CtIP), and factors involved in TC-NER such as XPF and XPG, are implicated in excising the DNA at R-loops, generating DNA breaks in the process (Goulielmaki et al. 2021; Makharashvili et al. 2018; Sollier et al. 2014; Stork et al. 2016). Whether this actively promotes genome stability by facilitating R-loop resolution, or is a pathological byproduct from sites with prolonged R-loop formation, is uncertain.

Helicases and translocase represent another important class of enzyme that resolve R-loops. In bacteria, helicases such as DinG, UvrD, and Rep genetically interact with RNase H, and resolve replication stress resulting from HO collisions (Boubakri et al. 2010). In humans and yeast, the DNA:RNA helicase Senataxin (SETX in human; Sen1 in yeast) plays a major role in R-loop resolution to limit TRC-induced DNA damage (Alzu et al. 2012; Cohen et al. 2018; Costantino and Koshland 2018; Mischo et al. 2011; Skourti-Stathaki et al. 2011), although Senataxin, as a helicase capable of unwinding not only DNA:RNA hybrid, but also dsDNA and dsRNA (Kim, Choe, and Seo 1999), has also been shown to participate in Pol III termination and replication termination (Choudhary et al. 2023; Rivosecchi et al. 2019). In *S. cerevisiae*, the Pif1 family replicative helicases – Pif1 and Rrm3, on top of transcription-independent general regulation of replication fidelity (Choudhary et al. 2023), promotes replication through various structures and sequences prone to TRC, including rDNA loci (Ivessa, Zhou, and Zakian 2000; Torres, Bessler, and Zakian 2004), highly transcribed euchromatic

regions (Azvolinsky et al. 2009; Felipe-Abrio et al. 2014), as well as G4s and R-loops (Dahan et al. 2018; Kumar et al. 2021; Schauer et al. 2020; Varon et al. 2023). Multiple members of the RecQ family helicase, including Bloom syndrome protein (BLM) and Werner syndrome helicase (WRN), on top of its canonical functions in DNA metabolism (Chu and Hickson 2009), also contribute to R-loop resolution (Chang et al. 2017; Marabitti et al. 2019; Tan et al. 2020). A host of DEAD box RNA-helicases has been found to cause R-loop accumulation and genome instability in their absence, and/or display DNA:RNA hybrid unwinding activity *in vitro* (Yang et al. 2023). Some notable examples include DHX9 (Chakraborty and Grosse 2011; Cristini et al. 2018), DDX5 (Mersaoui et al. 2019; Sessa et al. 2021), and DDX21 (Kim et al. 2020; Song et al. 2017). Finally, several fork remodelers, including SMARCAL1, ZRANB3, and FANCM, have been shown to efficiently zip-up dsDNA, thereby displacing the RNA from DNA:RNA hybrid (Hodson et al. 2022; Pugliese et al. 2019).

In higher eukaryotes, R-loops, especially promoter-proximal ones, frequently reside in GC-rich sequences that are also prone to forming G4s; this G4/DNA:RNA hybrid structure, known as G-loops (Duquette et al. 2004), poses a significant threat to replisome progression as the two structures reinforces the stability of each other (De Magis et al. 2019; Kumar et al. 2021). Therefore, helicases such as regulator of telomere elongation (RTEL) and Fanconi anemia (FA) protein J (FANCJ), appear to limit R-loop-induced genome instability by processing G4 structures (Castillo Bosch et al. 2014; Kotsantis et al. 2020; W. T. C. Lee et al. 2021; Wu, Shin-ya, and Brosh Jr. 2008).

1.4.4 Fork response in face of replication stress

The replication machinery has long been known to respond dynamically to obstacles and cellular stresses (Berti, Cortez, and Lopes 2020; Branzei and Foiani 2010). On top of the leading and lagging strand DNAPs Pol ε and Pol δ respectively, the primase Pol α, as well as the replicative CMG helicase composed of the Mcm2-7 complex, Cdc45, and GINS complex (composed of Sld5, Psf1, Psf2, and Psf3), the replisome also consists of many accessory factors that regulate the activity of the

replisome. One such factor is the fork protection complex (FPC), comprising the heterodimer Tof1 and Csm3 (Swi1 and Swi3 in *S. pombe*; TIMELESS and TIPIN in humans), the checkpoint protein Mrc1 (CLASPIN in human), and the accessory factor Ctf4 (Mcl1 in *S. pombe*, AND-1 in human). FPC serves important regulatory functions in promoting processivity and controlling the speed of replication in face of stress (Errico and Costanzo 2012; Patel and Kim 2023). In *S. cerevisiae* cells lacking Tof1 or Mrc1, and in human cells depleted of TIMELESS, DNA combing shows a global decrease in replication speed (Tourrière et al. 2005; Ünsal-Kaçmaz et al. 2007), suggesting FPC is required for efficient elongation. The underlying mechanism appears to be a dynamic regulation to promote fork stability, rather than merely stimulating replication. For example, Tof1/Csm3 and Swi1/Swi3 are required for stable fork pausing at RFBs, and their absence leads to fork collapse and necessitates fork restart by recombination-dependent replication (RDR, see below) (Calzada et al. 2005; Noguchi et al. 2003, 2004). At a global level, replication slows down in the presence of HU, but disrupting Tof1 and Mrc1 leads to elevated fork velocity despite the underlying stress (Katou et al. 2003).

Intrinsically, the discontinuous nature of lagging strand synthesis permits lesion bypass; but lesion blocking leading strand synthesis generally leads to the uncoupling between the CMG helicase and the DNAPs (Taylor and Yeeles 2018). Here, FPC coordinates the activities of DNA synthesis and parent strand unwinding to limit fork uncoupling. Structurally, the Tof1/Csm3 heterodimer interacts with the Mcm2-7 complex but is ahead of the helicase itself (Baretić et al. 2020; Jones et al. 2021), and *in vitro* it inhibits the ATPase activity of the helicase (Cho et al. 2013). FPC also interacts with Pol ε and stimulates its activity, but this association is dynamic, as determined through single molecule studies (Aria et al. 2013; Lewis et al. 2017). Despite the built-in mechanism, fork uncoupling appears to be fairly common, and very low doses of genotoxic treatment can trigger global fork uncoupling without activating the replication checkpoint (Zellweger et al. 2015). Fork uncoupling entails the accumulation of unreplicated ssDNA, which is rapidly coated by the ssDNA-binding heterotrimer replication protein A (RPA) (Bhat and Cortez 2018); ssDNA-RPA, together with other co-activators

recruited to a stalled fork, in turn activates the replication checkpoint kinase ATR (Mec1 and Rad3 in *S. cerevisiae* and *S. pombe* respectively) (Byun et al. 2005; Saldivar, Cortez, and Cimprich 2017). Once activated, ATR phosphorylates and thereby activates a crucial effector, CHK1 (Rad53 and Cds1 *S. cerevisiae* and *S. pombe* respectively), and together the two kinases trigger global responses such as cell cycle arrest and blocking origin firing. Activated ATR also regulates individual fork behavior by phosphorylating replisome components such as Mcm2-7, FPC, as well as many fork remodeling enzymes (see below) (Errico and Costanzo 2012). This directly affects the recruitment of repair and restart factors to stalled forks, modifying the fork repair pathway choice. In *S. cerevisiae*, *rad53*Δ mutants under genotoxic stress accumulate replication intermediates and have a high level of collapsed forks, indicating defects in fork stabilization (Lopes et al. 2001; Tercero and Diffley 2001).

Fork uncoupling followed by the accumulation of RPA-coated ssDNA appears to be a universal trigger to initiate fork remodeling (Berti et al. 2020; Kondratick, Washington, and Spies 2021; Sale 2012). Depending on the nature of the lesion, the fork can undergo damage bypass, which includes repriming synthesis downstream of the lesion; the error-prone translesion synthesis (TLS) pathway; and the error-free template switching. Replication forks can also undergo fork remodeling and replication restart via a number of homology-dependent repair pathways. In certain cases, the replication fork is cleaved by endonucleases, leading to controlled fork collapse and the broken fork is restarted using HR factors (Conti and Smogorzewska 2020).

Repriming is a lesion bypass pathway that acts via synthesizing a new primer downstream of the lesion. Lesions affecting the lagging strand are efficiently bypassed, due to the inherently discontinuous nature of synthesis. This has been shown *in vitro* for both *E. coli* and *S. cerevisiae* replisomes (McInerney and O'Donnell 2004; Taylor and Yeeles 2018). Using *Xenopus* egg extract, it has also been shown that the primase Pol α is recruited to stalled forks to promote lagging strand bypass (Parrilla-Castellar and Karnitz 2003; Van et al. 2010). Leading strand repriming is also observed, albeit

less inefficient than on the lagging strand. In *E. coli*, leading strand synthesis only transiently stalls when encountering a lesion, and is reinitiated downstream using the canonical DnaG primase (Yeeles and Marians 2011, 2013). In *S. cerevisiae*, the leading strand can be reprimed by Pol α, although this occurs at a low frequency and only at forks stalled by specific lesions (Taylor and Yeeles 2018, 2019). In metazoans, a specialized TLS polymerase with inherent primase activity, PrimPol (Primase/Polymerase), allows fork restart after a leading strand lesion (Tirman et al. 2021).

TLS refers to the use of specialized DNAPs instead of the replicative polymerases to replicate past lesions with a high error rate (Ma, Tang, and Guo 2020; McVey et al. 2016). TLS is triggered by RPA accumulated onto ssDNA, which recruits Rad6/Rad18 to monoubiquitinate PCNA (Davies et al. 2008). This in turn recruits various TLS polymerases via their C-terminal ubiquitin-binding domain (Bienko et al. 2005; Kannouche, Wing, and Lehmann 2004). PrimPol can also mediate TLS, and is recruited noncanonically, in a PCNA-independent way (Tirman et al. 2021). PCNA can also be polyubiquitinated by Rad5, which signals the switch from TLS to template switching, in which the nascent strand bypasses the lesion on one template by jumping onto another DNA strand to continue synthesis. Whether a fork will utilize TLS, template switching before undergoing further fork remodeling events remain poorly understood (Kondratick et al. 2021; Sale 2012).

When bypass mechanisms are not utilized, the uncoupled fork undergoes remodeling and processing to stabilize the stalled fork and to facilitate restart. Critical to this process is the formation of Rad51 filament onto ssDNA. Widely known for its role in HR-based DSB, the evolutionarily ancient protein Rad51 also has genetically separable functions in regulating fork dynamics (Bhat and Cortez 2018; Bonilla et al. 2020; Shinohara et al. 1992). By itself, Rad51 cannot displace RPA, but requires RAD51 mediators: in vertebrates the main RAD51 loader is BRCA2, and Rad52 is the functional equivalent in yeast (Sung 1997:199). A number of accessory factors are involved in fine-tuning the

biochemical activity of Rad51 filament assembly and stability, underscoring its central role in fork remodeling.

One mode of fork remodeling involves the conversion of the replication fork into a four-way junction, known as Holliday junction, by a process called fork reversal. It involves the backward translocation of the fork, re-annealing the two newly synthesized strands. Originally thought of as a pathological by-product of a collapsed fork, fork reversal is now known to be a common physiological response that contributes to DNA damage tolerance (Berti et al. 2020; Neelsen and Lopes 2015; Qiu et al. 2021). Many factors participate in fork reversal. Efficient fork reversal requires RAD51 (Zellweger et al. 2015), but its action is noncanonical, as the process is BRCA2-independent (Mason et al. 2019; Mijic et al. 2017), although once formed, canonical BRCA2-mediated RAD51 filament stabilizes the reversed fork (Bhat and Cortez 2018; Mijic et al. 2017). Disrupting Rad51 accumulation can therefore affect fork reversal. For example, RADX, a metazoan-specific protein, displaces RAD51 and therefore limits fork reversal (Bhat et al. 2018; Dungrawala et al. 2017); similarly, the RecQ family helicase RECQ5 unwinds RAD51 filament to prevent excessive fork reversal (Chappidi et al. 2019). Multiple helicases have been shown to both promote fork reversal and unwind the reversed forks. This includes the RecQ family helicases BLM and WRN (Kanagaraj et al. 2006; Machwe et al. 2006; Machwe, Karale, et al. 2011; Machwe, Lozada, et al. 2011), RAD54 (Bugreev, Rossi, and Mazin 2011), and the SNF2 family chromatin remodeler SMARCAL1 (Bétous et al. 2013; Couch et al. 2013). Interestingly, SMARCAL1 has been shown to have substrate specificity, being recruited to stalled forks via RPA, and promotes fork reversal when the leading strand in blocked, while inhibiting reversal when the lagging strand is blocked instead. Other helicases appear to preferentially promote fork reversal. This includes the UvrD family helicase FBH1 (Fugger et al. 2015); ZRANB3, which is recruited to stalled forks via binding to polyubiquitinated PCNA (Vujanovic et al. 2017); HLTF, which is recruited by binding to the 3'-OH group of leading strand DNA via the HIRAN domain (Achar et al. 2015; Kile et al. 2015); and the FA protein FANCM (Gari, Décaillet, Delannoy, et al. 2008; Gari, Décaillet, Stasiak,

et al. 2008). Finally, the RecQ family helicase RECQ1 appears to strictly unwind the reversed fork, and DNA2 mediates end cleavage of the reversed fork to promote its resolution (Berti et al. 2013; Hu et al. 2012; Thangavel et al. 2015). These helicases and nucleases have different binding affinity to various replication intermediates, but exactly how they are coordinated and selected remains poorly understood.

Fork reversal is thought to promote genome stability in multiple ways (Bhat and Cortez 2018; Thakar and Moldovan 2021). First, it slows down and stabilizes the replication fork, allowing time for repair or for replication to be completed from a nearby converging fork. However, the regressed arm is known to be susceptible to various nucleases, and factors such as RAD51/BRCA2, as well as the end-joining factor Ku are recruited to promote fork stability by limiting resection (Teixeira-Silva et al. 2017). Second, fork reversal places the lesion back into duplex DNA, allowing excision repair. Third, in cases where the lesion occurs on only one strand, fork reversal provides an undamaged template from a nascent strand to another, allowing bypass synthesis. Finally, structure-specific endonucleases such as MUS81/EME1, MUS81/EME2, SLX1/SLX4 can promote fork incision, allowing for repair by RDR (Neelsen and Lopes 2015; Wyatt and West 2014).

Regardless of whether the stalled fork is reversed or not, replication fork restart mechanisms allow resumption of DNA synthesis once the stress is removed. As described above, helicases such as RECQ1 can catalyze branch migration, converting the reversed fork back to a three-way junction. Nucleases such as WRN and DNA2 can process the regressed arm into canonical fork structure. Additionally, reversed forks can be restarted in a HR-dependent way, in which controlled resection of the regressed arm allows for the formation of Rad51 filament, which allows for strand invasion ahead of the Holliday junction (Ait Saada et al. 2018; Chakraborty, Schirmeisen, and Lambert 2023).

1.4.5 Mechanisms and responses to TRC

Naked R-loops can be bypassed in both CD- and HO-TRCs. Whereas naked R-loops in HO-TRC are bypassed by the lagging strand, they are translocated by the CMG helicase in CO-TRCs, and can be efficiently bypassed with Pol α repriming synthesis with the R-loop as primer. If the 5'-end of the R-loop is not annealed, the helicase can unwind the DNA:RNA hybrid, releasing the RNA in the process (Kumar et al. 2021). When the R-loop is associated with a RNAP – as is expected in most physiological conditions – the outcome is less clear. RNAP engages both strands of DNA during transcription (Barnes et al. 2015; Osman and Cramer 2020), necessitating alternative restart mechanisms. Nevertheless, PrimPol has been shown to facilitate leading strand bypass of HO-TRC in a $(GAA)_n$ region prone to R-loop and G4 formation (Šviković et al. 2019). The CMG helicase can also bypass protein-DNA crosslink (Sparks et al. 2019), suggesting the possibility of replication bypass of RNAP. Extensive fork remodeling has also been implicated in TRC. In one study using human cells, replication fork restart after R-loop-induced stalling is shown to be partly dependent on fork reversal factors RECQ5 and the fork incision enzyme MUS81/EME1, suggesting fork reversal and cleavage as one of the responses to TRC (Chappidi et al. 2019). Such activity appears to be tightly regulated, as TRC-triggered fork reversal and MUS81 activity can activate ATR, which in turn inhibits MUS81, limiting excessive fork cleavage (Matos et al. 2019).

As mentioned in the previous section, the stability of RNAP directly influences its potential to induce replication stress, and a number of factors are involved in resolving stalled RNAP and associated R-loops. In the case of TRC, replication stress response has been shown to actively influence RNAP stability, facilitating conflict resolution. In bacteria, UvrD and Rep, the accessory helicases that associate with the replisome, can remove stalled RNAP, facilitating replisome progression (Hawkins et al. 2019). In eukaryotes too, same replicative factors have dual functions in transcriptional regulation. ATAD5 is a PCNA unloader to facilitate replisome removal after replication completion, and is also responsible for PCNA de-ubiquitination during DDR, finetuning downstream process triggered by

PCNA post-translational modification (K. Lee et al. 2012). Curiously, ATAD5 has also been shown to interact with RNA helicases implicated in R-loop resolution, such as DHX9, DDX5, DDX21 (Kim et al. 2020). Recently, observations in human cells suggest Pol II also signals its removal on encountering a replication fork. In particular, active Pol II recruits TRIM28, an E3 ligase that mediates PCNA SUMOylation, which is recognized by chromatin remodelers such as FACT, and is therefore hypothesized to facilitate Pol II removal (Li et al. 2018, 2020).

ATR signaling has also been implicated in promoting Pol II removal. In yeast, Mec1 physically interacts with the transcription regulators PAF1 complex (PAF1C) and histone remodeler INO80 complex; phosphorylation of PAF1C is required for efficient Pol II removal in the presence of HU stress to promote replication (Poli et al. 2016). Agreeing with this, INO80 co-localizes with R-loop and participates in limiting R-loop-induced replication stress (Prendergast et al. 2020). A recent study also provides evidence that Mec1 signaling facilitates Pol III eviction to limit replication stress (Hurst et al. 2021).

In summary, despite our understanding of the potential of transcription to cause genome instability, and the fork response to replication stress, exactly how the two machineries respond to their encounter remain poorly understood. Further research is required into elucidating the factors influencing fork respond pathway choice in face of the transcription machinery, and the rules governing whether the RNAP is bypassed or removed.

1.5 Exploring the role of RNAi in limiting transcription-replication stress

RNAi has a well-documented chromatin function in transcription regulation. As described above, nuclear Argonautes of both *S. pombe* (Ago1) and plants (AGO4/6 in *A. thaliana*) are loaded with siRNA to target nascent transcripts and mediate CTGS and RdDM respectively (Martienssen and Moazed 2015; Wendte and Pikaard 2017). In mouse, *C. elegans*, and *D. melanogaster*, certain PIWI

proteins also mediate TGS via targeting nascent RNA through their associated piRNAs (Onishi, Yamanaka, and Siomi 2021; Ozata et al. 2019).

Accumulating evidence suggests that RNAi, beyond acting on silent heterochromatin, can also be targeted to euchromatic regions, sometimes via a noncanonical, sRNA-independent mechanism (Nazer, Gómez Acuña, and Kornblihtt 2022). In *D. melanogaster*, one study has shown the AGO2-DCR2 complex interacts with promoter-proximally paused Pol II and negative elongation factor (NELF) to repress the expression of heat-shock-induced genes, and the recruitment appears to depend on sRNA mapping to the antisense strand (Cernilogar et al. 2011). In another study, also in *D. melanogaster*, AGO1 has been shown to physically interact with Pol II, as well as with the Mediator complex (Zaytseva et al. 2020) – a large, multi-subunit transcriptional co-activator (Soutourina 2018) – and to act as a transcriptional repressor of the growth factor Myc. In *A. thaliana*, AGO1 binds to TSSs and TTSs in a sRNA-dependent manner, and acts as a transcriptional co-activator (Liu et al. 2018). As described above, the same was observed for *D. melanogaster*, where AGO2 localized to actively paused genes, and was proposed to fine tune transcription elongation in coordination with NELF (Cernilogar et al. 2011; Nazer, Dale, Chinen, et al. 2018; Nazer, Dale, Palmer, et al. 2018). In mammalian cells too, human AGO2 was proposed to be recruited via promoter-derived RNA to promote transcription (Matsui et al. 2013). Therefore, there is evidence for Argonaute acting as both a transcriptional activator and repressor, and via sRNA-dependent and independent ways. The exact mechanism of its recruitment is unclear, and likely differs among species, although DNA:RNA hybrids – which is abundant in promoter with a paused RNAP (see above) – have been proposed as the binding site for Argonautes (Nazer et al. 2022).

Dicer has also been shown to interact with euchromatic transcriptional processes. As mentioned above, *D. melanogaster* DCR2 interacts with AGO2 at promoters (Cernilogar et al. 2011); human DICER too, interacts with Pol II and chromatin, and immunoprecipitation-mass spectrometry (IP-MS)

indicates that nuclear phosphorylated DICER interacts with many general transcription factors including Mediator (Reyes-Castro et al. 2023; White et al. 2014). Recently, DICER has been shown to bind and cleave R-loops, and has also been implicated in binding to Pol II transcription termination paused sites (Camino et al. 2023; Hatchi et al. 2021). In particular, DICER, AGO1, and AGO2 are involved in the generation of a population of sRNA called single-stranded, DNA-damage-associated sRNA (sdRNA) at the site of Pol II pausing. Knocking down either factors leads to accumulation of ssDNA breaks accumulate that can be rescued by transfecting a sequence-specific sdRNA (Hatchi et al. 2021). In mESCs lacking Dicer, the chromosome segregation defect can be suppressed by mutating BRD4 (Gutbrod et al. 2022), which, limits R-loop-induced TRC by facilitating efficient transcription elongation (Edwards et al. 2020; Lam et al. 2020). This suggests that Dicer, too, has a role in transcription regulation, potentially at paused sites where R-loops accumulate.

RNAi occurs in S-phase to promote epigenetic inheritance, suggesting the need to coordinate with replication in space and time (Kloc et al. 2008; Li, Martienssen, and Cande 2011), and Dcr1 helps to terminate transcription at rDNA, tRNA genes, as well as highly transcribed Pol II transcripts to limit replication stress (Castel et al. 2014; Zaratiegui et al. 2011). In the absence of Dcr1, persistent DNA damage is observed, and cells progressively lose rDNA copies. We therefore set out to use *S. pombe* to further dissect the consequences to transcription and replication in the absence of Dcr1. We discovered that Dcr1 regulates Pol II pausing at the promoter, engaging Ago1 and sRNA, and in doing so limits mis-regulation of transcription elongation, which induces replication stress. The process is dependent on R-loops, and the role of Dcr1 becomes more important when R-loops accumulate in RNase H-deficient cells. An intact, fully functional Dcr1 is important for this function, but we found that the helicase domain plays a prominent role to genome stability, attributing a novel function to this domain. In the absence of Dcr1, DNA damage accumulates around TSS, and replication progresses slower when encountering transcription head-on. Replication forks also stall more frequently, necessitating the use

of recombination-dependent fork restart pathway. We hypothesize Dcr1 acts as a functional equivalent to the Integrator complex, which terminates pathological, paused Pol II in higher eukaryotes.

Chapter 2: Materials and methods

2.1 Yeast strains and culture

All strains used in this study are detailed in Table S1. All cultures were grown at 30°C in standard media with supplement (YES). Knockout mutants were generated following lithium-acetate transformation protocol (Murray, Watson, and Carr 2016) with cassettes generated using primers listed in Table S2. Higher order mutants were either generated by further direct transformation or by crosses on ME plates. For spot assays, mid-log phase cells were harvested and spotted with 10-fold serial dilutions. Cells were let grown for 3 – 5 days at 30 °C before being photographed. For doubling time analyses, overnight cultures were diluted and let grown into early log phase, before O.D. measurements were taken every ~60 minutes. Doubling time was estimated by fitting the data with an exponential curve using a simple R script. G_0 survival assay was performed by Benjamin Roche as previously described (Roche, Arcangioli, and Martienssen 2016).

2.2 Purification of Dcr1

Dcr1 purification was performed by Sonali Bhattacharjee. FLAG-Dcr1 strain was tested for functional silencing. 5 L of YES medium was inoculated with 10 – 15 mL of saturated overnight culture and grown to O.D. of 1 – 1.5. Cells were spun at room temperature and washed with distilled water and frozen for storage at -80 ˚C. The cell pellet was then resuspended in equal volumes lysis buffer (50 mM HEPES (pH 7.6), 300 mM potassium acetate, 5 mM magnesium acetate, 20 mM β-glycerol phosphate, 1 mM EGTA, 1 mM EDTA, 0.1% (v/v) NP-40) containing protease inhibitors. The suspension was aliquoted into 500 µL fractions in microcentrifuge tubes to which an equal amount of acid washed glass beads was added. The cells were disrupted in a FastPrep machine (4 rounds of disruption at 6 m/s). The cell lysate was then spun at 14,000 rpm for 15 min at 4 °C. The supernatant was transferred to a 50 mL Falcon tube and incubated with 500 µL of pre-washed anti-Flag-M2 agarose (Sigma) for 2 - 3 hrs at 4 °C. The beads and immobilized proteins were harvested by centrifugation at 500 × g, loaded on a Bio-

Rad Polyprep column and washed three times with 10 ml lysis buffer minus proteases. Bound protein was eluted with 3 × 500 µL fractions with the same buffer containing 0.2 mg/mL 3 × Flag peptide (Sigma).

2.3 Electrophoretic mobility shift assay

EMSA assays were performed by Sonali Bhattacharjee. Reaction mixtures (20 µL) consisted of 0.5 nM labelled synthetic nucleic acid substrate (Table S3) in Binding Buffer (50 mM Tris-HCl, pH 8.0, 1 mM DTT, 100 µg/mL BSA, 6% v/v glycerol). Reactions were started by adding proteins as indicated and held on ice for 15 min. The reaction mixtures were then loaded onto a pre-equilibrated 4 % native polyacrylamide gel in low ionic strength buffer (6.7 mM Tris-HCl pH 8.0), 3.3 mM sodium acetate, 2 mM EDTA pH 8.0). Samples were run in the gels at 200 V for 90 min with continuous buffer recirculation throughout. For all experiments, both buffer and gel were pre-cooled at 4 °C, and electrophoresis was done at room temperature. Gels were dried on 3 MM Whatman paper and exposed to phosphorimager screens overnight. Exposed screens were scanned using a Fuji FLA-3000 PhosphorImager. All the quantification was done with ImageQuant software (Fuji ImageGauge). All assays were repeated three times to ensure reproducibility.

2.4 Microscale thermophoresis

MST experiment was performed by Sonali Bhattacharjee. The sequences of oligonucleotides used are listed in table S3. DNA was labeled using the 5' EndTag nucleic acid labeling system (Vector laboratories, MB-9001), with Alexa Fluor^{TM} 647 C_2 Maleimide (ThermoFisher, A20347). DNA:RNA hybrid was annealed in a 20 µL reaction consisting of 125 ng of labeled DNA, an equimolar amount of RNA, 1.2 µL of 5M NaCl, and 16.8 µL 1M TE pH 7.0. 500 pM of DNA:RNA hybrid and 500 nM of Dicer was used for MST using the Monolith NT.1155 pico machine.

2.5 PRO-seq

PRO-seq libraries were performed as described (Judd et al. 2020), except cell permeabilization, run-on, and RNA extraction were performed following Mahat et al. 2016 to adapt for yeast cells. Briefly, cells were permeabilized and run-on was performed with 2-biotin, omitting biotin-11-ATP and biotin-11-GTP. Total RNA was extracted using hot phenol approach as described (Mahat et al. 2016). The RNA was base hydrolyzed and excess unincorporated biotin-NTPs were removed before undergoing on-bead library prep as detailed in Judd et al. 2020. The libraries were sequenced on Illumina NextSeq platform. Reads were processed and filtered using fastp (Chen et al. 2018), mapped with Bowtie2 (Langmead and Salzberg 2012), and clipped to the 5' position using Bedtools (Quinlan and Hall 2010) to map the position of Pol II at nucleotide resolution. The resulting BedGraph file was normalized by the total amount of reads and converted to BigWig format before being analyzed on R using custom scripts. Pausing indices (PIs) and termination indices (CIs) were calculated as previously described (Booth et al. 2016) – PI was defined as the ratio between the number of reads from annotated TSS to +150 bp, and the number of reads from the +250 bp to annotated TTS, and for CI, it was defined as written in Booth *et al.*, 2016, "the ratio of the highest density 100 bp window within 500 bp downstream from the CPS to the gene body". The window was first identified in WT, and the same window was used for other mutants.

2.6 RT-qPCR and RNA-seq

Total RNA was purified from mid-log phase cells using Direct-zol RNA Miniprep Kit (Zymo Research) following manufacturer's instructions, including the use of ZR BashingBead Lysis Tubes to lyse open the cells in TRI Reagent. DNA was removed using DNase I (Zymo Research) and purified using RNA Clean & Concentrator (Zymo Research).

For RT-qPCR, cDNA was generated from 1 µg of total RNA using SuperScript IV Reverse Transcriptase (Invitrogen 18090010) and random hexamer following the manufacturer's instruction.

The cDNA was diluted 1:20 and 2 µL of diluted cDNA was used per reaction. PowerUp SYBR Green Master Mix (Applied Biosystems) was used and measurements were taken using QuantStudio 5 or 6 machines (Applied Biosystems). The runs were analyzed with the ΔΔCt method, with *Act1* as control.

For RNA-seq, Ribosomal RNAs were depleted using RiboMinus Transcriptome Isolation Kit, Yeast (Invitrogen), and libraries were made using NEBNext Ultra II Directional RNA Library Prep Kit (NEB). The barcoded multiplex libraries were pooled and sequenced on Illumina NextSeq platform. The reads were trimmed using cutadapt (Martin 2011) and quantified using Salmon (Patro et al. 2017), using transcriptome annotation data from PomBase. Downstream data analyses were performed on R using custom scripts and with DESeq2 (Love, Huber, and Anders 2014).

2.7 sRNA-seq

Total RNA was purified as described above, and libraries were prepared using NextFlex Small RNA-seq v3 Kits (PerkinElmer) and sequenced on NextSeq Illumina platform. Reads were first filtered and trimmed using fastp (Chen et al. 2018). Duplicated reads and reads smaller than 20 nt or larger than 70 nt were discarded. Reads were mapped mapped to the *S. pombe* genome using Bowtie2 (Langmead and Salzberg 2012), and normalized to RPM before analysis using custom R scripts.

2.8 Suppressor screen

EMS mutagenesis was carried out as previously described (Winston 2008). Briefly, 1 x 10^9 the triple mutant yeast cells were harvested at mid-log phase, washed with sterile water and resuspended in 1.5 ml of 0.1 M sodium phosphate buffer (pH 7.0) and treated with 50 µL of EMS (Sigma M0880) for 1 h, 30 °C. 0.2 mL of treated cells was moved to 8 mL of sterile 5% sodium thiosulfate to inactivate the EMS. Cells were washed, resuspended in sterile water and plated on YES plate supplemented with 5 mM HU. Single colonies were allowed to recover on YES plate before re-streaking to HU plates to

verify suppression. For whole-genome sequencing, genomic DNA was purified using Quick-DNA Fungal/Bacterial Kits (ZymoResearch). DNA library was constructed NebNext Ultra II DNA Library Prep Kit for Illumina (NEB E7645). Barcoded DNA library was sequenced using Illumina NextSeq500 Paired-End 76 bp and analyzed as previously described (Roche et al. 2016). Briefly, reads were adapter-trimmed and quality-filtered using Sickle (paired-end mode), then mapped to the *S. pombe* genome using Bowtie2 (Langmead and Salzberg 2012). Duplicate reads were removed using Samtools, and SNPs were called using FreeBayes to find SNPs present in suppressor strain but absent in the parental strain (Garrison and Marth 2012).

Ten suppressors were isolated that conferred resistance to CPT (Fig. 2.1a-b, Table 1). Suppressor #1 (LS03) carried a mutation in the *top1* allele (*top1-W647**), truncating the C-terminal domain of Top1, which contains the catalytic tyrosine residue that forms transient covalent linkage with DNA, and that which is stabilized by CPT (Redinbo et al. 1998). Re-introduction of this allele indeed rendered every strain CPT-insensitive, but had little effect on TBZ or HU sensitivity (Fig. 2.1c). The result validated the specificity of the EMS screen. Examining the rest of the suppressors, we found multiple alleles involved in transcriptional processes and decided to focus on them. One allele, *paf1-D65N*, was found in the suppressor #6 (LS08), mutated the key subunit of the Paf1 complex (Paf1C) which plays a key role in Pol II initiation, elongation, and termination (Chen et al. 2015; Jaehning 2010). The mutation is a cancer-associated mutation in the COSMIC database, and is shown to disrupt a highly conserved residue critical for stabilizing the interaction between Paf1 and Ctr9, another Paf1C subunit (Xie et al. 2018). We therefore tested this allele by re-introducing the allele to fresh mutants, but we did not observe the allele conferring any CPT resistance (Fig. 2.1d). In *S. pombe*, the Paf1C is shown to inhibit spurious sRNA-based heterochromatin formation (Kowalik et al. 2015), either from sRNA produced from an artificially introduced hairpin, or from Dcr1-independent sRNA, referred to as primal RNA (priRNA) (Halic and Moazed 2010), which appears to be degradation product of highly transcribed genes. In Paf1C mutants, ectopic heterochromatin islands indeed formed stochastically

(Kowalik et al. 2015). Therefore, the original suppressor might have gained CPT resistance via random disruption of gene expression, which would explain why such suppression was not observed in freshly introduced strains, although we did not rule out that the suppression was caused by other alleles in the original suppressor.

Two additional alleles were tested, and they also failed to suppress the triple mutant beyond the original suppressor. One was *clr2-T497N*, mutating the a subunit of the SHREC silencing complex (Sugiyama et al. 2007), and its re-introduction to various mutants failed to confer CPT resistance (Fig. 2.1e). Another was *prl53*, which was recovered in 2 out of 10 suppressors (Table 1). *Prl53* was annotated as a highly transcribed lncRNA on PomBase, though it completely overlaps co-directionally with a short protein-coding gene, SPAC27E2.11c, raising the possibility that it could be a mis-annotated, bona fide protein-coding gene. We performed reverse transcription followed by PCR (RT-PCR) and found that *prl53* and SPAC27E2.11c were distinct transcripts (Fig. 2.1f); *prl53* was therefore likely a legitimate lncRNA. Nevertheless, we backcrossed LS11 to the triple mutant and the presence of the *prl53* SNP (chr1:4009719 T->C) did not correlate with CPT resistance (Fig. 2.1g-h). The reason for the inefficiency in obtaining genuine CPT suppressors was unclear, although it could be that metabolic genes were preferentially selected than genuine transcriptional regulator, as many suppressors also carried alleles mutating metabolic genes.

The EMS screen for HU-resistance was performed similar to the CPT screen (Fig. 2.2a). The screen yielded multiple mutants affecting core transcription process, which is described in section 3.4. We also isolated and verified two "bypass" suppressors. The first allele, isolated in LS15, was *epl1-T449A*, a subunit of the NuA4 acetyltransferase complex. NuA4 complex acetylates histone H4, and plays critical functions in transcription regulation as well as nucleotide excision repair (NER) (Hodges, Plummer, and Wyrick 2019; Xu et al. 2016). In the case of H4 acetylation, global H4 acetylation is mediated by the Piccolo subcomplex comprising the catalytic subunit Esa1 together with Eaf6, Yng2,

and the N-terminus of Epl1 (Hodges et al. 2019). However, we found that *epl1-T449A* was able to suppress specifically the HU sensitivity of *dcr1*Δ single mutant at 5mM (Fig. 2.2b), without noticeable effect in the *rnh1*Δ *rnh201*Δ double mutant nor the triple mutant. *Epl1-T449A* was also able to suppress the CPT sensitivity of *dcr1*Δ alone, suggesting a function other than in R-loop processing. In the suppressor LS27, only one SNP was called from WGS data, which led to *pof1-S449C*. This was verified by backcrossing and checking whether HU resistance was correlated with the presence of the SNP (Fig. 2.2c). Pof1 is a F-box protein that has been shown to downregulate Zip1, a transcription factor that is activated in response to abiotic stress (Harrison et al. 2005); the HU resistance could then be explained by general up-regulation of stress-resistance gene, especially since prolonged HU exposure is known to induce the formation of reactive oxygen species (ROS) (Singh and Xu 2016).

In partaking the genetic analyses throughout this project, additional phenotypes of *dcr1* – namely CHX and cold sensitivity – were revealed, especially when under certain genetic conditions. As genes related to translation were up-regulated in the triple mutant (see Section 3.5), a hypothesis explaining the sickness in the triple mutant was growth mis-regulation; this prompted us into testing whether CHX, a translation inhibitor, and whether slowing down growth at low temperature would have effects in the mutants. We did not find suppression by growing the triple mutant under low temperature, and *dcr1*Δ displayed mild CHX sensitivity (Fig. 2.3a). Unexpectedly, we observed the presence of suppressor alleles affecting transcription enhanced the sensitivities of *dcr1*Δ to these conditions. Both *rpb1-T481K* and *tfa2-L238** negatively interacted with *dcr1*Δ in the presence of CHX (Fig. 2.3a-b). The effect for *rpb1-T481K* was specific to *dcr1*Δ, whereas *tfa2-L238** also had a mild interaction with *rnh1*Δ *rnh201*Δ. Additionally, in the *tfa2-L238** background, *dcr1*Δ and *rnh1*Δ *rnh201*Δ both had a cold sensitivity phenotype (Fig. 2.3a).

We also discovered that the helicase domain of Dcr1 was involved in the novel phenotypes, that which also supported *dcr1-K38A* being a dominant allele (see Section 4.3). *dcr1*Δ was able to

suppress the CHX sensitivity of *med20*Δ, but this was not the case for *dcr1-K38R* nor *dcr1-K38A* (Fig. 2.3c), and in fact, the *dcr1-K38A* single mutant was hypersensitive to CHX. Finally, only *dcr1-K38A*, but not *dcr1-K38R* nor *dcr1*Δ, failed to grow at a lower temperature (Fig. 2.3c).

Table 1. EMS suppressor screen for CPT-resistance. Causative SNP for LS03 was verified by reintroduction into the triple mutant. When the causative SNPs were not verified, the most likely SNP(s) among the candidates were highlighted.

Suppressor	Causative SNP	Candidate SNPs	Other SNPs
LS03	**Top1-W647***	-	chr1:5337536 G->C (smc5); chr2:3325781 C->G (dca7); chr3:113406 G->C (mug135)
LS04	-	**Ubr1-T1371K**	chr1:3791335 A->T (emc5); chr2:3370202 T->A (rrn6); chr3:1199092 A->G (fah2)
LS05	-	**Swr1-L461F**	chr1:1315009 C->T (tRNA); chr2:38471 G->A; chr2:878995 G->A (adl1); chr2:2139752 G->A (mtd1); chr2:2398878 G->A (gcn2); chr2:3703878 G->A (utp4); chr2:3752032 G->A (smp2); chr2:4227429 C->T (trp4)
LS06	-	**Rad24-D209Y**	chr1:5512081 G->T (SPAC869.04); chr2:2368572 C->G (nep2/ulp1); chr2:2890520 A->G (SPNCRNA.1560); chr3:2072136 T->C (tRNA)
LS07	-	-	chr1:3367019 G->C (SPAC26A3.14c); chr2:237545 C->T (atg2); chr2:1562541 A->G (ask1); chr2:3280993 A->C (trs1); chr2:4256817 A->G (SPBC1652.02); chr2:4328161 T->C (vps1302)
LS08	-	**Paf1-D65N**	chr1:1578113 T->G; chr1:2742566 C->A (rax2); chr1:5434616 T->C (pgt1)
LS09	-	**Prl53 (chr1:4009432 C->G)**	chr1:2854937 C->T (dph3); chr2:2887599 A->T; chr3:67231 G->C
LS10	-	**Clr2-T497N**	chr1:745633 A->C (ura1); chr1:4856951 A->C (mpd2)
LS11	-	**Prl53 (chr1:4009719 T->C)**	chr1:1449292 T->C
LS12	-	-	chr2:2824997 G->A (cyr1); chr3:572789 G->A (asp1); chr3:1645153 A->G (osr1)

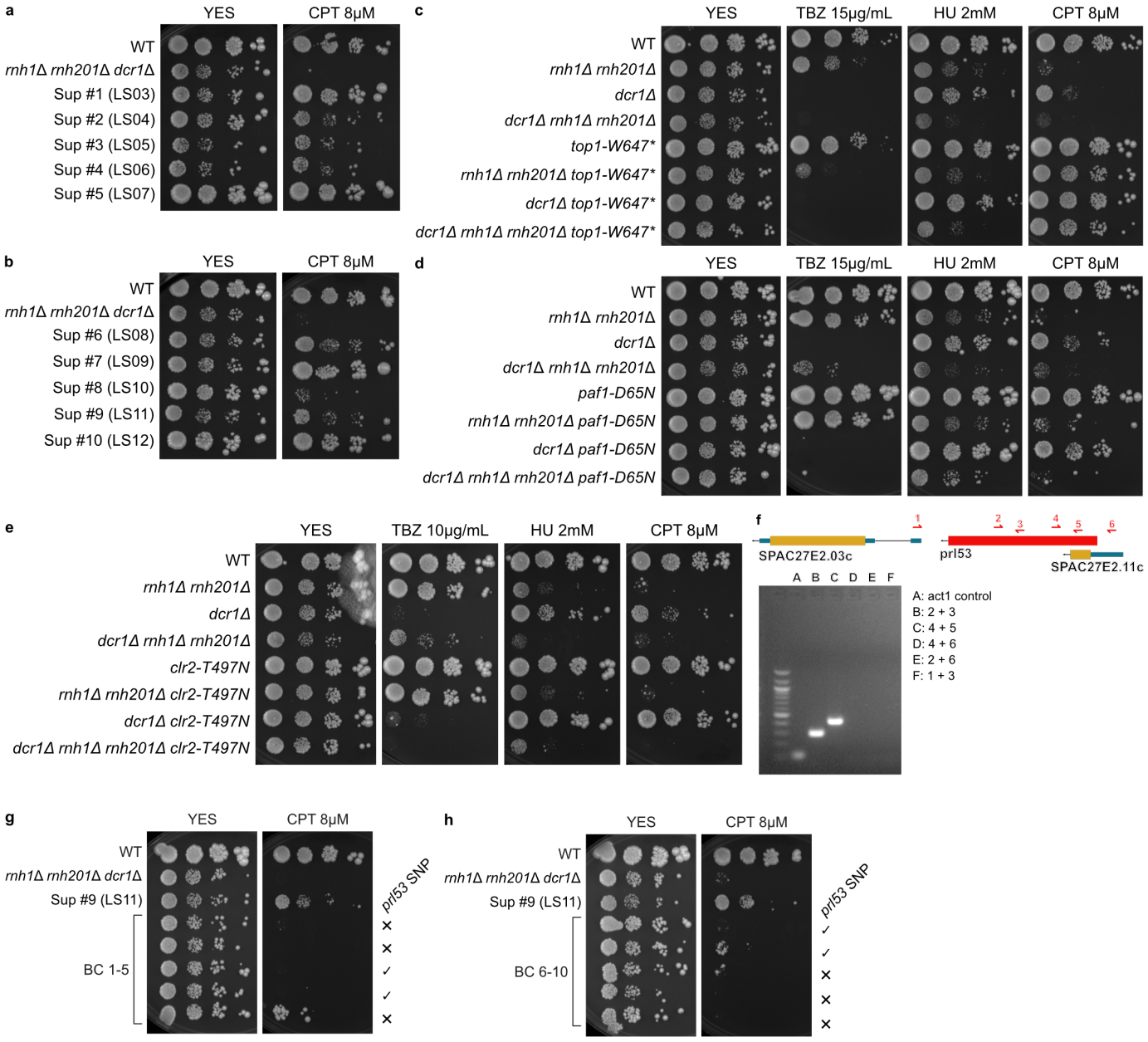
a
YES
CPT 8μM
WT
rnh1Δ rnh201Δ dcr1Δ
Sup #1 (LS03)
Sup #2 (LS04)
Sup #3 (LS05)
Sup #4 (LS06)
Sup #5 (LS07)
b
YES
CPT 8μM
WT
rnh1Δ rnh201Δ dcr1Δ
Sup #6 (LS08)
Sup #7 (LS09)
Sup #8 (LS10)
Sup #9 (LS11)
Sup #10 (LS12)
c
YES
TBZ 15μg/mL
HU 2mM
CPT 8μM
WT
rnh1Δ rnh201Δ
dcr1Δ
dcr1Δ rnh1Δ rnh201Δ
top1-W647*
rnh1Δ rnh201Δ top1-W647*
dcr1Δ top1-W647*
dcr1Δ rnh1Δ rnh201Δ top1-W647*
d
YES
TBZ 15μg/mL
HU 2mM
CPT 8μM
WT
rnh1Δ rnh201Δ
dcr1Δ
dcr1Δ rnh1Δ rnh201Δ
paf1-D65N
rnh1Δ rnh201Δ paf1-D65N
dcr1Δ paf1-D65N
dcr1Δ rnh1Δ rnh201Δ paf1-D65N
e
YES
TBZ 10μg/mL
HU 2mM
CPT 8μM
WT
rnh1Δ rnh201Δ
dcr1Δ
dcr1Δ rnh1Δ rnh201Δ
clr2-T497N
rnh1Δ rnh201Δ clr2-T497N
dcr1Δ clr2-T497N
dcr1Δ rnh1Δ rnh201Δ clr2-T497N
f
SPAC27E2.03c
prl53
SPAC27E2.11c
A B C D E F
A: act1 control
B: 2 + 3
C: 4 + 5
D: 4 + 6
E: 2 + 6
F: 1 + 3
g
YES
CPT 8μM
WT
rnh1Δ rnh201Δ dcr1Δ
Sup #9 (LS11)
BC 1-5
prl53 SNP
× × ✓ ✓ ×
h
YES
CPT 8μM
WT
rnh1Δ rnh201Δ dcr1Δ
Sup #9 (LS11)
BC 6-10
prl53 SNP
✓ ✓ × × ×

Figure 2.1. Triple mutant suppressor screen on CPT resistance.

(a,b) Spot assay of WT, the triple mutant *dcr1*Δ *rnh1*Δ *rnh201*Δ, and suppressors (a) #1-5 and (b) #6-10 resulting from an EMS mutagenesis screen. Cells were spotted with 10-fold dilution on YES plates without supplement or with CPT.

(c) Spot assay verification of one allele isolated, *top1-W647**, from the suppressor LS03.

(d,e) Spot assay verification of (d) *paf1-D65N* and (e) *clr2-T497N* from the suppressor LS08 and LS10, respectively.

(f) RT-PCR analysis of the *prl53* locus. Top: schematic of the *prl53* locus, highlighting annotated transcripts upstream and downstream. Graphics modified from PomBase. Red arrows indicate the primer used for PCR. Bottom: RT-PCR results showing the lack of amplification on lane D-F, suggesting *prl53* being a genuine lncRNA.

(g,h) Backcross analysis of LS11, carrying the *prl53* SNP (Chr1:4009432 C→G), showing the lack of correlation of CPT resistance to the presence of the SNP. SNPs in backcrosses (BC) were tested using dCAPs (see methods).

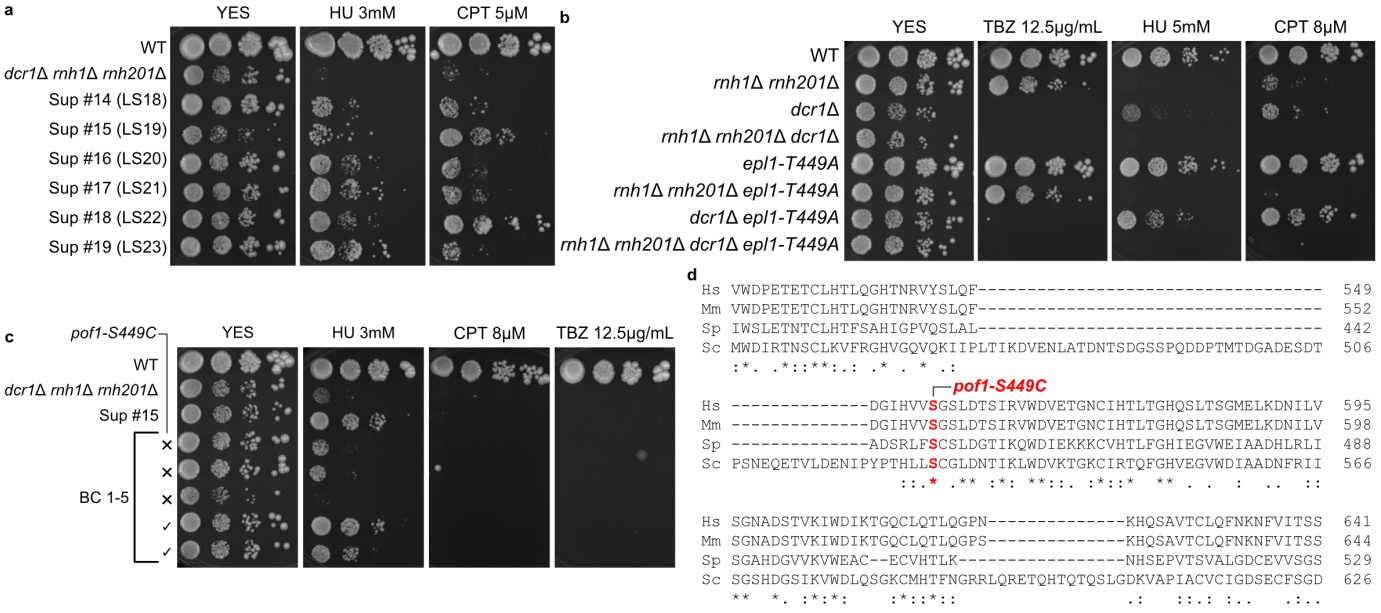

Figure 2.2. Verification of *epl1-T449A* and *pof1-S449C* from the HU suppressor screen.

(a) Representative spot assay of HU-resistant suppressors verification. WT, the triple mutant *dcr1*Δ *rnh1*Δ *rnh201*Δ, and HU-resistant colonies were spotted with 10-fold dilution on YES plates without supplement or with HU or CPT.

(b) Spot assay verification of *epl1-T449A* and from the suppressor LS15. Cells were plated with 10-fold dilution on YES plates without supplement or with TBZ, HU, or CPT.

(c) Backcross verification of LS27, carrying the *pof1-S449C*, showing the correlation of HU resistance to the presence of the SNP. Cells were plated with 10-fold dilution on YES plates without supplement or with TPZ, HU, or CPT. SNPs in backcrosses (BC) were tested using dCAPs (see methods).

(d) Sequence alignment of a select region of *pof1* from *Saccharomyces cerevisiae* (Sc), *S. pombe* (Sp), *Homo sapiens* (Hs), and *Mus musculus* (Mm). Alignment was done using Clustal Omega with default setting. *Pof1-S449* is highlighted in red, showing conservation among multiple species.

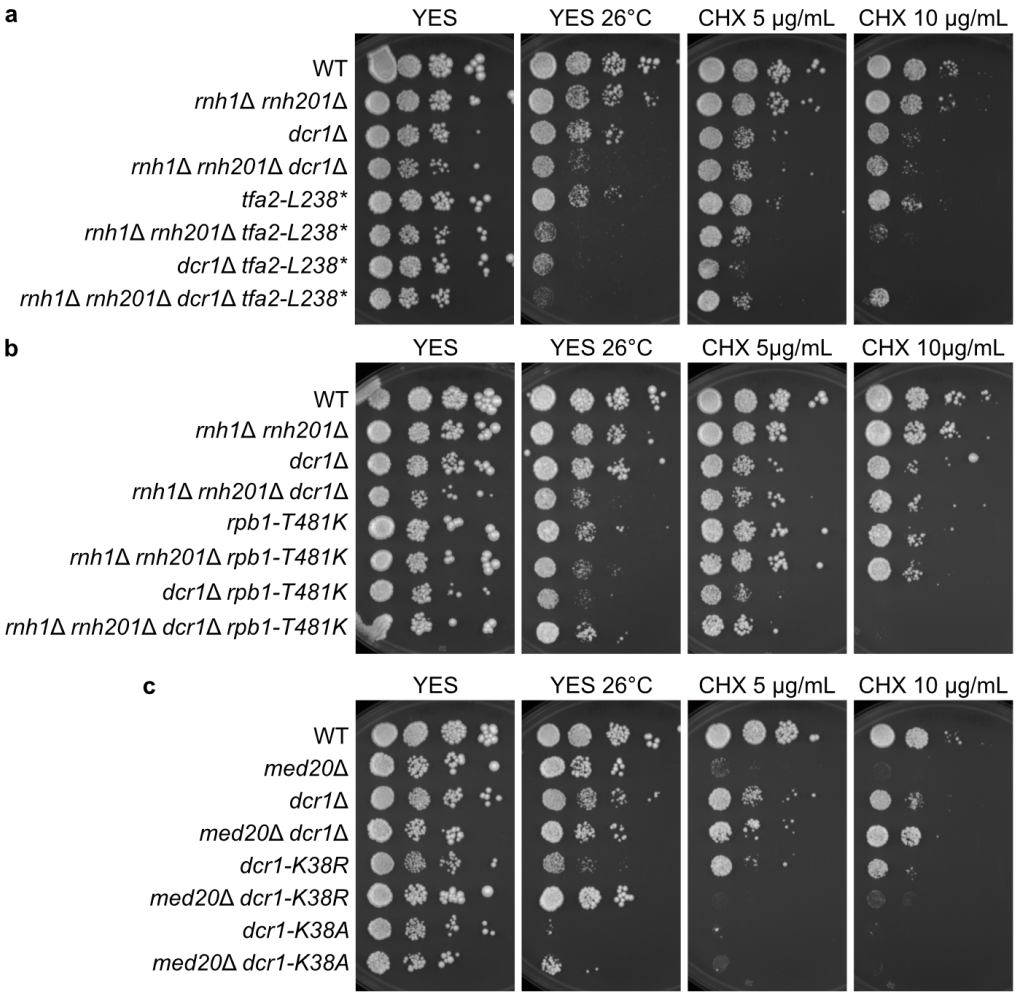

Figure 2.3. Cold and cycloheximide sensitivity of *dcr1*Δ cells in the presence of R-loops.

(a-b) Spot assay of WT, *dcr1*Δ, *rnh1*Δ *rnh201*Δ, and the triple mutant in combination with (a) *tfa2-L238** or (b) *rpb1-T481K,* with 10-fold dilution on YES plates in either low temperature or in the presence of cycloheximide (CHX).

(c) Spot assay of WT and *med20*Δ in combination with *dcr1* helicase alleles (*K38R* and *K38A*) and *dcr1*Δ, with 10-fold dilution on YES plates in either low temperature or in the presence of CHX.

2.9 Chromatin immunoprecipitation (ChIP) and ChIP-seq

ChIP was performed as described (Kim et al. 2014) with slight modifications. Briefly, 40 mL of mid-log phase cells in YES were crosslinked with 1% formaldehyde for 20 minutes and quenched with 360 mM glycine and 2.4 mM Tris for 5 minutes. Whole cell extracts were then prepared with FastPrep-24 and the chromatin was sheared with BioRuptor using 15 cycles of 30s ON/30s OFF. 2 µg of antibodies were pre-conjugated to 15 µL of Pierce Protein A/G Magnetic Beads (Thermo Scientific) for ~3 hours at 4 °C before being added to the sheared chromatin and were incubated overnight at 4 °C. The beads were washed and de-crosslinked with proteinase K and overnight incubation at 65°C. ChIP DNA Clean & Concentrator (Zymo Research) was used to clean up the DNA, and libraries were prepared using NEBNext Ultra II DNA Library Prep Kit (NEB). Indexed libraries were sequenced on NextSeq Illumina platform. For data processing, the demultiplexed reads were first trimmed with cutadapt (Martin 2011) before mapping to the genome using Bowtie2 (Langmead and Salzberg 2012). Reads were converted to sorted bam files using Samtools (Li et al. 2009), which were then used to generate normalized tracks using deepTools (Ramírez et al. 2014) and further analyzed using custom R scripts.

2.10 GLOE-seq

GLOE-seq libraries were prepared as described (Sriramachandran et al. 2020) except Zymolyase 100T was used instead of 20T for a more efficient spheroplasting. Data analyses were performed using custom R scripts.

2.11 Long-read sequencing analysis of replication pattern

For replication analysis, the strain FY2317 (from Forsburg lab) carrying the *hsv-tk* and *hENT1* transgenes (Hodson, Bailis, and Forsburg 2003) was used for pulse-chase experiments. Additional mutants were created from FY2317 specifically for replication analyses (Table S1). All strains were

tested for 5-fluoro-2'-deoxyuridine (FuDR, Sigma F0503) sensitivity and dot blots were performed to confirm capability of BrdU incorporation (data not shown). The experimental procedure of pulse-chasing experiment largely followed that described in (Theulot et al. 2022), and DNA extraction from (Hennion et al. 2020), with slight modification. Briefly, 650 μM of BrdU was added to 50 mL of mid-log phase cells for 2 minutes, before being chased with 6.5 mM of thymidine for 20 minutes. The cells were then pelleted, washed twice with water, before being spheroplasted with 125 μL of 50 mg/mL zymolyase 100T in 2 mL of Y1 buffer (1M sorbitol, 100 mM EDTA, pH 8.0, 14 mM β-mercaptoethanol), for ~30 minutes at 30 °C or until > 90% cell lysis when made 1% with SDS. Spheroplasts were then pelleted and lysed in 500 μL of 10% SDS, and incubated with 15 μL RNase A (Thermo Scientific) for 30 minutes at 50 °C. The lysate was cooled on ice, and 10 mL of TE and 5 mL of 5M potassium acetate was added. After 10 minutes on ice, the lysate was cleared by centrifuging at 5,000 x g at 4 °C for 10 minutes. 1 volume of isopropanol was added to precipitate the DNA, and was hooked using bent glass tip and washed twice with 70% ethanol. The hmwDNA was resuspended by incubating in 100 μL of TE at 50 °C for 30 minutes and its integrity confirmed by gel electrophoresis. 2 μg of hmwDNA was gently sheared by slowly pipetting up and down with a p200 tip, and library was prepared using ligation sequence kit SQK-LSK109 (ONT) and sequenced using R9.4.1 chemistry flow cells. Fork detection and replication speed analyses were done using NanoForkSpeed (Theulot et al. 2022).

2.12 Replication slippage assay

Replication slippage assays were performed by the Sarah Lambert laboratory (Institut Curie, Paris Orsay). 5-FOA (EUROMEDEX, 1555) resistant colonies were grown on uracil-containing plates with or without thiamine for 2 days at 30 ºC. They were subsequently inoculated into EMMg supplemented with uracil, with or without thiamine, for 24 hours. Cells were diluted and plated on EMMg complete (for cell survival) and on EMMg uracil-free plates, both supplemented with 60 μM

thiamine. To determine the reversion frequency, colonies were counted after 5 to 7 days of incubation at 30 ºC as previously described (Iraqui et al, 2012).

2.13 Analysis of replication intermediates by bi-dimensional gel electrophoresis.

2DGE experiments were performed by the Sarah Lambert laboratory (Institut Curie, Paris Orsay). For analysis of fork progression within rDNA, 2×10^9 exponentially growing cells were mixed with 50 ml of frozen Azide-Stop solution (0.5 M NaOH, 0.4 M EDTA, 0.2% sodium azide) and spun down at 1,521 × g, 10 min at 4 °C. The pellet was washed in 20 mL cold water and spun at 3,434 × g, 5 min at 4 °C. Cells were resuspended in 5 mL NIB buffer (17% glycerol, 50 mM MOPS pH 7.2, 150 mM potassium acetate, 2 mM magnesium chloride, 500 µM spermidine and 150 µM spermine, 25 mg/ml of Lysing enzyme and 10 mg/mL of zymolyase 100T) and incubated at 37 °C for 15 min. Four volumes of water were added and cells were spun down at 3,434 × g, 5 min at 4 °C. 5 mL of G2 buffer (Genomic DNA buffer set, Qiagen) was added to the pellet and cells were gently resuspended and incubated with 200 µL of 10 mg/mL RNase A, 200 µl of 20 mg/mL proteinase K, and 1.5% lauroylsarcosine, at 50 °C for 1 hour. Cells were spun down at 3,434 × g, 5 min at 4 °C. The supernatant was further incubated with 100 µL of RNase A, 100 µL of proteinase K for 1 hour at 37°C, whereas the pellet was resuspended in 5 mL of Buffer G2 with 100 µL of RNase A, 100 µL of proteinase K, 1.5% lauroylsarcosine and incubated at 37 °C for 1 hour. Both the “pellet” and “supernatant” fractions were spun down at 3,434 × g, 5 min at 4 °C and supernatants were transferred onto Genomic-tip 100/g columns (Qiagen) according to the manufacturer instructions. DNA was eluted using 50 °C pre-warmed elution buffer and precipitated with isopropanol. 5 µg of genomic DNA was digested with either 60 Units of *BamHI* or 60 Units of *HindIII* and *KpnI* enzymes. Precipitated DNA was run on 0.4% agarose gel for the first dimension and a 1% agarose gel for the second dimension. DNA was capillary transferred in 10X SSC onto nylon membranes and probed with a radio-labeled ^{32}P DNA probe corresponding to the 1,354 bp *EcoRI-EcoRI* fragment from rDNA unit (obtained by PCR using the

following primers: GAATTCGGTAAGCGTTGGATTG and GAATTCTTCTTTCACATCTCC) for *BamHI*-digested sample or corresponding to 1,340 bp fragment of rDNA (obtained by PCR using the following primers: CATGGTTACGGTTACATTGG and CCATCCCATATTTCGCACGA) for *HindII-KpnI*-digested samples. Quantitative densitometry analysis of the resulted Southern-blots was carried using a phosphor-imager (Typhoon-trio) and ImageQuant software (GE healthcare).

For replication analysis at the *RTS1*-RFB locus, 2.5×10^9 exponentially growing cells were treated with 0.1% sodium azide and mixed with frozen EDTA. Genomic DNA was crosslinked upon trimethyl psoralen (0.01 mg/mL, TMP, Sigma, T6137) addition to cell suspensions, for 5 min in the dark with occasional swirling. Cells were then irradiated with UV-A (365 nm) for 90 s at a constant flow of 50 mW/cm^2 (Kramarz, Saada, and Lambert 2021). Cell lysis was performed using 0.625 mg/mL lysing enzymes (Sigma, L1412) and 0.5 mg/mL zymolyase 100 T (Amsbio, 120493-1). Resulting spheroplasts were embedded into 2% low-melting agarose (Lonza, 50081) plugs. Next, plugs were incubated overnight at 55 °C, in a digestion buffer with 1 mg/mL of proteinase K (Euromedex, EU0090), prior to washing and storage in TE buffer (50 mM Tris, 10 mM EDTA) at 4 °C. DNA digestion was performed using 60 units per plug of restriction enzyme *Ase*I (NEB, R0526M). Samples were treated with beta-agarase (NEB, M0392L) and RNase A (Roche, 11119915001) and equilibrated to 0.3 M NaCl. Replication intermediates (RIs) were purified using BND cellulose columns (Sigma, B6385; Biorad, 731-1550), as previously described (Lambert et al. 2010). dsDNA was eluted by washing with 0.8 M NaCl, 10mM Tris-HCl (pH 7.5), and 1 mM EDTA. DNA containing single-stranded regions, such as RIs, was eluted by addition of 3 ml of 1 M NaCl, 10 mM Tris-HCl (pH 7.5), 1 mM EDTA, and 1.8% caffeine (Sigma, C-8960). RIs were precipitated with glycogen (Roche, 1090139001) and then separated by two-dimensional electrophoresis using 0.35 % and 0.9 % (+EtBr) agarose gels (1x TBE) for the first and second dimensions, respectively. Migrated DNA was transferred to a nylon membrane (Perkin-Elmer, NEF988001PK) in 10× SSC and probed with ^{32}P-radiolabeled *ura4* probe (TaKaRa *Bca*BEST^{TM} Labeling Kit, 6046 and alpha-^{32}P dCTP, Perkin-Elmer, BLU013Z250UC) in Ultra-Hyb

buffer (Invitrogen, AM8669) at 42 °C. Signal of replication intermediates was collected in phosphor-imager software (Typhoon-trio) and quantified by densitometric analysis with ImageQuantTL software (GE healthcare). The ‘tail signal’ was normalized to the overall signal corresponding to arrested forks.

Chapter 3: Dcr1 limits R-loop-induced genome instability

3.1 Summary

Although widely known for its post-transcriptional function, RNA interference (RNAi) plays an important role in the nucleus critical to genome stability (Castel and Martienssen 2013; Gutbrod and Martienssen 2020). In the fission yeast *Schizosaccharomyces pombe*, Dicer (Dcr1) is required for small RNA (sRNA)-dependent transcriptional silencing of pericentromeric heterochromatin (Volpe et al. 2002). Furthermore, Dicer also plays an RNAi-independent role in releasing RNA polymerase II (Pol II) to limit transcription-replication conflicts (TRCs) (Castel et al. 2014; Zaratiegui et al. 2011). Here, we show that Dcr1 resolves TRCs by regulating promoter-proximal, co-transcriptional R-loops. In RNase H-deficient cells, which accumulate pathological R-loops, deleting Dcr1 caused hypersensitivity to genotoxic stresses reflecting TRCs. Genetic evidence from suppressor screens, and genomic evidence from genome-wide transcriptional analysis, implicated Dcr1 in regulating nascent transcription and promoter-proximal pausing when R-loops accumulated. We also detected sRNA of 24 – 40 nt from promoters, and its generation depended redundantly on Dcr1 and RNase H. The genome instability phenotype of *dcr1*Δ can be suppressed by further deleting Ago1. Therefore, Dcr1 has a novel function in resolving paused Pol II to limit TRCs, the role of which depends on Ago1 and promoter-proximal sRNA.

3.2 Introduction

RNA interference (RNAi), widely known for its post-transcriptional gene regulatory functions, has an ancient and fundamental role in heterochromatic silencing and genome stability (Castel et al. 2014; Castel and Martienssen 2013; Gutbrod and Martienssen 2020; Volpe et al. 2002; Zaratiegui et al. 2011). In the fission yeast *Schizosaccharomyces pombe*, disruption of any of the RNAi components – Dicer (Dcr1), Argonaute (Ago1), or the RNA-dependent RNA polymerase Rdp1 – impairs pericentromeric heterochromatin formation and cohesin recruitment, leading to chromosome mis-

segregation and failure to grow on the microtubule inhibitor TBZ (Hall et al. 2003; Volpe et al. 2003). Beyond centromere functions, RNAi also assists in DNA damage response (Carmichael et al. 2004), and in plants and animals, small RNAs (sRNAs) are generated proximal to damage sites that are thought to promote repair (Lee et al. 2009; Wei et al. 2012).

We previously discovered that Dcr1 releases Pol II to limit TRCs (Castel et al. 2014; Roche et al. 2016; Zaratiegui et al. 2011). Such function appeared to be independent of canonical RNAi. For example, only *dcr1*Δ, but not *ago1*Δ, accumulated Rad52 foci, indicating persistent DNA damage (Zaratiegui et al. 2011); *dcr1*Δ progressively lost rDNA copies over meiotic generations, but this was not observed in *ago1*Δ, nor in the RNase III catalytic dead allele *dcr1-5* (Castel et al. 2014). Dicer-dependent chromosomal phenotypes have also been observed in mouse embryonic stem cells (mESCs) and interact with similar suppressor and enhancer mutations as in fission yeast suggesting broad conservation (Gutbrod et al. 2022). Nevertheless, how transcriptional processes are regulated by Dicer, and how this prevents genome instability, remains poorly understood.

R-loops are three-stranded nucleic acid structure consisting of a DNA:RNA hybrid with the displaced single-stranded DNA (ssDNA), and are thought to occur predominantly co-transcriptionally (Brickner et al. 2022). Physiological R-loops can be beneficial, but mis-regulated R-loops can become pathological, obstructing DNA replication and causing DNA damage and genome instability (García-Muse and Aguilera 2019; see Section 1.4.3). Two conserved ribonucleases, RNase H1 and RNase H2, are dedicated to degrade the RNA moiety of DNA:RNA hybrids in eukaryotes (Cerritelli and Crouch 2009). They operate partly redundantly (Lockhart et al. 2019) and in the double mutant *rnh1*Δ *rnh201*Δ, cells become hypersensitive to genotoxic agents such as hydroxyurea (HU) and camptothecin (CPT) (Zhao et al. 2018), underscoring the importance of R-loop removal to genome stability. In this chapter, I describe my genetic analyses showing a negative interaction between *dcr1* and RNase H, followed by a suppressor screen highlighting the important role of Dcr1 in mediating early transcriptional process.

This is followed by a genome-wide study of nascent transcription, supporting the role of Dcr1 in acting around promoter-proximal pause sites. Finally, we investigate the connection of this function of Dcr1 in relationship with canonical RNAi components – sRNA and Ago1.

3.3 Dcr1 negatively interacts with RNase H

Datasets for DRIP-seq and DRIPc-seq (DNA:RNA Immunoprecipitation followed by cDNA conversion and sequencing) have previously been generated by our laboratory from both WT and *dcr1*Δ cells in *S. pombe*, and extensive R-loop accumulation was documented at both rDNA and centromeric repeats (Castel et al., 2014; and Jie Ren, unpublished). Subsequently, DNA:RA hybrids have been found to accumulate at individual highly expressed genes in Hela cells when Dicer was knocked down (Camino et al. 2023). In order to determine the effects of Dicer on genes in *S. pombe*, I re-analyzed our DRIPc-seq data and observed a strand-specific global increase in R-loop accumulation in euchromatic genes (Fig. 3.1a). Thousands of genes were affected, especially highly expressed genes, indicating that Dicer was required for removal of R-loops associated with expressed genes genome-wide. In our laboratory too, we also found that *S. pombe* Dcr1 binds to R-loops and DNA:RNA hybrid, with a relatively high affinity as determined using microscale thermophoresis (Fig. 3.1b,c; Sonali Bhattacharjee, unpublished).

In order to investigate the role of Dicer in processing R-loops, I decided to create higher order mutants with RNase H1 and RNase H2 which accumulate pathological R-loops genome wide. RNase H1 is monomeric and is encoded by the *rnh1* gene, and RNase H2 is heterotrimeric, encoded by *rnh201, rnh202,* and *rnh203*, of which *rnh201* encodes the catalytic subunit (Hyjek et al. 2019). I therefore introduced *rnh1*Δ and *rnh201*Δ knockouts into *dcr1*Δ cells and measured growth rate. Whereas *rnh1*Δ and *rnh201*Δ single mutants displayed no growth defects, *dcr1*Δ and *rnh1*Δ *rnh201*Δ cells doubled ~50% slower than WT (Fig. 3.1d). The growth rate of *rnh1*Δ *rnh201*Δ double mutants confirmed that RNase H1 and H2 play a largely redundant role (Lockhart et al. 2019). While we observed no negative

interactions between *dcr1*Δ and with either *rnh1*Δ or *rnh201*Δ single mutants, strikingly, the triple mutant *dcr1*Δ *rnh1*Δ *rnh201*Δ divided ~2.5× times slower than WT. This suggested Dcr1 became critical to for growth when R-loops accumulated. Compared to *dcr1*Δ cells, the triple mutant cells were elongated, branching, and with multiple septa and nuclei (Fig. 3.1e-f), suggesting that the triple mutant had a severe replication defect. To test this, we checked for growth defect of the mutants in the presence of the replication stress-inducing drugs HU and camptothecin (CPT). While both HU and CPT introduce replication stress, they do so via distinct mechanisms. HU inhibits the enzyme ribonucleotide reductase (RNR), which converts ribonucleotides (NTPs) to dNTPs, the substrates for DNA synthesis. As a result, the cellular dNTP pool is depleted, slowing down replication forks, and activating the replication checkpoint (Singh and Xu 2016). CPT, on the other hand, triggers replication stress by generating obstacles to replication. In cells, topoisomerase I relieves DNA supercoiling tension, and an intermediary step involves a transient covalent linkage between the enzyme and DNA. CPT stabilizes this covalent linkage, creating a protein adduct as well as a single-stranded break; Collision between the replication fork and such obstacles leads to double-stranded breaks, or permanent arrest of the fork (Liu et al. 2000).

In order to determine sensitivity to genotoxic agents in a quantitative manner, I decided to perform spot assays of various mutant combinations of *dcr1*Δ, *rnh1*Δ, and *rnh201*Δ. Cells were grown in the presence of increasing doses of HU and CPT and serial 10-fold dilutions plated on media supplemented with each agent (Fig. 3.1g-h). The *rnh1*Δ *rnh201*Δ double mutant was highly HU- and CPT-sensitive as previously reported (Zhao et al. 2018). Strikingly, *dcr1*Δ hypersensitized RNase H-deficient cells to genotoxic agents (Fig. 3.1g-h), indicating that Dcr1 becomes important in limiting replication stress when R-loops accumulate. We noticed a stronger negative interaction between *dcr1*Δ and *rnh201*Δ than with *rnh1*Δ, especially in the presence of HU (Fig. 3.1g). This might be due to the additional roles of RNase H2 and that it accounts for the majority of RNase H activity in cells. While both RNase H1 and H2 can process R-loops, RNase H2 is capable of performing ribonucleotide

excision repair (RER), a process by which ribonucleoside monophosphates (rNMPs) incorporated during DNA replication is excised for repair (Williams, Lujan, and Kunkel 2016). Additionally, RNase H2 has recently been shown to promote recombination-dependent replication restart (Audoynaud et al. 2023). In face of replication obstacles, replication forks slow down or are completely arrested, requiring rescue from neighboring fork in the opposite direction or by restart via HR-dependent processes. Replication restart requires ssDNA that is generated by exonuclease to degrade the nascent strand. It has been demonstrated that the RNA primer at the 5' end of the Okazaki fragment inhibits nascent strand degradation, and RNase H2 promotes replication restart by removing the DNA:RNA hybrid (Audoynaud et al. 2023). These two additional functions of RNase H2 might account for the stronger interaction between *dcr1*Δ and *rnh201*Δ.

An explanation to this negative interaction phenotype is that Dcr1 directly participates in R-loop processing; in that case, overexpressing RNase H would make *dcr1*Δ more resistant to replication stress. However, this was not observed when a *nmt41* promoter was used to overexpress *rnh1* in *dcr1*Δ (Fig. 3.2a-b), suggesting that Dcr1 did not limit TRC by directly participating in R-loop metabolism. Given the genetic interaction between Dcr1 and RNase H, we also tested whether Dcr1 would interact with the R-loop-processing helicases, Sen1 and Dbl8, both of which are homologues of the human Senataxin (SETX) (Skourti-Stathaki et al. 2011). We observed no obvious growth defects under the conditions tested for both *sen1*Δ and *dbl8*Δ, nor any negative interaction between *dcr1* and *dbl8* (Fig. 3.2c-d). Unexpectedly, *dcr1*Δ *sen1*Δ double mutants were more resistant to CPT than *dcr1*Δ cells (Fig. 3.2c). This was contrary to our prediction considering the known transcription and replication roles of SETX. However, a proteomic study in *S. pombe* identified Sen1 and Dbl8 as predominantly interacting with Pol III and Pol I, respectively (Rivosecchi et al. 2019); therefore, our observations could be explained if Pol II loci are the main Dcr1-regulated targets.

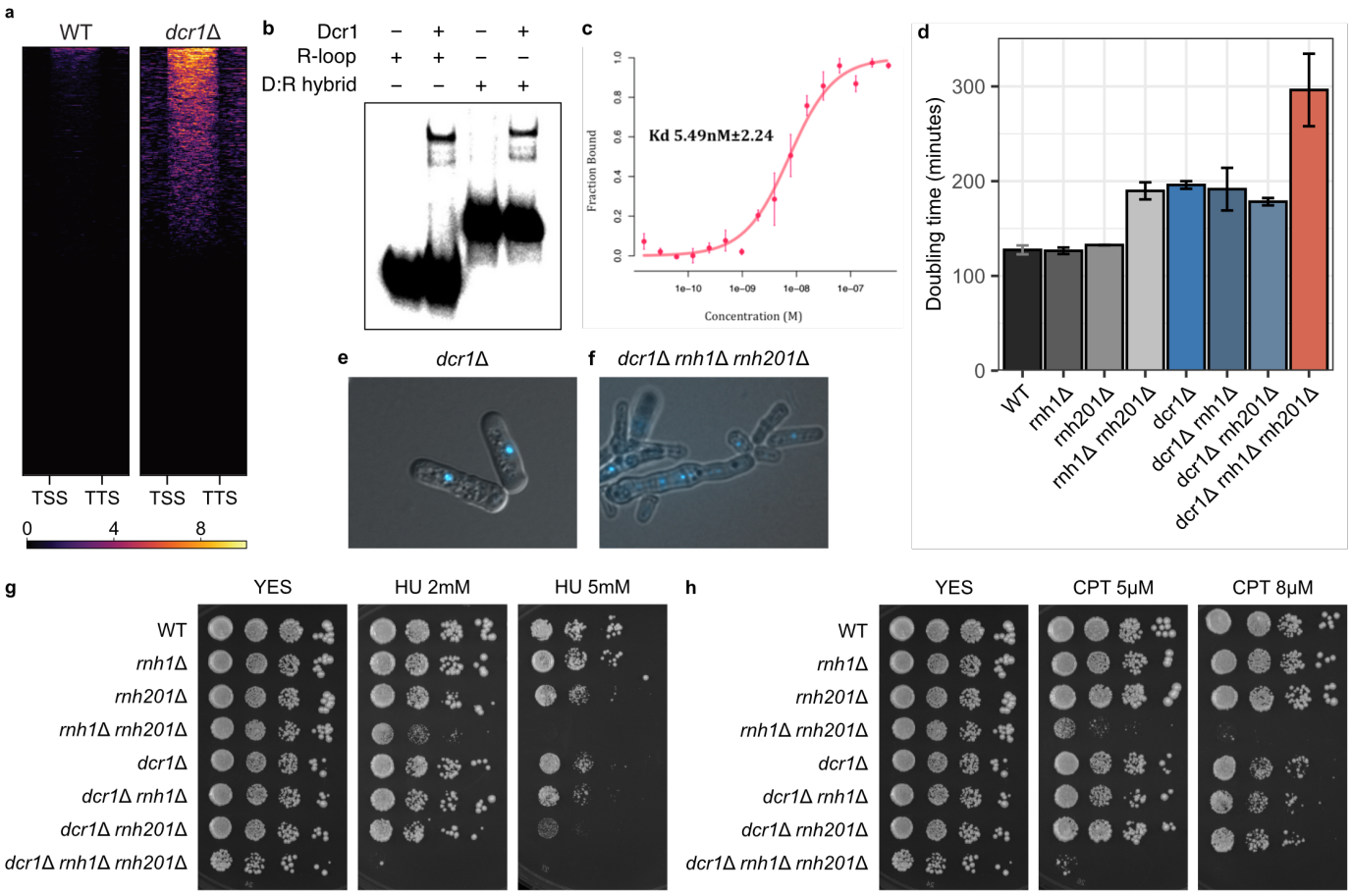
a
WT
dcr1Δ
TSS TTS TSS TTS
0 4 8
b
Dcr1 − + − +
R-loop + + − −
D:R hybrid − − + +
c
Kd 5.49nM±2.24
Fraction Bound
Concentration (M)
d
Doubling time (minutes)
WT
rnh1Δ
rnh201Δ
rnh1Δ rnh201Δ
dcr1Δ
dcr1Δ rnh1Δ
dcr1Δ rnh201Δ
dcr1Δ rnh1Δ rnh201Δ
e
dcr1Δ
f
dcr1Δ rnh1Δ rnh201Δ
g
YES
HU 2mM
HU 5mM
h
YES
CPT 5μM
CPT 8μM

Figure 3.1. Dicer protects against replication stress in the presence of R-loops.

(a) Heatmaps of DRIPc-seq signals in WT and *dcr1*Δ at annotated mRNA transcripts ± 500 bp. Values are RPM normalized.

(b) Electrophoretic mobility shift assay (EMSA) showing Dcr1 binds R-loops and DNA:RNA hybrids *in vitro*.

(c) Microscale thermophoresis (MST) assay of Dcr1 and R-loops.

(d) Doubling time analyses of WT and combinations of *rnh1*Δ, *rnh201*Δ, and *dcr1*Δ. N = 2. Error bars represent standard deviation.

(e,f) Representative images of *dcr1*Δ and *dcr1*Δ *rnh1*Δ *rnh201*Δ cells with DAPI staining respectively.

(g,h) Spot assay of WT and combinations of *rnh1*Δ, *rnh201*Δ, and *dcr1*Δ with 10-fold dilution on YES plates without supplement or with varying doses of the genotoxic agents hydroxyurea (HU) and camptothecin (CPT).

DRIPc-seq of WT and *dcr1*Δ was performed by Jie Ren.

***In vitro* Dcr1 binding assays were performed by Sonali Bhattacharjee.**

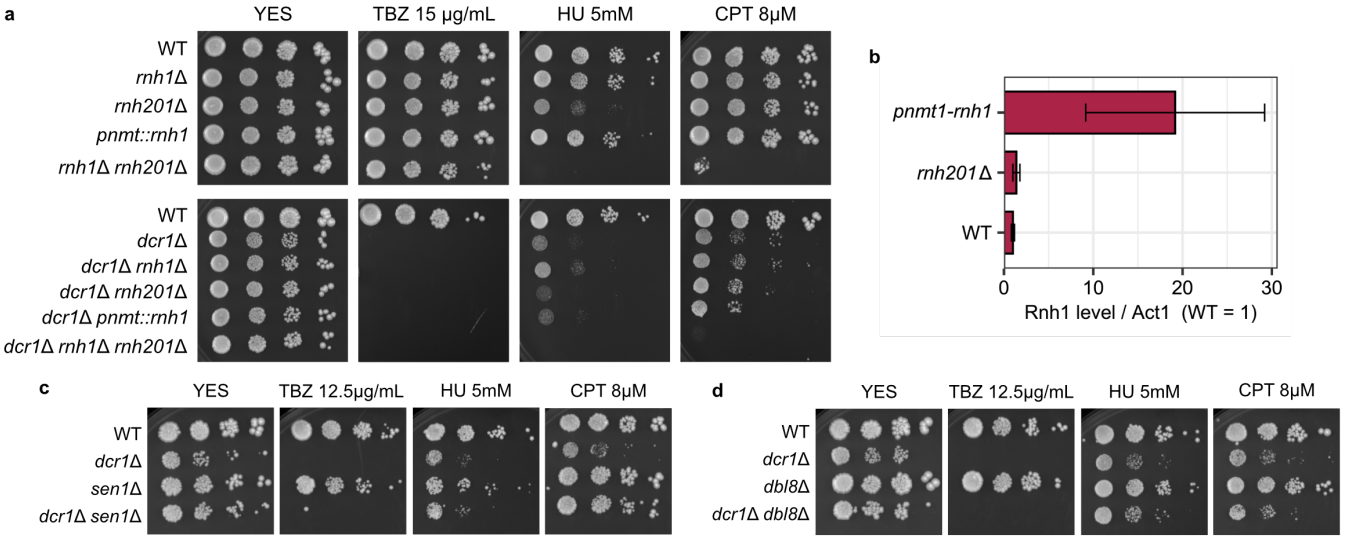

Figure 3.2. Analyses of *dcr1* with other R-loop modulators.

(a) Spot assay of WT and *dcr1*Δ, in combinations with *rnh1*Δ, *rnh201*Δ, *rnh1*Δ *rnh201*Δ, or an RNase H1-overexpressing strain *pnmt1::rnh1*. Cells were spotted with 10-fold dilution on YES plates without supplement or with varying doses of TBZ, HU, and CPT.

(b) RT-qPCR quantification of the expression of *rnh1* in WT, *rnh201*Δ, and the RNase H1-overexpressing strain. Expression levels were normalized to *act1*, WT =1. N = 2. Error bars represent SEM.

(c,d) Spot assay of WT, *dcr1*Δ with *sen1*Δ (c) or *dbl8*Δ (d) with 10-fold dilution on YES plates without supplement or with varying doses of TBZ, HU and CPT.

3.4 Genetic analysis of the *dcr1*Δ genome instability phenotype

The negative genetic interaction between *dcr1* and *rnh1 rnh201* prompted us to perform further genetic studies. Past studies identified multiple suppressors of canonical RNAi phenotypes in *dcr1*Δ. For example, TFIIS, encoded by *tfs1*, is a non-essential general transcription factor (GTF) that promotes Pol II processivity and regulates Pol II backtracking (Kulish and Struhl 2001); its deletion confers TBZ resistance in *ago1*Δ and *dcr1*Δ cells, presumably by reducing productive transcription at the pericentromeric repeats (Reyes-Turcu et al. 2010). In a similar vein, deletion of *mst2*, which encodes a H3K14 acetyltransferase, rescues the pericentromeric heterochromatin defects in RNAi mutants by reducing the level of the active mark H3K14ac and therefore ectopic transcription in the centromere (Reddy et al. 2011). Our laboratory previously discovered that *dcr1*Δ had severe defects in the entry as well as maintenance of the cellular quiescent (G_0) stage during nitrogen starvation (Roche et al. 2016), and a suppressor screen that restored viability identified multiple alleles of transcription regulators. These included *tbp1-D156Y*, encoding the highly conserved TATA-binding protein (TBP) involved in promoter melting and transcription initiation of Pol I, II, III (Cormack and Struhl 1992); *med31-ins*, an allele of the Med31 subunit of the mediator complex replacing the conserved phenylalanine F23 with 5 amino acids (Linder and Gustafsson 2004); as well as *fcp1-F580**, premature termination of the protein phosphatase that removes the phosphorylation at the serine 2 (pS2) of the Pol II C-terminal domain (CTD) repeats (Hausmann, Erdjument-Bromage, and Shuman 2004).

Notably, the suppressor *tbp1-D156Y*, despite being isolated in a G_0 viability screen (Roche et al. 2016), was also able to suppress the TBZ sensitivity of *dcr1*Δ indicating a heterochromatic function in dividing cells (see above). We therefore crossed these five mutants into the triple mutant *dcr1*Δ *rnh1*Δ *rnh201*Δ and assessed whether they could rescue the replication stress phenotype. As shown in Fig. 3.3a, all the suppressor mutants were able to confer TBZ resistance to the triple mutant, agreeing with previous findings. They were also all able to suppress the HU sensitivity of the triple mutant, although the effect was relatively weak in *tbp1-D156Y* and *tfs1*Δ. The suppressibility of CPT was

weaker, and we only observed robust suppression in *mst2*Δ and *fcp1-F580**. We further investigated TFIIS – because of its interesting property in regulating transcription elongation and termination – by isolating combination of mutants of *tfs1*Δ, *dcr1*Δ, and *rnh1*Δ *rnh201*Δ from crosses. To our surprise, in two separate biological replicates we failed to observe any suppression of by *tfs1*Δ (Fig. 3.3b-c); in fact, there was moderate negative interaction between *tfs1*Δ and *dcr1*Δ in the presence of CPT. This might be due to the variegated effect of *tfs1*Δ, as previously noted (Reyes-Turcu et al. 2010). Altogether, the variable suppressibility of these alleles suggests that, while multiple phenotypes of Dcr1 can be regulated by mutating GTFs, the genome instability phenotype in *dcr1*Δ is not due simply to the level of transcription, nor necessarily at the pericentromeric region, although remarkably, all the alleles tested here regulates early transcription, hinting at the possibility that this might the step where Dcr1 acts on.

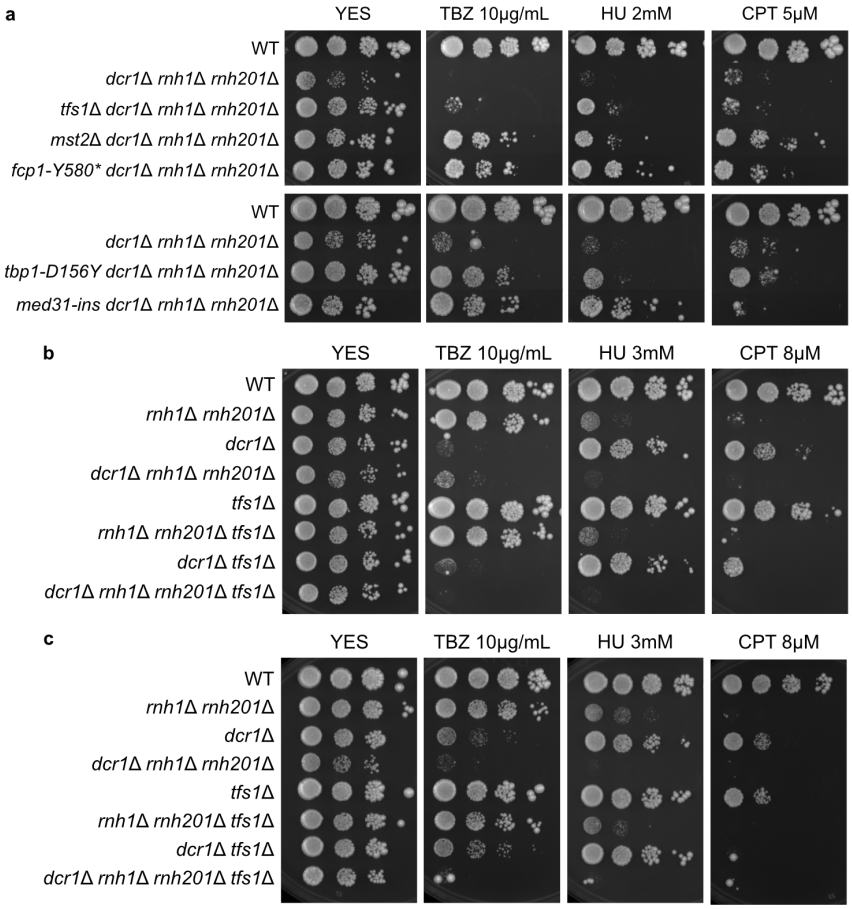

Figure 3.3. *dcr1* suppressors restore replication stress resistance in the presence of R-loops.

(a) Spot assay of the triple mutant *dcr1*Δ *rnh1*Δ *rnh201*Δ with various alleles of general transcription factors (GTFs) previously found to suppress silencing and quiescence defects in *dcr1*Δ: *tfs1*Δ, *mst2*Δ, *fcp1-Y580**, *tbp1-D156Y*, and *med31-ins*. See main text for details. Cells were plated with 10-fold dilution on YES plates without supplement or with TBZ or HU to test for drug sensitivity.

(b,c) Two independent replicates of spot assays of WT and combinations of *rnh1*Δ, *rnh201*Δ, *dcr1*Δ, and *tfs1*Δ with 10-fold dilution on YES plates without supplement or with varying doses of TBZ, HU, and CPT.

To follow up on these results, I decided to isolate new suppressors with an ethyl methanesulfonate (EMS) mutagenesis screen. Here, I treated the triple mutant with EMS and plated cells with either CPT or HU. Drug-resistant colonies were streaked back onto YES plates before verifying the drug resistance with spot assay. The new strains were sequenced and SNPs were identified by comparing with the genome of the original triple mutant. We first isolated ten suppressors that conferred resistance to CPT. On average, each suppressor carried 4 – 6 SNPs, and we decided to verify candidate SNPs by direct transformation. As described in section 2.5, except for the *top1* allele (*top1-W647**), independent alleles of known regulators *paf1* and *clr2* failed to confer CPT resistance in fresh strains indicating the screen was problematic. Because of this we decided to repeat the EMS screen for HU resistance. A total of 14 HU suppressors were isolated and sequenced, of which I identified the causative SNPs for 8 of them (Table 2). The HU screen performed more efficiently than the CPT screen, but many of the suppressors on HU were also resistant to CPT. On top two "bypass" suppressors – *epl1-T449A* and *pof1-S449C* (described in section 2.5), several alleles were identified in general transcription factors (GTFs) which had more specific predicted functions in mediating TRCs.

One such allele was *tfa2-L238** (LS22), a premature truncation in the gene encoding TFIIEβ, the small subunit of the heterodimeric GTF TFIIE (Fig. 3.4a). This allele conferred HU resistance specifically to the triple mutant, but not to *rnh1*Δ *rnh201*Δ or *dcr1*Δ alone. Interestingly, *tfa2-L238** was sensitive to TBZ, and it negatively interacted with *rnh1*Δ *rnh201*Δ in the presence of TBZ or CPT. Consistently, we observed an up-regulation of the centromeric transcripts *dg* and *dh* in *tfa2-L238**, but not *epl1-T449A*, consistent with a loss of heterochromatic silencing (Fig. 3.4b). TFIIE functions closely with TFIIH to promote the last steps of transcription initiation, by stimulating DNA melting to form the transcriptionally competent preinitiation complex (PIC) (Compe et al. 2019; Goodrich and Tjian 1994; Nogales, Louder, and He 2017). Although IUPred3 (Erdős, Pajkos, and Dosztányi 2021) predicted the mutation truncated a largely disordered region (Fig. 3.4c). structural studies in *S. cerevisiae* revealed the region contains the "E-tether" of Tfa2, which contacts Ssl2 (Ptr8 in *S. cerevisiae*;

XPB in human) (Schilbach et al. 2021), a subunit of the TFIIH complex that promotes promoter opening via its ATPase/DNA translocase activity (Compe and Egly 2016). Biochemical assay suggested this contact stimulated Ssl2 *in vitro* (Lin and Gralla 2005; Watanabe et al. 2003). In light of this, I predicted the allele *tfa2-L238** conferred HU resistance in the triple mutant by reducing the efficiency of Pol II promoter escape.

Two alleles were validated that directly affected the large subunits of the Pol II holoenzyme: *rpb2-R1118H* in LS16, and *rpb1-T481K* in LS21 (Fig. 3.4d-e). These mutations are located within the catalytic center, in physical proximity to each other (Fig. 3.4f). In each case, suppression was specific to HU, but not in CPT or TBZ, and primarily affected acting the triple mutant, although at higher doses of HU we observed mild suppression of the *rnh1*Δ *rnh201*Δ double mutant as well (not shown). In all multi-subunit RNAPs, phosphodiester bond synthesis activity is catalyzed by coordinating two Mg^{2+} ions with three conserved aspartate residues, arranged in the invariant motif DFDGD (Sosunov et al. 2003, 2005) (Fig. 3.4f-g). *rpb1-T481K* disrupts the threonine residue N-terminal to this motif (Fig. 3.4f-g) and is aligned with the phenylalanine residue. This threonine residue is highly conserved in Pol II, but is frequently replaced with cysteine in other polymerases (e.g. Pol III) (Cramer, Bushnell, and Kornberg 2001; Haag, Pontes, and Pikaard 2009). Its exact function is not known, but in *S. cerevisiae*, disruption of the asparagine residue C-terminal to the DFDGD motif (*rpb1-N488D*, or *N494* in *S. pombe*) leads to a decrease in transcription elongation rate and is thought to impair initiation as well (Malagon et al. 2006). Since the *rpb1-T481K* mutation replaces threonine with lysine with a long side chain, we speculate it might misalign the phenylalanine residue, thereby displacing the catalytic triad, impairing Pol II processivity.

The *rpb2-R1118H* allele also disrupts a highly conserved residue in the "switch 3" region of Pol II (Cramer et al. 2001; Gnatt et al. 2001) (Fig. 3.4h). As Pol II transitions from holoenzyme into a transcribing, elongating state, the clamp swings by about 30^{o} and five "switch" regions are re-folded

into directly contacting the template DNA and the RNA within the transcription bubble (Cramer et al. 2001; Gnatt et al. 2001); R1118, in particular, contacts the -2 nucleotide of the template DNA (Gnatt et al. 2001) (Fig. 3.4f). These nucleic acid contacts ensure proper three-dimensional ordering within the active center, and promote the stability of the transcribing complex. Indeed, studies of Pol III found that mutating the arginine R1061 in *S. cerevisiae*, equivalent to *rpb2-R1118* in *S. pombe*, led to defects in processive elongation, concomitant with frequent pausing and elevated termination frequency (Bobkova et al. 1999; Shaaban et al. 1996; Shaaban, Krupp, and Hall 1995). Altogether, the two alleles affecting the Pol II enzyme suggested Pol II itself triggered replication stress in the triple mutant, and that affecting its dynamics – initiation, elongation, and/or processivity – reduced its potential to trigger the stress.

Table 2. EMS suppressor screen for HU-resistance. Causative SNPs were verified with either co-segregation analysis through backcrosses, or by reintroduction into the triple mutant. When the causative SNPs were not verified, the most likely SNP(s) among the candidates were highlighted. N.D.: Not determined.

Suppressor	Sterile?	Causative SNP	Candidate SNPs
LS15	No	**Epl1-T449A**	SPNCRNA.857 (chr1:2872396 A->G); Map4-S326syn; Prl10 (chr3:1839843 C->G); an intergenic SNP (chr2:3020359 C->G)
LS16	Yes	**Rpb2-R1118H**	Esc1-S338C; Gas1-S516syn; Sea3-H321R; Syt22-R526G; Sld5-G192A; Fes1-D232V; Dbp8-R345Q; Snp22-Q269P
LS17	N.D.	-	Many (37 SNPs)
LS18	Yes	-	**Utp5-E601D; Ubr1-P1524S**
LS19	N.D.	-	3 SNPs on **Edc1** leading to truncation; Synonymous SNPs on Mde5, SPNCRNA.253, Wtf1, and Rga3
LS20	No	**Med20-Y44S**	Cul1-R330syn; a tRNA gene (chr2:820558 C->T)
LS21	Yes	**Rpb1-T481K**	Tlg2 (5'UTR); Agl1-G491A; Eno101 (5'UTR); Ptr3-P289A; Osh6 (intron); an intergenic SNP (chr1:4269071 T->C)
LS22	N.D.	**Tfa2-L238***	Nup132 (5'UTR); SPAC17A2.11 (5'UTR); Mas5-E362V; Tan1-I63P; Tif11 (3'UTR); Hrf1 (3'UTR); Vac14-N252K; Rrg1-S119P; SPCC18.17c-L18*
LS23	No	**Med20-W37A**	Pcs2 (3'UTR); Rpp0 (synonymous); one intergenic SNP (chr2:4471290 C->G)
LS24	No	-	**Cts1-V58L**; Spp42 (synonymous); Saf1 (3'UTR)
LS25	No	-	**Rok1-A388T**; Nte1-K806Q; Rpt3-D234A; one intergenic SNP (chr1:3022972 C->T)
LS26	No	**Med20 truncation**	Erd101-D176A; Kap113 (intron); one intergenic SNP (chr1:4415439 G->T)
LS27	No	**Pof1-S449C**	-
LS28	Yes	-	Gas5-V219syn; SPBC359.01-V342G; **Med15-L63***; SPBC83.05 (3'UTR); Map2 (5'UTR)

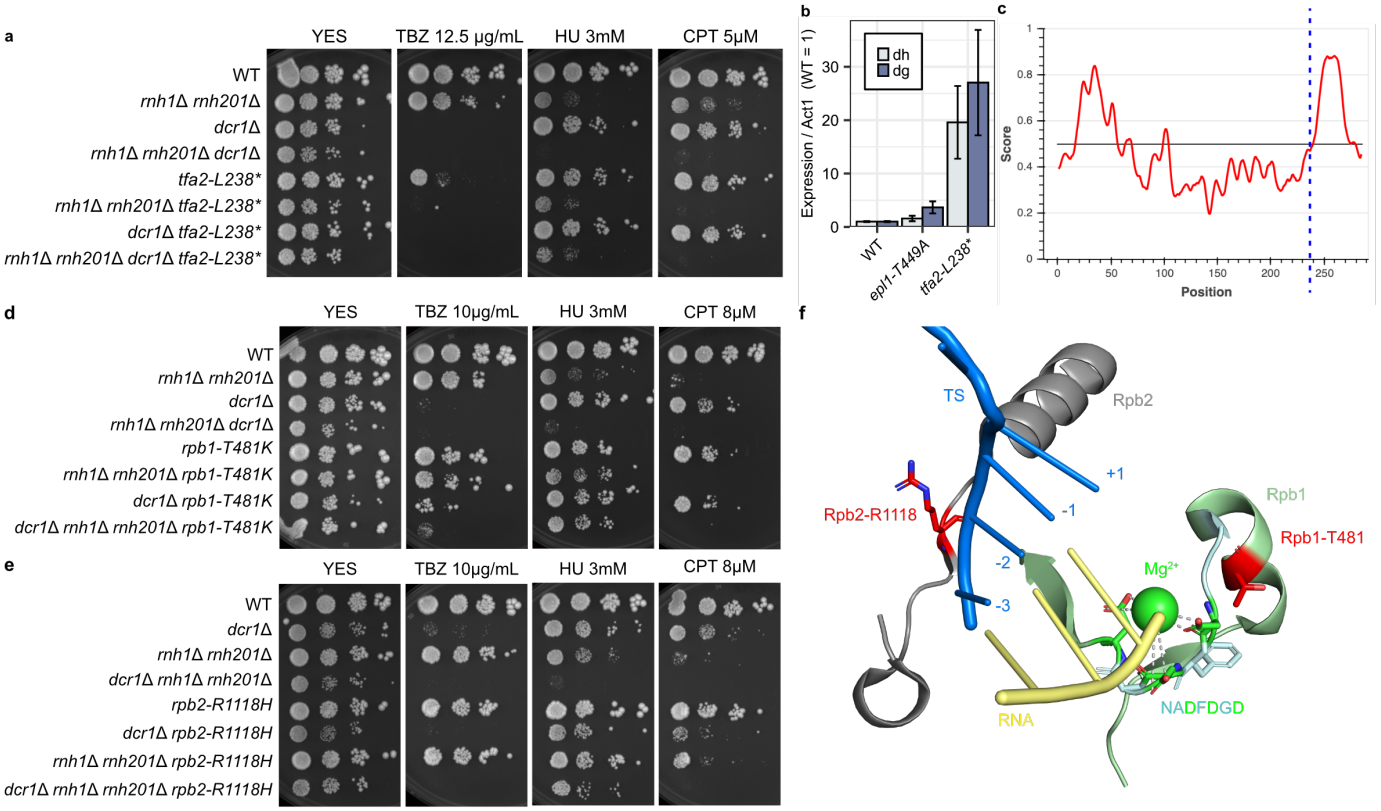

g **Rpb1**

```
Sp  GPDEH---PGAKYIIRDTGERIDLRYHKRAGDIPLRYGWRVERHIRDGDVVIFNRQPSLH  457
Sc  GPNEH---PGAKYVIRDSGDRIDLRYSKRAGDIQLQYGWKVERHIMDNDPVLFNRQPSLH  451
Hs  GNSQY---PGAKYIIRDNGDRIDLRFHPKPSDLHLQTGYKVERHMCDGDIVIFNRQPTLH  465
Mm  GNSQY---PGAKYIIRDNGDRIDLRFHPKPSDLHLQTGYKVERHMCDGDIVIFNRQPTLH  465
At  GPHPPPGKTGAKYIIRDDGQRLDLRYLKKSSDQHLELGYKVERHLQDGDFVLFNRQPSLH  465
    *        ****:*** *:*:***:  : .*  *. *::****: *.* *:*****:**

                rpb1-T481K ┐      ┌ Catalytic triad
Sp  KMSMMGHRIRVMPYSTFRLNLSVTSPYNADFDGDEMNMHVPQSEETRAEIQEITMVPKQI  517
Sc  KMSMMAHRVKVIPYSTFRLNLSVTSPYNADFDGDEMNLHVPQSEETRAELSQLCAVPLQI  511
Hs  KMSMMGHRVRILPWSTFRLNLSVTTPYNADFDGDEMNLHLPQSLETRAEIQELAMVPRMI  525
Mm  KMSMMGHRVRILPWSTFRLNLSVTTPYNADFDGDEMNLHLPQSLETRAEIQELAMVPRMI  525
At  KMSIMGHRIRIMPYSTFRLNLSVTSPYNADFDGDEMNMHVPQSFETRAEVLELMMVPKCI  525
    ***:*.**::::*:*********:*****:*****:*:*** *****: ::  **  *

Sp  VSPQSNKPVMGIVQDTLAGVRKFSLRDNFLTRNAVMNIMLWVPDWDGILPPPVILKPKVL  577
Sc  VSPQSNKPCMGIVQDTLCGIRKLTLRDTFIELDQVLNMLYWVPDWDGVIPTPAIIKPKPL  571
Hs  VTPQSNRPVMGIVQDTLTAVRKFTKRDVFLERGEVMNLLMFLSTWDGKVPQPAILKPRPL  585
Mm  VTPQSNRPVMGIVQDTLTAVRKFTKRDVFLERGEVMNLLMFLSTWDGKVPQPAILKPRPL  585
At  VSPQANRPVMGIVQDTLLGCRKITKRDTFIEKDVFMNTLMWWEDFDGKVPAPAILKPRPL  585
```

h **Rpb2**

```
                                                    Switch 3
Sp  SHGFQSRGFEVMYHGHTGRKLVAQVFLGPTYYQRLKHLVDDKIHARARGPVQILTRQPVE 1109
Sc  EHGYQSRGFEVMYNGHTGKKLMAQIFFGPTYYQRLRHMVDDKIHARARGPMQVLTRQPVE 1120
At  KCGYQMRGFERMYNGHTGRPLTAMIFLGPTYYQRLKHMVDDKIHSRGRGPVQILTRQPAE 1081
Mm  DYGYHLRGNEVLYNGFTGRKITSQIFIGPTYYQRLKHMVDDKIHSRARGPIQILNRQPME 1076
Hs  DYGYHLRGNEVLYNGFTGRKITSQIFIGPTYYQRLKHMVDDKIHSRARGPIQILNRQPME 1076
    . *:: ** * :*:*.**: : : :*:********:*:******:*.***:*:*.*** *

                ┌ rpb2-R1118H
Sp  GRSRDGGLRFGEMERDCQISHGCSSVLRERLFDCSDAYRVIVCDICGLIAI-ASYKKDSY 1168
Sc  GRSRDGGLRFGEMERDCMIAHGAASFLKERLMEASDAFRVHICGICGLMTVIAKLNHNQF 1180
At  GRSRDGGLRFGEMERDCMIAHGAAHFLKERLFDQSDAYRVHVCEVCGLIAI-ANLKKNSF 1140
Mm  GRSRDGGLRFGEMERDCQIAHGAAQFLRERLFEASDPYQVHVCNLCGIMAI-ANTRTHTY 1135
Hs  GRSRDGGLRFGEMERDCQIAHGAAQFLRERLFEASDPYQVHVCNLCGIMAI-ANTRTHTY 1135
    **************** *:**.: .*:****:: ** ::* :* :**:::: *. . . :
```

Figure 3.4. Mutations in the Pol II catalytic center and in TFIIE suppress *dcr1*Δ.

(a,b) Spot assay verification of (a) *rpb1-T481K* and (b) *rpb2-R1118H* from the suppressors LS21 and LS16, respectively. Cells were plated with 10-fold dilution on YES plates without supplement or with TBZ, HU, or CPT.

(c) Catalytic center of Pol II highlighting the two residues in red, Rpb1-T481 and Rpb2-R1118, whose mutation suppresses *dcr1*Δ. Note that Rpb1-T481 aligns with the catalytic triad (NADFDGD) coordinating a Mg^{2+} ion (green), and that Rpb2-R1118 is in proximity to the template strand (TS) DNA (blue). RNA is in yellow and the direction of RNA synthesis labeled with numbers on TS. Image generated from PDB:5vvs.

(d) Sequence alignment of a select region of Rpb1 from *Saccharomyces cerevisiae* (Sc), *S. pombe* (Sp), *Homo sapiens* (Hs), *Mus musculus* (Mm), and *Arabidopsis thaliana* (At). Alignment was done using Clustal Omega with default setting. *Rpb1-T481* is highlighted in red, and the catalytic triad coordinating the Mg^{2+} ion is highlighted in blue.

(e) Sequence alignment of a select region of *rpb1* from *Saccharomyces cerevisiae* (Sc), *S. pombe* (Sp), *Homo sapiens* (Hs), *Mus musculus* (Mm), and *Arabidopsis thaliana* (At). Alignment was done using Clustal Omega with default setting. *Rpb2-R1118H* is highlighted in red, and the switch 3 region is highlighted in blue.

(f) Spot assay verification of *tfa2-L238** from the suppressor LS22 performed as in (a).

(g) RT-qPCR quantification of the expression of *dg/dh* centromeric transcripts in *epl1-T449A* and *tfa2-L238**. Relative expression was normalized to *Act1*. N = 2 independent biological replicates. Error bars represent SEM.

(h) IUPred3 prediction of Tfa2 (UniProt: P79011) showing the disorder tendency. Vertical blue dotted line represents the approximate location of residue L238, that which was turned into a premature stop codon in LS22.

Finally, 3 out of 14 suppressors (LS20, 23, 26) carried mutations in the *med20* gene, which encodes a subunit of the Mediator complex (Larivière et al. 2012), and one suppressor, LS28, carried a truncation of Med15 (*med15-L63**), although this allele has not been verified. The three *med20* alleles were assigned *med20-1* to *med20-3*, and they disrupted conserved residues Y44S (*med20-1*) and W37A (*med20*-2), or, in the case of *med20-3*, caused a frameshift at F108, leading to premature termination at position 128 and truncation of roughly half of the protein (Fig. 3.5a). We confirmed the suppressors by backcrossing and genotyping the *med20* mutants (Fig. 3.5b-d).

Mediator is a large, multi-subunit complex that is critical for Pol II transcription (Richter et al. 2022; Soutourina 2018). It is generally required for PIC assembly, and aids gene-specific transcription factors (TFs) in recruiting Pol II and other GTFs. Beyond initiation, it also plays a role in promoting productive elongation (Richter et al. 2022). Structurally, Mediator can be subdivided into four modules: Head, Middle, Tail, and the CDK8 kinase modules (Harper and Taatjes 2018), and the complex as a whole forms extensive, dynamic contacts with Pol II and GTFs (Chen et al. 2021; Nozawa, Schneider, and Cramer 2017; Plaschka et al. 2015). Med20 is part of the Med8/18/20 'movable jaw' subcomplex within the head module of the Mediator, with Med8 being the structural bridge connecting the tight Med18-Med20 heterodimer to the rest of the head module (Larivière et al. 2012). The movable jaw establishes transient interactions with Pol II and GTF directly – Med8 contacts Rpb4 of the Rpb4-Rpb7 Pol II stalk, and Med18-Med20 contacts Rpb3-Rpb11, as well as the 'E-ribbon' of TFIIE (within the TFIIEα subunit, Tfa1 in *S. pombe*) and the 'B-ribbon' of TFIIB (Plaschka et al. 2016; Rengachari et al. 2021).

Studies in *S. pombe* have previously demonstrated that deleting subunits from the movable jaw module led to impaired pericentromeric silencing (Carlsten et al. 2012; Oya et al. 2013; Thorsen et al. 2012). In particular, *med18*Δ or *med20*Δ led to derepressed *dg/dh* repeat transcription, a decrease in the siRNA level, as well as a reduction in the H3K9me and Swi6 level as determined by chromatin

immunoprecipitation (ChIP). We therefore tested whether the replication stress phenotype would also be suppressed in *med20*Δ, and also whether the *med20* alleles isolated would lead to silencing defect. With spot assays, we found that both *med20-1* and *med20*Δ conferred HU resistance to *dcr1*Δ alone, the *rnh1*Δ *rnh201*Δ double mutant, as well as the triple mutant, and a mild suppression to CPT (Fig. 3.5e-f). Neither *med20-1* nor *med20*Δ single mutant was sensitive to TBZ, but interestingly, we observed only *med20-1*, but not *med20*Δ, was able to suppress the TBZ sensitivity of *dcr1*Δ single mutant. We next checked whether the mutants lost pericentromeric silencing by determining the expression level of *dg/dh* transcripts using RT-qPCR (Fig. 3.5g). Agreeing with previous studies, we found *med20*Δ had an elevated level of *dg/dh* expression; interestingly, we did not observe silencing defects in *med20-1*, and only *med20-1*, but not *med20*Δ was able to reduce the silencing defect of *dcr1*Δ. Thus, the roles of Med20 in pericentromeric silencing and in *dcr1*Δ-induced genome instability were functionally separable, implying the T-R stress-triggering loci lay beyond the centromere. Supporting this idea, we also found that *med20-1* was able to suppress the cellular quiescence phenotype of *dcr1*Δ (Fig. 3.5h), an additional role of Dcr1 that was independent to canonical centromeric function (Roche et al. 2016).

In summary, forward and reverse genetics suggested mis-regulation of Pol II transcription in *dcr1*Δ – and particularly when R-loops accumulated in the *rnh1*Δ *rnh201*Δ background – was the trigger to the replication stress phenotype. Notably, suppressor alleles isolated from the sensitized screen for R-loop dependent Dicer phenotypes pointed to the early steps of transcription – especially the transition from initiation to elongation – being the most critical. We therefore decided to investigate how transcription was mis-regulated using genome-wide approaches.

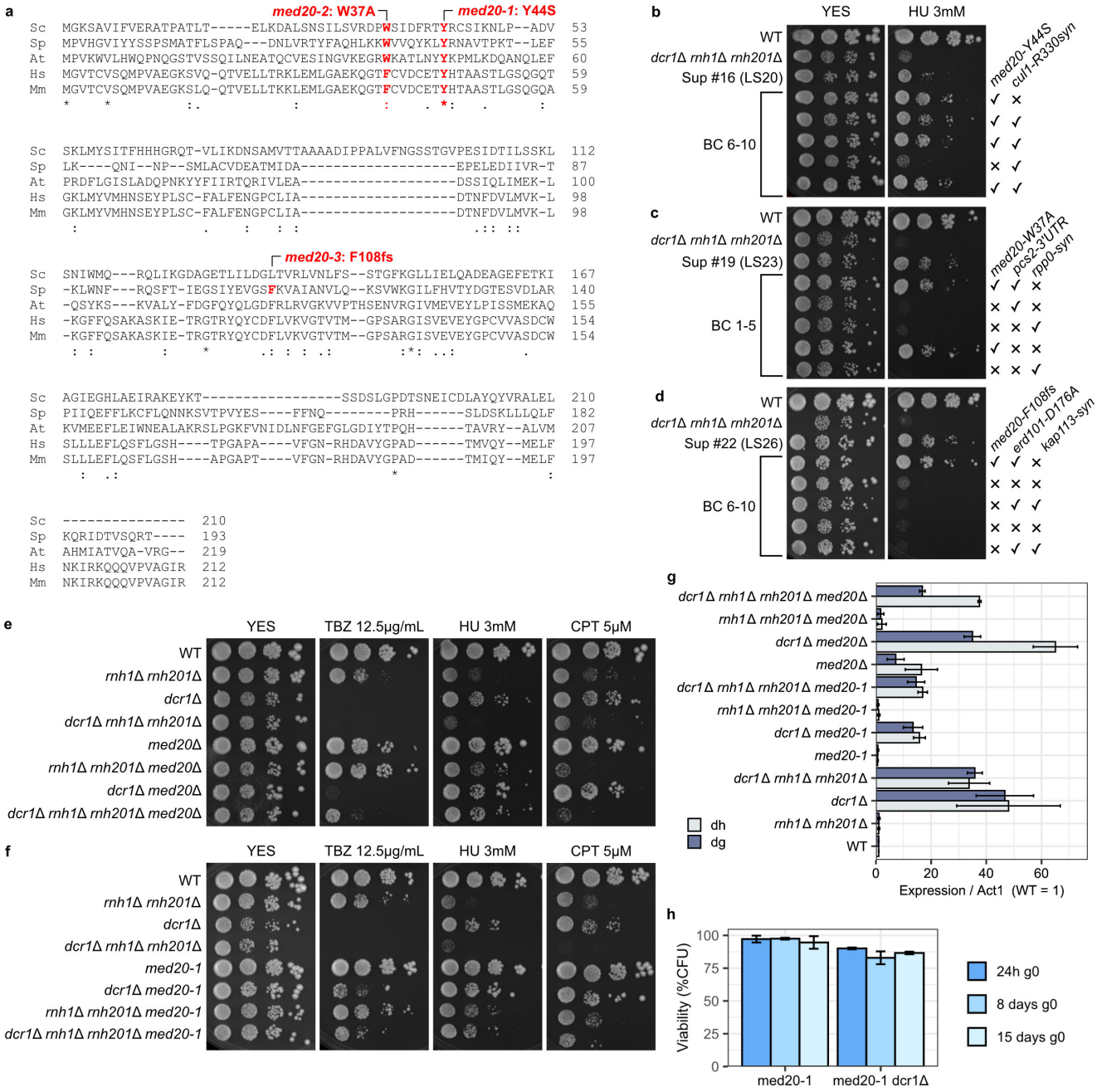
a
med20-2: W37A
med20-1: Y44S
Sc MGKSAVIFVERATPATLT-----ELKDALSNSILSVRDPWSIDFRTYRCSIKNLP--ADV 53
Sp MPVHGVIYYSSPSMATFLSPAQ---DNLVRTYFAQHLKKWVVQYKLYRNAVTPKT--LEF 55
At MPVKWVLHWQPNQGSTVSSQILNEATQCVESINGVKEGRWKATLNYYKPMLKDQANQLEF 60
Hs MGVTCVSQMPVAEGKSVQ-QTVELLTRKLEMLGAEKQGTFCVDCETYHTAASTLGSQGQT 59
Mm MGVTCVSQMPVAEGKSLQ-QTVELLTKKLEMLGAEKQGTFCVDCETYHTAASTLGSQGQA 59
Sc SKLMYSITFHHHGRQT-VLIKDNSAMVTTAAAADIPPALVFNGSSTGVPESIDTILSSKL 112
Sp LK----QNI--NP--SMLACVDEATMIDA-------------------EPELEDIIVR-T 87
At PRDFLGISLADQPNKYYFIIRTQRIVLEA-------------------DSSIQLIMEK-L 100
Hs GKLMYVMHNSEYPLSC-FALFENGPCLIA-------------------DTNFDVLMVK-L 98
Mm GKLMYVMHNSEYPLSC-FALFENGPCLIA-------------------DTNFDVLMVK-L 98
med20-3: F108fs
Sc SNIWMQ---RQLIKGDAGETLILDGLTVRLVNLFS--STGFKGLLIELQADEAGEFETKI 167
Sp -KLWNF---RQSFT-IEGSIYEVGSFKVAIANVLQ--KSVWKGILFHVTYDGTESVDLAR 140
At -QSYKS---KVALY-FDGFQYQLGDFRLRVGKVVPTHSENVRGIVMEVEYLPISSMEKAQ 155
Hs -KGFFQSAKASKIE-TRGTRYQYCDFLVKVGTVTM--GPSARGISVEVEYGPCVVASDCW 154
Mm -KGFFQSAKASKIE-TRGTRYQYCDFLVKVGTVTM--GPSARGISVEVEYGPCVVASDCW 154
Sc AGIEGHLAEIRAKEYKT-----------------SSDSLGPDTSNEICDLAYQYVRALEL 210
Sp PIIQEFFLKCFLQNNKSVTPVYES----FFNQ--------PRH------SLDSKLLLQLF 182
At KVMEEFLEIWNEALAKRSLPGKFVNIDLNFGEFGLGDIYTPQH------TAVRY--ALVM 207
Hs SLLLEFLQSFLGSH----TPGAPA----VFGN-RHDAVYGPAD------TMVQY--MELF 197
Mm SLLLEFLQSFLGSH----APGAPT----VFGN-RHDAVYGPAD------TMIQY--MELF 197
Sc ---------------- 210
Sp KQRIDTVSQRT---- 193
At AHMIATVQA-VRG-- 219
Hs NKIRKQQQVPVAGIR 212
Mm NKIRKQQQVPVAGIR 212
b
YES
HU 3mM
WT
dcr1Δ rnh1Δ rnh201Δ
Sup #16 (LS20)
BC 6-10
med20-Y44S
cul1-R330syn
c
WT
dcr1Δ rnh1Δ rnh201Δ
Sup #19 (LS23)
BC 1-5
med20-W37A
pcs2-3'UTR
rpp0-syn
d
WT
dcr1Δ rnh1Δ rnh201Δ
Sup #22 (LS26)
BC 6-10
med20-F108fs
erd101-D176A
kap113-syn
e
YES
TBZ 12.5µg/mL
HU 3mM
CPT 5µM
WT
rnh1Δ rnh201Δ
dcr1Δ
dcr1Δ rnh1Δ rnh201Δ
med20Δ
rnh1Δ rnh201Δ med20Δ
dcr1Δ med20Δ
dcr1Δ rnh1Δ rnh201Δ med20Δ
f
YES
TBZ 12.5µg/mL
HU 3mM
CPT 5µM
WT
rnh1Δ rnh201Δ
dcr1Δ
dcr1Δ rnh1Δ rnh201Δ
med20-1
dcr1Δ med20-1
rnh1Δ rnh201Δ med20-1
dcr1Δ rnh1Δ rnh201Δ med20-1
g
dcr1Δ rnh1Δ rnh201Δ med20Δ
rnh1Δ rnh201Δ med20Δ
dcr1Δ med20Δ
med20Δ
dcr1Δ rnh1Δ rnh201Δ med20-1
rnh1Δ rnh201Δ med20-1
dcr1Δ med20-1
med20-1
dcr1Δ rnh1Δ rnh201Δ
dcr1Δ
rnh1Δ rnh201Δ
WT
dh
dg
0
20
40
60
Expression / Act1 (WT = 1)
h
Viability (%CFU)
100
75
50
25
0
med20-1
med20-1 dcr1Δ
24h g0
8 days g0
15 days g0

Figure 3.5. Suppression of *dcr1*Δ by *med20* mutations.

(a) Sequence alignment of *med20* from *Saccharomyces cerevisiae* (Sc), *S. pombe* (Sp), *Homo sapiens* (Hs), *Mus musculus* (Mm), and *Arabidopsis thaliana* (At). Alignment was done using Clustal Omega with default setting. SNPs for the three alleles, labeled *med20-1* to *med20-3*, are highlighted in red. *Med20-3* leads to a frameshift at F108, leading to truncation at residue 128.

(b-d) Backcross verification of (b) *med20-1,* (c) *med20-2*, and (d) *med20-3* alleles respectively. Cells were plated with 10-fold dilution on YES plates without supplement or with HU to test for drug sensitivity. SNPs in backcrosses (BC) were tested using dCAPs (see methods).

(e-f) Spot assay to test the suppression activity of (e) *med20*Δ and (f) *med20-1*. Cells were plated with 10-fold dilution on YES plates without supplement or with TBZ or HU to test for drug sensitivity.

(g) RT-qPCR quantification of the expression of *dg/dh* centromeric transcripts in various mutants. Fold change was calculated relative to *Act1* and WT. N = 2 - 3 independent biological replicates. Error bars represent SEM. Note only *med20*Δ but not *med20-1* has silencing defect, and that *med20-1* could mildly suppress silencing defect in *dcr1*Δ.

(h) Viability assay of G_0 entry and quiescence maintenance in prototroph *med20-1* and *med20-1 dcr1*Δ. *dcr1*Δ has severe G_0 entry and maintenance defect (Roche et al. 2016), and *med20-1* was able to almost fully suppress this phenotype of *dcr1*Δ.

3.5 Dcr1 mediates global promoter-proximal pausing in the presence of R-loops

To understand how transcription was affected by *dcr1*Δ in the presence of R-loops, we performed total RNA-seq to quantify gene expression in various mutants. In the *dcr1*Δ single mutant, the *rnh1*Δ *rnh201*Δ double mutant, and the triple mutant, genes were mostly up- rather than down-regulated (Fig. 3.6a). As previously described (Atkinson et al. 2018; Marasovic, Zocco, and Halic 2013), *dcr1* deletion did not drastically change the transcriptome – only 184/6820 (2.7%) of annotated transcripts were significantly upregulated (Fig. 3.6a, orange dots). Annotated centromeric transcripts were reproducibly upregulated in both *dcr1*Δ and the triple mutant (Fig. 3.6a, blue dots). Gene ontology analysis using AnGeLi (Bitton et al. 2015) revealed no specific gene sets being enriched, except for those related to oxidoreductive and core environmental stress. This set of genes was also upregulated in *rnh1*Δ *rnh201*Δ as well as in the triple mutant, and was slightly more deregulated in the triple mutant (Fig. 3.6b,c), suggesting a shared regulatory mechanism that involved both Dcr1 and RNase H. Using DESeq2 (Love et al. 2014) for statistical analyses, we investigated genes that were specifically upregulated in the triple mutant. Even with a relaxed selection criterion ($\log_2$ fold-change >1, adjusted p-value < 10^{-6}), only 15 genes were significantly upregulated (Fig. 3.6d, top panel). Of note, 6 genes (*tef101, tef102, tef103, SPAC29A4.02c, tef3, cpc2*) were linked to translation elongation. Although why elongation was specifically disrupted was unclear, the results suggested that the triple mutant was under translational stress, potentially stemming from disrupted transcription fidelity.

RNA-seq was also performed in various mutants in combination of *med20-1* or *med20*Δ, both being suppressors of the genome stability phenotype of *dcr1*Δ (Fig. 3.5e-f). While we did not find drastic changes to the transcriptome (not shown) – which was surprising considering Med20, being a subunit of Mediator complex, presumably would act globally – we found that both *med20* mutants were able to suppress the upregulation of the genes upregulated in *dcr1*Δ (Fig. 3.6b). The alleles were also able to suppress the genes specifically upregulated in the triple mutant (Fig. 3.6d, middle and bottom panel), although the effect was stronger in *med20-1* than in *med20*Δ.

Overall, the RNA-seq data showed that the disruption of Dcr1 or RNase H did not lead to substantial changes to the transcriptome. Since Dcr1 is involved in sRNA biogenesis, we performed sRNA-seq to see how RNase H mutant would affect the sRNA population. Centromeric sRNA was absent *dcr1*Δ and in the triple mutant, and was not affected in the *rnh1*Δ *rnh201*Δ double mutant, as expected (not shown), agreeing with the RNA-seq results showing de-repression of centromeric transcripts in *dcr1*Δ (Fig. 3.6). As the genetic studies described above suggested transcriptional mis-regulation as underlying the genome stability phenotype, we generated genome-wide profile of all sRNA mapped to all annotated Pol II transcripts (Fig. 3.7a). In mammals, non-productive, R-loop-associated Pol II is terminated at promoter proximal paused site by the Integrator complex (Welsh and Gardini 2023; Xu et al. 2023), releasing short RNA in the process (Stein et al. 2022). We detected a strong peak of sRNA at TSS in WT, reflecting early transcript termination. This promoter-derived sRNA population ranged predominantly between 25 – 40 nt (Fig. 3.7b), broadly agreeing with early termination products (Beckedorff et al. 2020). We did not see any changes to this promoter-derived sRNA in *dcr1*Δ and only a mild decrease in the *rnh1*Δ *rnh201*Δ double mutant, but this population of sRNA was completely absent in the triple mutant (Fig. 3.7a), suggesting its biogenesis depended redundantly on both Dcr1 and RNase H. We also noted in the triple mutant the absence of an sRNA peak at the TTS. sRNA derived from the TTS could represent products from cleavage-based termination; as we noted no substantial changes to Pol II density at TTS in any mutants (see below, Fig. 3.8e), the lack of TTS sRNA peak in the triple mutant could be due to a switch into cleavage-independent termination. As Ago1 is an effector protein that binds sRNA, we also analyzed Ago1-associated sRNA in WT and *dcr1*Δ from data generated in Halic and Moazed, 2010. Curiously, we found that in *dcr1*Δ a prominent peak at TTS emerged (Fig. 3.7c). As sRNA at TTS was present even in the absence of Dcr1 (Fig. 3.7a), we concluded that Dcr1-independent transcription termination generated sRNA that would be loaded into Ago1.

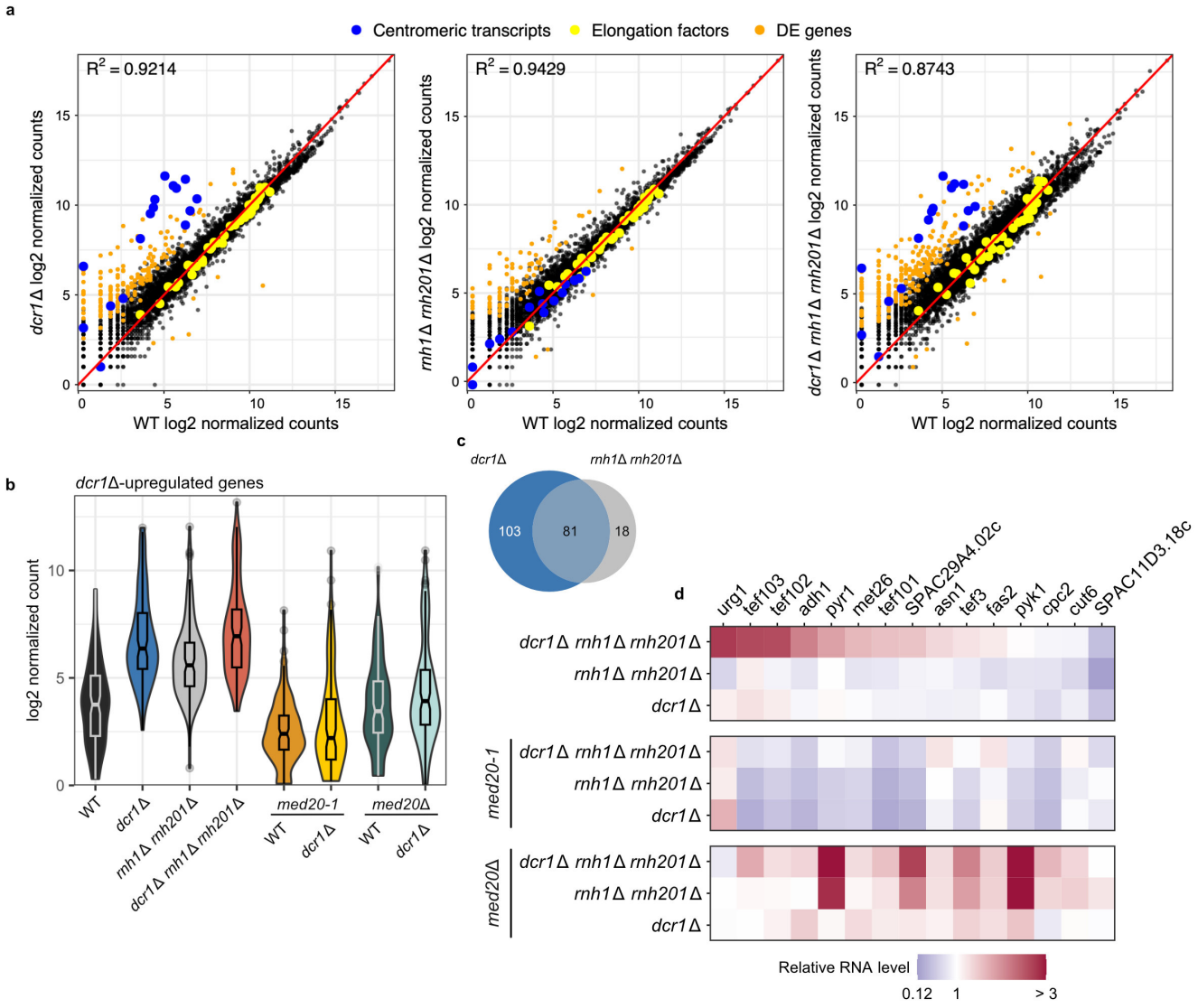
a
Centromeric transcripts
Elongation factors
DE genes
R2 = 0.9214
R2 = 0.9429
R2 = 0.8743
dcr1Δ log2 normalized counts
rnh1Δ rnh201Δ log2 normalized counts
dcr1Δ rnh1Δ rnh201Δ log2 normalized counts
WT log2 normalized counts
b
dcr1Δ-upregulated genes
log2 normalized count
WT
dcr1Δ
rnh1Δ rnh201Δ
dcr1Δ rnh1Δ rnh201Δ
med20-1
med20Δ
c
dcr1Δ
rnh1Δ rnh201Δ
103
81
18
d
urg1
tef103
tef102
adh1
pyr1
met26
tef101
SPAC29A4.02c
asn1
tef3
fas2
pyk1
cpc2
cut6
SPAC11D3.18c
dcr1Δ rnh1Δ rnh201Δ
rnh1Δ rnh201Δ
dcr1Δ
med20-1
med20Δ
Relative RNA level
0.12
1
> 3

Figure 3.6. RNA-seq analyses of *dcr1*Δ mutants in the presence of R-loops.

(a) Correlation of normalized RNA-seq read counts for each gene (N = 6,387) between WT and *dcr1*Δ (left), *rnh1*Δ *rnh201*Δ (middle), and *dcr1*Δ *rnh1*Δ *rnh201*Δ (right). Blue dots indicate centromeric transcripts, defined as annotated genes within the centromere on PomBase. Yellow dots highlight transcription elongation factors (GO:0008023) and termination factors (GO:0006369). Orange dots are significantly differentially expressed genes, defined as Log_2 fold-change > 2, and with adjusted p-values < 0.05.

(b) Violin plot of log_2 normalized expression of *dcr1*Δ upregulated genes in various mutants. *dcr1*Δ upregulated genes were defined as in (a).

(c) Venn diagram of genes upregulated in *dcr1*Δ and in *rnh1*Δ *rnh201*Δ showing a largely overlapping list of genes misregulated in both mutants.

(d) Heatmap showing the relative RNA count, normalized to WT, of 15 genes upregulated specifically in the triple mutant *dcr1*Δ *rnh1*Δ *rnh201*Δ, in various mutants.

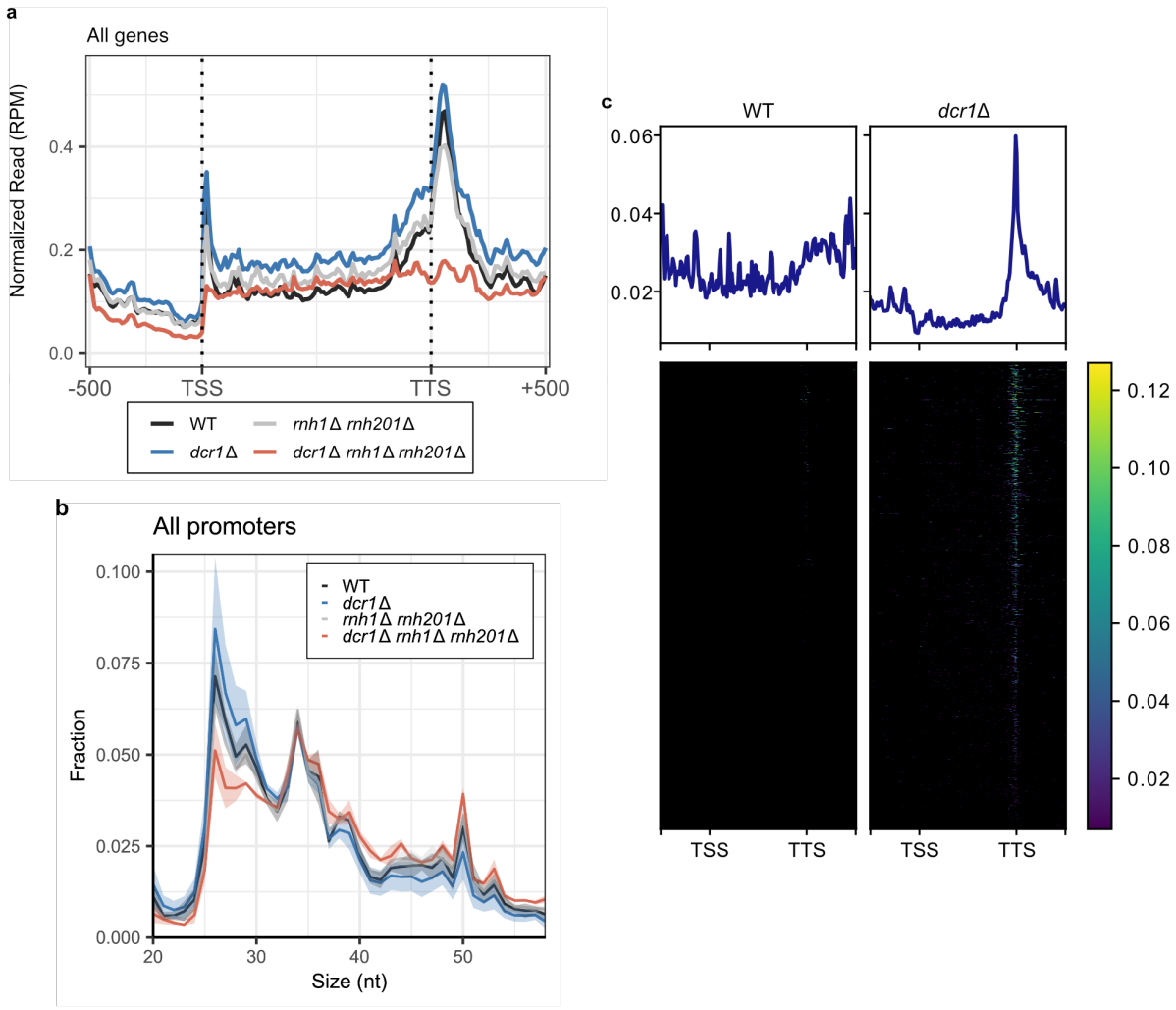

Figure 3.7. Dcr1 and RNase H generate promoter-proximal sRNA.

(a) Profile plot of mean normalized sRNA-seq signal in WT, *dcr1*Δ, *rnh1*Δ *rnh201*Δ, and the triple mutant within gene body ± 500 bp of all annotated genes.

(b) Size distribution of promoter-proximal sRNA in WT, *dcr1*Δ, *rnh1*Δ *rnh201*Δ, and the triple mutant.

(c) Heatmaps of Ago1-associated sRNA signals in WT and *dcr1*Δ at annotated mRNA transcripts ± 500 bp. Values are RPM normalized. Data from Halic and Moazed, 2010.

As the genetic studies described above suggested transcriptional mis-regulation as underlying the genome stability phenotype, and that promoter-proximal sRNA was affected in the triple mutant, we decided to directly study nascent transcription using precision run-on sequencing (PRO-seq) (Mahat et al. 2016). In PRO-seq, a nuclear transcriptional run-on reaction was performed with bulky biotin-NTPs, which led to transcriptional arrest; sequencing biotin-enriched RNA and mapping the first nucleotide would yield a global snapshot of active RNAPs at a near single-nucleotide resolution. In Fig. 3.8a, I generated genome-wide profile of all annotated genes in *S. pombe* in WT, with TSSs updated using the previously published PRO-cap data (Booth et al. 2016). Immediately downstream of the TSS was a prominent peak, corresponding to the promoter-proximal pause site of Pol II, agreeing with previous findings that genes in *S. pombe*, like those in many other higher eukaryotes, are frequently paused (Booth et al. 2016; Chivu et al. 2023). Downstream of annotated TTSs – also known as cleavage and polyadenylation sites (CPSs) – was another broad peak that corresponded to Pol II slowing down for eviction.

Other kinds of transcription behavior can be inferred from PRO-seq data. When the same genome profile was generated for PRO-seq data on *rpb1-T481K*, which we speculated would affect processivity (Fig. 3.4, see above), we observed a progressive decrease in read count along the gene body, as well as an absence of a typical peak downstream of TTS (Fig. 3.8b). This is reminiscent to the "slow" Pol II mutant phenotype (Fong et al. 2015); we speculate these mutants destabilize Pol II, making the holoenzyme less of an obstacle to replication and hence reducing replication stress. The amount of pausing can be quantified by calculating the pausing index (PI), defined as the ratio of the number of reads in the promoter to that of the rest of the gene body (Booth et al. 2016), and as shown in Fig. 3.8c, *rpb1-T481K* had a PI level similar to WT. Similarly, the amount of pausing or slowing down beyond the TTS can be quantified with the termination index (CI) (See methods), which was dramatically reduced in the *rpb1-T481K* mutant (Fig. 3.8d).

When the same genome-wide profile was generated for *dcr1*Δ, *rnh1*Δ *rnh201*Δ, and the triple mutant and compared with WT, we indeed observed more drastic changes to pausing than to termination (Fig. 3.8e-g). In the absence of RNase H, we observed an increase in the amount of pausing, suggesting efficient R-loop processing was required for pause release. This was in agreement with studies in mammalian cells, which showed a positive correlation between R-loop levels and the degree of pausing (Chen et al. 2017). *dcr1*Δ had a WT level of pausing, but the triple mutant, despite having a WT level of paused peak, had a higher amount of reads along the gene body, indicating that Dcr1 prevented unscheduled pause escape, especially when the paused state was triggered by the absence of RNase H. As shown for all annotated genes (Fig. 3.8f,h), deletion of *rnh1* and *rnh201* led to a significant increase of pausing, and further deleting *dcr1* brought the PI below that of WT.

We did not observe any drastic changes to termination (Fig. 3.8g,i), although a slight drop of CI was observed in the triple mutant. A decrease of CI could be due to an elevated read count along the gene body, or a reduction in Pol II density beyond CPS; judging from the profile plot (Fig. 3.8e), we concluded an elevated read count along the gene body better explained the phenotype of the triple mutant. Indeed, after normalizing the PI and CI of each transcript to WT, we observed a more noticeable shift in densities only in PI, but not CI (Fig. 3.8f-g). The pausing defect was more drastic in the top 10% paused genes (Fig. 3.8j), and was correlated with expression level (Fig. 3.8k), supporting a specific role of Dcr1 in pause regulation. From RNA-seq data, we observed no expression level changes to genes involved in transcription elongation and termination (Fig. 3.6a, yellow dots), arguing against the possibility that the pause defect observed here could be due to mis-regulation of such factors.

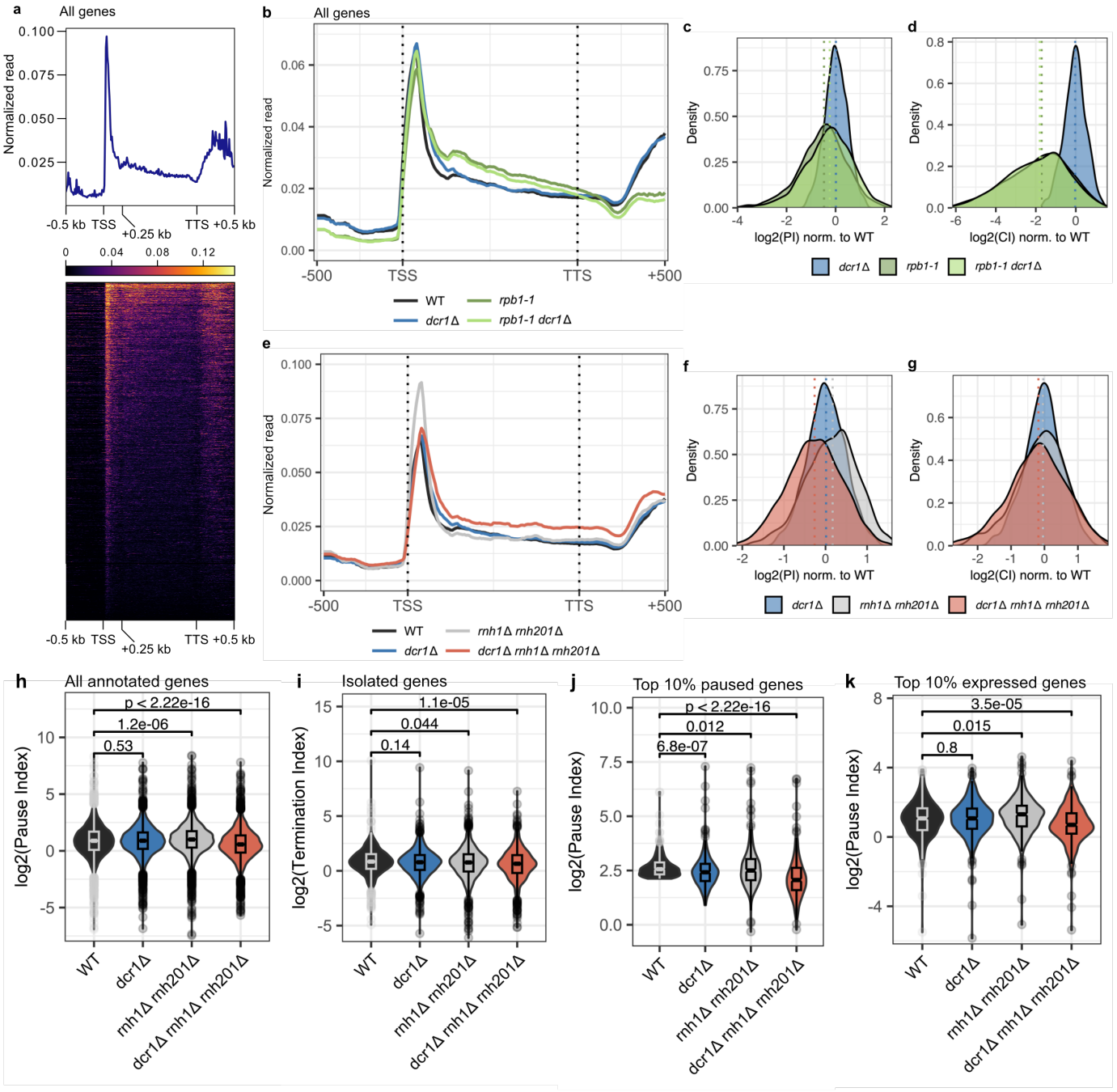
a
All genes
Normalized read
0.100
0.075
0.050
0.025
-0.5 kb TSS
+0.25 kb
TTS +0.5 kb
0
0.04
0.08
0.12
b
All genes
Normalized read
0.06
0.04
0.02
0.00
-500
TSS
TTS
+500
WT
rpb1-1
dcr1Δ
rpb1-1 dcr1Δ
c
Density
0.75
0.50
0.25
0.00
-4
-2
0
2
log2(PI) norm. to WT
d
Density
0.8
0.6
0.4
0.2
0.0
-6
-4
-2
0
log2(CI) norm. to WT
dcr1Δ
rpb1-1
rpb1-1 dcr1Δ
e
Normalized read
0.100
0.075
0.050
0.025
0.000
-500
TSS
TTS
+500
WT
rnh1Δ rnh201Δ
dcr1Δ
dcr1Δ rnh1Δ rnh201Δ
f
Density
0.75
0.50
0.25
0.00
-2
-1
0
1
log2(PI) norm. to WT
g
Density
0.6
0.4
0.2
0.0
-2
-1
0
1
log2(CI) norm. to WT
dcr1Δ
rnh1Δ rnh201Δ
dcr1Δ rnh1Δ rnh201Δ
h
All annotated genes
log2(Pause Index)
p < 2.22e-16
1.2e-06
0.53
10
5
0
-5
WT
dcr1Δ
rnh1Δ rnh201Δ
dcr1Δ rnh1Δ rnh201Δ
i
Isolated genes
log2(Termination Index)
1.1e-05
0.044
0.14
15
10
5
0
-5
WT
dcr1Δ
rnh1Δ rnh201Δ
dcr1Δ rnh1Δ rnh201Δ
j
Top 10% paused genes
log2(Pause Index)
p < 2.22e-16
0.012
6.8e-07
10.0
7.5
5.0
2.5
0.0
WT
dcr1Δ
rnh1Δ rnh201Δ
dcr1Δ rnh1Δ rnh201Δ
k
Top 10% expressed genes
log2(Pause Index)
3.5e-05
0.015
0.8
8
4
0
-4
WT
dcr1Δ
rnh1Δ rnh201Δ
dcr1Δ rnh1Δ rnh201Δ

Figure 3.8. Dicer is required for promoter-proximal pausing in the presence of R-loops.

(a) Heatmap and mean normalized PRO-seq signal of all annotated transcripts in WT. TSSs are adjusted based on published PRO-cap data (Booth *et al.*, 2016).

(b) Profile plot of mean normalized PRO-seq signal of all annotated transcripts in WT, *dcr1*Δ (blue), *rpb1-1* (*rpb1-T481K*) (dark green), and *rpb1-1 dcr1*Δ (light green).

(c,d) Density plot of (c) PIs and (d) CIs of all annotated genes for *dcr1*Δ, *rpb1-1,* and *rpb1-1 dcr1*Δ after normalization to WT. Dotted lines represent median for each genotype.

(e) Profile plot of mean normalized PRO-seq read of all annotated genes in WT, *dcr1*Δ (blue), *rnh1*Δ *rnh201*Δ (grey) and *dcr1*Δ *rnh1*Δ *rnh201*Δ (red). The increase in read counts along the gene body reflects unscheduled PolII release in *dcr1*Δ *rnh1*Δ *rnh201*Δ.

(f,g) Density plot of (f) PIs and (g) CIs of all annotated genes after normalization to WT. Dotted lines represent median for each genotype.

(h) Violin plot of pausing indices (PIs) computed for all annotated genes from PRO-seq data. P-values represent results of one-way ANOVA. See methods for details.

(i) Violin plot of termination indices (CIs) computed from PRO-seq data. P-values represent results of one-way ANOVA. Isolated genes were used to limit confoundment from read counts from neighboring genes. See methods for details.

(j,k) Violin plots of PIs computed for all (j) top 10% paused genes and (k) top 10% expressed genes from PRO-seq data. P-values represent results of one-way ANOVA. Top 10% paused genes were determined from WT PRO-seq data, and top 10% expressed genes were determined from WT RNA-seq data, both generated in this study.

The role of Dcr1 in limiting unscheduled Pol II pause release was consistent with the results from our genetic studies described above. Among all the suppressor alleles, *med20* mutants displayed the strongest suppression; we therefore assessed how *med20-1* would affect nascent transcription dynamics when introduced into *dcr1*Δ and *rnh1*Δ *rnh201*Δ mutants (Fig. 3.9). Introducing *med20-1* into WT led to an increase in PI, and in *dcr1*Δ mutant *med20-1* caused an even more substantial increase in PI (Fig. 3.9b-d). On the contrary, *rnh1*Δ *rnh201*Δ already had elevated pausing, and *med20-1* led to a reduction of PI below that of WT (Fig. 3.9e-g). Finally, we observed no statistical differences in PI between the triple mutant and the quadruple mutant (Fig. 3.9a,h-j), although the gene body Pol II density appeared to be reduced to WT level (Fig. 3.9h) and there was a slight decrease of termination index (Fig. 3.9j). How *med20-1* led to distinct Pol II pause behavior was difficult to infer from the PRO-seq data alone; regardless, it was evident that early transcription was predominantly affected, but not to other stages of the transcription cycle. Additionally, the fact that *med20-1* had opposite effects on pausing in *dcr1*Δ (enhancement) and in *rnh1*Δ *rnh201*Δ (reduction) suggested that promoter-proximal Pol II was affected in a distinct way in each mutant, therefore responding differently when Med20 function was disrupted.

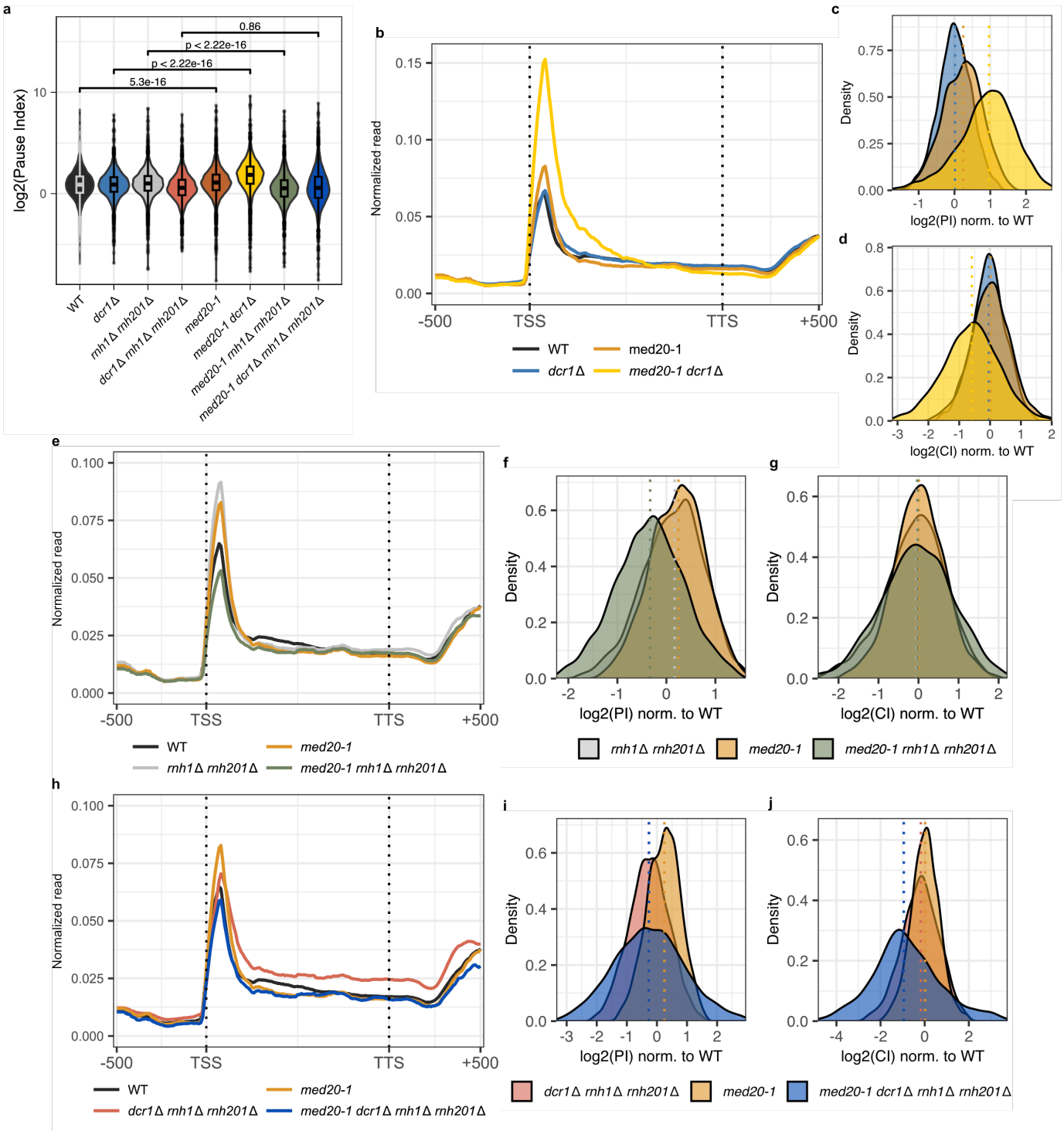
a
log2(Pause Index)
0.86
p < 2.22e-16
p < 2.22e-16
5.3e-16
WT
dcr1Δ
rnh1Δ rnh201Δ
dcr1Δ rnh1Δ rnh201Δ
med20-1
med20-1 dcr1Δ
med20-1 rnh1Δ rnh201Δ
med20-1 dcr1Δ rnh1Δ rnh201Δ
b
Normalized read
-500
TSS
TTS
+500
WT
med20-1
dcr1Δ
med20-1 dcr1Δ
c
Density
log2(PI) norm. to WT
d
Density
log2(CI) norm. to WT
e
Normalized read
WT
med20-1
rnh1Δ rnh201Δ
med20-1 rnh1Δ rnh201Δ
f
Density
log2(PI) norm. to WT
g
Density
log2(CI) norm. to WT
rnh1Δ rnh201Δ
med20-1
med20-1 rnh1Δ rnh201Δ
h
Normalized read
WT
med20-1
dcr1Δ rnh1Δ rnh201Δ
med20-1 dcr1Δ rnh1Δ rnh201Δ
i
Density
log2(PI) norm. to WT
j
Density
log2(CI) norm. to WT
dcr1Δ rnh1Δ rnh201Δ
med20-1
med20-1 dcr1Δ rnh1Δ rnh201Δ

Figure 3.9. Med20 is required for unscheduled Pol II release in *dcr1*Δ in the presence of R-loops.

(a) Violin plot of pausing indices (PIs) computed for all annotated genes from PRO-seq data. P-values represent results of one-way ANOVA. See methods for details.

(b) Profile plot of mean normalized PRO-seq signal of all annotated transcripts in WT, *dcr1*Δ, *med20-1*, and *med20-1 dcr1*Δ.

(c,d) Density plot of (c) PIs and (d) CIs of all annotated genes for *dcr1*Δ, *med20-1,* and *med20-1 dcr1*Δ after normalization to WT. Dotted lines represent median for each genotype.

(e-g) Same as (b-d), except for *rnh1*Δ *rnh201*Δ in combination with *med20-1*.

(h-j) Same as (h-j), except for *dcr1*Δ *rnh1*Δ *rnh201*Δ in combination with *med20-1*. The decrease in read counts along the gene body reflects unscheduled PolII release in *med20-1 dcr1*Δ *rnh1*Δ *rnh201*Δ.

3.6 Ago1 is required for *dcr1*Δ-induced genome instability

As described in previous sections, the genome stability function of Dcr1 appeared independent to its role in pericentromeric silencing. For example, suppressors such as *epl1-T449A* and *rpb2-R1118H* did not confer TBZ resistance to *dcr1*Δ, nor did they lead to silencing defects by themselves (Fig. 2.2, 3.4). Alleles of *med20* also indicated the two functions of Dcr1 were genetically separable (Fig. 3.5). Curiously, although both Dcr1 and Ago1 had been implicated in a separate RNAi-independent pathway in DNA damage checkpoint activation (Carmichael et al. 2004), the rDNA copy loss phenotype was not observed in *ago1*Δ (Castel et al. 2014). We therefore investigated whether the genome instability phenotype of *dcr1*Δ depended on Ago1, and found that only *dcr1*Δ, but not *ago1*Δ, had growth defects in high doses of HU and CPT (Fig. 3.10a). This prompted us to perform further genetic studies on *ago1*.

We first tested whether *ago1* would interact with RNase H in a similar way to that of *dcr1*. We observed no interaction between *ago1*Δ and *rnh1*Δ or *rnh201*Δ individually, but *ago1* deletion suppressed the HU- and CPT-sensitivity of the *rnh1*Δ *rnh201*Δ, acting in the opposite way to *dcr1*Δ, which sensitized the genotoxic drug sensitivity of the double mutant (Fig. 3.10b). It was previously proposed that Ago1 acted downstream of Dcr1 in the regulation of cell cycle checkpoint and cytokinesis (Carmichael et al. 2004), based on the observation that overexpressing Ago1 in *dcr1*Δ, but not vice versa, restored the septation index and resistance to HU. We therefore constructed combinations of mutants with *dcr1*Δ, *ago1*Δ, and *rnh1*Δ *rnh201*Δ (Fig. 3.10c). We observed no negative interaction between *dcr1*Δ and *ago1*Δ, as the double mutant appeared phenotypically identical to *dcr1*Δ. Strikingly, *ago1*Δ was able to repress the ability of *dcr1*Δ to hypersensitize the RNase H mutant *rnh1*Δ *rnh201*Δ to both HU and CPT (Fig. 3.10c). We also investigated how *med20*Δ, as a genome instability suppressor of *dcr1*Δ (Fig. 3.5), would interact with *ago1*Δ under various conditions (Fig. 3.10d). Both *dcr1*Δ and *ago1*Δ, but not *med20*Δ, were acutely sensitive to TBZ, as expected. However, *med20*Δ was able to confer TBZ resistance to *ago1*Δ, but not to *dcr1*Δ. Additionally, *med20*Δ was sensitive to cycloheximide (CHX, see also section 2.8), which was suppressed in double mutants with *dcr1*Δ, but

not *ago1*Δ. These results above suggested Ago1 was required for *dcr1*Δ to sensitize *rnh1*Δ *rnh201*Δ, in contrast to previous reports that Ago1 overexpression suppressed *dcr1*Δ (Carmichael et al. 2004).

As we showed that Dcr1 regulates promoter-proximal Pol II pausing (Fig. 3.8) and sRNA generation (Fig. 3.7), and since Ago1 binds sRNA, we wondered if the localization of Ago1 depended on Dcr1. We performed Ago1 ChIP-seq in *dcr1*Δ alone, the *rnh1*Δ *rnh201*Δ double mutant, as well as the triple mutant. Ago1 accumulated downstream of TSS in WT, and was reduced by *dcr1*Δ and *rnh1*Δ *rnh201*Δ, but was most severe in the triple mutant (Fig. 3.10e). As this coincided with promoter-derived sRNA, we hypothesize that Ago1 is bound by this promoter-derived sRNA, and that the recruitment of Ago1 to the promoter depended on the activity of Dcr1 and RNase H. At TTS, *dcr1*Δ reduced Ago1 recruitment to TTS in an RNase H-independent manner. We speculate this might reflect the role of Dcr1 in transcription termination (Castel et al. 2014).

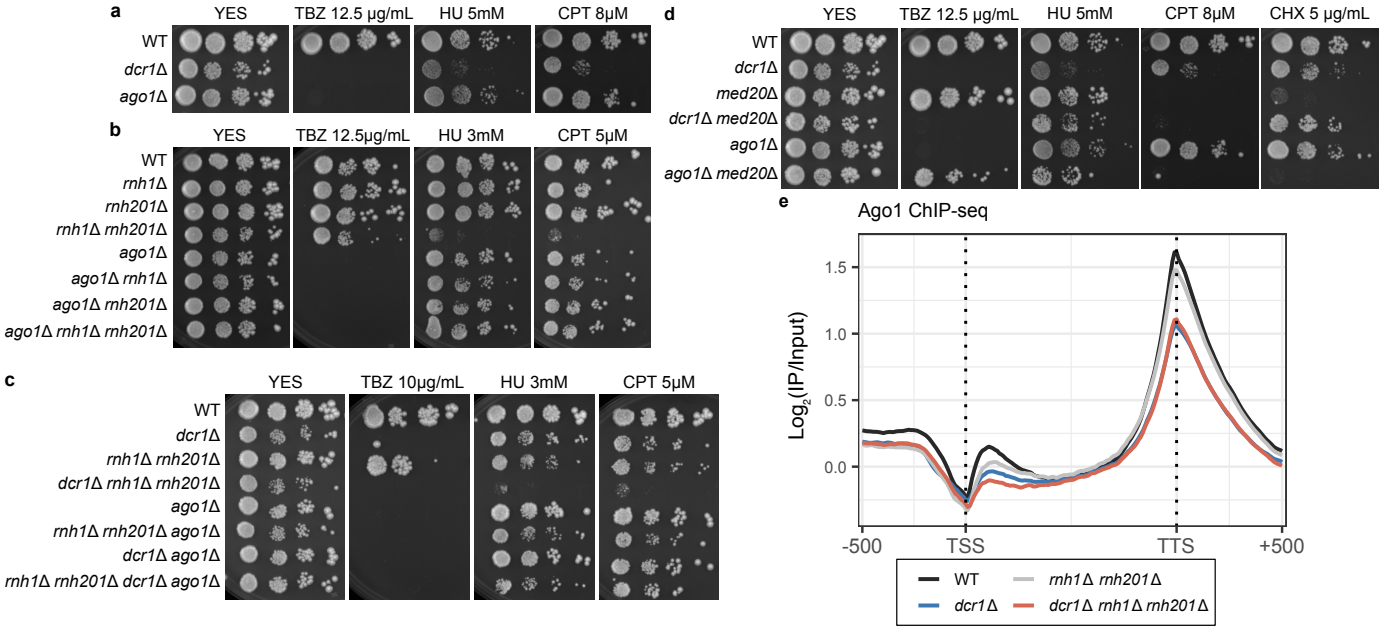

Figure 3.10. *ago1*Δ suppresses *dcr1*Δ-induced genome instability in the presence of R-loops.

(a) Spot assay of WT, *dcr1*Δ, and *ago1*Δ with 10-fold dilution on YES plates without supplement or with TBZ, HU, or CPT and tested for drug sensitivity.

(b) Spot assay of WT and combinations of *rnh1*Δ, *rnh201*Δ, and *ago1*Δ with 10-fold dilution on YES plates without supplement or with varying doses of TBZ, HU, and CPT.

(c) Spot assay of WT and combinations of *rnh1*Δ, *rnh201*Δ, *ago1*Δ, and *dcr1*Δ with 10-fold dilution on YES plates without supplement or with varying doses of TBZ, HU, and CPT.

(d) Spot assay of WT and combinations of *dcr1*Δ, *ago1*Δ, and *med20*Δ with 10-fold dilution on YES plates without supplement or with varying doses of TBZ, HU, and CPT.

(e) Distribution of log2 normalized Ago1 ChIP-seq reads in WT, *dcr1*Δ, *rnh1*Δ *rnh201*Δ, and triple mutant within gene body ± 500 bp of all annotated genes.

3.7 Discussion

Three lines of evidence suggested Dcr1 participates in regulating the early steps of transcription. First, we observed a genome-wide increase of R-loops (Fig. 3.1a), a common co-transcriptional by-product (Brickner et al. 2022); this was also observed in a recent study conducted in mammalian cells (Camino et al. 2023). Second, both forward and reverse genetic studies (Figs. 3.3-5) identified multiple alleles implicated in early transcription, including the TATA-binding protein *tbp1*; subunits of mediator including *med31* and *med20* (*med15* in the suppressor LS28 was not verified); *epl1*, a subunit of the Piccolo NuA4 acetyltransferase complex, implicated in promoter H4 acetylation (see Section 2.5); *fcp1*, a phosphatase that removes pS2 at Pol II CTD, the mark that is associated with elongating Pol II; and *tfa2*, the small subunit of the TFIIE complex involved in stimulating promoter escape. Third, PRO-seq analyses of nascent transcription dynamics revealed modifications in promoter-proximal pausing, but relatively little change in termination behavior (Fig. 3.8). This was further supported by *med20-1*, a Dcr1 suppressor, having dramatically enhanced pausing especially in *dcr1*Δ (Fig. 3.9).

In the triple mutant *dcr1*Δ *rnh1*Δ *rnh201*Δ, cells became elongated and often with multiple septa and nuclei (Fig. 3.1d). One explanation for the replication phenotypes therefore, could be defective cell cycle checkpoint enactment, potentially leading to mitotic progression before DNA synthesis was complete. This is indeed well documented in RNAi mutants (Carmichael et al. 2004; Kloc et al. 2008) and while we could not completely rule out its contribution in this study, this was unlikely to be the main cause for several reasons. First, while both *dcr1*Δ and *ago1*Δ were checkpoint defective, only *dcr1*Δ was sensitive to a high dose of genotoxic drugs (Fig. 3.10a). Additionally, only *dcr1*Δ, but not *ago1*Δ, negatively interacted with *rnh1*Δ *rnh201*Δ (Fig. 3.10b), ruling out the possibility that both performed identical functions in the same pathway. In fact, that *ago1*Δ was able to partially suppress the triple mutant phenotype (Fig. 3.10c) implicated Ago1 as being required for the *dcr1*Δ phenotype to manifest. Together with the previous finding that *ago1*Δ, unlike that of *dcr1*Δ, did not

lose rDNA copies over meiotic generations (Castel et al. 2014), we therefore concluded that defective checkpoint regulation alone was insufficient to explain the data presented in this study.

The fact that the role of Dcr1 in pause release was only revealed in the presence of certain genetic backgrounds (e.g., *rnh1*Δ *rnh201*Δ or *med20-1*) implied that Dcr1, unlike GTFs, did not actively engage in normal transcription initiation, but rather impacted specific situations in which the transcription machinery became pathological, that which may therefore became an obstacle to replication stress. In the RNase H-defective background, the initiation-to-elongation process was hampered, leading to an increase in pausing. This appeared to require Dcr1, as the triple mutant had a WT level of pause peak, but an excess gene-body run on. We therefore hypothesize Dcr1 resolves pathologically arrested Pol II around the promoter, thereby limiting its contribution as an obstacle to replication. This explains that i) in *tfa2-L238**, an overall decrease in TFIIH-mediated elongation stimulation compensated for the loss of inhibition in *dcr1*Δ; ii) in *med20-1*, the mechanism was similar to that of *tfa2-L238**, except that it probably acted upstream, reducing the conversion efficiency of PIC to initially transcribing complex (ITC) (Hantsche and Cramer 2017). This explains also the decrease in pausing in *med20-1 rnh1*Δ *rnh201*Δ as there was overall less initiation. It should be noted that the interactions are likely dynamic and complex. Indeed, the Med8/18/20 submodule is known to interact with TFIIE and TFIIH, therefore playing a direct role in stimulating elongation (Rengachari et al. 2021), although a recent structural study provided evidence that the TFIIE/H complex traveled with Pol II beyond initiation, only dissociating when the pausing factors DSIF and NELF were recruited (Zhan et al. 2023). Finally, iii) in *rpb1-T481K* and *rpb2-R1118H*, alleles that directly affected the Pol II catalytic core, replication stress was reduced by reducing the stability and/or processivity of Pol II. This was supported by the PRO-seq data showing a gradual decrease in gene body signal, as well as a drastic decrease in termination peak. Hence, despite pathological elongation in the absence of Dcr1, Pol II was less of an obstacle to the replication fork.

First documented in the 1980s (Rougvie and Lis 1988), promoter-proximal pausing is now known to be a critical checkpoint to regulate gene expression (Core and Adelman 2019). It involves Pol II being actively held in a transcriptionally poised state by associating with the negative elongation factor (NELF) and the DRB sensitivity-inducing factor (DSIF) complexes (Core and Adelman 2019). Pol II is then either licensed into productive elongation through the action of the P-TEFb complex, or terminated via a recently described function of the Integrator complex, of which the INTS11 subunit mediates RNA endonucleolytic cleavage, releasing Pol II (Beckedorff et al. 2020; Stein et al. 2022; Xu et al. 2023). A recent PRO-seq study across the tree of life provided insight into the similarities and differences of pausing behavior among species (Chivu et al. 2023). In many animals including humans and mice, the pause peaks are focused, peaking at around 20 – 60 bp downstream of TSSs; this is correlated with the presence of a metazoan-specific NELF complex. In species without NELF, including *S. pombe* and *Zea mays*, pausing still occurs and is mediated by the eukaryotic-specific DSIF and pTEF-b complexes, although the peaks are broader and further downstream of the promoter (~100 bp in our data). Since most recent structural studies were conducted using human (and *Sus scrofa*) proteins and promoter templates, and that a structural study of paused Pol II – especially that in the absence of NELF, and in *S. pombe* is still lacking, how the TSS-pause site distance influences GTF dynamics beyond initiation, and therefore how Dcr1 would fit in the scenario, remains uncertain. Nevertheless, given that the promoter architecture of *S. pombe* is highly similar to that of other higher eukaryotes (Schwer et al. 2009; Yang and Ponticelli 2012), unlike that of *S. cerevisiae*, in which PICs universally scan downstream of promoters for TSSs (Qiu et al. 2020), we believe the observations from structural studies are valid in explaining our results. The fact that *S. cerevisiae* lacks both pausing and Dicer also leads us into speculating that this function of Dcr1 is conserved among other eukaryotes.

How might Dcr1 function in promoter-proximal processes? We note multiple parallel characteristics between Dcr1 and Integrator. First, Integrator is recruited to promoter-proximally paused Pol II (Fianu et al. 2021), and in human cells DICER cooperates with BRCA1 and AGO1/2 to

generate small RNA at Pol II pause sites (Hatchi et al. 2021), suggesting DICER is also recruited to paused Pol II. This is further supported by our observation that Dcr1 regulates pausing at Pol II loci. Second, Integrator is shown to stably interact with the heterotrimeric complex sensor of single-stranded DNA (SOSS), which contains the ssDNA-binding protein SSB1 (Xu et al. 2023); Integrator is therefore proposed to be recruited to promoter-proximal R-loops, via its displaced ssDNA strand. Human DICER, too, has been shown to bind and cleave R-loops (Camino et al. 2023); *S. pombe* Dcr1 also binds to R-loops (Fig. 3.1b-c), though we did not observe any cleavage activity. Therefore, both Dicer and Integrator share common mechanism in its recruitment. Third, Integrator terminates paused Pol II via a cleavage mechanism, generating short RNA in the process (Beckedorff et al. 2020). Our results indicate that promoter-proximal sRNA is dependent partly on a functional Dcr1, broadly agreeing with human DICER cleaving R-loops (Camino et al. 2023) and generating sRNA at paused sites (Hatchi et al. 2021). Lastly, the Pol II removal function of Integrator has been shown to limit R-loop-induced replication stress (Bhowmick et al. 2023), parallel to our finding that Dcr1 limits replication stress when R-loops accumulate. Therefore, we propose Dcr1 in *S. pombe* is the functional equivalent of the Integrator complex in higher eukaryotes, terminating pathological Pol II at the promoter and generating sRNA in the process. Indeed, in *C. elegans*, Integrator is implicated in the biogenesis of piRNA by terminating promoter-proximally paused Pol II (Beltran et al. 2021), suggesting an intimate connection between early RNAP termination and RNAi.

Chapter 4: Characterization of genome instability phenotype in *dcr1*Δ

4.1 Summary

In the previous chapter, we found that deleting Dcr1 causes hypersensitivity to genotoxic stress in RNase H-deficient cells which accumulate pathological R-loops. Genetic and genomic evidence implicated Dcr1 in regulating promoter proximal pausing in the presence of R-loops, which also accumulate in Dicer mutants. Here, we implicate the helicase domain of Dicer in this essential catalytic function and investigate the consequences for DNA replication and repair. In the absence of Dcr1, DNA breaks accumulated around transcription start sites (TSSs) rather than around replication origins, and DNA replication processivity and speed were impaired in a manner dependent on transcriptional activity and directionality. Our results demonstrate a novel nuclear function of Dcr1 inresolving transcription-replication conflicts, which we speculate to be ancestral before being co-opted into the RNAi pathway.

4.2 Introduction

In Chapter 3 we showed that Dcr1 limits transcription-induced replication stress especially when R-loops accumulate, but mechanistically how this is achieved is unclear. In particular, previous studies showed that *dcr1-5* – an RNase III catalytic dead allele – had no defects in rDNA copy maintenance, unlike *dcr1*Δ which caused progressive loss of rDNA (Castel et al. 2014). On the other hand, as described in Section 1.2, the Archaeal Hef helicase is thought to be the closest homolog to the helicase domain of Dcr1; this suggested a possibility that the helicase domain could be involved in the genome stability function of Dcr1. In parallel, the consequences to genome stability – other than a progressive loss of rDNA copies – are poorly understood. To address these questions, in this chapter I investigate how Dcr1 mediates its genome maintenance function via a domain deletion study, and the consequence to genome stability in *dcr1*Δ by using multiple genomic, genetic, and molecular techniques. Given the role of Dcr1 in mediating the transcriptional process described in Chapter 3, we

also study how replication is impaired in scenarios where transcription activity is high, and in the case of *rnh1*Δ *rnh201*Δ, where pathological R-loops impede replication.

4.3 Domain analyses of the genome maintenance function of Dcr1

To investigate which domains and/or catalytic functions of Dcr1 are critical for its genome maintenance role, we created various *dcr1* mutants (Fig. 4.1a), including the deletions of the N-terminal helicase domain (*ΔHel*), the DUF283 domain (*ΔDUF*), the PAZ domain (*ΔPAZ*, Fig. 4.1b), as well as the C-terminal 103 amino acids (ΔC103) containing a dsRBD domain as well as a nuclear retention signal (Barraud et al. 2011); we also generated *dcr1-K38R* and *dcr1-K38A*, disrupting the conserved DExD helicase Walker A motif and inhibiting ATP hydrolysis and binding, respectively (MacRae et al. 2006).

In all alleles tested, pericentromeric silencing was lost, as determined by RT-qPCR measurement of *dg/dh* transcript levels (Fig. 4.1c), and cells were TBZ-sensitive to varying degrees (Fig. 4.1d), indicating that an intact, functional Dcr1 was required for proper centromeric function. Unexpectedly, *dcr1-K38A*, but neither *dcr1-K38R* nor *dcr1-ΔHel*, caused acute CPT sensitivity (Fig. 4.1d). We validated the result with strains generated independently (Fig. 4.2a), and it was further verified with backcross (Fig. 4.2b). As the helicase deletion did not have a CPT phenotype, *dcr1-K38A* thus likely represented a dominant negative allele.

Given the CPT-sensitivity phenotype, we next evaluated the genome instability phenotype of *dcr1-K38A* with the rDNA copy number maintenance assay (Castel et al. 2014). F0 mutants were created fresh via transformation and crossed to generate F1-3 progeny following successive meioses. rDNA copy number was estimated by DNA-qPCR normalizing to Act1. As shown, whereas *dcr1-K38R* displayed a maintenance profile similar to that of WT, *dcr1-K38A* led to a rapid loss of rDNA copy over meiotic generations (Fig. 4.2c). Comparing rDNA copy number between F0 and F3, *dcr1-K38A*

displayed the most severe loss of rDNA copy, even more than *dcr1*Δ (Fig. 4.2d), again suggestive of a dominant phenotype.

We next performed PRO-seq with the helicase mutants, and we found a pausing defect only in *dcr1-K38A*, but not *dcr1-K38R* (Fig. 4.2e-f) and no significant termination defect (Fig. 4.2g), phenocopying the triple mutant (Fig. 3.9b, e). We introduced *med20*Δ into *dcr1-K38R/A* and observed a suppression of only *dcr1-K38R* but not *dcr1-K38A* (Fig. 4.2h). This suppressibility further supported our conclusion that the helicase activity of Dcr1 was involved in genome maintenance, and that the *dcr1-K38A* allele was dominant negative.

The PRO-seq results and the genetic interaction with *med20*Δ pointed to the possibility that the helicase of Dcr1 might be responsible for the R-loop-induced genome instability as observed in the triple mutant under genotoxic stress (Fig. 3.1e-f). To test this, we introduced *rnh1*Δ *rnh201*Δ in various *dcr1* mutants (Fig. 4.3). Whereas *dcr1-K38R* and *dcr1-K38A* indeed interacted negatively with *rnh1*Δ *rnh201*Δ, similar interaction was also observed in all the other alleles tested, including *dcr1-5*. Therefore, the helicase activity alone was insufficient, though required, for the role of Dcr1 in protecting against R-loop-induced genome instability, and that the transcriptional stress induced by *dcr1-K38A*, as manifested in the dominant phenotype of CPT sensitivity, was distinct from the stress when R-loops accumulated.

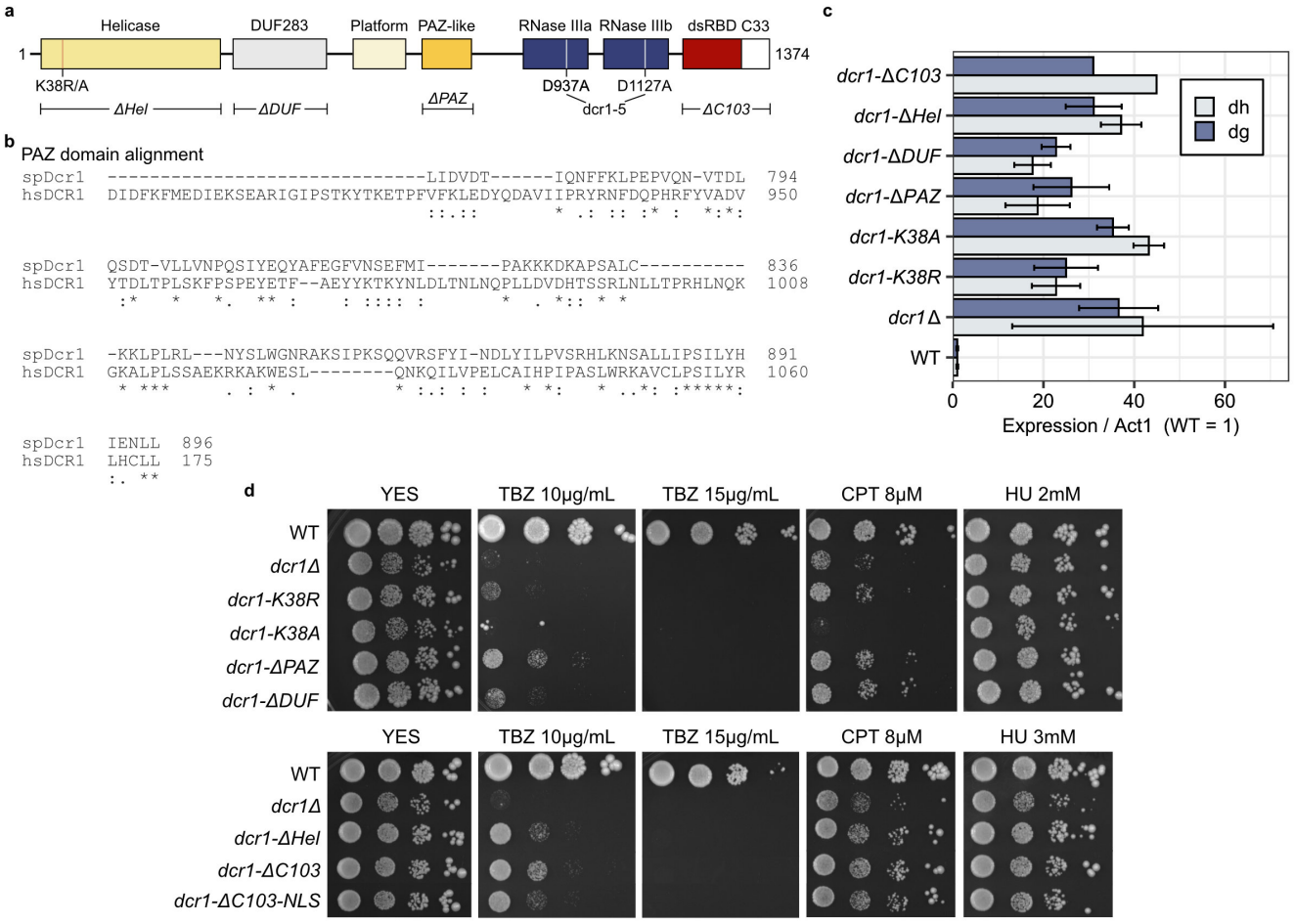
a
Helicase
DUF283
Platform
PAZ-like
RNase IIIa
RNase IIIb
dsRBD C33
1
1374
K38R/A
D937A
D1127A
dcr1-5
ΔHel
ΔDUF
ΔPAZ
ΔC103
b
PAZ domain alignment
spDcr1 -----------LIDVDT------IQNFFKLPEPVQN-VTDL 794
hsDCR1 DIDFKFMEDIEKSEARIGIPSTKYTKETPFVFKLEDYQDAVIIPRYRNFDQPHRFYVADV 950
spDcr1 QSDT-VLLVNPQSIYEQYAFEGFVNSEFMI-------PAKKKDKAPSALC---------- 836
hsDCR1 YTDLTPLSKFPSPEYETF--AEYYKTKYNLDLTNLNQPLLDVDHTSSRLNLLTPRHLNQK 1008
spDcr1 -KKLPLRL---NYSLWGNRAKSIPKSQQVRSFYI-NDLYILPVSRHLKNSALLIPSILYH 891
hsDCR1 GKALPLSSAEKRKAKWESL--------QNKQILVPELCAIHPIPASLWRKAVCLPSILYR 1060
spDcr1 IENLL 896
hsDCR1 LHCLL 175
c
dcr1-ΔC103
dcr1-ΔHel
dcr1-ΔDUF
dcr1-ΔPAZ
dcr1-K38A
dcr1-K38R
dcr1Δ
WT
dh
dg
0
20
40
60
Expression / Act1 (WT = 1)
d
YES
TBZ 10μg/mL
TBZ 15μg/mL
CPT 8μM
HU 2mM
WT
dcr1Δ
dcr1-K38R
dcr1-K38A
dcr1-ΔPAZ
dcr1-ΔDUF
YES
TBZ 10μg/mL
TBZ 15μg/mL
CPT 8μM
HU 3mM
WT
dcr1Δ
dcr1-ΔHel
dcr1-ΔC103
dcr1-ΔC103-NLS

Fig. 4.1. Domains of Dcr1 required for genome stability.

(a) Domain architecture of *S. pombe* Dcr1, highlighting the mutants used in this study. Not drawn to scale.

(b) Sequence alignment between human Dicer (hsDCR1) and putative *S. pombe* Dcr1 (spDcr1), which is deleted in the allele *dcr1-ΔPAZ*.

(c) RT-qPCR quantification of the expression of *dg/dh* centromeric transcripts in various *dcr1* alleles. Fold change was calculated relative to *Act1* and WT. N = 3 independent biological replicates. Error bars represent SEM. All *dcr1* alleles lost silencing, indicating the entire *dcr1* was important for centromeric function.

(d) Spot assay of various *dcr1* alleles. Cells were plated with 10-fold dilution on YES plates without supplement or with TBZ, CPT, or HU to test for drug sensitivity. All *dcr1* alleles were sensitive to TBZ, although to slightly varying extent. Note only *dcr1-K38A* was acutely sensitive to CPT, worse than *dcr1*Δ.

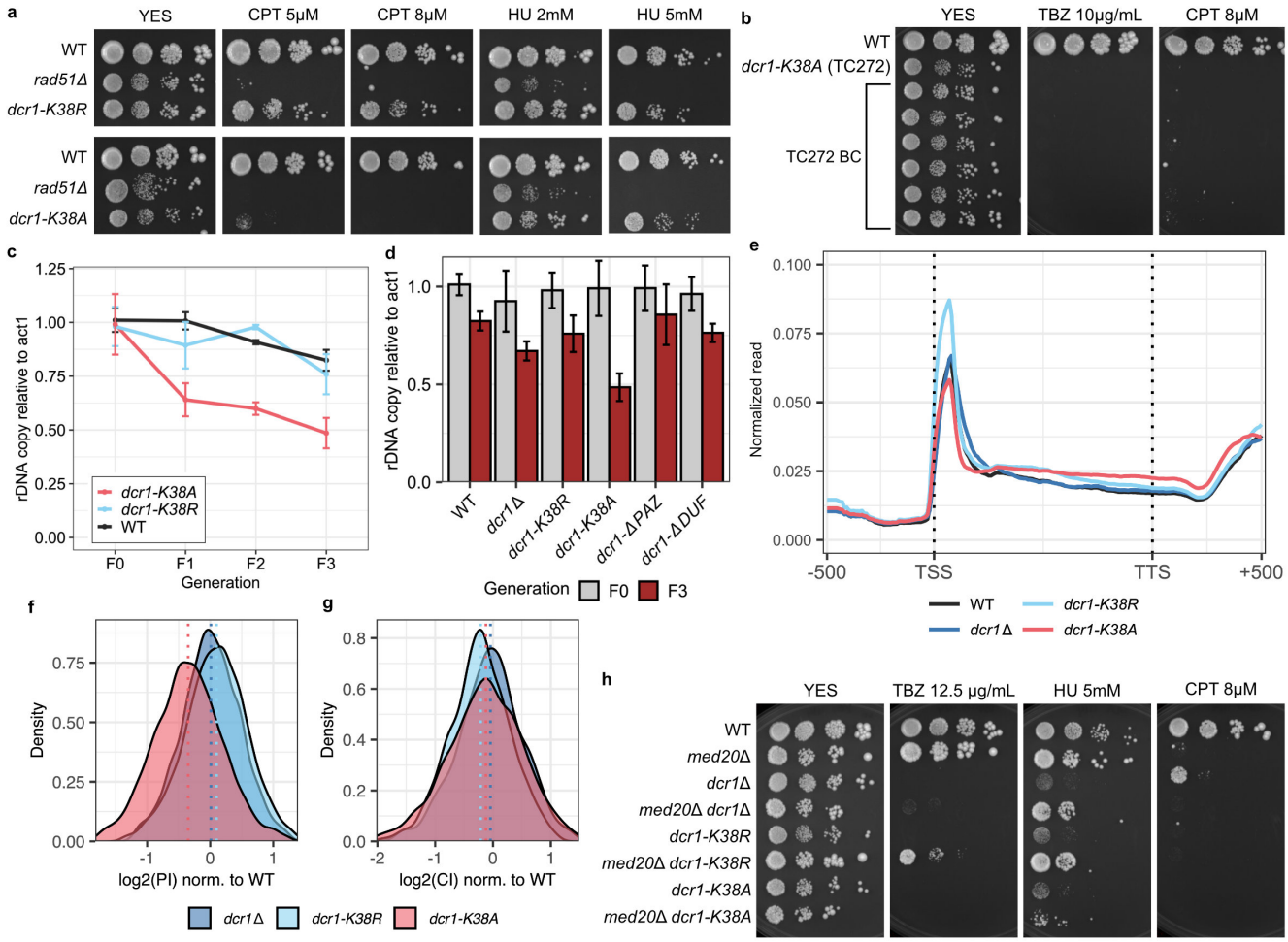
a
YES
CPT 5μM
CPT 8μM
HU 2mM
HU 5mM
WT
rad51Δ
dcr1-K38R
WT
rad51Δ
dcr1-K38A
b
YES
TBZ 10μg/mL
CPT 8μM
WT
dcr1-K38A (TC272)
TC272 BC
c
rDNA copy relative to act1
1.25
1.00
0.75
0.50
0.25
0.00
dcr1-K38A
dcr1-K38R
WT
F0
F1
F2
F3
Generation
d
rDNA copy relative to act1
1.0
0.5
0.0
WT
dcr1Δ
dcr1-K38R
dcr1-K38A
dcr1-ΔPAZ
dcr1-ΔDUF
Generation
F0
F3
e
Normalized read
0.100
0.075
0.050
0.025
0.000
-500
TSS
TTS
+500
WT
dcr1-K38R
dcr1Δ
dcr1-K38A
f
Density
0.75
0.50
0.25
0.00
-1
0
1
log2(PI) norm. to WT
g
Density
0.8
0.6
0.4
0.2
0.0
-2
-1
0
1
log2(CI) norm. to WT
dcr1Δ
dcr1-K38R
dcr1-K38A
h
YES
TBZ 12.5 μg/mL
HU 5mM
CPT 8μM
WT
med20Δ
dcr1Δ
med20Δ dcr1Δ
dcr1-K38R
med20Δ dcr1-K38R
dcr1-K38A
med20Δ dcr1-K38A

Fig. 4.2. The helicase domain of Dcr1 contributes to pausing and genome stability.

(a) Spot assays of WT, *dcr1-K38R*, and *dcr1-K38A* on YES plates without supplement or with varying concentrations of CPT and HU. *Rad51*Δ serves as positive control.

(b) Backcross analysis of TC272, a strain carrying the *dcr1-K38A* allele alongside a cassette conferring hygromycin resistance. Hygromycin-resistant colonies were selected from backcross and the SNP for *dcr1-K38A* was confirmed using dCAPs

(c) qPCR quantification of relative rDNA copy number (WT F0 = 1) in WT, *dcr1-K38R*, and *dcr1-K38A* over meiotic generations.

(d) qPCR quantification of relative rDNA copy number (WT F0 = 1) in various *dcr1* alleles in F0 and F3 generation.

(e) Heatmap and mean normalized PRO-seq signal of all annotated transcripts in WT, *dcr1*Δ, *dcr1-K38R*, and *dcr1-K38A*.

(f-g) Density plot of (f) PIs and (g) CIs of all annotated genes in *dcr1*Δ, *dcr1-K38R*, and *dcr1-K38A* after normalization to WT. Dotted lines represent median for each genotype.

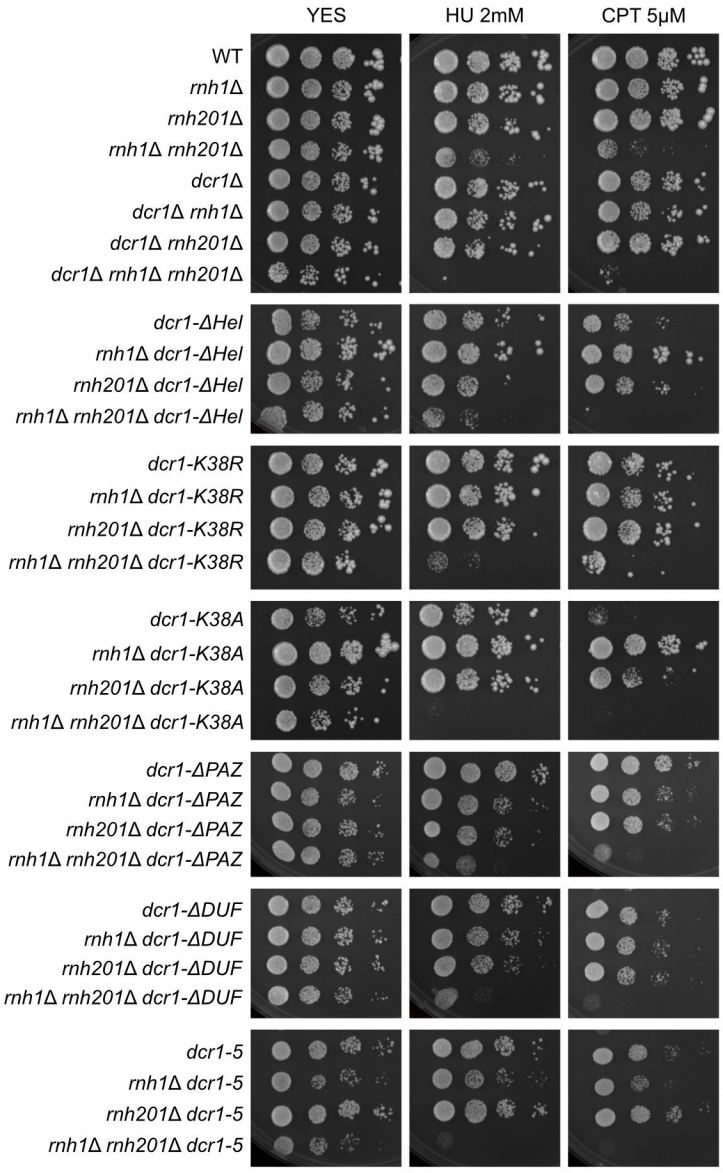

Fig. 4.3. Domains of Dcr1 required for resistance to replication stress in the presence of R-loops. Spot assays of various *dcr1* alleles crossed to *rnh1*Δ and *rnh201*Δ. Cells were plated with 10-fold dilutions on YES plates without supplement or with HU or CPT to test for drug sensitivity. All *dcr1* alleles negatively interacted with *rnh1*Δ *rnh201*Δ, including the *dcr1-5* allele, suggesting the function from an intact Dcr1 was required for genome maintenance.

4.4 DNA damage accumulates at promoters in the absence of Dcr1

All the evidence presented above suggested that Dcr1 modulates nascent transcription dynamics to limit replication stress; we next investigated the consequences of genome instability in *dcr1*Δ. Phosphorylated histone H2A.X (γH2A.X) is one of the earliest responses to DNA damage (Nakamura et al. 2004; Rogakou et al. 1998), and we prepared chromatin immunoprecipitation followed by sequencing (ChIP-seq) libraries to probe for DNA damage genome-wide. Aligning the reads from both H2A and γH2A.X ChIP-seq to all annotated genes, we observed a trough upstream of TSS, corresponding to the nucleosome-depleted region (NDR) (Lantermann et al. 2010), though the +1 and -1 nucleosomes were not easily detectable via meta-analysis of ChIP sequencing data. After normalizing γH2A.X with H2A, we found an enrichment of phosphorylation over the H2A upstream of TSSs in *dcr1*Δ, *rnh1*Δ *rnh201*Δ, as well as in the triple mutant *dcr1*Δ *rnh1*Δ *rnh201*Δ (Fig. 4.4a), indicating persistent DNA damage around promoters.

We further investigated the nature of damage with GLOE-seq (genome-wide ligation of 3'-hydroxy (OH) ends followed by sequencing) (Sriramachandran et al. 2020). GLOE-seq is a technique that permits the detection of free 3'-OH nicks in the genome at a single-nucleotide resolution. In native genomic DNA (gDNA), the method detects both single-strand breaks (SSBs) as well as DSBs. On a genome-wide level, we observed a genome-wide increase in DNA breaks in the triple mutant (Fig. 4.4b). Aligning the reads sense or antisense to transcription, we observed in both WT and all mutants, there was a peak of DNA breaks downstream of pause sites in the sense direction. In the triple mutant, however, an additional peak accumulated upstream of the pause site, suggesting an increase in SSB along the transcription direction.

Okazaki fragments are an important physiological source of DNA nicks during replication, and in *S. cerevisiae* GLOE-seq was used in a DNA ligase depleted ($cdc9^{AID}$) background to enrich for lagging strand bias for origin mapping; in the ligase-proficient WT background, a leading strand bias

of breaks was observed instead (Sriramachandran et al. 2020). The authors attributed it to the fact that the leading strand DNAP Pol ε had a higher ribonucleotide misincorporation rate, and the removal of these ribonucleotides created nicks that could be sequenced. As *S. pombe* has no sequence-defined origin of replication, we compared the GLOE-seq data to a recently published Orc4 ChIP-seq dataset (Masuda et al. 2020). Strand bias of breaks can be quantified with the replication fork directionality (RFD) index, defined as the ratio of excess reverse strand read (Crick strand) to the total amount of reads within a genomic region; in this case, a positive RFD value downstream of an origin indicates excess DNA nicks from the lagging strand.

Calculating the RFD index indeed revealed a discernible pattern genome-wide (Fig. 4.4c). Comparing RFD around Orc4 peaks showed that *S. pombe*, unlike budding yeast, had a lagging strand bias (Fig. 4.4c). The bias was much less obvious in the triple mutant (Fig. 4.4c), and when RFD around all the annotated origins at oriDB (Siow et al. 2012) were aggregated, the triple mutant indeed displayed an RFD profile with a lower overall magnitude (Fig. 4.4d). This could be due to at least three reasons: a decrease in the amount of lagging strand breaks, an increase in leading strand breaks, or an overall decrease in the amount of replicative activity contributing to DNA breaks. Interestingly, we also observed a drastic leading strand bias immediately downstream of origins in WT (Fig. 4.4d), that was abrogated in both the *rnh1*Δ *rnh201*Δ and the triple mutant.

Taken together, our GLOE seq results indicate that DNA breaks accumulate on leading and lagging strands during replication, even in the presence of pathological R-loops induced in RNaseH mutants. In the absence of Dicer, however, breaks accumulate at promoters instead, accompanied by phosphorylated histone H2A.X. One interpretation of these results is that Dicer is required to process replication forks that have been stalled by R-loops resulting from TRCs. In the absence of Dicer, these forks collapse resulting in genome-wide replication stalling and repair by homologous recombination, accompanied by phosphorylation of histone H2A.X.

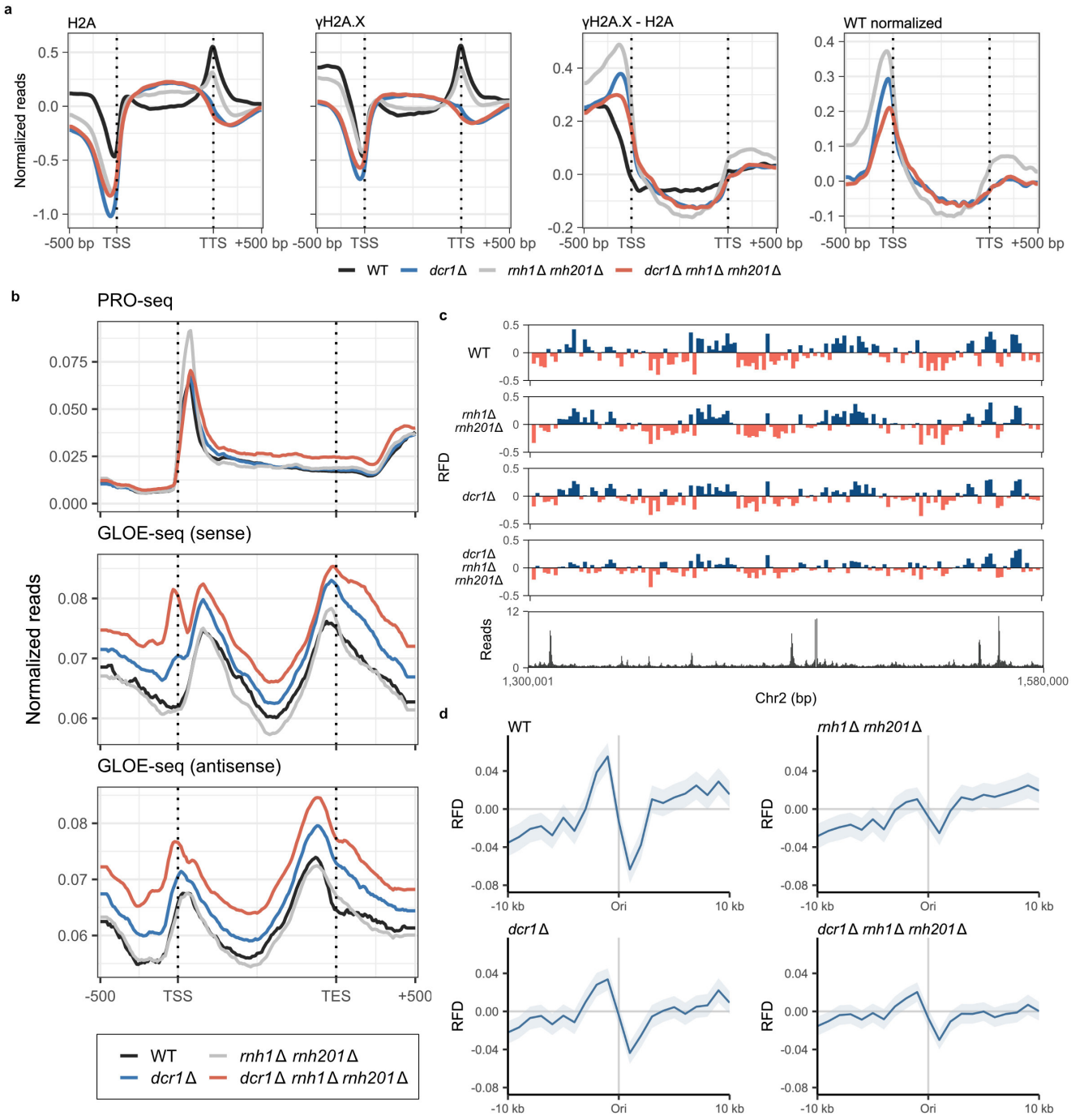
a
H2A
γH2A.X
γH2A.X - H2A
WT normalized
Normalized reads
-500 bp TSS TTS +500 bp
WT
dcr1Δ
rnh1Δ rnh201Δ
dcr1Δ rnh1Δ rnh201Δ
b
PRO-seq
GLOE-seq (sense)
GLOE-seq (antisense)
Normalized reads
-500 TSS TES +500
c
WT
rnh1Δ rnh201Δ
dcr1Δ
dcr1Δ rnh1Δ rnh201Δ
RFD
Reads
1,300,001
1,580,000
Chr2 (bp)
d
WT
rnh1Δ rnh201Δ
dcr1Δ
dcr1Δ rnh1Δ rnh201Δ
RFD
-10 kb Ori 10 kb

Fig. 4.4. Dcr1 prevents promoter-proximal DNA damage and replication defects in the presence of R loops.

(a) Distribution of (from left to right) log2 normalized H2A, γH2A.X, γH2A.X - H2A, and WT-normalized γH2A.X - H2A reads in WT, *dcr1*Δ, *rnh1*Δ *rnh201*Δ, and triple mutant within gene body ± 500 bp of all annotated genes.

(b) Distribution of normalized GLOE-seq reads in in WT, *dcr1*Δ, *rnh1*Δ *rnh201*Δ, and triple mutant within gene body ± 500 bp of all annotated genes aligned according to sense or antisense direction to transcription. PRO-seq signal from Fig. 3.9 plotted at the top for comparison.

(c) Replication fork directionality (RFD) analysis of GLOE-seq data in various mutants. RFD is defined as the ratio of excess reverse (crick strand) reads within a region, which is calculated as (REV – FWD)/(REV + FWD). Bottom lane represents Orc4 ChIP-seq reads from Masuda *et al.*, 2020. Note the positive RFD values immediately downstream of an Orc4 peak, indicating a lagging strand bias.

(d) Metaplot of RFD signal after combining the results from ~750 replication origins defined in oriDB.

4.5 Dcr1 promotes replication progression through highly transcribed regions

The results above suggested a role of Dcr1 in regulating replication, prompting us to investigate how transcription mis-regulation affected replication fidelity. We collaborated with Sarah Lambert (Institut Curie, Paris Orsay) to probe replication fork structure and dynamics in the absence of *dcr1* using bi-dimensional gel electrophoresis (2DGE) and recombination assays. In eukaryotes, rDNA units are arranged in blocks of tandem repeats (Kobayashi 2014), and with its highly-transcribed nature, make them a hotspot of transcription-replication conflicts and genome instability. To mitigate the effect of TRC, individual rDNA units contain a strong replication origin and a replication fork barrier (RFB) to limit head-on collisions (Brewer, Lockshon, and Fangman 1992; Kobayashi 2003). Given the roles of Dcr1 in rDNA copy maintenance (Castel et al. 2014) (Fig. 4.2c-d), we analyzed replication fork progression within the two regions of the rDNA unit, covering either the programmed RFB or the origin (Fig. 4.5a-b). Both WT and *dcr1*Δ displayed the expected intensity along the Y-arc corresponding to programmed pausing along the RFB (Fig. 4.5c, bottom). In contrast, only *dcr1*Δ accumulated extra intensities along the ascending and descending Y-arc in the *HindIII/KpnI* restriction fragment (Fig. 4.5c, top). Additionally, we observed a moderate increase in the intensity corresponding to the X-spike in *dcr1*Δ, corresponding to joint molecules thought to be intermediates of homologous recombination. The results suggested that replication was hampered in *dcr1*Δ when progressing through highly transcribed units.

One limitation in studying rDNA clusters was that the transcriptional activity of individual rDNA units was highly heterogeneous; for example, not all rDNA units are actively transcribed, and inactive rRNA genes can be heterochromatinized (McStay and Grummt 2008). We therefore further probed how *dcr1*Δ affected fork progression with an engineered *RTS1-RFB* fork stalling assay (Lambert et al. 2005) (Fig. 4.5d). Here, a Rtf1-bound *RTS1* blocked replisome progression in a polar manner, requiring rescue by recombination-dependent replication (RDR). RDR is prone to replication slippage (RS) (Carr and Lambert 2021), and can be detected with *ura*$^{+}$ reversion arising from the segmental-

duplicated *ura4-sd20* allele (Iraqui, Chekkal, Jmari, Pietrobon, Fréon, Costes, and Sarah A. E. Lambert 2012). The absence of Dcr1 resulted in a slight decrease (~1.4-fold reduction) of RS downstream of RFB (Fig. 4.5e). In contrast, the frequency of upstream RS showed ~3-fold increase compared to WT (Fig. 4.5e). This may indicate that nascent strand degradation (Carr and Lambert 2021) was more extensive, resulting in more fork-restart occurring downstream from the RFB in *dcr1*Δ. Agreeing with this hypothesis, 2DGE at the RFB (Fig. 4.5f-g) revealed a strong signal corresponding to arrested forks at the *RTS1* barrier accumulated when RFB was activated. Exo1-mediated resected forks could be detected as a tail descending towards the linear arc (Ait Saada et al. 2017; Teixeira-Silva et al. 2017), and the signal was more intense in *dcr1*Δ (Fig. 4.5h). Out data suggested that Dcr1 represented a novel player in preventing resection of unprotected forks during HR-mediated fork restart.

To further investigate how replication was hampered in *dcr1*Δ, we employed nanopore long-read sequencing to estimate replication speed of individual forks in a genome-wide manner (Theulot et al. 2022). Conventional, single-molecule methods of analyzing DNA replication speed, such as DNA fiber and combing analyses (Bianco et al. 2012), are low-throughput and lack sequence information. Recent progress in long-read sequencing has opened up the possibility to perform replication studies in a high-throughput, high-resolution manner. In particular, nanopore sequencing using Oxford Nanopore Technology (ONT) allows sequencing native genomic DNA, along with the detection of modified nucleotides (Hennion et al. 2022; Müller et al. 2019; Theulot et al. 2022). In a typical experiment, cells are pulsed with modified nucleotide (such as the thymidine analogue 5-bromo-2'-deoxyuridine, BrdU) that is incorporated into nascent DNA during replication. With a trained model, the modified nucleotide can be detected using ONT, and information about the site and speed of replication can be extracted from the data.

We started by creating *dcr1*Δ, *rnh1*Δ *rnh201*Δ, as well as the triple mutant in an *S. pombe* strain capable of incorporating exogenous nucleosides (Hodson et al. 2003). We then performed pulse-chase

labeling with BrdU, and detection using NanoForkSpeed (Theulot et al. 2022), a procedure that allows the detection of BrdU incorporated during replication. As shown in Fig. 4.6a, BrdU incorporation could be detected in individual DNA molecules of >60 kb long, and based on the characteristic rise and fall of BrdU signal densities from pulse-chase labeling, replication forks were automatically detected and their speed estimated. In WT, we observed a median fork velocity of ~1.8 kb/min in WT (Fig. 4.6b), agreeing broadly with estimates in eukaryotes (Técher et al. 2013), though individual fork speed varied drastically, ranging from 0.5 to 3.6 kb/min (after removing top and bottom 1% of outliers).

Inspecting all replication forks genome-wide, we observed changes to global replication speed in various mutants. The mean replication speed dropped slightly in *dcr1*Δ, by ~0.1kb, and was further decreased in the triple mutant, by another ~0.15kb to 1.55 kb/min (Fig. 4.6b). Curiously, we observed a modest increase in speed in the *rnh1*Δ *rnh201*Δ mutants, which was surprising considering that R-loop accumulation is usually associated with impeded fork progression.

NanoForkSpeed also provided genomic location as well as the direction of the replication forks, which we could leverage to correlate fork speed with various genomic features. As a proof of principle, we extracted all the replication forks that overlapped with annotated rDNA loci, and separated them into co-directional or head-on fork progression with the rRNA transcription direction. We observed a substantial decrease in replication speed when the fork proceeded head-on with transcription (Fig. 4.6c), thereby directly showing an influence of transcriptional activity to replication speed. Unfortunately, the current read depth precluded statistically meaningful analyses of fork behavior at the rDNA loci for various mutants. However, we also collected all replication forks overlapping annotated mRNA genes and classified them as being co-directional or head-on. As shown in Fig. 4.6d, we observed only in the triple mutant a significant reduction in replication speed as forks travelled head-on. Therefore, Dcr1 promoted fork progression through R-loop-induced replication obstacles.

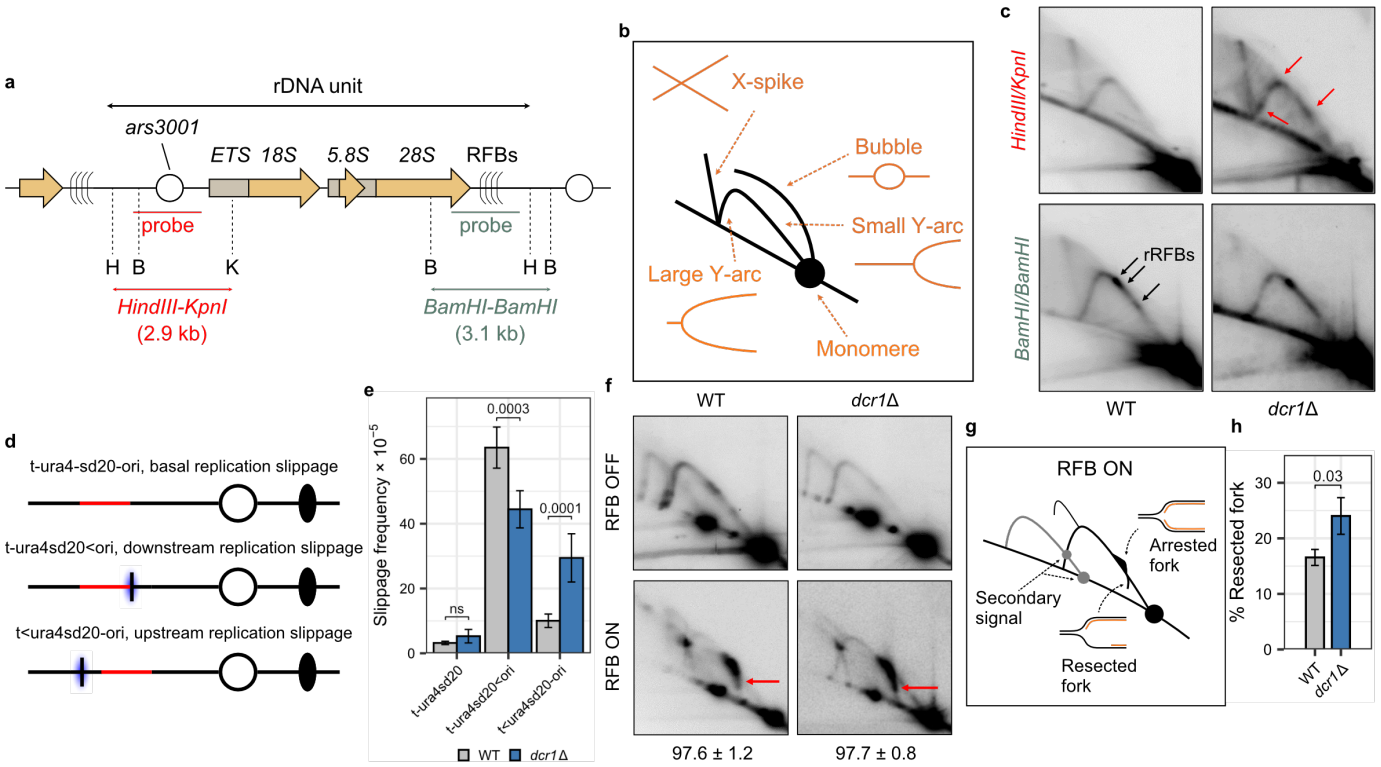
a
rDNA unit
ars3001
ETS
18S
5.8S
28S
RFBs
probe
probe
H B
K
B
H B
HindIII-KpnI
(2.9 kb)
BamHI-BamHI
(3.1 kb)
b
X-spike
Bubble
Small Y-arc
Large Y-arc
Monomere
c
HindIII/KpnI
BamHI/BamHI
rRFBs
WT
dcr1Δ
d
t-ura4-sd20-ori, basal replication slippage
t-ura4sd20<ori, downstream replication slippage
t<ura4sd20-ori, upstream replication slippage
e
Slippage frequency × 10−5
0.0003
0.0001
ns
t-ura4sd20
t-ura4sd20<ori
t<ura4sd20-ori
WT
dcr1Δ
f
WT
dcr1Δ
RFB OFF
RFB ON
97.6 ± 1.2
97.7 ± 0.8
g
RFB ON
Arrested fork
Secondary signal
Resected fork
h
% Resected fork
0.03
WT
dcr1Δ

Fig. 4.5. Dcr1 promotes replication through highly transcribed regions and limits fork resection.

(a) Schematic of an rDNA unit located on the chromosome III. Probes and restriction sites are indicated. H: *HindIII* B: *BamHI*, K: *KpnI*, ars; autonomously replicating sequence, ETS: external transcribed spacer, RFB: programmed and polar replication fork barrier. The orange arrows indicate the transcription unit of rRNA.

(b) Illustration representing the expected migration behavior of replication intermediates (RI) analyzed by bidimensional gel electrophoresis (2DGE). The "Y arc" is a series of Y-shaped RI, resulting from the replication fork progression within the DNA fragment analyzed. The "bubble arc" corresponds to the firing of the replication origin. The vertical X-spike results from X-shaped DNA joint molecules corresponding to RIs.

(c) Representative images of RI analysis by 2DGE within the *BamHI-BamHI* restriction fragment (bottom panels) or the *HindIII-KpnI* restriction fragment (Top panels) in indicated strains. Black arrows indicate the position of the programmed RFBs and red arrows indicate the fork pausing signal revealed in RNAi mutants.

(d) Diagrams of constructs containing the reporter allele *ura4-sd20 (red bar)*, associated or not to the *RTS1*-RFB (blue bars) on chromosome III. The RFB is integrated 5 kb away from a strong replication origin (ori). Black oval indicates centromere position. After thiamine removal, forks traveling from the centromere toward the telomere are blocked in a polar manner. The *ura4-sd20* allele contains a 20 nt duplication flanked by micro-homology. When the *ura4-sd20* allele is replicated by a restarted fork, the non-processive DNA synthesis undergoes replication slippage resulting in the deletion of the duplication and the restoration of a functional *ura4* $^{+}$ gene.

(e) Frequency of replication slippage in indicated strains and constructs. Bars indicate mean values ± 95 % confidence interval. Statistical analysis was performed using Student's t-test, compared to *WT*.

(f) Representative 2DGE analysis in indicated strains and conditions. The red arrow indicates the "tail" signal in WT and *dcr1*Δ strain. Numbers indicate the efficiency of the RFB ± standard deviation (SD).

(g) Schematics of RIs observed within the *AseI* restriction fragment in RFB ON condition using *ura4* as probe. Gray lines indicate secondary signal caused by partial digestion of psoralen-cross linked RIs. (h) "Tail" quantification from (g). Bars indicate mean values ± SEM. Statistical analysis was performed using Student's t-test, compared to WT.

2DGE and replication slippage experiments were performed by Sarah Lambert laboratory.

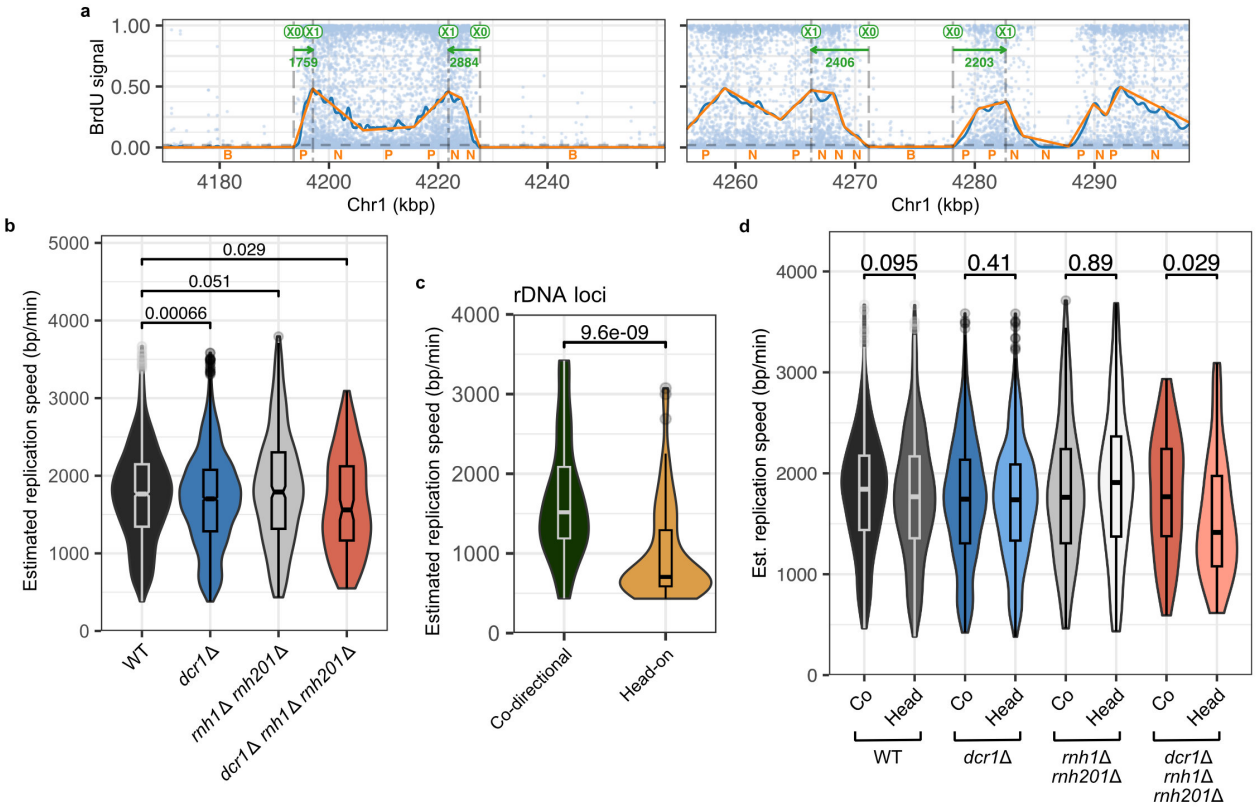
a
BrdU signal
1.00
0.50
0.00
X0 X1
1759
X1 X0
2884
B P N P P N N B
4180
4200
4220
4240
Chr1 (kbp)
X1 X0
2406
X0 X1
2203
P N P N N N B P P N N P N P N
4260
4270
4280
4290
Chr1 (kbp)
b
Estimated replication speed (bp/min)
5000
4000
3000
2000
1000
0
0.029
0.051
0.00066
WT
dcr1Δ
rnh1Δ rnh201Δ
dcr1Δ rnh1Δ rnh201Δ
c
rDNA loci
9.6e-09
Estimated replication speed (bp/min)
Co-directional
Head-on
d
Est. replication speed (bp/min)
0.095
0.41
0.89
0.029
Co
Head
WT
dcr1Δ
rnh1Δ rnh201Δ
dcr1Δ rnh1Δ rnh201Δ

Fig. 4.6. Dcr1 prevents transcription-replication collisions in the presence of R-loops.

(a) Example of individual nanopore sequencing reads from pulse-labelled WT (FY2317) cells, showing BrdU contents after processing using NanoForkSpeed. Figures generated using software in Theulot *et al.*, 2022. Replication forks are automatically detected as rightward, leftward, diverging and converging forks. Light blue dots: raw data from the BrdU detection tool Megalodon, representing the probability of BrdU at each thymidine position. The raw data is smoothened and is represented as the blue curve, further simplified using the Ramer-Doublas-Peucker algorithm (RDP), which is ultimately used to detect forks, labelled as green arrows in the diagram, fork velocity (bp/min, in green) indicated below. Refer to Theulot *et al.*, 2022 for detail.

(b) Violin plot showing the global estimated replication speed distribution in various genotypes. P-values represent results of one-way ANOVA.

(c) Violin plot showing the estimated replication speed distribution for all replication forks mapped to the rDNA loci, separated according to head-on or co-transcription to the direction of rRNA transcription. P-values represent results of one-way ANOVA.

(d) Violin plot showing the estimated replication speed distribution for all replication forks mapped to all annotated mRNA transcripts, separated according to head-on or co-transcription to the direction of transcription direction, and by genotype. P-values represent results of one-way ANOVA.

4.6 Discussion

We concluded from our domain analysis that the helicase domain of Dcr1 appeared to play a more prominent role in maintaining genome stability. We discovered *Dcr1-K38A*, but not *Dcr1-K38R*, resulted in additional genome instability phenotypes. While the RNase III-dead *dcr1-5* mutant did not have a rDNA copy maintenance phenotype (Castel et al. 2014), every domain deletion mutants tested here appeared to lose rDNA copy at a degree comparable to *dcr1*Δ, an exception being *dcr1-K38A*, which was more severe than *dcr1*Δ. Although not directly tested in Dcr1, one can assume mutating Walker A lysine to arginine and alanine would abolish ATP hydrolysis and binding respectively, as in the case of the Rad51 class recombinases (D. Sharma et al. 2013). Indeed, *D. melanogaster* Dcr-2 displayed distinct nucleic acid enzymatic activities when incubated with or without ATP, or with the non-hydrolyzable ATPγS (Singh et al. 2021), suggesting that in Dicer too, ATP binding and hydrolysis were separable events, exerting different influences to Dicer's activity. We speculate that *Dcr1-K38A*, void of bound ATP, adopts a conformation that, instead of processing R-loops, traps itself onto chromatin, obstructing replication.

Nevertheless, from our genetic analysis of introducing various *dcr1* alleles into RNase H mutants (Fig. 4.3), we concluded that a fully functional Dcr1 was required to limit R-loop-induced replication stress. This function is likely not prevalent under physiological condition and is therefore enhanced only in a *rnh1*Δ *rnh201*Δ background. Under this condition, we observed a loss of promoter-proximal pausing in the triple mutant (Fig. 3.7), explaining the negative interaction between *dcr1-5* and *rnh1*Δ *rnh201*Δ. Together with the findings on *dcr1-K38R/A*, we speculate that Dcr1 is recruited via its ATPase/helicase domain to promoter-proximal R-loops – further stabilized in paused and potentially backtracked Pol II (Castillo-Guzman and Chédin 2021) – and uses its RNase III catalytic activity for resolution.

We further characterized the consequences for genome stability in the absence of *dcr1*Δ. In both *dcr1*Δ and *rnh1*Δ *rnh201*Δ, we observed accumulation of γH2A.X around TSSs (Fig. 4.4a), but only in the triple mutant did it manifest as a detectable GLOE-seq peak representing DNA breaks (Fig. 4.4b). This suggests that the absence of either Dcr1 or RNase H activates the DNA damage response (DDR) pathway, in agreement with γH2A.X being one of the earliest damage markers, which does not necessarily mean the presence of a DNA break (Cleaver, Feeney, and Revet 2011; Nakamura et al. 2004). From the GLOE-seq results we also observed a decrease in a lagging strand bias in the triple mutant (Fig. 4.4c,d). While this could be due to an increase in leading or a reduction in lagging strand breaks, or a general decrease in replication speed, an interesting possibility is that replication forks, and associated breaks, were accumulating at promoters rather than at origins, due to the presence of paused Pol II and unresolved R-loops.

We tested this possibility with 2DGE, as well as with single molecule replication mapping using long read sequencing. In *dcr1*Δ, we found that replication was indeed hampered at the rDNA unit (Fig. 4.5), as well as a slight global decrease in replication speed (Fig. 4.6b). When transcription was disrupted in the presence of R-loops, deleting *dcr1*Δ led to a further reduction in replication speed (Fig. 4.6b), but was more severe when fork progression clashed head-on with transcription (Fig. 4.6d). We also observed an increase in replication fork slippage in *dcr1*Δ when the *ura4* gene was placed upstream of the programmed replication fork barrier (Fig. 4.5d,e). Replication slippage as a mutational signature can be used as a proxy to measure the extent of replication restart via recombination (Carr and Lambert 2021), which requires end resection to generate ssDNA for loading homologous recombination factors. The increase in upstream replication slippage suggested a more extensive nascent strand degradation, promoting recombination further downstream of the RFB. Indeed, we observed from 2-dimensional gel electrophoresis that end resection was more severe in *dcr1*Δ (Fig. 4.5f-h). We conclude that Dicer does indeed mediate replication-transcription collisions via R-loops and paused Pol II, which are resolved in

its absence by fork resection and restart by homologous recombination. Direct examination of forks in mutant genotypes by transmission electron microscopy will further test this conclusion.

Chapter 5: Conclusion and future directions

Cells defective in RNAi have long been known to display genome instability phenotypes such as chromosomal segregation errors (Gutbrod et al. 2022; Gutbrod and Martienssen 2020; Hall et al. 2003; Volpe et al. 2003; Zaratiegui et al. 2011). Accumulating evidence in recent years has shown that Dcr1 has additional genome stability functions beyond that of classical RNAi, although a mechanism is lacking (Zaratiegui et al. 2011). Since nuclear RNAi in *S. pombe* plays a critical function in coordinating S phase-specific CTGS with that of replication, and in doing so ensuring faithful propagation of epigenetic information (Castel et al. 2014; Kloc et al. 2008; Li et al. 2011; Zaratiegui et al. 2011), a hypothesis of Dcr1 being involved in limiting TRC was proposed. R-loops are frequently associated with genome instability (see Section 1.4.3), and in our laboratory, we found that *S. pombe* DNA:RNA hybrid accumulated at rDNA repeats in *dcr1*Δ cells (Castel et al. 2014), and in mESCs, BRD4, which resolves R-loops (Edwards et al. 2020; Lam et al. 2020), was identified as a strong suppressor of *Dicer*$^{-/-}$ (Gutbrod et al. 2022). Additionally, Dicer from both *S. pombe* and human can bind R-loops (Fig. 3.1b-c, Camino et al. 2023). Despite strong evidence of Dicer in limiting TRC, and a link to R-loops, exactly how Dicer limits TRC and the consequence to genome stability in its absence remain poorly understood.

Here, we conducted a series of genetic studies in *S. pombe* to further dissect the *dcr1*Δ phenotype when R-loops accumulate in RNase H-deficient *rnh1*Δ *rnh201*Δ cells. We found that Dcr1 regulates early transcriptional activity of Pol II near promoters and terminators to prevent replication stress. This was supported by genetic experiments with known and new suppressors, as well as genome-wide nascent transcription studies using PRO-seq. We found a population of sRNA of the size between 24 – 40 nt that mapped to the promoter, and to the terminator, whose biogenesis depended redundantly on Dcr1 and RNase H. sRNAs of exactly this size-range have been detected in human cancer cells, where they depend on Dicer and BRCA1 and coincide with R-loops at the actin gene terminator,

although genome-wide studies have not been performed (Hatchi et al. 2021). The genome instability phenotype of *dcr1*Δ required the presence of Ago1, as *ago1*Δ suppressed HU and CPT sensitivity in *dcr1*Δ cells. Ago1 was recruited to promoters and especially to terminators, and its recruitment depended on both Dcr1 and RNase H, as the ChIP-seq signal decreased in significantly in the triple mutant.

We performed domain analyses of Dcr1 and found that while an intact Dcr1 with both catalytic functions – ATPase and RNase III – was important in preventing R-loop-induced replication stress, the ATPase/helicase domain played a more direct role, and that a catalytic dead allele, *dcr1-K38A*, appeared dominant, causing more genome instability than when the helicase was deleted. We next employed a series of genomic approaches to further characterize the genome instability phenotype in *dcr1*Δ, and discovered that DNA damage, manifested in DNA breaks, was enriched around TSSs and terminators of mRNA genes. Our data also suggested Dcr1 played a more direct role in protecting replication forks, as manifested in altered RFD profiles genome-wide. This agreed with work from our collaborator Sarah Lambert, demonstrating that Dcr1 promoted replication progression through highly transcribed units and prevented unprotected fork degradation. Finally, we conducted a replication dynamics study using long read sequencing after BrdU incorporation, and discovered that in the triple mutant *dcr1*Δ *rnh1*Δ *rnh201*Δ a direct slowing down of replication speed as the fork progressed head-on to transcription units, further supporting the role of Dcr1 in preventing TRCs in the presence of R-loops.

With respect to transcription, we observed a global decrease in pausing index in the triple mutant (Fig. 3.8e,f) due to a higher read count at the gene body suggesting aberrant pause escape. However, not all genes were affected to the same degree and indeed, a substantial number of genes had a higher PI than WT (Fig. 3.8f). It would be important to identify the subset of genes and their associated features that are 'TRC hotspots' requiring the action of Dcr1. The pausing defect correlated partly with

gene expression (Fig. 3.8k) but we observed a stronger dependency on genes already having a high PI in WT (Fig. 3.8j). In animals, actively paused genes are associated with developmentally regulated genes, or genes that require rapid response to environmental stimuli (Core and Adelman 2019); in fact, Dicer-dependent promoter-proximal pausing was first identified *in vivo* in *D. melanogaster* in the promoters of heat-shock responsive genes (Cernilogar et al. 2011). Our RNA-seq results showed that *dcr1*Δ and *rnh1*Δ *rnh201*Δ shared a similar set of up-regulated genes that were related to environmental stress (Fig. 3.6c), potentially supporting that in *S. pombe* too, dynamically expressed genes are actively held in a paused state and are subjected to Dcr1 regulation.

Another, non-mutually exclusive set of genes regulated by Dicer could be those that are prone to promoter R-loop formation. In our DRIPc-seq data we failed to detect promoter-specific R-loops enrichment in the *dcr1*Δ single mutant (Fig. 3.1a). This might be due to two reasons. First, given the lack of apparent pausing defect globally in the *dcr1*Δ single mutant (Fig. 3.8e-f), R-loops at TRC hotspots might be efficiently resolved by other mechanisms such as RNase H. Second, promoter-associated R-loops, as mentioned in section 1.4.3, are distinct from gene-body R-loops associated with elongating RNAP. In particular, promoter-associated R-loops tend to be shorter and less stable; it was therefore proposed that DRIP-based method, which involved DNA fragmentation and deproteinization, could further destabilize these R-loops, making them refractory to be captured and sequenced (Castillo-Guzman and Chédin 2021). In this case, *in vivo* approaches such as MapR (Yan and Sarma 2020), which is based on a CUT&RUN (cleavage under targets and release using nuclease) approach with catalytically inactive RNase H, may be more suitable for detecting promoter-associated R-loops. Unfortunately, successful CUT&RUN based sequencing has not reported for *S. pombe* and requires significant modifications from the protocol designed for *S. cerevisiae*. We successfully performed MapR in mammalian cells, and managed to perform CUT&RUN in *S. pombe*, although performing MapR in *S. pombe* would require further optimization of the protocol; these are described in detail in Appendix 1.

We detected sRNA mapped to the promoter and to the terminator from the transcribed strand, which depended on both Dcr1 and RNase H in a redundant manner (Fig. 3.7). We did not find promoter-proximal antisense sRNAs, suggesting they were cleavage products from nascent transcripts. Whether the sRNA serves a functional role remains unclear. They could be the consequences of Dcr1 and RNase H terminating Pol II via an endonucleolytic mechanism; further, they could be important in recruiting Ago1. Human Dicer has been shown process R-loops *in vitro*, cleaving the RNA moiety at 20 – 23 nt from the 3' end (Camino et al. 2023), and in our laboratory, we found that *S. pombe* Dcr1 was able to bind R-loops too (Fig. 3.1b,c). On the other hand, Ago1 has been hypothesized to be recruited via its binding to R-loops (Nazer et al. 2022). In fact, the PIWI domain of Argonautes resembles an RNase H domain (Song et al. 2004), and prokaryotic Argonautes often display strong affinity towards DNA substrates (see Section 1.2). Ago1 acts downstream of Dcr1 (Carmichael et al. 2004), and we found that Ago1 was indeed recruited to the TSSs and especially the TTSs by Dicer and RNase H (Fig. 3.10). We therefore tested whether the promoter-derived sRNA serves to recruit Ago1. Rationalizing that promoter sRNA were dicer-independent in the presence of RNase H, we mapped sRNA reads from *dcr1*Δ cells recovered by RNA-immunoprecipitation (RIP) for Ago1-associated sRNA (Halic and Moazed 2010). We found that Ago1 bound small RNA mapped to the TTSs, resembling Ago1 in this respect, although read lengths (36 nt) prohibited estimating the length distribution of the sRNA (data not shown). We will further examine the role of Ago1 in processing R-loops using previously characterized catalytic mutants that lose other silencing functions (Irvine et al. 2006).

Unexpectedly, we found that *dcr1*Δ did not negatively interact with *sen1*Δ (Fig. 3.2c), which is well known to process R-loops: in human cells, Senataxin (SETX) is an R-loop resolving helicase involved in mediating Pol II pausing, termination, and DSBs (Cohen et al. 2018; Hasanova et al. 2023; Skourti-Stathaki et al. 2011). In *S. cerevisiae* too, Sen1 is known to mediate Pol II transcription termination, and in doing so, limits replication stress (Alzu et al. 2012; Mischo et al. 2011; Porrua and

Libri 2013). In *S. pombe*, the function of Sen1 appeared to be distinct, being involved in terminating Pol III transcription (Legros et al. 2014; Rivosecchi et al. 2019). Another homolog, Dbl8, is recruited to DSBs (Yu et al. 2013). While it remains to be tested whether Sen1 and Dbl8 operate redundantly, the lack of negative interaction between *dcr1*Δ and either *sen1*Δ or *dbl8*Δ suggests that Dcr1, rather than acting as a global R-loop regulator, participates specifically at Pol II transcription units that are co-regulated by other R-loop factors (such as RNase H). Alternatively, as Sen1 is a DNA:RNA helicase, it might function in the same pathway as Dcr1. In this case, it would be interesting to see if *sen1*Δ also negatively interacts with *rnh1*Δ *rnh201*Δ under genotoxic stress, in similar manner to what we observed for *dcr1*Δ. While the rDNA copy loss phenotype in *dcr1*Δ cycling cells (Castel et al. 2014) might implicate Dcr1 in Pol I regulation, Dcr1 appears to play a more prominent role in regulating Pol I during cellular quiescence G_0 (Roche et al. 2016); in cycling *dcr1*Δ cells, Pol II accumulated at rDNA repeats instead (Castel et al. 2014; Roche et al. 2016). In fact, Pol II activity at rDNA loci has been widely documented and is proposed to play a role in regulating rDNA copy number (Abraham et al. 2020; Kobayashi and Ganley 2005; Watase and Yamashita 2024).

In our domain analyses (Section 4.3), we found that both the helicase deletion mutant (*dcr1-ΔHel*) and the RNase III dead mutant (*dcr1-5*) negatively interacted with *rnh1*Δ *rnh201*Δ in a similar way as *dcr1*Δ (Fig. 4.3). The Walker A motif mutant, *dcr1-K38R*, was also phenotypically similar to *dcr1*Δ. This suggested both the ATPase and RNase III activities were important for resolving TRCs. On the other hand, *dcr1-K38A* appeared phenotypically dominant, causing acute CPT sensitivity and enhanced rDNA copy loss (Fig. 4.1-2). Performing ChIP on Dcr1 had been difficult in *S. pombe*, partly due to its low expression level, and we speculate that Dcr1 resolving paused Pol II is a dynamic event, thereby evading capture by conventional ChIP. If *dcr1-K38A* indeed traps itself onto chromatin as we speculate (see Section 4.6), then it should be more stabilized and potentially can be ChIPed. We also note that *sen1*Δ suppressed the CPT sensitivity of *dcr1*Δ at high CPT doses (Fig. 3.2c); it would be interesting to see if *sen1*Δ could also suppress *dcr1-K38A*.

S. pombe is an excellent model organism for studying the nuclear function of Dcr1, owing to its simple yet intact RNAi pathway; the lack of miRNA eliminates confounding factors in interpreting phenotypes. Given that the epigenetic, chromosome segregation, and replication machineries are well conserved between *S. pombe* and other eukaryotes, we believe the function of Dcr1 in resolving TRC is conserved. The findings in human cells that *Dicer*$^{-/-}$ knockout displays chromosome segregation defects (Gutbrod et al. 2022), that Dicer binds and processes R-loops (Camino et al. 2023), and that Dicer-dependent sRNA is generated at transcription termination paused sites (Hatchi et al. 2021) all support this nuclear role of Dicer in mammals. *S. pombe* Dcr1 retains a catalytically active ATPase that alters the cleavage preference of dsRNA, and is required for proper centromeric siRNA biogenesis, although ATP-independent dsRNA cleavage by Dcr1-K38A was also observed (Colmenares et al. 2007). In animals, the ancestral Dicer is predicted to have a catalytically active helicase domain; in deuterostomes the emergence of additional antiviral proteins such as RIG-I-like receptors (RLRs) and the expansion of adaptive immunity is correlated with the loss of ATPase activity in Dicer (Aderounmu et al. 2023). Indeed, human Dicer remains capable of generating sRNA *in vitro* when the helicase domain is deleted (MacRae et al. 2006), and mammalian Dicer does not appear to require ATP for its function. Nevertheless, the helicase domain is relatively well conserved, and human Dicer has intact Walker A and B motifs (Kidwell, Chan, and Doudna 2014). The function of the mammalian Dicer helicase remains elusive; it has been shown to act as a platform to recruit accessory factors (Hansen et al. 2020), but this cannot explain the conservation of the catalytic residues. In a recent preprint, it was shown that human Dicer can hydrolyze ATP when incubated with an equimolar amount of ATP, but not when ATP was in ~500-fold excess (Ciechanowska et al. 2023). Therefore, we speculate in mammals too, a function of the helicase domain of Dicer may be specific to cleaving R-loops and therefore in maintaining genome stability.

As described in Section 1.2, recent metagenomic and phylogenetic studies have shed light on the evolutionary history of RNAi, suggesting Argonaute and Dicer had distinct functions before being co-opted into silencing pathways (Torri et al. 2022). LECA, as descendants of Asgard Archaea (Williams et al. 2013), very likely evolved with a pre-existing, functional Argonaute (Leão et al. 2023). Dicer, on the other hand, appeared to be a truly eukaryote-specific fusion protein with domains of bacterial and archaeal origins (Shabalina and Koonin 2008). Notably, the closest prokaryotic homolog to Dicer's helicase is that of an archaeal protein, Hef (Shabalina and Koonin 2008; Sinha et al. 2018), which participates in resolving stalled replication forks (Lestini et al. 2010). The evolutionary origin of Argonautes and Dicer is still an active area of investigation, although a recent preprint found that Asgard Argonaute has RNA-guided RNA cleavage activity, and is located in an operon that also encodes a DExD domain helicase and a protein containing an RNase III/dsRBD domain (Bastiaanssen et al. 2023), suggesting the emergence of a proto-RNAi pathway before LECA.

Nevertheless, as proposed by Torri *et al.*, RNAi was likely dispensable in LECA for genome defense; in fact, even in prokaryotes the presence of pAgos did not correlate with a decrease in TE number (Ryazansky, Kulbachinskiy, and Aravin 2018). Additionally, small noncoding RNA can function without a protein partner, which is proposed to be more ancient than RNAi (Chen and Zhou 2023). All chromatin metabolism – transcription, replication, repair, and epigenetic inheritance – uses the same DNA molecule, and have therefore been co-evolving since the emergence of DNA as the basis of inheritance. Therefore, it is perhaps not surprising that many proteins are found to regulate multiple processes. For example, as mentioned in Section 1.4, many helicases that unwind dsDNA for fork remodeling also unwind R-loops. In *S. pombe*, the leading strand DNAP Cdc20, the HR repair factors Rad51 and Rad54, as well as the Pol II subunits Rpb2 and Rpb7 are all required for proper heterochromatic silencing (Djupedal et al. 2005; Kato 2005; Li et al. 2011; Onaka et al. 2016), highlighting their interconnectedness. As for Dicer, we and others have shown that it can bind to DNA:RNA hybrids (Fig. 3.1b-c, Camino et al. 2023), and the helicase domain of *Sporotrichum*

thermophile Dicer-2 can hydrolyze ATP when DNA:RNA hybrid is added (Kidwell et al. 2014). Additionally, the helicase of human Dicer can bind both ssDNA and ssRNA (Ciechanowska et al. 2023). For Argonaute, as most pAgos are catalytically inactive and virtually none mediates exclusively RNA-guided RNA targeting like eAgos, its ancestral function likely lies in DNA-based mechanism. As mentioned, the long, catalytically active pAgo of *T. thermophilus* facilitates replication termination with a DNA cleavage mechanism (Jolly et al. 2020). In *Natronobacterium gregoryi*, the long pAgo mediates recombination in a way that is independent of its catalytic activity (Fu et al. 2019). Therefore, in Eukaryotes, Dicer and Argonaute in general might have functions beyond RNA processing.

Replication origins are often found near TSSs, generating TRC (See section 1.4.2; Hu and Stillman 2023). In the Saccharomycetaceae family, the emergence of sequence-specific replication origins of and a silent information regulator (SIR)-based gene silencing mechanism correlate with the loss of RNAi, which is thought to increase TRC (Hu et al. 2020). Our finding in *S. pombe* supports this hypothesis, placing RNAi as a key player at the promoter region to coordinate transcription and replication. Given the evolutionary context and the results presented here, we speculate the ancient function of Dicer and Argonaute predating the emergence of a silencing pathway lies in that of limiting replication stress.

Chapter 6: Appendix 1 – CUT&RUN-based method for R-loop profiling

6.1 Introduction

CUT&RUN has become increasingly popular as an alternative to ChIP for its simpler workflow, and high signal-to-noise ratio. For genome-wide R-loop studies, MapR was recently developed as a simplified CUT&RUN workflow by using a custom enzyme with a catalytically dead RNase H fused to MNase (Yan et al. 2019; Yan and Sarma 2020). As described in Section 1.4.3 and in Chapter 5, *in situ* approaches such as CUT&RUN are predicted to better detect short, promoter-proximal R-loops. However, while a CUT&RUN protocol exists for *S. cerevisiae* (Brahma and Henikoff 2019), it has not been used in *S. pombe* owing the differences in cellular physiology. In particular, the CUT&RUN protocol for *S. cerevisiae* involves nuclei extraction, which is difficult in *S. pombe*. In this chapter, I describe the MapR experiment I performed on moues embryonic stem cells (mESCs) with Joshua Steinberg in our laboratory, and my optimization on performing CUT&RUN in *S. pombe*.

6.2 Materials and methods

6.2.1 mESCs tissue culture and MapR

Tissue culture was performed by Joshua Steinberg. mESC tissue culture was performed as described in Gutbrod *et al*. 2022. Briefly, cells were grown in 2i + LIF medium at 37 ºC and 5% CO_2, on culture dishes coated with gelatin. For inducible *Dicer1*$^{flx/flx}$ knockout, cells were treated with hydroxytamoxifen (OHT) at a final concentration of 1 µM. MapR was performed largely following Yan & Sarma 2020, including in-house purification of GST-MNase and GST-RHΔ-MNase. 3.5 x 10^6 cells were used per MapR experiment, and for *Dicer1*$^{flx/flx}$ cells were harvested after 8 days of OHT treatment.

6.2.2 Nuclei extraction and CUT&RUN for *S. pombe*

A working, but yet to be optimized, protocol for performing CUT&RUN in fission yeast is described here. The protocol involves two major steps: nuclei isolation and the actual CUT&RUN. Nuclei isolation can be done ahead of time and the resulting nuclei can be frozen in -80 ºC indefinitely. For CUT&RUN, the whole procedure takes 2 days, and extra time is required for the preparation of DNA-seq libraries.

Stock solutions

1. 20% w/v BSA in water. Store at -20 ºC.
2. 0.1 M Calcium chloride
3. 1 M Citric acid
4. 0.5 M EDTA pH 8.0
5. 0.2 M EGTA pH 8.0
6. 1 M HEPES-KOH pH 7.5
7. 1 M HEPES-KOH pH 7.9
8. 1 M Manganese chloride
9. 1 M PIPES-NaOH pH 6.3. Store in dark at 4 ºC.
10. 2 M Potassium chloride
11. 1 M Sodium citrate
12. 5 M Sodium chloride
13. 5 M Sorbitol
14. 2 M Sucrose

Stock buffers:

1. SCSa – 20 mM sodium citrate, 1 M sorbitol. Store at RT.
2. SCSb – 20 mM citric acid, 1M sorbitol. Store at RT.
3. 10X protease inhibitor (10X Pi) – dissolve 1 tablet of Roche COmplete protease inhibitor in 5 mL of H_2O. Store for up to 1 week at 4 ºC.
4. 10X salt buffer (10X SB) – make fresh every experiment as spermidine is unstable in solution. Keep on ice throughout.

	Stock	**Final conc. (10X)**	**20 mL**
HEPES pH 7.5	1 M	200 mM	4 mL
NaCl	5 M	1.5 M	6 mL
Spermidine	Pure; 6.4 M	5 mM	15.6 µL
H_2O	--	--	10 mL

Buffers:

SCS buffer

SCS buffer is prepared by mixing SCSa and SCSb until pH reaches 5.8. Empirically 35 mL SCSa and 15 mL SCSb works for me. SCS buffer can be stored at RT.

SPC buffer (no Pi)

Store for up to 6 months at 4 ºC.

	Stock	**Final conc.**	**10 mL**
PIPES pH 6.3	1 M	200 mM	2 mL
Sorbitol	5 M	1 M	2 mL
$CaCl_2$	0.1 M	0.1 mM	10 µL
H_2O	--	--	6 mL

SPC buffer
Since protease inhibitor is stable for only 1 week, SPC should not be stored > 1 week too.

	Stock	**Final conc.**	**50 mL**
PIPES pH 6.3	1 M	200 mM	10 mL
Sorbitol	5 M	1 M	10 mL
$CaCl_2$	0.1 M	0.1 mM	50 µL
10X Pi	10X	1X	5 mL
H_2O	--	--	25 mL

Ficoll buffer
Ficoll buffer is best made fresh but can be stored at 4 ºC for a few weeks. To make 25 mL Ficoll buffer, dissolve 2.25 g Ficoll PM-400 in 15 mL of water and add 500 µL of 1M PIPES pH 6.3 and 125 µL 0.1 M $CaCl_2$. Top up to 25 mL water once the Ficoll dissolved.

Wash buffer (WB)
Prepare fresh every time.

	Stock	**Final conc.**	**1 mL**
10X SB	10X	1X	100 µL
10X PI	1X	1X	100 µL
H_2O	--	--	800 µL

NIB buffer
Prepare fresh every time.

	Stock	**Final conc.**	**1 mL**
10X SB	10X	1X	100 µL
10X PI	10X	1X	100 µL
Sucrose	2M	1.2 M	600 µL
H_2O		--	200 µL

Dig-Wash buffer (DW)
Prepare fresh every time. DW can be stored overnight at 4 ºC.

	Stock	**Final conc.**	**50 mL**
10X SB	10X	1X	5 mL
10X PI	10X	1X	5 mL
Digitonin	5% (w/v)	0.02% (w/v)	200 µL
H_2O		--	To 50 mL

Bead-binding buffer
Store at 4 ºC for up to 6 months.

	Stock	**Final conc.**	**50 mL**
HEPES-KOH pH 7.9	1 M	20 mM	1 mL
KCl	2 M	10 mM	250 µL
$CaCl_2$	0.1 M	1 mM	500 µL
$MnCl_2$	1 M	1 mM	50 µL
H_2O	--	--	48.2 mL

Pre-block buffer

Prepare fresh every time.

	Stock	Final conc.	1 mL
10X SB	10X	1X	100 µL
10X PI	10X	1X	100 µL
Digitonin	5% (w/v)	0.02% (w/v)	4 µL
EDTA	0.5 M	2 mM	4 µL
BSA	20% (w/v)	3% (w/v)	150 µL
H_2O	--	--	642 µL

Block buffer

Prepare fresh every time. Can be stored overnight at 4 ºC.

	Stock	Final conc.	2 mL
10X SB	10X	1X	200 µL
10X PI	10X	1X	200 µL
Digitonin	5% (w/v)	0.02% (w/v)	8 µL
EDTA	0.5 M	2 mM	8 µL
BSA	20% (w/v)	0.1% (w/v)	10 µL
H_2O	--	--	1574 µL

2X STOP buffer

	Stock	Final conc.	1 mL
NaCl	5 M	150 mM	30 µL
EDTA	0.5 M	20 mM	40 µL
EGTA	0.2 M	4 mM	20 µL
Digitonin	5% (w/v)	0.02% (w/v)	4 µL
RNase A	--	--	5 µL
Spike-in DNA	10 pg/mL	10 pg/µL	1 µL
H_2O	--	--	900 µL

Nuclei isolation

The protocol is a combination from Flor-Parra *et al.* 2014 and Orsi *et al.* 2015. First the protoplast is prepared using lallzyme; protoplasts are then subjected to a hypotonic shock to lyse the plasma membrane. A simple sucrose gradient then removes the debris to yield relatively clean nuclei. The following protocol describes the preparation of nuclei from 500 mL of culture. Depending on the sensitivity required 10 mL worth of cell is enough for a single CUT&RUN experiment. The protocol can be scaled up or down as suitable.

1. Inoculate from an overnight culture and grow *S. pombe* until mid-log phase.
2. Harvest the cells by centrifugation, and wash twice in 15 mL of SCS buffer.
3. Resuspend the cells in 25 mL of SCS buffer supplemented with 2.5 g of lallzyme (0.1g/mL).
4. Incubate at RT, checking under light microscope until >90% of cells become rounded (for WT this typically equals 15-20 minutes).
5. Harvest the cells and wash once with 15 mL of SCS buffer.
    - From this point onwards everything should be kept on ice if possible.

6. Wash once with 25 mL cold SPC+Pi buffer.
7. Resuspend the pelet in 0.5 mL SPC buffer without protease inhibitor.
8. Add to 25 mL cold Ficoll buffer, mix by inverting up and down a few times.
9. Centrifuge 10 min at 7,500 x g at 4ºC.
10. Wash the pellet with 10 mL of cold SPC+Pi buffer.
11. Centrifuge 10 min at 4,200 x g at 4ºC.
12. Repeat step 10 – 11 for a total of two washes.
13. Resuspend the pellet in 5 mL of cold SPC+Pi buffer.
14. Aliquot as desired and snap-freeze in liquid N_2. The nuclei can be stored indefinitely at -80ºC.

Note: at this point the nuclei are still "crude nuclei", contaminated with cellular debris. To allow for efficient binding to concanavalin-A beads one must perform a sucrose gradient centrifugation to isolate the nuclei from the debris. This can be done before or after snap-freezing. The protocol here performs such clean-up post-freezing in a smaller scale.

***S. pombe* CUT&RUN with nuclei**

Based on observation, 20 µL of bead slurry is sufficient for binding nuclei isolated from 10 mL of culture. One should expect clear supernatant (tiny loss of material is acceptable) and flaky bead when binding is successful. The protocol largely follows the original CUT&RUN protocol (Skene & Henikoff, 2017) so modifications can be made as necessary (e.g., optimizing salt condition for diffusion of large complexes).

Part 1: Nuclei clean-up

- Note: This can also be done before snap-freezing the nuclei.
- For convenience this protocol uses 2 mL tube in a fixed angle table-top refrigerated centrifuge for sucrose gradient. 50 mL of culture worth of nuclei can be processed per 2 mL tube.

1. Thaw an aliquot of nuclei on ice, and spin at 4,000 x g for 3 min.
2. Remove supernatant and resuspend in 500 µL of cold WB.
3. Transfer the cells in WB to an empty 2 mL tube. Add 1 mL of cold NIB from the bottom so the cell suspension is on top of the NIB.
4. Centrifuge 15 min at 12,000 rpm at 4 ºC.
   - It's a good time to prepare the beads while the nuclei are in centrifuge (see below).
5. After the centrifugation, a sticky white mess should be deposited onto the side of the tube, and semi-transparent nuclei should be pelleted. Carefully remove as much white mess as and remove all supernatant. Resuspend the pellet in an appropriate amount of cold DW.
   - For each separate CUT&RUN experiment cells are resuspended in 200 µL. If a tube of nuclei is to be used for 5 CUT&RUN experiments one can resuspend the pellet in 1 mL of DW.

Part 2: CUT&RUN reaction

- Note: Before the addition of primary antibodies every step should be performed at room temperature.

1. Activate the beads – beads can be prepared in bulk.

i. Resuspend the Concanavalin-A beads by pipetting or gently flicking the bottle. Transfer an appropriate amount into a DNA LoBind tube.
    - For example, if 5 CUT&RUN reactions each with 10 mL culture worth of nuclei, take 100 µL of beads.
ii. Transfer to a magnetic rack and remove the storage buffer.
iii. Resuspend in 1 mL of Bead Binding buffer.
iv. Clear in a magnetic rack and remove the supernatant.
v. Repeat steps iii-iv twice for a total of three washes.
vi. Resuspend the beads in DW, same volume as the amount being taken.
    - For example, resuspend 100 µL of beads with 100 µL of DW.

2. Binding the cells to beads:
    i. Add an appropriate amount of activated beads to an appropriate amount of cells. See above for reference.
    ii. Rotate at RT for > 5 minutes.
        - Usually 10 – 15 minutes is sufficient. The beads should start to clump and form distinct particles or flakes.
    iii. Quick spin and stand to clear in a magnetic rack and remove the supernatant.

3. Preparation of nuclei for primary antibodies:
    i. Resuspend the beads gently in 1 mL of Pre-Block buffer.
        - From here onwards, since the nuclei are bound to the beads they will inevitably look flaky. There is no need to resuspend into fine particulate; breaking the large clumps into multiple smaller flakes is sufficient for efficient diffusion of antibodies.
    ii. Rotate at RT for 5 minutes.
    iii. Quick spin and stand to clear in a magnetic rack and remove the supernatant.
    iv. Repeat step i – iii, this time using 1 mL of Block buffer.
    v. Resuspend the beads in 200 µL of Block buffer.
    vi. Transfer to a 0.2 mL PCR tube.
        - Since the beads will be rotated overnight, keeping the suspension in a small volume prevents the beads from getting stuck in places where the buffer could not reach.

4. Add 1 µL of primary antibody for a 1:200 dilution. Mix by pipetting gently. The amount of antibodies added can be modified as needed.
    - The amount of primary antibody to cells is the most variable step in the current protocol, and needs to be optimized for every antibody.
5. Rotate overnight at 4°C.
6. The next day, quickly spin the tubes and transfer the bead suspension to a 1.5 mL DNA LoBind tube.
7. Binding of pAG-MNase:
    i. Stand to clear in a magnetic rack and remove the supernatant.
    ii. Wash the beads by gently resuspending in 1 mL of DW buffer.
    iii. Repeat the wash with DW buffer for a total of 2 washes.
    iv. Resuspend the beads in 50 µL Block buffer.

v. Add 1.5 µL of pAG-MNase. Mix by gently pipetting.
vi. Transfer to a new DNA LoBind tube, incubate at 4°C for 1 hour with rotation.
    - Transferring to a new tube allows the liquid to stay in the bottom of the tube through surface tension, so no clumps get stuck at the side of the tube.
    - While the tubes are incubating, prepare the 2X STOP buffer and chill that and 0.1M $CaCl_2$ on ice.

8. Quickly spin down and stand to clear in a magnetic rack.
9. Remove the supernatant and wash twice with 1 mL DW buffer.
10. Resuspend the beads in 150 µL DW buffer.
11. Place on ice for at least 2 min to chill to 0°C.
12. Add 3 µL of cold 0.1M $CaCl_2$, mix by gently pipetting or flicking
13. Incubate at 4°C for 30 minutes, flicking occasionally.
14. After 30 minutes, stop the reaction by adding 150 µL 2X STOP buffer. Mix by pipetting gently.
15. Release the cleaved fragment by incubating at 37°C for 10 minutes.
16. Centrifuge 4,000 x g at 4°C for 3 minutes.
17. Place the tubes on a magnetic rack and stand to clear. Transfer the supernatant to a clean 2 mL DNA LoBind tube.
    - 2 mL tube is used because Zymo Research's ChIP DNA Clean and Concentrator kit requires adding 5x volume of binding buffer.
18. Add 1.5 µL of 20% w/v SDS and 2 µL of proteinase K. Incubate at 70°C for 10 minutes.
19. Clean up the DNA using Zymo Research's ChIP DNA Clean and Concentrator. The eluted DNA can be used to prepare sequencing libraries.

6.3 Results and Discussion

We decided to replicate the MapR experiment in a small-scale sequencing experiment using HeLa cells. We compared our MapR results with that performed in the original publication that used HEK293 cells, which showed promoter-proximal R-loops at the *GBAP1* locus (Fig. S1a, top panel). Our sequencing run yielded a better signal-to-noise ratio, as well as very clear enrichment of R-loops at the promoters (Fig. S1a, bottom panel). Given the positive results, we proceeded to generating Dicer1$^{-/-}$ cells for MapR.

Full Dicer knockout is lethal in mammals, and we used an OHT-inducible knockout *Dicer*$^{flx/flx}$ mESC cell line. After 8 days of OHT treatment, the cells adopted abnormal morphology just as the *Dgcr8*$^{-/-}$ cells (Fig. S1b), and began to lose viability (Fig. S1c). We confirmed the knockout by Western blot (Fig. S1d) and performed MapR as described above. Unfortunately, the read depth obtained for

this pilot study was insufficient for analyzing the effect of Dicer knockout on R-loop dynamics at various gene features. Nevertheless, we observed a clear enrichment of R-loops at the pericentromeric repeats (Fig. S1e). In one replicate of Dicer1 knockout, there appeared to be a slight increase in the overall level, although further experiment is required to verify the results. When aligning to all genes, we obtained a very clear enrichment of R-loops accumulating at the TSS over negative control (Fig. S1f), as expected. Surprisingly, we did not detect any R-loops accumulating around TTS (Fig. S1g), as previously reported in HeLa cells (Hatchi et al., 2021). While the insufficient read depth could be an explanation, we also speculate this might be due to that R-loops at TTS being less efficiently captured by MapR.

In parallel, I also made an effort into developing a working CUT&RUN protocol in *S. pombe*, so that MapR could be performed. During testing, we realized that enzymatic treatment to digest the cell wall of *S. pombe*, while allowing antibodies to enter cells, rendered the cells incapable of binding to Concanavalin-A beads. In *S. cerevisiae*, CUT&RUN was performed after nuclei extraction (Brahma and Henikoff 2019), but an efficient nuclei extraction protocol in *S. pombe* suitable for sequencing was lacking. I therefore decided to optimize such a protocol, and for this, I combined a protoplasting protocol using Lallzyme (Flor-Parra et al. 2014), nuclei extraction using mild hypotonic shock (Orsi et al. 2015), followed by nuclei clean-up using a simple fractionation (adopted from an in-house protocol, which was modified from Keogh et al. 2006). The resulting nuclei were relatively clean and could then be bound onto Concanavalin-A beads for CUT&RUN (Methods).

I performed a MNase experiment on digitonin-permeabilized nuclei to test whether they were suitable for CUT&RUN based experiment. As shown (Fig. S2a), the no enzyme control (NE) showed that the DNA was mostly high molecular weight, meaning the nuclei extraction process did not damage the chromatin. When MNase was added and activated, a characteristic nucleosome ladder was observed. With this, we proceeded to performing several test-runs of CUT&RUN. We first tested with an antibody

against pS5 of Pol II, which is known to be enriched in Pol II early in the transcription cycle (Eick and Geyer 2013). We tested the sensitivity of the protocol using nuclei from 10 mL and 1 mL worth of log-phase cells. While in no enzyme control we did not detect any substantial enrichment over the bottom 10% or top 10% expressed genes, we detected enrichment over the gene body in top 10% expressed genes when the α-pS5 antibody was used (Fig. S2b,c). Strikingly, we observed a better enrichment when 10 times less nuclei were used, suggesting that a careful titration of antibody to nuclei was needed for the CUT&RUN protocol. We also tested our protocol with histone H3 and H3K9me2 antibodies (Fig. S2d), and observed a clear enrichment of H3K9me2 at the centromere (Fig. S2d, left) but not at any random genomic loci (Fig. S2d. right).

Overall, we have developed a working CUT&RUN protocol, but we noted the protocol is far from optimized. First, careful titration of antibody to nuclei is required, which sometimes requires substantial amount of testing. Second, the signal to noise ratio is still suboptimal compared to what has been achieved using mammalian cells; this might be due to contamination from cellular debris or lysed nuclei arising during the experimental procedure, or could be from non-specific binding of the antibody. Third, as the protocol was assembled from several other methods, and future optimization will test whether this can be further simplified, streamlining the experimental procedure.

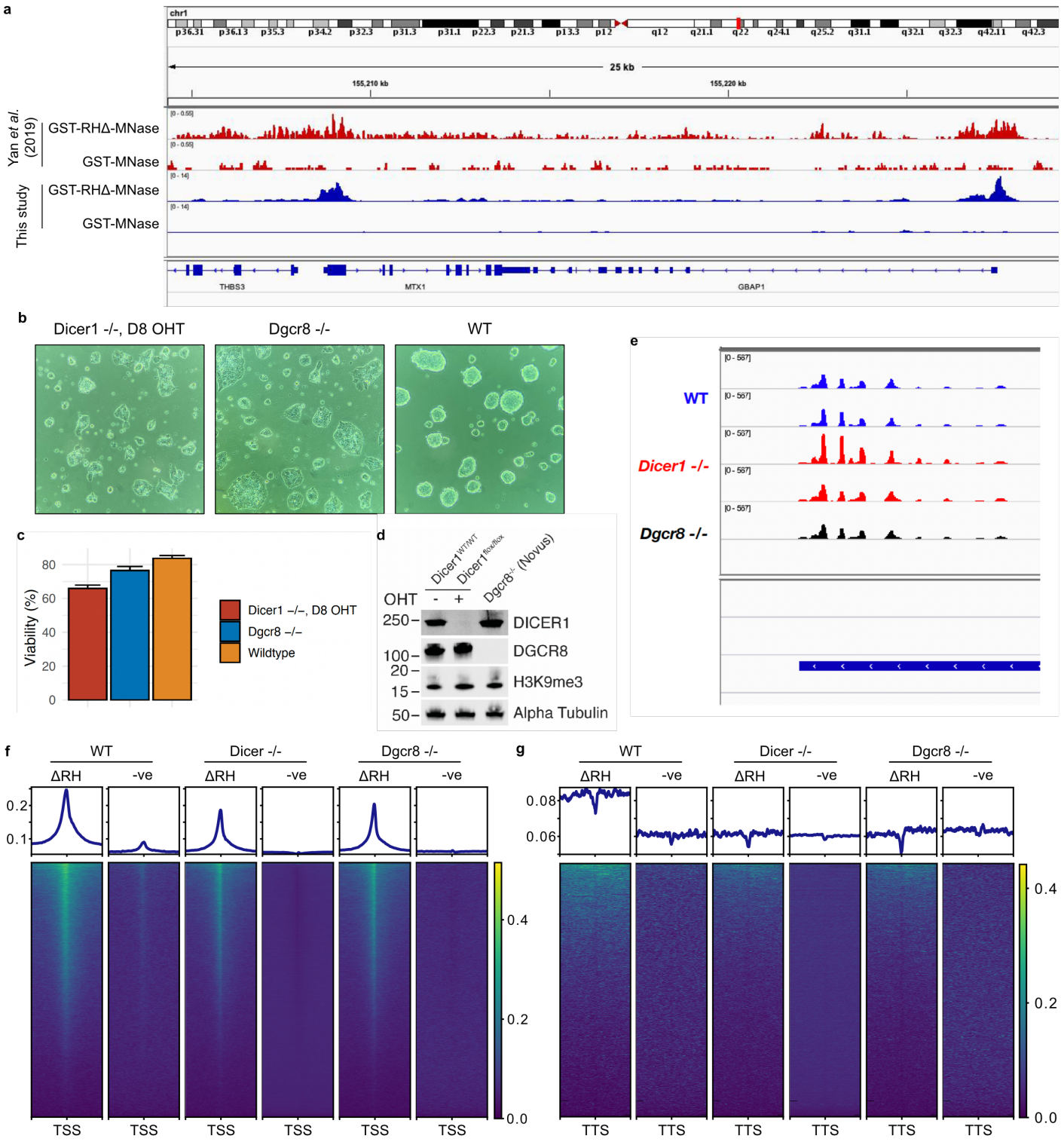
a
chr1
25 kb
155,210 kb
155,220 kb
Yan et al. (2019)
GST-RHΔ-MNase
GST-MNase
This study
GST-RHΔ-MNase
GST-MNase
THBS3
MTX1
GBAP1
b
Dicer1 -/-, D8 OHT
Dgcr8 -/-
WT
c
Viability (%)
Dicer1 –/–, D8 OHT
Dgcr8 –/–
Wildtype
d
OHT
DICER1
DGCR8
H3K9me3
Alpha Tubulin
e
WT
Dicer1 -/-
Dgcr8 -/-
f
WT
Dicer -/-
Dgcr8 -/-
ΔRH
-ve
TSS
g
TTS

Figure S1. MapR in HeLa and mESCs

(a) Example genome browser view comparing the MapR experiment in Yan *et al*., 2019 using HEK293 cells, and our pilot study using HeLa cells. Note the peaks at the TSSs of *MTX1* and *GBAP1* showing reproducible results.

(b) Representative images of Dicer1$^{-/-}$, Dgcr8$^{-/-}$, and WT mESCs.

(c) Viability counts of mESCs of various genotypes at the time of harvest. Error bars represent SEM.

(d) Western blot showing successful knockout at respective genotypes. Global H3K9me3 level remained unchanged. Tubulin was used as loading control.

(e) Genome browser view of a region of the mouse pericentromeric region at chromosome 9 (~3,000-3,005kb; GSAT_mm)

(f,g) Heatmap and mean normalized mapR signal of all annotated transcripts, centered to (f) TSS and (g) TTS with 3kb upstream and downstream, in various genotypes. ΔRH: MapR experiment using GST-RHΔ-MNase; -ve: negative control using GST-MNase. Values represent noralized read count (CPM).

Tissue culture for HeLa and mESC, viability assay, and Western blot were conducted by Joshua Steinberg.

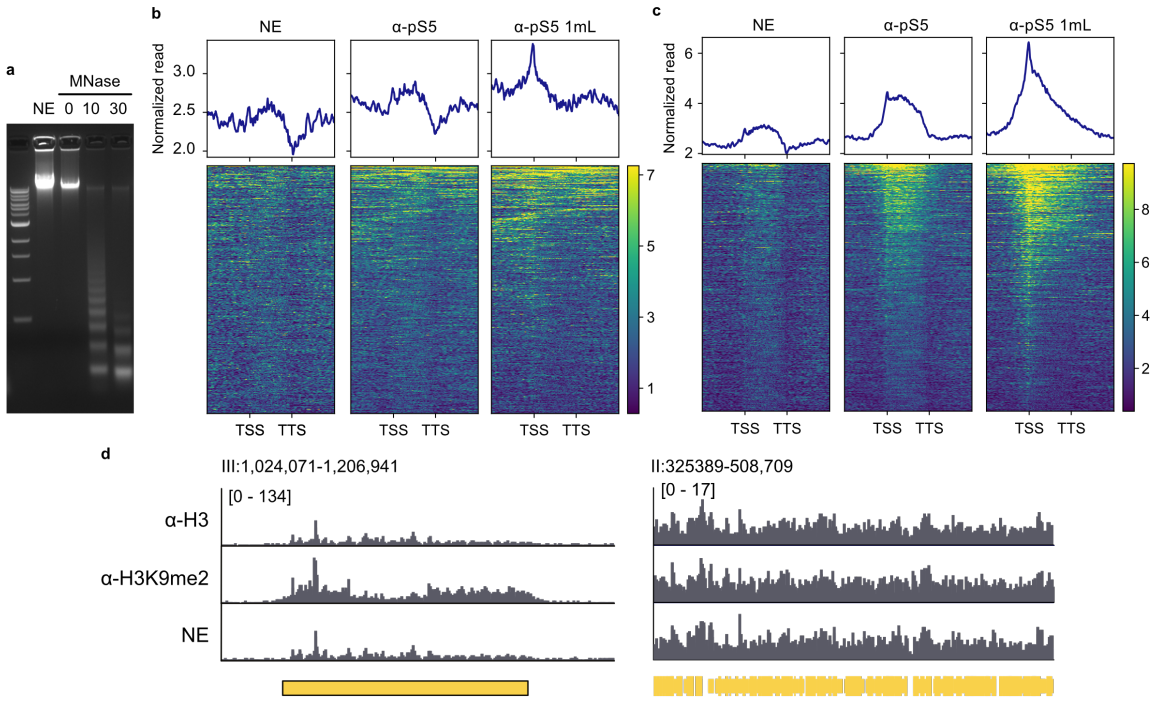

Figure S2. Optimization of CUT&RUN in *S. pombe*

(a) MNase activity assay on digitonin permeabilized *S. pombe* nuclei. Cells from 0.5 L of culture were prepped into nuclei and snap-frozen into 10 aliquots. For MNase activity assay, 1 aliquot was thawed on ice and resuspended in 160 µL of freshly prepared dig-wash buffer (20 mM HEPES pH 7.5, 150 mM NaCl, 2 mM $CaCl_2$, 0.5 mM spermidine, 0.02% w/v digitonin). MNase purified in-house was added to a final concentration of 1.5 µM, and the reaction was incubated at 37 ºC. At 0, 10, 30 minutes, 25 µL of the reaction was mixed with an equal volume of 2X STOP buffer (150 mM NaCl, 20 mM EDTA pH 8.0, 4 mM EGTA pH 8.0, 2% w/v SDS) prechilled on ice. The reactions were then treated with 2 µL 10 mg/mL RNase A at 37 ºC for 15 min and DNA was extracted using PhChl.

(b,c) Heatmap and mean normalized CUT&RUN signal of (b) bottom 10% expressed genes and (c) top 10% expressed genes for no enzyme (NE) control, CUT&RUN performed with 10 mL and 1mL cell culture worth of nuclei against α-pS5 antibody targeting Pol II.

(d) Genome browser view of *S. pombe* chromosome III centromere (left), and a random region (right) of CUT&RUN performed in WT cells using anti-histone H3 (α-H3), anti-H3K9me2, or NE control.

Chapter 7: Appendix 2 – supplementary tables

Table S1 – List of strains used in this study

Strain name	Mating type	Genotype	Reference	Use
BR00	h-		972	WT
BR51	h+			WT
BR245	h-	*dcr1-5* (D908A, D1127A)	Roche et al., 2016	Fig. 4.3
BR370	h-	*dcr1Δ::hphMX*	Roche et al., 2016	Fig. 3.3a
BR371	h+	*dcr1Δ::hphMX*	Roche et al., 2016	Fig. 3.2c,d; 3.4e
CC11		*dcr1Δ::hphMX sen1Δ::kanMX*	This study	Fig. 3.2c
CC15		*dcr1Δ::hphMX dbl8Δ::kanMX*	This study	Fig. 3.2d
FY2317	h+	*leu1-32::[hENT1 leu1+] his7-366::[hsv-tk his7+] ura4-D18 ade6-M210*	Hodson et al., 2003	Fig. 4.6
RM52	h+	*ade6-DN/N,leu1-32,ura4-DS/E,imr1L::ura4+,otr1R::ade6+, hphMX6-purg1-3FLAG-dcr1*	Sonali Bhattacharjee	Fig. 3.1b,c
TC45	h-	*dcr1-K38R::hphMX*	This study	
TC48	h-	*dcr1-K38A::hphMX*	This study	
TC91	h+	*rnh1Δ::hphMX*	This study	Fig. 3.1d; 3.10b
TC92	h+	*rnh1Δ::hphMX*	This study	Fig. 3.1d,g,h; 3.2a
TC94	h+	*rnh201Δ::natMX*	This study	Fig. 3.1d; 3.10b
TC95	h+	*rnh201Δ::natMX*	This study	Fig. 3.1d,g,h; 3.2a
TC98	h+	*hphMX-:pnmt1-rnh1*	This study	Fig. 3.2a
TC119	h-	*dcr1-K38R::hphMX*	This study	
TC123	h-	*dcr1-K38A::hphMX*	This study	
TC127	h+	*rnh1Δ::hphMX rnh201Δ::natMX*	This study	Fig. 3.1d
TC128	h+	*rnh1Δ::hphMX rnh201Δ::natMX*	This study	Throughout
TC131	h+	*mat1PΔ17:LEU2 ura4-DS/E ade6-DN/N leu1-32 otr1R(SphI)::ade6+ imr1L(NcoI)::ura4+ rad51Δ::kanMX*	This study	Fig. 4.2a
TC151	h-	*dcr1-K38R::hphMX*	This study	
TC155	h-	*dcr1-K38A::hphMX*	This study	
TC167	h+	*dcr1Δ::kanMX*	This study	Fig. 3.1d
TC168	h+	*dcr1Δ::kanMX*	This study	Throughout
TC171	h+	*rnh1Δ::hphMX dcr1Δ::kanMX*	This study	Fig. 3.1d
TC172	h+	*rnh1Δ::hphMX dcr1Δ::kanMX*	This study	Fig. 3.1d,g,h; 3.2a
TC175	h+	*rnh201Δ::natMX dcr1Δ::kanMX*	This study	Fig. 3.1d
TC176	h+	*rnh201Δ::natMX dcr1Δ::kanMX*	This study	Fig. 3.1d,g,h; 3.2a
TC180		*hphMX::pnmt1-rnh1 dcr1Δ::kanMX*	This study	Fig. 3.2a
TC187	h+	*rnh1Δ::hphMX rnh201Δ::natMX dcr1Δ::kanMX*	This study	Fig. 3.1d
TC188	h+	*rnh1Δ::hphMX rnh201Δ::natMX dcr1Δ::kanMX*	This study	Throughout
TC207	h-	*dcr1-K38R::hphMX*	This study	

TC211	h-	*dcr1-K38A::hphMX*	This study	
TC255	h-	*dcr1-K38R::hphMX*	This study	Fig. 4.1d
TC256	h-	*dcr1-K38R::hphMX*	This study	Fig. 2.3c; 4.2a,h; 4.3
TC271	h-	*dcr1-K38A::hphMX*	This study	Fig. 4.1d
TC272	h-	*dcr1-K38A::hphMX*	This study	Fig. 2.3c; 4.2a,h; 4.3
TC277	h-	*dcr1Δ::hphMX*	This study	Fig. 4.1d
TC304	h-	*dcr1-ΔPAZ::hphMX*	This study	Fig. 4.1d
TC307	h-	*dcr1-ΔDUF::hphMX*	This study	Fig. 4.1d
TC320	h+	*rnh201Δ::natMX dcr1-K38R::hphMX*	This study	Fig. 4.3
TC323	h-	*rnh201Δ::natMX dcr1-K38A::hphMX*	This study	Fig. 4.3
TC326	h-	*rnh1Δ::kanMX dcr1-K38R::hphMX*	This study	Fig. 4.3
TC329	h+	*rnh1Δ::kanMX dcr1-K38A::hphMX*	This study	Fig. 4.3
TC332	h+	*rnh1Δ::kanMX rnh201Δ::natMX dcr1-K38R::hphMX*	This study	Fig. 4.3
TC335	h+	*rnh1Δ::kanMX rnh201Δ::natMX dcr1-K38A::hphMX*	This study	Fig. 4.3
TC338	h+	*rnh1Δ::kanMX dcr1-ΔPAZ::hphMX*	This study	Fig. 4.3
TC342	h+	*rnh201Δ::natMX dcr1-ΔPAZ::hphMX*	This study	Fig. 4.3
TC344	h+	*rnh1Δ::kanMX rnh201Δ::natMX dcr1-ΔPAZ::hphMX*	This study	Fig. 4.3
TC347	h+	*rnh1Δ::kanMX dcr1-ΔDUF::hphMX*	This study	Fig. 4.3
TC351	h+	*rnh201Δ::natMX dcr1-ΔDUF::hphMX*	This study	Fig. 4.3
TC352	h+	*rnh1Δ::kanMX rnh201Δ::natMX dcr1-ΔDUF::hphMX*	This study	Fig. 4.3
TC372	h-	*dcr1-ΔHel::hphMX*	This study	Fig. 4.3
TC375	h-	*rnh1Δ::hphMX rnh201Δ::natMX dcr1Δ::kanMX tbp1-D156Y*	This study	Fig. 3.3a
TC378	h-	*rnh1Δ::hphMX rnh201Δ::natMX dcr1Δ::kanMX med31-ins*	This study	Fig. 3.3a
TC381	h-	*dcr1-ΔC103::hphMX*	This study	
TC416	h-	*rnh1Δ::hphMX rnh201Δ::natMX dcr1Δ::kanMX tfs1Δ::kanMX*	This study	Fig. 3.3a
TC419	h-	*rnh1Δ::hphMX rnh201Δ::natMX dcr1Δ::kanMX mst2Δ::kanMX*	This study	Fig. 3.3a
TC422	h-	*rnh1Δ::hphMX rnh201Δ::natMX dcr1Δ::kanMX fcp1-Y580*::kanMX*	This study	Fig. 3.3a
TC441	h-	*clr2-T497N::kanMX*	This study	Fig. 2.1e
TC445	h-	*paf1-D65N::kanMX*	This study	Fig. 2.1d
TC459	h-	*top1-W647*::kanMX*	This study	Fig. 2.1c
TC495	h-	*clr2-T497N::kanMX rnh1Δ::hphMX rnh201Δ::natMX*	This study	Fig. 2.1e
TC497	h-	*clr2-T497N::kanMX dcr1Δ::kanMX*	This study	Fig. 2.1e
TC498	h-	*clr2-T497N::kanMX dcr1Δ::kanMX rnh1Δ::hphMX rnh201Δ::natMX*	This study	Fig. 2.1e
TC502	h-	*paf1-D65N::kanMX rnh1Δ::hphMX rnh201Δ::natMX*	This study	Fig. 2.1d
TC505	h-	*paf1-D65N::kanMX dcr1Δ::kanMX*	This study	Fig. 2.1d
TC508	h-	*paf1-D65N::kanMX dcr1Δ::kanMX rnh1Δ::hphMX6 rnh201Δ::natMX6*	This study	Fig. 2.1d
TC526	h-	*top1-W647*::kanMX rnh1Δ::hphMX rnh201Δ::natMX*	This study	Fig. 2.1c
TC529	*h+*	*top1-W647*::kanMX dcr1Δ::kanMX*	This study	Fig. 2.1c

TC530	h-	*top1-W647*::kanMX dcr1Δ::kanMX rnh1Δ::hphMX rnh201Δ::natMX*	This study	Fig. 2.1c
TC532	h+	*tfs1Δ::kanMX*	This study	Fig. 3.3b
TC534	h+	*rnh1Δ::hphMX rnh201Δ::natMX tfs1Δ::kanMX*	This study	Fig. 3.3b
TC536	h-	*dcr1Δ::kanMX tfs1Δ::kanMX*	This study	Fig. 3.3c
TC537		*dcr1Δ::kanMX tfs1Δ::kanMX*	This study	Fig. 3.3b
TC539	h-	*rnh1Δ::hphMX rnh201Δ::natMX dcr1Δ::kanMX tfs1Δ::kanMX*	This study	Fig. 3.3c
TC540	h-	*rnh1Δ::hphMX rnh201Δ::natMX dcr1Δ::kanMX tfs1Δ::kanMX*	This study	Fig. 3.3b
TC564	h-	*med20Δ::kanMX*	This study	Fig. 2.3c; 3.5e; 3.10d; 4.2h
TC571	h+	*med20-1*	This study	Fig. 3.5f
TC572	h-	*epl1-T449A*	This study	Fig. 2.5b
TC575	h-	*dcr1Δ::kanMX med20-1*	This study	Fig. 3.5f
TC579	h-	*rnh1Δ::hphMX rnh201Δ::natMX med20-1*	This study	Fig. 3.5f
TC583	h-	*rnh1Δ::hphMX rnh201Δ::natMX dcr1Δ::kanMX med20-1*	This study	Fig. 3.5f
TC587	h-	*dcr1Δ::kanMX epl1-T449A*	This study	Fig. 2.2b
TC591	h-	*rnh1Δ::hphMX rnh201Δ::natMX epl1-T449A*	This study	Fig. 2.2b
TC595	h-	*rnh1Δ::hphMX rnh201Δ::natMX dcr1Δ::kanMX epl1-T449A*	This study	Fig. 2.2b
TC607	h-	*rnh1Δ::hphMX rnh201Δ::natMX dcr1Δ::hphMX*	This study	Fig. 3.4b
TC608	h+	*rnh1Δ::hphMX rnh201Δ::natMX dcr1Δ::hphMX*	This study	Fig. 3.5c
TC621	h+	*dcr1Δ::hphMX med20Δ::kanMX*	This study	Fig. 2.3c; 3.5e; 3.10d; 4.2h
TC622	h+	*rnh1Δ::hphMX rnh201Δ::natMX med20Δ::kanMX*	This study	Fig. 3.5e
TC624	h+	*rnh1Δ::hphMX rnh201Δ::natMX dcr1Δ::hphMX med20Δ::kanMX*	This study	Fig. 3.5e
TC644	h+	*rpb1-T481K::kanMX6*	This study	Fig. 2.3b; 3.4a
TC648	h+	*tfa2-L238*::kanMX*	This study	Fig. 2.3a; 3.4a
TC649	h+	*rnh1Δ::hphMX rnh201Δ::natMX rpb1-T481K::kanMX6*	This study	Fig. 2.3b; 3.4a
TC652	h+	*dcr1Δ::hphMX rpb1-T481K::kanMX6*	This study	Fig. 2.3b; 3.4a
TC653	h+	*rnh1Δ::hphMX rnh201Δ::natMX dcr1Δ::hphMX rpb1-T481K::kanMX6*	This study	Fig. 2.3b; 3.4a
TC654	h+	*rnh1Δ::hphMX rnh201Δ::natMX tfa2-L238*::kanMX*	This study	Fig. 2.3a; 3.4a
TC657	h+	*dcr1Δ::kanMX tfa2-L238*::kanMX*	This study	Fig. 2.3a; 3.4a
TC661	h-	*ago1Δ::hphMX*	This study	Fig. 3.10
TC665	h+	*rnh1Δ::hphMX rnh201Δ::natMX dcr1Δ::kanMX tfa2-L238*::kanMX*	This study	Fig. 2.3a; 3.4a
TC666	h-	*ago1Δ::hphMX med20Δ::kanMX*	This study	Fig. 3.10d
TC669	h-	*dcr1K38R::hphMX med20Δ::kanMX*	This study	Fig. 2.3c; 4.2h
TC672	h-	*dcr1K38A::hphMX med20Δ::kanMX*	This study	Fig. 2.3c; 4.2h
TC673	h-	*sen1Δ::kanMX*	This study	Fig. 3.2c
TC677	h-	*dbl8Δ::kanMX*	This study	Fig. 3.2d
TC727	h+	*leu1-32::[hENT1 leu1+] his7-366::[hsv-tk his7+] ura4-D18 ade6-M210 dcr1Δ::hphMX*	This study	Fig. 4.6
TC730	h+	*rnh1Δ::kanMX ago1Δ::hphMX*	This study	Fig. 3.10c
TC733	h-	*rnh201Δ::natMX ago1Δ::hphMX*	This study	Fig. 3.10c
TC736	h-	*rnh1Δ::kanMX rnh201Δ::natMX ago1Δ::hphMX*	This study	Fig. 3.10c,d

TC748	h+	*leu1-32::[hENT1 leu1+] his7-366::[hsv-tk his7+] ura4-D18 ade6-M210 rnh1Δ::kanMX rnh201Δ::natMX*	This study	Fig. 4.6
TC750	h+	*leu1-32::[hENT1 leu1+] his7-366::[hsv-tk his7+] ura4-D18 ade6-M210 rnh1Δ::kanMX rnh201Δ::natMX dcr1Δ::hphMX*	This study	Fig. 4.6
TC752		*rnh1Δ::hphMX dcr1-5*	This study	Fig. 3.3
TC753		*rnh201Δ::natMX dcr1-5*	This study	Fig. 3.3
TC755		*rnh1Δ::hphMX rnh201Δ::natMX dcr1-5*	This study	Fig. 3.3
TC757	h+	*ago1Δ::hphMX rnh1Δ::hphMX rnh201Δ::natMX dcr1Δ::kanMX*	This study	Fig. 3.10c
TC759	h-	*rpb2-R1118H::kanMX*	This study	Fig. 3.4e
TC761	h-	*rnh1Δ::hphMX dcr1-ΔHel::hphMX*	This study	Fig. 3.3
TC763	h+	*rnh201Δ::natMX dcr1-ΔHel::hphMX*	This study	Fig. 3.3
TC765	h-	*rnh1Δ::hphMX rnh201Δ::natMX dcr1-ΔHel::hphMX*	This study	Fig. 3.3
TC767		*rnh1Δ::hphMX rnh201Δ::natMX rpb2-R1118H::kanMX*	This study	Fig. 3.4e
TC777	h-	*dcr1Δ::hphMX rpb2-R1118H::kanMX*	This study	Fig. 3.4e
TC779	h+	*rnh1Δ::hphMX rnh201Δ::natMX dcr1Δ::hphMX rpb2-R1118H::kanMX*	This study	Fig. 3.4e

Table S2 – List of primers used in this study

Name	Sequence (5'-3')	Use
Ago1-InF1	CAGCATCGCAATAATGTCGG	KO genotype
Ago1-InR1	GCCCAAGATCTAATAGGAGC	KO genotype
Clr2_L6	CAGTTAATCTGCTGCCCAACATTG	Clr2-T497N cassette
Clr2_L7	AACGTGGAACCTATTTGGTATCTTCC	Clr2-T497N cassette
Clr2_L8	TAATTAACCCGGGGATCCGTCGACCCCTATCTTTCTCTG TAATTTATGAAATGCAAAAG	Clr2-T497N cassette
Clr2_L9	AAACGAGCTCGAATTCATCGATGATAAACTATTTGTGT TGAATTAGAGATGGGATATA	Clr2-T497N cassette
Clr2_T497N_F	AGGAGATTTAAATTACAATTCAGAAGTGAAAGAAC	Clr2-T497N cassette
Clr2_T497N_R	GTTCTTTCACTTCTGAATTGTAATTTAAATCTCCT	Clr2-T497N cassette
Clr2-T497N-dCAPs-F	TGAGCCTTGGTTCGTAAAAGGAGATTTAAATTAGA	Clr2-T497N dCAPs
Clr2-T497N-dCAPs-R	ATTTCAGACAGTAAATATTCATAAAAATCGTCATCG	Clr2-T497N dCAPs
Cul1_A3	GCTCGACCAAAACTGCAGTGAGGATATC	Cul1-R330 dCAPs; SphI cuts WT
Cul1-R330syn_dCAPs	CCTGATCTCTTGACAAACTCCTCAAATGCATG	Cul1-R330 dCAPs; SphI cuts WT
Dbl8_InF1	GGCTCAAGTGAAAAGTGCCG	Dbl8 KO genotype
Dbl8_InR1	GACGCGTTACATTGGCATCC	Dbl8 KO genotype
Dbl8_L1	AATCACAAACTTCGGATTATAATGGG	Dbl8 KO cassette
Dbl8_L2	TAATTAACCCGGGGATCCGTCGACCTGATGTCCACACA GCACTCG	Dbl8 KO cassette

Dbl8_L5	AAACGAGCTCGAATTCATCGATGATAAGCCGATTTAGGTTTTAGTATGAG	Dbl8 KO cassette
Dbl8_L6	AGAATATACTGGTGCATTTGTCCTG	Dbl8 KO cassette
Dcr1_A14	GAATGGATATTTCAAGTTTTCTACTTCC	Dcr1-K38R/A dCAPs; BglII cuts WT
Dcr1_A4	GGAATGAATGAGCTTGTACAAACAC	Dcr1-K38R/A cassette
dcr1_delta_hel_1F	GAATGGATATTTCAAGTTTTCTACTTACTGATGATATCGTCTATGAAG	Dcr1-delta-Hel cassette
dcr1_delta_hel_1R	CTTCATAGACGATATCATCAGTAAGTAGAAAACTTGAAATATCCATTC	Dcr1-delta-Hel cassette
Dcr1_deltaDUF_1F	GTTTGTCTATAAGACCCATACGAATCAGACTAACTGCATACAACCC	Dcr1-delta-DUF cassette
Dcr1_deltaDUF_1R	GGGTTGTATGCAGTTAGTCTGATTCGTATGGGTCTTATAGACAAAC	Dcr1-delta-DUF cassette
Dcr1_deltaPAZ_1F	GGCGACCAATAAGTTTTCAATATGTAATTTAAAAAAATTTTGGATAGTGTCAAC	Dcr1-delta-PAZ cassette
Dcr1_deltaPAZ_1R	GTTGACACTATCCAAAATTTTTTTAAATTACATATTGAAAACTTATTGGTCGCC	Dcr1-delta-PAZ cassette
Dcr1_K38A_F	GTAATGTCGCACCAGCGCCCGTTCTC	Dcr1-K38A cassette
Dcr1_K38A_R	GAGAACGGGCGCTGGTGCGACATTAC	Dcr1-K38A cassette
Dcr1_K38R_F	GTAATGTCCTACCAGCGCCCGTTCTC	Dcr1-K38R cassette
Dcr1_K38R_R	GAGAACGGGCGCTGGTAGGACATTAC	Dcr1-K38R cassette
Dcr1_L10	TATGAACGATATCGTAGAGAGCAGC	Dcr1-delta-PAZ cassette
Dcr1_L7	TAATTAACCCGGGGATCCGTCGACCTTATGTTGTAAAAAACTACCACCTAC	Dcr1-K38R/A, delta-PAZ, and delta-DUF cassette
Dcr1_L8	AAACGAGCTCGAATTCATCGATGATACGCACTTTAATAAAAAATGATTAAACG	Dcr1-K38R/A, delta-PAZ, and delta-DUF cassette
Dcr1_L9	CCTATGTTCCGATAAGAGCAGGC	Dcr1-K38R/A, delta-PAZ, and delta-DUF cassette
Dcr1-InF1	TCCGCAGATGTTAAAGCCTG	KO genotype; Also Dcr1-deltaDUF cassette
Dcr1-InR1	CCTACTCCTTACTGGCTTGC	KO genotype
Dcr1-K38R/A-dCAPS	TATCAACTTCACAGCAAGTAAGATC	Dcr1-K38R/A dCAPs with Dcr1_A14; BglII cuts WT
Erd101_A3	TCAACGTGGGTTGAGGAAAAGC	Erd101 dCAPs; EcoRV cuts WT
Erd101-D176A_dCAPs	AGTGCTTTAGCATATGATGTGAATATTTCAGAAACAATGATA	Erd101 dCAPs with A3; EcoRV cuts WT
Kap113_A3	GCACGAGTTTTGGCAGTTATGC	Kap113 dCAPs; XbaI cuts WT
Kap113-int1_dCAPs	AAAAAGTTGAAAATTCAAAAGATTTTGCTTTGATCGTCTA	Kap113 dCAPs with A3; XbaI cuts WT
Med20_A3	GCCAGCATGCTGGGATTAATGTTTTG	dCAPs primer

Med20_A6	CGGCAGTCCTTTACTATTGAAGGTT	dCAPs primer with Med20_A7 for Med20-3; DraI cuts WT
Med20_A7	CGACGGACTCAGTACCATCGTAA	dCAPs primer with Med20_A6 for Med20-3; DraI cuts WT
Med20-W37A_dCAPs3	TATTTCTTATGATTGATGATTTCAAGATCTAACTTTGAATTTCAGACATA	dCAPs primer with Med20_A3 for Med20-2; NdeI cuts WT
Med20-Y44S_dCAPs3	AAAAATTCTAAAGTTTTTGGAGTGACAGCATTTCCG	dCAPs primer with Med20_A3 for Med20-1; BspEI cuts mutant
p30_qPCR_F	CCATATCAATTTCCCATGTTCC	RT-qPCR
p30_qPCR_R	CATCAAGCGAGTCGAGATGA	RT-qPCR
p33_qPCR_F	TATCCTGCGTCTCGGTATCC	RT-qPCR
p33_qPCR_R	CTGTTCGTGAATGCTGAGAAAG	RT-qPCR
Paf1_D65N_F	GAATGCCGCTTAATTTGGCCGGAATAACTG	Paf1-D65N cassette
Paf1_D65N_R	CAGTTATTCCGGCCAAATTAAGCGGCATTC	Paf1-D65N cassette
Paf1_In1R	TTCAAGCCCTGTGCTATTGACATG	Paf1-D65N cassette
Paf1_L6	AAGCAACTTTATTTAGTTTTGGACATAACGC	Paf1-D65N cassette
Paf1_L8	AAACGAGCTCGAATTCATCGATGATAAGGTGATACAATCGACGCAAAATCC	Paf1-D65N cassette
Paf1_L9	TAATTAACCCGGGGATCCGTCGACCCGATGTTCACTCACTGTAGTCCAATTTC	Paf1-D65N cassette
Paf1-D65N-dCAPs-F	ATCTCCTTCAAAAAATCCAGTTATTCCGGCGATAT	Paf1-D65N dCAPs
Paf1-D65N-dCAPs-R	ATGCCTTACCAAATTTTGTATCAACTTTAGTTCAAG	Paf1-D65N dCAPs
Pcs2_A3	ATAATTGTAAAAAATTTGTTCATGGCTCTATGTAAACT	Pcs2 dCAPs; PstI cuts mutant
Pcs2-3'utr-dCAPs	ACTGGGTGTTGTAGTTCAAGCTGCTGTAAAAATACCTGCA	Pcs2 dCAPs with Pcs2_A3; PstI cuts mutant
pnmt1-AB	AAACGAGCTCGAATTCATCGATGATATCGCCATAAAAGACAGAATAAGTC	Rnh1 Overexpression
pnmt1-Rnh1	GCACGCTTATTTCCACCCATGATTTAACAAAGCGACTATAAG	Rnh1 Overexpression
Pof1_A3	TCATACTTTCAGTGCTCATATTGGCCC	Pof1-S449C dCAPs; XbaI cuts WT
Pof1-S449C-dCAPs	ATTTTTTCTTCTCGATGTCCCATTGCTTTATTGTGCCGTCCAATGATCTA	Pof1-S449C dCAPs; XbaI cuts WT
Rnh1_InF1	GGAAGTCGCTACTCCTCGTC	Rnh201 KO genotype
Rnh1_InR1	ATTGCTGTCAGAGCGGATGG	Rnh201 KO genotype
Rnh1_L1	AGAGGCCAACAGAGATGAGG	Rnh1 KO cassette
Rnh1_L2	TAATTAACCCGGGGATCCGTCGACCCGGGTTTGCTTATTTACTAGCTG	Rnh1 KO cassette

Rnh1_L5	AAACGAGCTCGAATTCATCGATGATATTGAAAAGTATAGATTCGGAGCTAAG	Rnh1 KO cassette
Rnh1_L6	CTGTGAATGTTCGTTTCAAAACC	Rnh1 KO cassette
Rnh1_Pnmt1	TATAGTCGCTTTGTTAAATCATGGGTGGAAATAAGCGTGC	Rnh1 Overexpression
Rnh1_qPCR_1F	ACGGTCGTATGCTTTGCTTC	RT-qPCR
Rnh1_qPCR_1R	ACCTTTCACCTGATCCGACG	RT-qPCR
Rnh1-L7	AACAACAAGGTGTATCCATCAAGG	Rnh1 Overexpression
Rnh201_InF1	TGTCGCTTACTGTCCAGTCG	Rnh201 KO genotype
Rnh201_InR1	CACTCGGTAGTTCGAGCGTC	Rnh201 KO genotype
Rnh201_L1	CTTGTATGCAGGCTTCGATTGC	Rnh201 KO cassette
Rnh201_L2	TAATTAACCCGGGGATCCGTCGACCAGCGGTACTACGGTAAAACG	Rnh201 KO cassette
Rnh201_L5	AAACGAGCTCGAATTCATCGATGATACATTGCTTCGTGCTTTTGGA	Rnh201 KO cassette
Rnh201_L6	CGAGATTCCACAACAAAGCGG	Rnh201 KO cassette
Rpb1_A3	CACGAGTTTCTTCTGACTGAGGGACATGC	Rpb1-T481K dCAPs; PacI cuts mutant
Rpb1_L10	CCAAGGTAACGTTCTTAGAAGAAACAC	Rpb1-T481K cassette
Rpb1_L7	GATCTTTCTGCTGTATACAGGAATAAATTTATC	Rpb1-T481K cassette
Rpb1_L8	TAATTAACCCGGGGATCCGTCGACCGTGTACTAGCCACCCTGTGATAAAC	Rpb1-T481K cassette
Rpb1_L9	AAACGAGCTCGAATTCATCGATGATACCTATACTGACTTTTCTGCACCGTG	Rpb1-T481K cassette
Rpb1_T481K_F	CCGATTAAACTTGTCAGTTAAGTCTCCTTATAATGCTG	Rpb1-T481K cassette
Rpb1_T481K_R	CAGCATTATAAGGAGACTTAACTGACAAGTTTAATCGG	Rpb1-T481K cassette
Rpb1-T481K_dCAPs	GCCGTACTCGACATTCCGATTAAACTTGTTAATTA	Rpb1-T481K dCAPs; PacI cuts mutant
Rpb2_L10	CAAAGCGTGACGTTTCCACTCC	Rpb2-R1118 cassette
Rpb2_L7	CCCGTTGAAACTCAACAATGCG	Rpb2-R1118 cassette
Rpb2_L8	TAATTAACCCGGGGATCCGTCGACCGATCTTAAAGAAGCTATCATTTATTTACATAAGC	Rpb2-R1118 cassette
Rpb2_L9	AAACGAGCTCGAATTCATCGATGATACGATCATCCTTCTGTATGTTCATGC	Rpb2-R1118 cassette
Rpb2_R1118H_dCAPs_1	ACTCGTCAACCCGTTGAAGGCAGATCTAGAGATGGTGGCGATC	Rpb2-R1118H dCAPs with L8; PvuI cuts WT
Rpb2_R1118H_for	GGTGGCCTTCACTTTGGAGAAATGG	Rpb2-R1118 cassette
Rpb2_R1118H_rev	CCATTTCTCCAAAGTGAAGGCCACC	Rpb2-R1118 cassette
Rpp0_A3	CAAAGTAGCCTCGGAAGGACCA	Rpp0 dCAPs with A3; KpnI cuts WT
Rpp0_A4	CACTGGTATGGAACCCGGTAAGAC	Rpp0 dCAPs with A4; KpnI cuts WT
Sen1_InF1	AGGATCGCACCGTTACCTTC	Sen1 KO genotype
Sen1_InR1	GTCGCTCTTGTTGGCGTATC	Sen1 KO genotype

Sen1_L1	TCGGTGAAACAACGTTTATTTGG	Sen1 KO cassette
Sen1_L2	TAATTAACCCGGGGATCCGTCGACCCCAATGCTGACCC TCTTTACTAG	Sen1 KO cassette
Sen1_L5	AAACGAGCTCGAATTCATCGATGATAGTTGTACCACTA AATACGCATC	Sen1 KO cassette
Sen1_L6	TGGCCTTCTTCACCTATTATAGACTG	Sen1 KO cassette
Tfa2_L10	CAGCTTATTTGAATTCAAATGATGGAC	Tfa2_L238* cassette
Tfa2_L238*_F	ACTTGGAAAATACGGTTAAAAGCCCACTAGCGTGG	Tfa2_L238* cassette
Tfa2_L238*_R	CCACGCTAGTGGGCTTTTAACCGTATTTTCCAAGT	Tfa2_L238* cassette
Tfa2_L7	CTACTAACTAGCTCCCGTGGCC	Tfa2_L238* cassette
Tfa2_L8	AAACGAGCTCGAATTCATCGATGATAGTCGAAATAGAA AGATCAGTTATGTATTGAAAGG	Tfa2_L238* cassette
Tfa2_L9	TAATTAACCCGGGGATCCGTCGACCGCACAAAAGGGA AAGATAAGAATTTCTG	Tfa2_L238* cassette
Top1_L10	GCTATACCGGAACTTGTGCCAATCTG	Top1-W647* cassette
Top1_L7	CTGGTTCTTTAAAGCGTCGAGTATATC	Top1-W647* cassette
Top1_L8	TAATTAACCCGGGGATCCGTCGACCTTGTATATTGAATT TGATGATCGTAACAGGC	Top1-W647* cassette
Top1_L9	AAACGAGCTCGAATTCATCGATGATAGCCAAGCTGCTG CTTTTTTAATCTTTATAC	Top1-W647* cassette
Top1_W647*_F	CATTACCGATTCATGAATCGTAAAACATC	Top1-W647* cassette
Top1_W647*_R	GATGTTTTACGATTCATGAATCGGTAATG	Top1-W647* cassette
Top1-W647*-dCAPs-F	TCTAGTTCGTAAAGTGTCTCGTGATGTTTTAGGAT	Top1-W647* dCAPs
Top1-W647*-dCAPs-R	GGATGAGACTGCGAAAAATGATGC	Top1-W647* dCAPs

Table S3 – Oligonucleotide sequences for biochemical assays

Name	Sequence (5'-3')	Use
DNA1	GGGTGAACCTGCAGGTGGGCGGCTGCTCATCG TAGGTTAGTTGGTAGAATTCGGCAGCGTC	Anneal with DNA2 for R-loops
DNA2	GACGCTGCCGAATTCTACCAGTGCCTTGCTAG GACATCTTTGCCCACCTGCAGGTTCACCC	DNA:RNA and R-loops
RNA	AAAGAUGUCCUAGCAAGGCAC	Anneal with DNA2 for DNA:RNA and R-loops

Chapter 8: References

Abraham, Karan J., Negin Khosraviani, Janet N. Y. Chan, Aparna Gorthi, Anas Samman, Dorothy Y. Zhao, Miling Wang, Michael Bokros, Elva Vidya, Lauren A. Ostrowski, Roxanne Oshidari, Violena Pietrobon, Parasvi S. Patel, Arash Algouneh, Rajat Singhania, Yupeng Liu, V. Talya Yerlici, Daniel D. De Carvalho, Michael Ohh, Brendan C. Dickson, Razq Hakem, Jack F. Greenblatt, Stephen Lee, Alexander J. R. Bishop, and Karim Mekhail. 2020. "Nucleolar RNA Polymerase II Drives Ribosome Biogenesis." *Nature* (December 2018). doi: 10.1038/s41586-020-2497-0.

Achar, Yathish Jagadheesh, David Balogh, Dante Neculai, Szilvia Juhasz, Monika Morocz, Himabindu Gali, Sirano Dhe-Paganon, Česlovas Venclovas, and Lajos Haracska. 2015. "Human HLTF Mediates Postreplication Repair by Its HIRAN Domain-Dependent Replication Fork Remodelling." *Nucleic Acids Research* 43(21):10277–91. doi: 10.1093/nar/gkv896.

Achar, Yathish Jagadheesh, and Marco Foiani. 2017. "Coordinating Replication with Transcription." Pp. 455–87 in *DNA Replication: From Old Principles to New Discoveries*, *Advances in Experimental Medicine and Biology*, edited by H. Masai and M. Foiani. Singapore: Springer.

Aderounmu, Adedeji M., P. Joseph Aruscavage, Bryan Kolaczkowski, and Brenda L. Bass. 2023. "Ancestral Protein Reconstruction Reveals Evolutionary Events Governing Variation in Dicer Helicase Function" edited by V. Dötsch. *eLife* 12:e85120. doi: 10.7554/eLife.85120.

Aguilera, Andrés. 2002. "The Connection between Transcription and Genomic Instability." *The EMBO Journal* 21(3):195–201. doi: 10.1093/emboj/21.3.195.

Ait Saada, Anissia, Sarah A. E. Lambert, and Antony M. Carr. 2018. "Preserving Replication Fork Integrity and Competence via the Homologous Recombination Pathway." *DNA Repair* 71:135–47. doi: 10.1016/j.dnarep.2018.08.017.

Ait Saada, Anissia, Ana Teixeira-Silva, Ismail Iraqui, Audrey Costes, Julien Hardy, Giulia Paoletti, Karine Fréon, and Sarah A. E. Lambert. 2017. "Unprotected Replication Forks Are Converted into Mitotic Sister Chromatid Bridges." *Molecular Cell* 66(3):398-410.e4. doi: 10.1016/j.molcel.2017.04.002.

Akerman, Ildem, Bahar Kasaai, Alina Bazarova, Pau Biak Sang, Isabelle Peiffer, Marie Artufel, Romain Derelle, Gabrielle Smith, Marta Rodriguez-Martinez, Manuela Romano, Sandrina Kinet, Peter Tino, Charles Theillet, Naomi Taylor, Benoit Ballester, and Marcel Méchali. 2020. "A Predictable Conserved DNA Base Composition Signature Defines Human Core DNA Replication Origins." *Nature Communications* 11(1):4826. doi: 10.1038/s41467-020-18527-0.

Alzu, Amaya, Rodrigo Bermejo, Martina Begnis, Chiara Lucca, Daniele Piccini, Walter Carotenuto, Marco Saponaro, Alessandra Brambati, Andrea Cocito, Marco Foiani, and Giordano Liberi. 2012. "Senataxin Associates with Replication Forks to Protect Fork Integrity across RNA-Polymerase-II-Transcribed Genes." *Cell* 151(4):835–46. doi: 10.1016/j.cell.2012.09.041.

Aria, Valentina, Mariarita De Felice, Roberta Di Perna, Shuji Uno, Hisao Masai, Juhani E. Syväoja, Barbara van Loon, Ulrich Hübscher, and Francesca M. Pisani. 2013. "The Human Tim-Tipin Complex Interacts Directly with DNA Polymerase ϵ and Stimulates Its Synthetic Activity *." *Journal of Biological Chemistry* 288(18):12742–52. doi: 10.1074/jbc.M112.398073.

Aristarkhov, A., A. Mikulskis, J. G. Belasco, and E. C. Lin. 1996. "Translation of the adhE Transcript to Produce Ethanol Dehydrogenase Requires RNase III Cleavage in Escherichia Coli." *Journal of Bacteriology* 178(14):4327–32. doi: 10.1128/jb.178.14.4327-4332.1996.

Atkinson, Sophie R., Samuel Marguerat, Danny A. Bitton, Maria Rodríguez-López, Charalampos Rallis, Jean François Lemay, Cristina Cotobal, Michal Malecki, Pawel Smialowski, Juan Mata, Philipp Korber, François Bachand, and Jürg Bähler. 2018. "Long Noncoding RNA Repertoire and Targeting by Nuclear Exosome, Cytoplasmic Exonuclease, and RNAi in Fission Yeast." *Rna* 24(9):1195–1213. doi: 10.1261/rna.065524.118.

Audoynaud, Charlotte, Kamila Schirmeisen, Anissia Ait Saada, Armelle Gesnik, Paloma Fernández-Varela, Virginie Boucherit, Virginie Ropars, Anusha Chaudhuri, Karine Fréon, Jean-Baptiste Charbonnier, and

Sarah A. E. Lambert. 2023. “RNA:DNA Hybrids from Okazaki Fragments Contribute to Establish the Ku-Mediated Barrier to Replication-Fork Degradation.” *Molecular Cell* 0(0). doi: 10.1016/j.molcel.2023.02.008.

Axtell, Michael J., Jakub O. Westholm, and Eric C. Lai. 2011. “Vive La Différence: Biogenesis and Evolution of microRNAs in Plants and Animals.” *Genome Biology* 12(4):221. doi: 10.1186/gb-2011-12-4-221.

Azvolinsky, Anna, Paul G. Giresi, Jason D. Lieb, and Virginia A. Zakian. 2009. “Highly Transcribed RNA Polymerase II Genes Are Impediments to Replication Fork Progression in Saccharomyces Cerevisiae.” *Molecular Cell* 34(6):722–34. doi: 10.1016/j.molcel.2009.05.022.

Baaklini, Imad, Chadi Hraiky, Fabien Rallu, Yuk-Ching Tse-Dinh, and Marc Drolet. 2004. “RNase HI Overproduction Is Required for Efficient Full-Length RNA Synthesis in the Absence of Topoisomerase I in Escherichia Coli.” *Molecular Microbiology* 54(1):198–211. doi: 10.1111/j.1365-2958.2004.04258.x.

Bachl, Jürgen, Chris Carlson, Vanessa Gray-Schopfer, Mark Dessing, and Carina Olsson. 2001. “Increased Transcription Levels Induce Higher Mutation Rates in a Hypermutating Cell Line1.” *The Journal of Immunology* 166(8):5051–57. doi: 10.4049/jimmunol.166.8.5051.

Baretić, Domagoj, Michael Jenkyn-Bedford, Valentina Aria, Giuseppe Cannone, Mark Skehel, and Joseph T. P. Yeeles. 2020. “Cryo-EM Structure of the Fork Protection Complex Bound to CMG at a Replication Fork.” *Molecular Cell* 78(5):926-940.e13. doi: 10.1016/j.molcel.2020.04.012.

Barlow, Jacqueline H., Robert B. Faryabi, Elsa Callén, Nancy Wong, Amy Malhowski, Hua Tang Chen, Gustavo Gutierrez-Cruz, Hong-Wei Sun, Peter McKinnon, George Wright, Rafael Casellas, Davide F. Robbiani, Louis Staudt, Oscar Fernandez-Capetillo, and André Nussenzweig. 2013. “Identification of Early Replicating Fragile Sites That Contribute to Genome Instability.” *Cell* 152(3):620–32. doi: 10.1016/j.cell.2013.01.006.

Barnes, Christopher O., Monica Calero, Indranil Malik, Brian W. Graham, Henrik Spahr, Guowu Lin, Aina E. Cohen, Ian S. Brown, Qiangmin Zhang, Filippo Pullara, Michael A. Trakselis, Craig D. Kaplan, and Guillermo Calero. 2015. “Crystal Structure of a Transcribing RNA Polymerase II Complex Reveals a Complete Transcription Bubble.” *Molecular Cell* 59(2):258–69. doi: 10.1016/j.molcel.2015.06.034.

Barra, V., and D. Fachinetti. 2018. “The Dark Side of Centromeres: Types, Causes and Consequences of Structural Abnormalities Implicating Centromeric DNA.” *Nature Communications* 9(1). doi: 10.1038/s41467-018-06545-y.

Barraud, Pierre, Stephan Emmerth, Yukiko Shimada, Hans Rudolf Hotz, Frédéric H. T. Allain, and Marc Bühler. 2011. “An Extended dsRBD with a Novel Zinc-Binding Motif Mediates Nuclear Retention of Fission Yeast Dicer.” *EMBO Journal* 30(20):4223–35. doi: 10.1038/emboj.2011.300.

Bastiaanssen, Carolien, Pilar Bobadilla Ugarte, Kijun Kim, Yanlei Feng, Giada Finocchio, Todd A. Anzelon, Stephan Köstlbacher, Daniel Tamarit, Thijs J. G. Ettema, Martin Jinek, Ian J. MacRae, Chirlmin Joo, Daan C. Swarts, and Fabai Wu. 2023. *RNA-Guided RNA Silencing by an Asgard Archaeal Argonaute*. *preprint*. Microbiology. doi: 10.1101/2023.12.14.571608.

Bayne, Elizabeth H., Sharon A. White, Alexander Kagansky, Dominika A. Bijos, Luis Sanchez-Pulido, Kwang Lae Hoe, Dong Uk Kim, Han Oh Park, Chris P. Ponting, Juri Rappsilber, and Robin C. Allshire. 2010. “Stc1: A Critical Link between RNAi and Chromatin Modification Required for Heterochromatin Integrity.” *Cell* 140(5):666–77. doi: 10.1016/j.cell.2010.01.038.

Beckedorff, Felipe, Ezra Blumenthal, Lucas Ferreira daSilva, Yuki Aoi, Pradeep Reddy Cingaram, Jingyin Yue, Anda Zhang, Sadat Dokaneheifard, Monica Guiselle Valencia, Gabriel Gaidosh, Ali Shilatifard, and Ramin Shiekhattar. 2020. “The Human Integrator Complex Facilitates Transcriptional Elongation by Endonucleolytic Cleavage of Nascent Transcripts.” *Cell Reports* 32(3):107917. doi: 10.1016/j.celrep.2020.107917.

Beletskii, A., and Ashok S. Bhagwat. 1996. “Transcription-Induced Mutations: Increase in C to T Mutations in the Nontranscribed Strand during Transcription in Escherichia Coli.” *Proceedings of the National Academy of Sciences* 93(24):13919–24. doi: 10.1073/pnas.93.24.13919.

Bell, Stephen P., and Karim Labib. 2016. “Chromosome Duplication in Saccharomyces Cerevisiae.” *Genetics* 203(3):1027–67. doi: 10.1534/genetics.115.186452.

Bell, Stephen P., and Bruce Stillman. 1992. “ATP-Dependent Recognition of Eukaryotic Origins of DNA Replication by a Multiprotein Complex.” *Nature* 357(6374):128–34. doi: 10.1038/357128a0.

Beltran, Toni, Elena Pahita, Subhanita Ghosh, Boris Lenhard, and Peter Sarkies. 2021. “Integrator Is Recruited to Promoter-proximally Paused RNA Pol II to Generate Caenorhabditis Elegans piRNA Precursors.” *The EMBO Journal* 40(5):e105564. doi: 10.15252/embj.2020105564.

Bernard, P., J. F. Maure, J. F. Partridge, S. Genier, J. P. Javerzat, and R. C. Allshire. 2001. “Requirement of Heterochromatin for Cohesion at Centromeres.” *Science* 294(5551):2539–42. doi: 10.1126/science.1064027.

Bernstein, Emily, Sang Yong Kim, Michelle A. Carmell, Elizabeth P. Murchison, Heather Alcorn, Mamie Z. Li, Alea A. Mills, Stephen J. Elledge, Kathryn V. Anderson, and Gregory J. Hannon. 2003. “Dicer Is Essential for Mouse Development.” *Nature Genetics* 35(3):215–17. doi: 10.1038/ng1253.

Berti, Matteo, Arnab Ray Chaudhuri, Saravanabhavan Thangavel, Shivasankari Gomathinayagam, Sasa Kenig, Marko Vujanovic, Federico Odreman, Timo Glatter, Simona Graziano, Ramiro Mendoza-Maldonado, Francesca Marino, Bojana Lucic, Valentina Biasin, Matthias Gstaiger, Ruedi Aebersold, Julia M. Sidorova, Raymond J. Monnat, Massimo Lopes, and Alessandro Vindigni. 2013. “Human RECQ1 Promotes Restart of Replication Forks Reversed by DNA Topoisomerase I Inhibition.” *Nature Structural and Molecular Biology* 20(3):347–54. doi: 10.1038/nsmb.2501.

Berti, Matteo, David Cortez, and Massimo Lopes. 2020. “The Plasticity of DNA Replication Forks in Response to Clinically Relevant Genotoxic Stress.” *Nature Reviews Molecular Cell Biology* 21(10):633–51. doi: 10.1038/s41580-020-0257-5.

Bertoli, Cosetta, Jan M. Skotheim, and Robertus A. M. de Bruin. 2013. “Control of Cell Cycle Transcription during G1 and S Phases.” *Nature Reviews Molecular Cell Biology* 14(8):518–28. doi: 10.1038/nrm3629.

Besnard, Emilie, Amélie Babled, Laure Lapasset, Ollivier Milhavet, Hugues Parrinello, Christelle Dantec, Jean-Michel Marin, and Jean-Marc Lemaitre. 2012. “Unraveling Cell Type–Specific and Reprogrammable Human Replication Origin Signatures Associated with G-Quadruplex Consensus Motifs.” *Nature Structural & Molecular Biology* 19(8):837–44. doi: 10.1038/nsmb.2339.

Bétous, Rémy, Frank B. Couch, Aaron C. Mason, Brandt F. Eichman, Maria Manosas, and David Cortez. 2013. “Substrate-Selective Repair and Restart of Replication Forks by DNA Translocases.” *Cell Reports* 3(6):1958–69. doi: 10.1016/j.celrep.2013.05.002.

Bhat, Kamakoti P., and David Cortez. 2018. “RPA and RAD51: Fork Reversal, Fork Protection, and Genome Stability.” *Nature Structural and Molecular Biology* 25(6):446–53. doi: 10.1038/s41594-018-0075-z.

Bhat, Kamakoti P., Archana Krishnamoorthy, Huzefa Dungrawala, Edwige B. Garcin, Mauro Modesti, and David Cortez. 2018. “RADX Modulates RAD51 Activity to Control Replication Fork Protection.” *Cell Reports* 24(3):538–45. doi: 10.1016/j.celrep.2018.06.061.

Bhowmick, Rahul, Kavi P. M. Mehta, Mads Lerdrup, and David Cortez. 2023. “Integrator Facilitates RNAPII Removal to Prevent Transcription-Replication Collisions and Genome Instability.” *Molecular Cell*. doi: 10.1016/j.molcel.2023.05.015.

Bianco, Julien N., Jérôme Poli, Julie Saksouk, Julien Bacal, Maria Joao Silva, Kazumasa Yoshida, Yea Lih Lin, Hélène Tourrière, Armelle Lengronne, and Philippe Pasero. 2012. “Analysis of DNA Replication Profiles in Budding Yeast and Mammalian Cells Using DNA Combing.” *Methods* 57(2):149–57. doi: 10.1016/j.ymeth.2012.04.007.

Bienko, Marzena, Catherine M. Green, Nicola Crosetto, Fabian Rudolf, Grzegorz Zapart, Barry Coull, Patricia Kannouche, Gerhard Wider, Matthias Peter, Alan R. Lehmann, Kay Hofmann, and Ivan Dikic. 2005. “Ubiquitin-Binding Domains in Y-Family Polymerases Regulate Translesion Synthesis.” *Science* 310(5755):1821–24. doi: 10.1126/science.1120615.

Bitton, Danny A., Falk Schubert, Shoumit Dey, Michal Okoniewski, Graeme C. Smith, Sanjay Khadayate, Vera Pancaldi, Valerie Wood, and Jürg Bähler. 2015. “AnGeLi: A Tool for the Analysis of Gene Lists from Fission Yeast.” *Frontiers in Genetics* 6(NOV):1–9. doi: 10.3389/fgene.2015.00330.

Bloom, Kerry S. 2014. “Centromeric Heterochromatin: The Primordial Segregation Machine.” *Annual Review of Genetics* 48(1):457–84. doi: 10.1146/annurev-genet-120213-092033.

Bobkova, Ekaterina V., Natasha Habib, Gemma Alexander, and Benjamin D. Hall. 1999. “Mutational Analysis of the Hydrolytic Activity of Yeast RNA Polymerase III *.” *Journal of Biological Chemistry* 274(30):21342–48. doi: 10.1074/jbc.274.30.21342.

Bohmert, Karen, Isabelle Camus, Catherine Bellini, David Bouchez, Michel Caboche, and Christoph Benning. 1998. “AGO1 Defines a Novel Locus of Arabidopsis Controlling Leaf Development.” *The EMBO Journal* 17(1):170–80. doi: 10.1093/emboj/17.1.170.

Bonilla, Braulio, Sarah R. Hengel, McKenzie K. Grundy, and Kara A. Bernstein. 2020. “RAD51 Gene Family Structure and Function.” *Annual Review of Genetics* 54:25–46. doi: 10.1146/annurev-genet-021920-092410.

Booth, Gregory T., Isabel X. Wang, Vivian G. Cheung, and John T. Lis. 2016. “Divergence of a Conserved Elongation Factor and Transcription Regulation in Budding and Fission Yeast.” *Genome Research* 26(6):799–811. doi: 10.1101/gr.204578.116.

Borges, Filipe, and Robert A. Martienssen. 2015. “The Expanding World of Small RNAs in Plants.” *Nature Reviews Molecular Cell Biology* 16(12):727–41. doi: 10.1038/nrm4085.

Boubakri, Hasna, Anne Langlois de Septenville, Enrique Viguera, and Bénédicte Michel. 2010. “The Helicases DinG, Rep and UvrD Cooperate to Promote Replication across Transcription Units in Vivo.” *The EMBO Journal* 29(1):145–57. doi: 10.1038/emboj.2009.308.

Bouzinba-Segard, Haniaa, Adeline Guais, and Claire Francastel. 2006. “Accumulation of Small Murine Minor Satellite Transcripts Leads to Impaired Centromeric Architecture and Function.” *Proceedings of the National Academy of Sciences* 103(23):8709–14. doi: 10.1073/pnas.0508006103.

Bowers, Jayson L., John C. W. Randell, Shuyan Chen, and Stephen P. Bell. 2004. “ATP Hydrolysis by ORC Catalyzes Reiterative Mcm2-7 Assembly at a Defined Origin of Replication.” *Molecular Cell* 16(6):967–78. doi: 10.1016/j.molcel.2004.11.038.

Brahma, Sandipan, and Steven Henikoff. 2019. “RSC-Associated Subnucleosomes Define MNase-Sensitive Promoters in Yeast.” *Molecular Cell* 73(2):238-249.e3. doi: 10.1016/j.molcel.2018.10.046.

Branzei, Dana, and Marco Foiani. 2010. “Maintaining Genome Stability at the Replication Fork.” *Nature Reviews Molecular Cell Biology* 11(3):208–19. doi: 10.1038/nrm2852.

Brewer, Bonita J. 1988. “When Polymerases Collide: Replication and the Transcriptional Organization of the E. Coli Chromosome.” *Cell* 53(5):679–86. doi: 10.1016/0092-8674(88)90086-4.

Brewer, Bonita J., Daniel Lockshon, and Walton L. Fangman. 1992. “The Arrest of Replication Forks in the rDNA of Yeast Occurs Independently of Transcription.” *Cell* 71(2):267–76. doi: 10.1016/0092-8674(92)90355-G.

Brickner, Joshua R., Jada L. Garzon, and Karlene A. Cimprich. 2022. “Walking a Tightrope: The Complex Balancing Act of R-Loops in Genome Stability.” *Molecular Cell* 82(12):2267–97. doi: 10.1016/j.molcel.2022.04.014.

Brill, Steven J., and Rolf Sternglanz. 1988. “Transcription-Dependent DNA Supercoiling in Yeast DNA Topoisomerase Mutants.” *Cell* 54(3):403–11. doi: 10.1016/0092-8674(88)90203-6.

Brison, Olivier, Sami El-Hilali, Dana Azar, Stéphane Koundrioukoff, Mélanie Schmidt, Viola Nähse, Yan Jaszczyszyn, Anne-Marie Lachages, Bernard Dutrillaux, Claude Thermes, Michelle Debatisse, and Chun-Long Chen. 2019. “Transcription-Mediated Organization of the Replication Initiation Program across Large Genes Sets Common Fragile Sites Genome-Wide.” *Nature Communications* 10(1):5693. doi: 10.1038/s41467-019-13674-5.

Brüning, Jan-Gert, and Kenneth J. Marians. 2020. “Replisome Bypass of Transcription Complexes and R-Loops.” *Nucleic Acids Research* 1–15. doi: 10.1093/nar/gkaa741.

Bruno, Federica, Cristóbal Coronel-Guisado, and Cristina González-Aguilera. 2024. “Collisions of RNA Polymerases behind the Replication Fork Promote Alternative RNA Splicing in Newly Replicated Chromatin.” *Molecular Cell* 84(2):221-233.e6. doi: 10.1016/j.molcel.2023.11.036.

Bubunenko, Mikhail, Donald L. Court, Abdalla Al Refaii, Shivalika Saxena, Alexey Korepanov, David I. Friedman, Max E. Gottesman, and Jean-Hervé Alix. 2013. "Nus Transcription Elongation Factors and RNase III Modulate Small Ribosome Subunit Biogenesis in Escherichia Coli." *Molecular Microbiology* 87(2):382–93. doi: 10.1111/mmi.12105.

Bugreev, Dmitry V., Matthew J. Rossi, and Alexander V. Mazin. 2011. "Cooperation of RAD51 and RAD54 in Regression of a Model Replication Fork." *Nucleic Acids Research* 39(6):2153–64. doi: 10.1093/nar/gkq1139.

Bühler, Marc, and Danesh Moazed. 2007. "Transcription and RNAi in Heterochromatic Gene Silencing." *Nature Structural & Molecular Biology* 14(11):1041–48. doi: 10.1038/nsmb1315.

Bühler, Marc, André Verdel, and Danesh Moazed. 2006. "Tethering RITS to a Nascent Transcript Initiates RNAi- and Heterochromatin-Dependent Gene Silencing." *Cell* 125(5):873–86. doi: 10.1016/j.cell.2006.04.025.

Burger, Kaspar, and Monika Gullerova. 2018. "Nuclear Re-Localization of Dicer in Primary Mouse Embryonic Fibroblast Nuclei Following DNA Damage." *PLOS Genetics* 14(2):e1007151. doi: 10.1371/journal.pgen.1007151.

Burger, Kaspar, Margarita Schlackow, and Monika Gullerova. 2019. "Tyrosine Kinase C-Abl Couples RNA Polymerase II Transcription to DNA Double-Strand Breaks." *Nucleic Acids Research* 47(7):3467–84. doi: 10.1093/nar/gkz024.

Burger, Kaspar, Margarita Schlackow, Martin Potts, Svenja Hester, Shabaz Mohammed, and Monika Gullerova. 2017. "Nuclear Phosphorylated Dicer Processes Double-Stranded RNA in Response to DNA Damage." *Journal of Cell Biology* 216(8):2373–89. doi: 10.1083/jcb.201612131.

Byrd, Alicia K., and Kevin D. Raney. 2012. "Superfamily 2 Helicases." *Frontiers in Bioscience-Landmark* 17(6):2070–88. doi: 10.2741/4038.

Byun, Tony S., Marcin Pacek, Muh-ching Yee, Johannes C. Walter, and Karlene A. Cimprich. 2005. "Functional Uncoupling of MCM Helicase and DNA Polymerase Activities Activates the ATR-Dependent Checkpoint." *Genes & Development* 19(9):1040–52. doi: 10.1101/gad.1301205.

Cabrini, Matteo, Marco Roncador, Alessandro Galbiati, Lina Cipolla, Antonio Maffia, Fabio Iannelli, Simone Sabbioneda, Fabrizio d'Adda di Fagagna, and Sofia Francia. 2021. "DROSHA Is Recruited to DNA Damage Sites by the MRN Complex to Promote Non-Homologous End Joining." *Journal of Cell Science* 134(6):jcs249706. doi: 10.1242/jcs.249706.

Calzada, Arturo, Ben Hodgson, Masato Kanemaki, Avelino Bueno, and Karim Labib. 2005. "Molecular Anatomy and Regulation of a Stable Replisome at a Paused Eukaryotic DNA Replication Fork." *Genes & Development* 19(16):1905–19. doi: 10.1101/gad.337205.

Camino, Lola P., Arijit Dutta, Sonia Barroso, Carmen Pérez-Calero, Jeffrey N. Katz, María García-Rubio, Patrick Sung, Belén Gómez-González, and Andrés Aguilera. 2023. "DICER Ribonuclease Removes Harmful R-Loops." *Molecular Cell*. doi: 10.1016/j.molcel.2023.09.021.

Carlsten, Jonas O., Zsolt Szilagyi, Beidong Liu, Marcela Davila Lopez, Erzsébet Szászi, Ingela Djupedal, Thomas Nyström, Karl Ekwall, Claes M. Gustafsson, and Xuefeng Zhu. 2012. "Mediator Promotes CENP-A Incorporation at Fission Yeast Centromeres." *Molecular and Cellular Biology* 32(19):4035–43. doi: 10.1128/mcb.00374-12.

Carmichael, Jon B., Patrick Provost, Karl Ekwall, and Tom C. Hobman. 2004. "Ago1 and Dcr1, Two Core Components of the RNA Interference Pathway, Functionally Diverge from Rdp1 in Regulating Cell Cycle Events in Schizosaccharomyces Pombe." *Molecular Biology of the Cell* 15(3):1425–35. doi: 10.1091/mbc.e03-06-0433.

Carr, Antony, and Sarah Lambert. 2021. "Recombination-Dependent Replication: New Perspectives from Site-Specific Fork Barriers." *Current Opinion in Genetics & Development* 71:129–35. doi: 10.1016/j.gde.2021.07.008.

Casper, Anne M., Paul Nghiem, Martin F. Arlt, and Thomas W. Glover. 2002. "ATR Regulates Fragile Site Stability." *Cell* 111(6):779–89. doi: 10.1016/S0092-8674(02)01113-3.

Castel, Stephane E., and Robert A. Martienssen. 2013. “RNA Interference in the Nucleus: Roles for Small RNAs in Transcription, Epigenetics and Beyond.” *Nature Reviews Genetics* 14(2):100–112. doi: 10.1038/nrg3355.

Castel, Stephane E., Jie Ren, Sonali Bhattacharjee, An Yun Chang, Mar Sánchez, Alberto Valbuena, Francisco Antequera, and Robert A. Martienssen. 2014. “Dicer Promotes Transcription Termination at Sites of Replication Stress to Maintain Genome Stability.” *Cell* 159(3):572–83. doi: 10.1016/j.cell.2014.09.031.

Castillo Bosch, Pau, Sandra Segura-Bayona, Wouter Koole, Jane T. van Heteren, James M. Dewar, Marcel Tijsterman, and Puck Knipscheer. 2014. “FANCJ Promotes DNA Synthesis through G-quadruplex Structures.” *The EMBO Journal* 33(21):2521–33. doi: 10.15252/embj.201488663.

Castillo-Guzman, Daisy, and Frédéric Chédin. 2021. “Defining R-Loop Classes and Their Contributions to Genome Instability.” *DNA Repair* 106(May). doi: 10.1016/j.dnarep.2021.103182.

Cayrou, Christelle, Philippe Coulombe, Alice Vigneron, Slavica Stanojcic, Olivier Ganier, Isabelle Peiffer, Eric Rivals, Aurore Puy, Sabine Laurent-Chabalier, Romain Desprat, and Marcel Méchali. 2011. “Genome-Scale Analysis of Metazoan Replication Origins Reveals Their Organization in Specific but Flexible Sites Defined by Conserved Features.” *Genome Research* 21(9):1438–49. doi: 10.1101/gr.121830.111.

Ceccaldi, Raphael, Beatrice Rondinelli, and Alan D. D’Andrea. 2016. “Repair Pathway Choices and Consequences at the Double-Strand Break.” *Trends in Cell Biology* 26(1):52–64. doi: 10.1016/j.tcb.2015.07.009.

Cecere, Germano, and Carlo Cogoni. 2009. “Quelling Targets the rDNA Locus and Functions in rDNA Copy Number Control.” *BMC Microbiology* 9:44. doi: 10.1186/1471-2180-9-44.

Cernilogar, Filippo M., Maria Cristina Onorati, Greg O. Kothe, A. Maxwell Burroughs, Krishna Mohan Parsi, Achim Breiling, Federica Lo Sardo, Alka Saxena, Keita Miyoshi, Haruhiko Siomi, Mikiko C. Siomi, Piero Carninci, David S. Gilmour, Davide F. V. Corona, and Valerio Orlando. 2011. “Chromatin-Associated RNA Interference Components Contribute to Transcriptional Regulation in Drosophila.” *Nature* 480(7377):391–95. doi: 10.1038/nature10492.

Cerritelli, Susana M., and Robert J. Crouch. 2009. “Ribonuclease H: The Enzymes in Eukaryotes.” *The FEBS Journal* 276(6):1494–1505. doi: 10.1111/j.1742-4658.2009.06908.x.

Cerutti, Heriberto, and J. Armando Casas-Mollano. 2006. “On the Origin and Functions of RNA-Mediated Silencing: From Protists to Man.” *Current Genetics* 50(2):81–99. doi: 10.1007/s00294-006-0078-x.

Cerutti, Lorenzo, Nina Mian, and Alex Bateman. 2000. “Domains in Gene Silencing and Cell Differentiation Proteins: The Novel PAZ Domain and Redefinition of the Piwi Domain.” *Trends in Biochemical Sciences* 25(10):481–82. doi: 10.1016/S0968-0004(00)01641-8.

Chakraborty, Prasun, and Frank Grosse. 2011. “Human DHX9 Helicase Preferentially Unwinds RNA-Containing Displacement Loops (R-Loops) and G-Quadruplexes.” *DNA Repair* 10(6):654–65. doi: 10.1016/j.dnarep.2011.04.013.

Chakraborty, Shrena, Kamila Schirmeisen, and Sarah AE Lambert. 2023. “The Multifaceted Functions of Homologous Recombination in Dealing with Replication-Associated DNA Damages.” *DNA Repair* 129:103548. doi: 10.1016/j.dnarep.2023.103548.

Chan, Simon W. L., Daniel Zilberman, Zhixin Xie, Lisa K. Johansen, James C. Carrington, and Steven E. Jacobsen. 2004. “RNA Silencing Genes Control de Novo DNA Methylation.” *Science* 303(5662):1336–1336. doi: 10.1126/science.1095989.

Chandramouly, Gurushankar, Jiemin Zhao, Shane McDevitt, Timur Rusanov, Trung Hoang, Nikita Borisonnik, Taylor Treddinick, Felicia Wednesday Lopezcolorado, Tatiana Kent, Labiba A. Siddique, Joseph Mallon, Jacklyn Huhn, Zainab Shoda, Ekaterina Kashkina, Alessandra Brambati, Jeremy M. Stark, Xiaojiang S. Chen, and Richard T. Pomerantz. 2021. “Polθ Reverse Transcribes RNA and Promotes RNA-Templated DNA Repair.” *Science Advances* 7(24):eabf1771. doi: 10.1126/sciadv.abf1771.

Chang, Emily Yun-Chia, Carolina A. Novoa, Maria J. Aristizabal, Yan Coulombe, Romulo Segovia, Richa Chaturvedi, Yaoqing Shen, Christelle Keong, Annie S. Tam, Steven J. M. Jones, Jean-Yves Masson, Michael S. Kobor, and Peter C. Stirling. 2017. “RECQ-like Helicases Sgs1 and BLM Regulate R-Loop–Associated Genome Instability.” *Journal of Cell Biology* 216(12):3991–4005. doi: 10.1083/jcb.201703168.

Chappidi, Nagaraja, Zuzana Nascakova, Barbora Boleslavska, Ralph Zellweger, Esin Isik, Martin Andrs, Shruti Menon, Jana Dobrovolna, Chiara Balbo Pogliano, Joao Matos, Antonio Porro, Massimo Lopes, and Pavel Janscak. 2019. "Fork Cleavage-Religation Cycle and Active Transcription Mediate Replication Restart after Fork Stalling at Co-Transcriptional R-Loops." *Molecular Cell* 1–14. doi: 10.1016/j.molcel.2019.10.026.

Chen, Fei Xavier, Ashley R. Woodfin, Alessandro Gardini, Ryan A. Rickels, Stacy A. Marshall, Edwin R. Smith, Ramin Shiekhattar, and Ali Shilatifard. 2015. "PAF1, a Molecular Regulator of Promoter-Proximal Pausing by RNA Polymerase II." *Cell* 162(5):1003–15. doi: 10.1016/j.cell.2015.07.042.

Chen, Liang, Jia Yu Chen, Xuan Zhang, Ying Gu, Rui Xiao, Changwei Shao, Peng Tang, Hao Qian, Daji Luo, Hairi Li, Yu Zhou, Dong Er Zhang, and Xiang Dong Fu. 2017. "R-ChIP Using Inactive RNase H Reveals Dynamic Coupling of R-Loops with Transcriptional Pausing at Gene Promoters." *Molecular Cell* 68(4):745-757.e5. doi: 10.1016/j.molcel.2017.10.008.

Chen, Qi, and Tong Zhou. 2023. "Emerging Functional Principles of tRNA-Derived Small RNAs and Other Regulatory Small RNAs." *Journal of Biological Chemistry* 299(10):105225. doi: 10.1016/j.jbc.2023.105225.

Chen, Shifu, Yanqing Zhou, Yaru Chen, and Jia Gu. 2018. "Fastp: An Ultra-Fast All-in-One FASTQ Preprocessor." *Bioinformatics* 34(17):i884–90. doi: 10.1093/bioinformatics/bty560.

Chen, Xiaoshu, Jian-Rong Yang, and Jianzhi Zhang. 2016. "Nascent RNA Folding Mitigates Transcription-Associated Mutagenesis." *Genome Research* 26(1):50–59. doi: 10.1101/gr.195164.115.

Chen, Xizi, Xiaotong Yin, Jiabei Li, Zihan Wu, Yilun Qi, Xinxin Wang, Weida Liu, and Yanhui Xu. 2021. "Structures of the Human Mediator and Mediator-Bound Preinitiation Complex." *Science* 372(6546). doi: 10.1126/science.abg0635.

Chen, Yu-Hung, Sarah Keegan, Malik Kahli, Peter Tonzi, David Fenyö, Tony T. Huang, and Duncan J. Smith. 2019. "Transcription Shapes DNA Replication Initiation and Termination in Human Cells." *Nature Structural & Molecular Biology* 26(1):67–77. doi: 10.1038/s41594-018-0171-0.

Chivu, Alexandra G., Abderhman Abuhashem, Gilad Barshad, Edward J. Rice, Michelle M. Leger, Albert C. Vill, Wilfred Wong, Rebecca Brady, Jeramiah J. Smith, Athula H. Wikramanayake, César Arenas-Mena, Ilana L. Brito, Iñaki Ruiz-Trillo, Anna-Katerina Hadjantonakis, John T. Lis, James J. Lewis, and Charles G. Danko. 2023. "Evolution of Promoter-Proximal Pausing Enabled a New Layer of Transcription Control." 2023.02.19.529146.

Cho, Won-Ho, Young-Hoon Kang, Yun-Young An, Inger Tappin, Jerard Hurwitz, and Joon-Kyu Lee. 2013. "Human Tim-Tipin Complex Affects the Biochemical Properties of the Replicative DNA Helicase and DNA Polymerases." *Proceedings of the National Academy of Sciences* 110(7):2523–27. doi: 10.1073/pnas.1222494110.

Chong, Shin Yen, Sam Cutler, Jing-Jer Lin, Cheng-Hung Tsai, Huai-Kuang Tsai, Sue Biggins, Toshio Tsukiyama, Yi-Chen Lo, and Cheng-Fu Kao. 2020. "H3K4 Methylation at Active Genes Mitigates Transcription-Replication Conflicts during Replication Stress." *Nature Communications* 11(1):809. doi: 10.1038/s41467-020-14595-4.

Choudhary, Ramveer, Joanna Niska-Blakie, Mohamood Adhil, Giordano Liberi, Yathish Jagadheesh Achar, Michele Giannattasio, and Marco Foiani. 2023. "Sen1 and Rrm3 Ensure Permissive Topological Conditions for Replication Termination." *Cell Reports* 42(7):112747. doi: 10.1016/j.celrep.2023.112747.

Christman, Michael F., Fred S. Dietrich, and Gerald R. Fink. 1988. "Mitotic Recombination in the rDNA of S. Cerevisiae Is Suppressed by the Combined Action of DNA Topoisomerases I and II." *Cell* 55(3):413–25. doi: 10.1016/0092-8674(88)90027-X.

Chu, Wai Kit, and Ian D. Hickson. 2009. "RecQ Helicases: Multifunctional Genome Caretakers." *Nature Reviews Cancer* 9(9):644–54. doi: 10.1038/nrc2682.

Ciccia, Alberto, and Stephen J. Elledge. 2010. "The DNA Damage Response: Making It Safe to Play with Knives." *Molecular Cell* 40(2):179–204. doi: 10.1016/j.molcel.2010.09.019.

Ciccia, Alberto, Neil McDonald, and Stephen C. West. 2008. “Structural and Functional Relationships of the XPF/MUS81 Family of Proteins.” *Annual Review of Biochemistry* 77(1):259–87. doi: 10.1146/annurev.biochem.77.070306.102408.

Ciechanowska, Kinga, Agnieszka Szczepanska, Kamil Szpotkowski, Klaudia Wojcik, Anna Urbanowicz, and Anna Kurzynska-Kokorniak. 2023. *The Human Dicer Helicase Domain Mediates ATP Hydrolysis and RNA Rearrangement*. *preprint*. Molecular Biology. doi: 10.1101/2023.06.28.546842.

Claussin, Clémence, Jacob Vazquez, and Iestyn Whitehouse. 2022. “Single-Molecule Mapping of Replisome Progression.” *Molecular Cell* 82(7):1372-1382.e4. doi: 10.1016/j.molcel.2022.02.010.

Cleaver, James E., Luzviminda Feeney, and Ingrid Revet. 2011. “Phosphorylated H2Ax Is Not an Unambiguous Marker for DNA Double-Strand Breaks.” *Cell Cycle* 10(19):3223–24. doi: 10.4161/cc.10.19.17448.

Cohen, Sarah, Nadine Puget, Yea-Lih Lin, Thomas Clouaire, Marion Aguirrebengoa, Vincent Rocher, Philippe Pasero, Yvan Canitrot, and Gaëlle Legube. 2018. “Senataxin Resolves RNA:DNA Hybrids Forming at DNA Double-Strand Breaks to Prevent Translocations.” *Nature Communications* 9(1):533. doi: 10.1038/s41467-018-02894-w.

Colmenares, Serafin U., Shane M. Buker, Marc Buhler, Mensur Dlakić, and Danesh Moazed. 2007. “Coupling of Double-Stranded RNA Synthesis and siRNA Generation in Fission Yeast RNAi.” *Molecular Cell* 27(3):449–61. doi: 10.1016/j.molcel.2007.07.007.

Compe, Emmanuel, and Jean-Marc Egly. 2016. “Nucleotide Excision Repair and Transcriptional Regulation: TFIIH and Beyond.” *Annual Review of Biochemistry* 85(1):265–90. doi: 10.1146/annurev-biochem-060815-014857.

Compe, Emmanuel, Carlos M. Genes, Cathy Braun, Frederic Coin, and Jean Marc Egly. 2019. “TFIIE Orchestrates the Recruitment of the TFIIH Kinase Module at Promoter before Release during Transcription.” *Nature Communications* 10(1). doi: 10.1038/s41467-019-10131-1.

Conti, Brooke A., and Agata Smogorzewska. 2020. “Mechanisms of Direct Replication Restart at Stressed Replisomes.” *DNA Repair* 95:102947. doi: 10.1016/j.dnarep.2020.102947.

Core, Leighton, and Karen Adelman. 2019. “Promoter-Proximal Pausing of RNA Polymerase II: A Nexus of Gene Regulation.” *Genes & Development* 33(15–16):960–82. doi: 10.1101/gad.325142.119.

Cormack, Brendan P., and Kevin Struhl. 1992. “The TATA-Binding Protein Is Required for Transcription by All Three Nuclear RNA Polymerases in Yeast Cells.” *Cell* 69(4):685–96. doi: 10.1016/0092-8674(92)90232-2.

Costantino, Lorenzo, and Douglas Koshland. 2018. “Genome-Wide Map of R-Loop-Induced Damage Reveals How a Subset of R-Loops Contributes to Genomic Instability.” *Molecular Cell* 71(4):487-497.e3. doi: 10.1016/j.molcel.2018.06.037.

Couch, Frank B., Carol E. Bansbach, Robert Driscoll, Jessica W. Luzwick, Gloria G. Glick, Rémy Bétous, Clinton M. Carroll, Sung Yun Jung, Jun Qin, Karlene A. Cimprich, and David Cortez. 2013. “ATR Phosphorylates SMARCAL1 to Prevent Replication Fork Collapse.” *Genes & Development* 27(14):1610–23. doi: 10.1101/gad.214080.113.

Court, Donald L., Jianhua Gan, Yu-He Liang, Gary X. Shaw, Joseph E. Tropea, Nina Costantino, David S. Waugh, and Xinhua Ji. 2013. “RNase III: Genetics and Function; Structure and Mechanism.” *Annual Review of Genetics* 47(1):405–31. doi: 10.1146/annurev-genet-110711-155618.

Cramer, Patrick, D. A. Bushnell, and R. D. Kornberg. 2001. “Structural Basis of Transcription: RNA Polymerase II at 2.8 Ångstrom Resolution.” *Science* 292(5523):1863–76. doi: 10.1126/science.1059493.

Cristini, Agnese, Matthias Groh, Maiken S. Kristiansen, and Natalia Gromak. 2018. “RNA/DNA Hybrid Interactome Identifies DXH9 as a Molecular Player in Transcriptional Termination and R-Loop-Associated DNA Damage.” *Cell Reports* 23(6):1891–1905. doi: 10.1016/j.celrep.2018.04.025.

Dahan, Danielle, Ioannis Tsirkas, Daniel Dovrat, Melanie A. Sparks, Saurabh P. Singh, Roberto Galletto, and Amir Aharoni. 2018. “Pif1 Is Essential for Efficient Replisome Progression through Lagging Strand G-Quadruplex DNA Secondary Structures.” *Nucleic Acids Research* 46(22):11847–57. doi: 10.1093/nar/gky1065.

Dai, Yaxin, Aili Zhang, Shan Shan, Zihua Gong, and Zheng Zhou. 2018. "Structural Basis for Recognition of 53BP1 Tandem Tudor Domain by TIRR." *Nature Communications* 9(1):2123. doi: 10.1038/s41467-018-04557-2.

Dang, Tuyen T., and Julio C. Morales. 2020. "XRN2 Links RNA:DNA Hybrid Resolution to Double Strand Break Repair Pathway Choice." *Cancers* 12(7):1821. doi: 10.3390/cancers12071821.

Datta, Abhijit, and Sue Jinks-Robertson. 1995. "Association of Increased Spontaneous Mutation Rates with High Levels of Transcription in Yeast." *Science* 268(5217):1616–19. doi: 10.1126/science.7777859.

Davies, Adelina A., Diana Huttner, Yasukazu Daigaku, Shuhua Chen, and Helle D. Ulrich. 2008. "Activation of Ubiquitin-Dependent DNA Damage Bypass Is Mediated by Replication Protein A." *Molecular Cell* 29(5):625–36. doi: 10.1016/j.molcel.2007.12.016.

De Magis, Alessio, Stefano G. Manzo, Marco Russo, Jessica Marinello, Rita Morigi, Olivier Sordet, and Giovanni Capranico. 2019. "DNA Damage and Genome Instability by G-Quadruplex Ligands Are Mediated by R Loops in Human Cancer Cells." *Proceedings of the National Academy of Sciences* 116(3):816–25. doi: 10.1073/pnas.1810409116.

Deaton, Am, and Adrian P. Bird. 2011. "CpG Islands and the Regulation of Transcription." *Genes & Development* 25(10):1010–22. doi: 10.1101/gad.2037511.1010.

Dedukh, Dmitrij, and Alla Krasikova. 2022. "Delete and Survive: Strategies of Programmed Genetic Material Elimination in Eukaryotes." *Biological Reviews* 97(1):195–216. doi: 10.1111/brv.12796.

Deltcheva, Elitza, Krzysztof Chylinski, Cynthia M. Sharma, Karine Gonzales, Yanjie Chao, Zaid A. Pirzada, Maria R. Eckert, Jörg Vogel, and Emmanuelle Charpentier. 2011. "CRISPR RNA Maturation by Trans-Encoded Small RNA and Host Factor RNase III." *Nature* 471(7340):602–7. doi: 10.1038/nature09886.

Deshpande, Atul M., and Carol S. Newlon. 1996. "DNA Replication Fork Pause Sites Dependent on Transcription." *Science* 272(5264):1030–33. doi: 10.1126/science.272.5264.1030.

Deshpande, Girish, Gretchen Calhoun, and Paul Schedl. 2005. "Drosophila Argonaute-2 Is Required Early in Embryogenesis for the Assembly of Centric/Centromeric Heterochromatin, Nuclear Division, Nuclear Migration, and Germ-Cell Formation." *Genes & Development* 19(14):1680–85. doi: 10.1101/gad.1316805.

Ditch, Scott, Mimi C. Sammarco, Ayan Banerjee, and Ed Grabczyk. 2009. "Progressive GAA·TTC Repeat Expansion in Human Cell Lines." *PLOS Genetics* 5(10):e1000704. doi: 10.1371/journal.pgen.1000704.

Djupedal, Ingela, Manuela Portoso, Henrik Spåhr, Carolina Bonilla, Claes M. Gustafsson, Robin C. Allshire, and Karl Ekwall. 2005. "RNA Pol II Subunit Rpb7 Promotes Centromeric Transcription and RNAi-Directed Chromatin Silencing." *Genes and Development* 19(19):2301–6. doi: 10.1101/gad.344205.

Doxzen, Kevin W., and Jennifer A. Doudna. 2017. "DNA Recognition by an RNA-Guided Bacterial Argonaute." *PLOS ONE* 12(5):e0177097. doi: 10.1371/journal.pone.0177097.

Drané, Pascal, Marie-Eve Brault, Gaofeng Cui, Khyati Meghani, Shweta Chaubey, Alexandre Detappe, Nishita Parnandi, Yizhou He, Xiao-Feng Zheng, Maria Victoria Botuyan, Alkmini Kalousi, William T. Yewdell, Christian Münch, J. Wade Harper, Jayanta Chaudhuri, Evi Soutoglou, Georges Mer, and Dipanjan Chowdhury. 2017. "TIRR Regulates 53BP1 by Masking Its Histone Methyl-Lysine Binding Function." *Nature* 543(7644):211–16. doi: 10.1038/nature21358.

Drobysheva, Arina V., Sofia A. Panafidina, Matvei V. Kolesnik, Evgeny I. Klimuk, Leonid Minakhin, Maria V. Yakunina, Sergei Borukhov, Emelie Nilsson, Karin Holmfeldt, Natalya Yutin, Kira S. Makarova, Eugene V. Koonin, Konstantin V. Severinov, Petr G. Leiman, and Maria L. Sokolova. 2021. "Structure and Function of Virion RNA Polymerase of a crAss-like Phage." *Nature* 589(7841):306–9. doi: 10.1038/s41586-020-2921-5.

Drolet, Marc. 2006. "Growth Inhibition Mediated by Excess Negative Supercoiling: The Interplay between Transcription Elongation, R-Loop Formation and DNA Topology." *Molecular Microbiology* 59(3):723–30. doi: 10.1111/j.1365-2958.2005.05006.x.

Dungrawala, Huzefa, Kamakoti P. Bhat, Rémy Le Meur, Walter J. Chazin, Xia Ding, Shyam K. Sharan, Sarah R. Wessel, Aditya A. Sathe, Runxiang Zhao, and David Cortez. 2017. "RADX Promotes Genome Stability

and Modulates Chemosensitivity by Regulating RAD51 at Replication Forks." *Molecular Cell* 67(3):374-386.e5. doi: 10.1016/j.molcel.2017.06.023.

Duquette, Michelle L., Priya Handa, Jack A. Vincent, Andrew F. Taylor, and Nancy Maizels. 2004. "Intracellular Transcription of G-Rich DNAs Induces Formation of G-Loops, Novel Structures Containing G4 DNA." *Genes & Development* 18(13):1618–29. doi: 10.1101/gad.1200804.

Durand-Dubief, Mickaël, and Philippe Bastin. 2003. "TbAGO1, an Argonaute Protein Required for RNA Interference, Is Involved in Mitosis and Chromosome Segregation in Trypanosoma Brucei." *BMC Biology*.

Durkin, Sandra G., and Thomas W. Glover. 2007. "Chromosome Fragile Sites." *Annual Review of Genetics* 41(1):169–92. doi: 10.1146/annurev.genet.41.042007.165900.

Dutta, Dipak, Konstantin Shatalin, Vitaly Epshtein, Max E. Gottesman, and Evgeny Nudler. 2011. "Linking RNA Polymerase Backtracking to Genome Instability in E. Coli." *Cell* 146(4):533–43. doi: 10.1016/j.cell.2011.07.034.

Eckert, Carrie A., Daniel J. Gravdahl, and Paul C. Megee. 2007. "The Enhancement of Pericentromeric Cohesin Association by Conserved Kinetochore Components Promotes High-Fidelity Chromosome Segregation and Is Sensitive to Microtubule-Based Tension." *Genes & Development* 21(3):278–91. doi: 10.1101/gad.1498707.

Edwards, Drake S., Rohin Maganti, Jarred P. Tanksley, Jie Luo, James J. H. Park, Elena Balkanska-Sinclair, Jinjie Ling, and Scott R. Floyd. 2020. "BRD4 Prevents R-Loop Formation and Transcription-Replication Conflicts by Ensuring Efficient Transcription Elongation." *Cell Reports* 32(12):108166. doi: 10.1016/j.celrep.2020.108166.

Eick, Dirk, and Matthias Geyer. 2013. "The RNA Polymerase II Carboxy-Terminal Domain (CTD) Code." *Chemical Reviews* 113(11):8456–90. doi: 10.1021/cr400071f.

Elías-Arnanz, Montserrat, and Margarita Salas. 1997. "Bacteriophage Φ29 DNA Replication Arrest Caused by Codirectional Collisions with the Transcription Machinery." *The EMBO Journal* 16(18):5775–83. doi: 10.1093/emboj/16.18.5775.

Erdős, Gábor, Mátyás Pajkos, and Zsuzsanna Dosztányi. 2021. "IUPred3: Prediction of Protein Disorder Enhanced with Unambiguous Experimental Annotation and Visualization of Evolutionary Conservation." *Nucleic Acids Research* 49(W1):W297–303. doi: 10.1093/nar/gkab408.

Errico, Alessia, and Vincenzo Costanzo. 2012. "Mechanisms of Replication Fork Protection: A Safeguard for Genome Stability." *Critical Reviews in Biochemistry and Molecular Biology* 47(3):222–35. doi: 10.3109/10409238.2012.655374.

Estrem, Brandon, and Jianbin Wang. 2023. "Programmed DNA Elimination in the Parasitic Nematode Ascaris." *PLOS Pathogens* 19(2):e1011087. doi: 10.1371/journal.ppat.1011087.

Evrin, Cecile, Pippa Clarke, Juergen Zech, Rudi Lurz, Jingchuan Sun, Stefan Uhle, Huilin Li, Bruce Stillman, and Christian Speck. 2009. "A Double-Hexameric MCM2-7 Complex Is Loaded onto Origin DNA during Licensing of Eukaryotic DNA Replication." *Proceedings of the National Academy of Sciences* 106(48):20240–45. doi: 10.1073/pnas.0911500106.

Fagard, Mathilde, Stéphanie Boutet, Jean-Benoit Morel, Catherine Bellini, and Hervé Vaucheret. 2000. "AGO1, QDE-2, and RDE-1 Are Related Proteins Required for Post-Transcriptional Gene Silencing in Plants, Quelling in Fungi, and RNA Interference in Animals." *Proceedings of the National Academy of Sciences* 97(21):11650–54. doi: 10.1073/pnas.200217597.

Felipe-Abrio, I., Juan Lafuente-Barquero, M. L. Garcia-Rubio, and Andrés Aguilera. 2014. "RNA Polymerase II Contributes to Preventing Transcription-Mediated Replication Fork Stalls." *The EMBO Journal* 34(2):236–50. doi: 10.15252/embj.201488544.

Fenstermaker, Tyler K., Svetlana Petruk, Sina K. Kovermann, Hugh W. Brock, and Alexander Mazo. 2023. "RNA Polymerase II Associates with Active Genes during DNA Replication." *Nature* 1–8. doi: 10.1038/s41586-023-06341-9.

Fianu, Isaac, Ying Chen, Christian Dienemann, Olexandr Dybkov, Andreas Linden, Henning Urlaub, and Patrick Cramer. 2021. "Structural Basis of Integrator-Mediated Transcription Regulation." *Science* 374(6569):883–87. doi: 10.1126/science.abk0154.

Flor-Parra, Ignacio, Jacob Zhurinsky, Manuel Bernal, Paola Gallardo, and Rafael R. Daga. 2014. “A Lallzyme MMX-Based Rapid Method for Fission Yeast Protoplast Preparation.” *Yeast* 31(2):61–66. doi: 10.1002/yea.2994.

Folco, Hernan Diego, Alison L. Pidoux, Takeshi Urano, and Robin C. Allshire. 2008. “Heterochromatin and RNAi Are Required to Establish CENP-A Chromatin at Centromeres.” *Science* 319(5859):94–97. doi: 10.1126/science.1150944.

Fong, Nova, Kristopher Brannan, Benjamin Erickson, Hyunmin Kim, Michael A. Cortazar, Ryan M. Sheridan, Tram Nguyen, Shai Karp, and David L. Bentley. 2015. “Effects of Transcription Elongation Rate and Xrn2 Exonuclease Activity on RNA Polymerase II Termination Suggest Widespread Kinetic Competition.” *Molecular Cell* 60(2):256–67. doi: 10.1016/j.molcel.2015.09.026.

Francia, Sofia, Matteo Cabrini, Valentina Matti, Amanda Oldani, and Fabrizio d’Adda di Fagagna. 2016. “DICER, DROSHA and DNA Damage Response RNAs Are Necessary for the Secondary Recruitment of DNA Damage Response Factors.” *Journal of Cell Science* 129(7):1468–76. doi: 10.1242/jcs.182188.

Francia, Sofia, Flavia Michelini, Alka Saxena, Dave Tang, Michiel De Hoon, Viviana Anelli, Marina Mione, Piero Carninci, and Fabrizio D’adda Di Fagagna. 2012. “Site-Specific DICER and DROSHA RNA Products Control the DNA-Damage Response.” *Nature* 488(7410):231–35. doi: 10.1038/nature11179.

French, Sarah. 1992. “Consequences of Replication Fork Movement Through Transcription Units in Vivo.” *Science* 258(5086):1362–65. doi: 10.1126/science.1455232.

Fu, Lei, Caiyun Xie, Zehua Jin, Zizhuo Tu, Li Han, Meilin Jin, Yaozu Xiang, and Anding Zhang. 2019. “The Prokaryotic Argonaute Proteins Enhance Homology Sequence-Directed Recombination in Bacteria.” *Nucleic Acids Research* 47(7):3568–79. doi: 10.1093/nar/gkz040.

Fugger, Kasper, Martin Mistrik, Kai J. Neelsen, Qi Yao, Ralph Zellweger, Arne Nedergaard Kousholt, Peter Haahr, Wai Kit Chu, Jiri Bartek, Massimo Lopes, Ian D. Hickson, and Claus Storgaard Sørensen. 2015. “FBH1 Catalyzes Regression of Stalled Replication Forks.” *Cell Reports* 10(10):1749–57. doi: 10.1016/j.celrep.2015.02.028.

Gadaleta, Mariana C., and Eishi Noguchi. 2017. “Regulation of DNA Replication through Natural Impediments in the Eukaryotic Genome.” *Genes* 8(3). doi: 10.3390/genes8030098.

Gaillard, Hélène, and Andrés Aguilera. 2013. “Transcription Coupled Repair at the Interface between Transcription Elongation and mRNP Biogenesis.” *Biochimica et Biophysica Acta (BBA) - Gene Regulatory Mechanisms* 1829(1):141–50. doi: 10.1016/j.bbagrm.2012.09.008.

Gaillard, Hélène, and Andrés Aguilera. 2016. “Transcription as a Threat to Genome Integrity.” *Annual Review of Biochemistry* 85(1):291–317. doi: 10.1146/annurev-biochem-060815-014908.

Gan, Wenjian, Zhishuang Guan, Jie Liu, Ting Gui, Keng Shen, James L. Manley, and Xialu Li. 2011. “R-Loop-Mediated Genomic Instability Is Caused by Impairment of Replication Fork Progression.” *Genes & Development* 25(19):2041–56. doi: 10.1101/gad.17010011.

Gao, Dongying, Ning Jiang, Rod A. Wing, Jiming Jiang, and Scott A. Jackson. 2015. “Transposons Play an Important Role in the Evolution and Diversification of Centromeres among Closely Related Species.” *Frontiers in Plant Science* 6.

Gao, Min, Wei Wei, Ming Ming Li, Yong Sheng Wu, Zhaoqing Ba, Kang Xuan Jin, Miao Miao Li, You Qi Liao, Samir Adhikari, Zechen Chong, Ting Zhang, Cai Xia Guo, Tie Shan Tang, Bing Tao Zhu, Xing Zhi Xu, Niels Mailand, Yun Gui Yang, Yijun Qi, and Jannie M. Rendtlew Danielsen. 2014. “Ago2 Facilitates Rad51 Recruitment and DNA Double-Strand Break Repair by Homologous Recombination.” *Cell Research* 24(5):532–41. doi: 10.1038/cr.2014.36.

Gao, Yunyi, Therese Solberg, Chundi Wang, and Feng Gao. 2023. “Small RNA-Mediated Genome Rearrangement Pathways in Ciliates.” *Trends in Genetics* 39(2):94–97. doi: 10.1016/j.tig.2022.10.001.

García-Muse, Tatiana, and Andrés Aguilera. 2019. “R Loops: From Physiological to Pathological Roles.” *Cell* 179(3):604–18. doi: 10.1016/j.cell.2019.08.055.

García-Pichardo, Desiré, Juan C. Cañas, María L. García-Rubio, Belén Gómez-González, Ana G. Rondón, and Andrés Aguilera. 2017. "Histone Mutants Separate R Loop Formation from Genome Instability Induction." *Molecular Cell* 66(5):597-609.e5. doi: 10.1016/j.molcel.2017.05.014.

García-Rubio, M., P. Huertas, S. González-Barrera, and A. Aguilera. 2003. "Recombinogenic Effects of DNA-Damaging Agents Are Synergistically Increased by Transcription in Saccharomyces Cerevisiae: New Insights Into Transcription-Associated Recombination." *Genetics* 165(2):457–66. doi: 10.1093/genetics/165.2.457.

García-Rubio, María, Paula Aguilera, Juan Lafuente-Barquero, José F. Ruiz, Marie-Noelle Simon, Vincent Geli, Ana G. Rondón, and Andrés Aguilera. 2018. "Yra1-Bound RNA–DNA Hybrids Cause Orientation-Independent Transcription–Replication Collisions and Telomere Instability." *Genes & Development* 32(13–14):965–77. doi: 10.1101/gad.311274.117.

Gari, Kerstin, Chantal Décaillet, Mathieu Delannoy, Leonard Wu, and Angelos Constantinou. 2008. "Remodeling of DNA Replication Structures by the Branch Point Translocase FANCM." *Proceedings of the National Academy of Sciences of the United States of America* 105(42):16107–12. doi: 10.1073/pnas.0804777105.

Gari, Kerstin, Chantal Décaillet, Alicja Z. Stasiak, Andrzej Stasiak, and Angelos Constantinou. 2008. "The Fanconi Anemia Protein FANCM Can Promote Branch Migration of Holliday Junctions and Replication Forks." *Molecular Cell* 29(1):141–48. doi: 10.1016/j.molcel.2007.11.032.

Garrison, Erik, and Gabor Marth. 2012. "Haplotype-Based Variant Detection from Short-Read Sequencing."

Giglia-Mari, Giuseppina, Angelika Zotter, and Wim Vermeulen. 2011. "DNA Damage Response." *Cold Spring Harbor Perspectives in Biology* 3(1):a000745. doi: 10.1101/cshperspect.a000745.

Gnatt, Averell L., Patrick Cramer, Jianhua Fu, David A. Bushnell, and Roger D. Kornberg. 2001. "Structural Basis of Transcription: An RNA Polymerase II Elongation Complex at 3.3 Å Resolution." *Science* 292(5523):1876–82. doi: 10.1126/science.1059495.

Gómez-González, Belén, and Andrés Aguilera. 2007. "Activation-Induced Cytidine Deaminase Action Is Strongly Stimulated by Mutations of the THO Complex." *Proceedings of the National Academy of Sciences* 104(20):8409–14. doi: 10.1073/pnas.0702836104.

Gong, Zhiyun, Yufeng Wu, Andrea Koblížková, Giovana A. Torres, Kai Wang, Marina Iovene, Pavel Neumann, Wenli Zhang, Petr Novák, C. Robin Buell, Jiří Macas, and Jiming Jiang. 2012. "Repeatless and Repeat-Based Centromeres in Potato: Implications for Centromere Evolution." *The Plant Cell* 24(9):3559–74. doi: 10.1105/tpc.112.100511.

González-Barrera, Sergio, María García-Rubio, and Andrés Aguilera. 2002. "Transcription and Double-Strand Breaks Induce Similar Mitotic Recombination Events in Saccharomyces Cerevisiae." *Genetics* 162(2):603–14. doi: 10.1093/genetics/162.2.603.

Goodrich, James A., and Robert Tjian. 1994. "Transcription Factors IIE and IIH and ATP Hydrolysis Direct Promoter Clearance by RNA Polymerase II." *Cell* 77(1):145–56. doi: 10.1016/0092-8674(94)90242-9.

Goulielmaki, Evi, Maria Tsekrekou, Nikos Batsiotos, Mariana Ascensão-Ferreira, Eleftheria Ledaki, Kalliopi Stratigi, Georgia Chatzinikolaou, Pantelis Topalis, Theodore Kosteas, Janine Altmüller, Jeroen A. Demmers, Nuno L. Barbosa-Morais, and George A. Garinis. 2021. "The Splicing Factor XAB2 Interacts with ERCC1-XPF and XPG for R-Loop Processing." *Nature Communications* 12(1):3153. doi: 10.1038/s41467-021-23505-1.

Green, Phil, Brent Ewing, Webb Miller, Pamela J. Thomas, and Eric D. Green. 2003. "Transcription-Associated Mutational Asymmetry in Mammalian Evolution." *Nature Genetics* 33(4):514–17. doi: 10.1038/ng1103.

Grimm, Christian, Primo Schaer, Peter Munz, and Jürg Kohli. 1991. "The Strong ADH1 Promoter Stimulates Mitotic and Meiotic Recombination at the ADE6 Gene of Schizosaccharomyces Pombe." *Molecular and Cellular Biology* 11(1):289–98. doi: 10.1128/mcb.11.1.289-298.1991.

Gros, Julien, Charanya Kumar, Gerard Lynch, Tejas Yadav, Iestyn Whitehouse, and Dirk Remus. 2015. "Post-Licensing Specification of Eukaryotic Replication Origins by Facilitated Mcm2-7 Sliding along DNA." *Molecular Cell* 60(5):797–807. doi: 10.1016/j.molcel.2015.10.022.

Gutbrod, M. J., B. Roche, J. I. Steinberg, A. A. Lakhani, K. Chang, A. J. Schorn, and R. A. Martienssen. 2022. "Dicer Promotes Genome Stability via the Bromodomain Transcriptional Co-Activator BRD4." *Nature Communications* 13(1):1001. doi: 10.1038/s41467-022-28554-8.

Gutbrod, Michael J., and Robert A. Martienssen. 2020. "Conserved Chromosomal Functions of RNA Interference." *Nature Reviews Genetics*. doi: 10.1038/s41576-019-0203-6.

Ha, Minju, and V. Narry Kim. 2014. "Regulation of microRNA Biogenesis." *Nature Reviews Molecular Cell Biology* 15(8):509–24. doi: 10.1038/nrm3838.

Haag, Jeremy R., Olga Pontes, and Craig S. Pikaard. 2009. "Metal A and Metal B Sites of Nuclear RNA Polymerases Pol IV and Pol V Are Required for siRNA-Dependent DNA Methylation and Gene Silencing" edited by F. Berger. *PLoS ONE* 4(1):e4110. doi: 10.1371/journal.pone.0004110.

Hage, Aziz El, Sarah L. French, Ann L. Beyer, and David Tollervey. 2010. "Loss of Topoisomerase I Leads to R-Loop-Mediated Transcriptional Blocks during Ribosomal RNA Synthesis." *Genes & Development* 24(14):1546–58. doi: 10.1101/gad.573310.

Halic, Mario, and Danesh Moazed. 2010. "Dicer-Independent Primal RNAs Trigger RNAi and Heterochromatin Formation." *Cell* 140(4):504–16. doi: 10.1016/j.cell.2010.01.019.

Hall, Ira M., Ken-ichi Noma, and Shiv I. S. Grewal. 2003. "RNA Interference Machinery Regulates Chromosome Dynamics during Mitosis and Meiosis in Fission Yeast." *Proceedings of the National Academy of Sciences* 100(1):193–98. doi: 10.1073/pnas.232688099.

Hamperl, Stephan, Michael J. Bocek, Joshua C. Saldivar, Tomek Swigut, and Karlene A. Cimprich. 2017. "Transcription-Replication Conflict Orientation Modulates R-Loop Levels and Activates Distinct DNA Damage Responses." *Cell* 170(4):774-786.e19. doi: 10.1016/j.cell.2017.07.043.

Hanawalt, Philip C., and Graciela Spivak. 2008. "Transcription-Coupled DNA Repair: Two Decades of Progress and Surprises." *Nature Reviews Molecular Cell Biology* 9(12):958–70. doi: 10.1038/nrm2549.

Hansen, Sarah R., Adedeji M. Aderounmu, Helen M. Donelick, and Brenda L. Bass. 2020. "Dicer's Helicase Domain: A Meeting Place for Regulatory Proteins." *Cold Spring Harbor Symposia on Quantitative Biology* LXXXIV:039750. doi: 10.1101/sqb.2019.84.039750.

Hantsche, Merle, and Patrick Cramer. 2017. "Conserved RNA Polymerase II Initiation Complex Structure." *Current Opinion in Structural Biology* 47:17–22. doi: 10.1016/j.sbi.2017.03.013.

Hao, Zhitai, Vladimir Svetlov, and Evgeny Nudler. 2021. "Rho-Dependent Transcription Termination: A Revisionist View." *Transcription* 12(4):171–81. doi: 10.1080/21541264.2021.1991773.

Harfe, Brian D., Michael T. McManus, Jennifer H. Mansfield, Eran Hornstein, and Clifford J. Tabin. 2005. "The RNaseIII Enzyme *Dicer* Is Required for Morphogenesis but Not Patterning of the Vertebrate Limb." *Proceedings of the National Academy of Sciences* 102(31):10898–903. doi: 10.1073/pnas.0504834102.

Harper, Thomas M., and Dylan J. Taatjes. 2018. "The Complex Structure and Function of Mediator." *Journal of Biological Chemistry* 293(36):13778–85. doi: 10.1074/jbc.R117.794438.

Harrison, Clare, Satoshi Katayama, Susheela Dhut, Dongrong Chen, Nie Jones, Jürg Bähler, and Takashi Toda. 2005. "SCFPof1-Ubiquitin and Its Target Zip1 Transcription Factor Mediate Cadmium Response in Fission Yeast." *EMBO Journal* 24(3):599–610. doi: 10.1038/sj.emboj.7600536.

Hasanova, Zdenka, Veronika Klapstova, Odil Porrua, Richard Stefl, and Marek Sebesta. 2023. "Human Senataxin Is a Bona Fide R-Loop Resolving Enzyme and Transcription Termination Factor." *Nucleic Acids Research* 51(6):2818–37. doi: 10.1093/nar/gkad092.

Hassan, A. Bassim, Rachel J. Errington, Nick S. White, Dean A. Jackson, and Peter R. Cook. 1994. "Replication and Transcription Sites Are Colocalized in Human Cells." *Journal of Cell Science* 107(2):425–34. doi: 10.1242/jcs.107.2.425.

Hatchi, Elodie, Liana Goehring, Serena Landini, Konstantina Skourti-Stathaki, Derrick K. DeConti, Fieda O. Abderazzaq, Priyankana Banerjee, Timothy M. Demers, Yaoyu E. Wang, John Quackenbush, and David

M. Livingston. 2021. “BRCA1 and RNAi Factors Promote Repair Mediated by Small RNAs and PALB2–RAD52.” *Nature* (February 2019). doi: 10.1038/s41586-020-03150-2.

Hausmann, Stéphane, Hediye Erdjument-Bromage, and Stewart Shuman. 2004. “Schizosaccharomyces Pombe Carboxyl-Terminal Domain (CTD) Phosphatase Fcp1: DISTRIBUTIVE MECHANISM, MINIMAL CTD SUBSTRATE, AND ACTIVE SITE MAPPING *.” *Journal of Biological Chemistry* 279(12):10892–900. doi: 10.1074/jbc.M312513200.

Hawkins, Michelle, Juachi U. Dimude, Jamieson A. L. Howard, Abigail J. Smith, Mark S. Dillingham, Nigel J. Savery, Christian J. Rudolph, and Peter McGlynn. 2019. “Direct Removal of RNA Polymerase Barriers to Replication by Accessory Replicative Helicases.” *Nucleic Acids Research* 47(10):5100–5113. doi: 10.1093/nar/gkz170.

Helmrich, Anne, Monica Ballarino, Evgeny Nudler, and Laszlo Tora. 2013. “Transcription-Replication Encounters, Consequences and Genomic Instability.” *Nature Structural and Molecular Biology* 20(4):412–18. doi: 10.1038/nsmb.2543.

Helmrich, Anne, Monica Ballarino, and Laszlo Tora. 2011. “Collisions between Replication and Transcription Complexes Cause Common Fragile Site Instability at the Longest Human Genes.” *Molecular Cell* 44(6):966–77. doi: 10.1016/j.molcel.2011.10.013.

Helmrich, Anne, Karen Stout-Weider, Klaus Hermann, Evelin Schrock, and Thomas Heiden. 2006. “Common Fragile Sites Are Conserved Features of Human and Mouse Chromosomes and Relate to Large Active Genes.” *Genome Research* 16(10):1222–30. doi: 10.1101/gr.5335506.

Hendriks, Giel, Fabienne Calléja, Harry Vrieling, Leon H. F. Mullenders, Jacob G. Jansen, and Niels de Wind. 2008. “Gene Transcription Increases DNA Damage-Induced Mutagenesis in Mammalian Stem Cells.” *DNA Repair* 7(8):1330–39. doi: 10.1016/j.dnarep.2008.04.015.

Henikoff, Steven, Kami Ahmad, and Harmit S. Malik. 2001. “The Centromere Paradox: Stable Inheritance with Rapidly Evolving DNA.” *Science* 293(5532):1098–1102. doi: 10.1126/science.1062939.

Henikoff, Steven, and Ali Shilatifard. 2011. “Histone Modification: Cause or Cog?” *Trends in Genetics* 27(10):389–96. doi: 10.1016/j.tig.2011.06.006.

Hennion, Magali, Jean Michel Arbona, Laurent Lacroix, Corinne Cruaud, Bertrand Theulot, Benoît Le Tallec, Florence Proux, Xia Wu, Elizaveta Novikova, Stefan Engelen, Arnaud Lemainque, Benjamin Audit, and Olivier Hyrien. 2020. “FORK-Seq: Replication Landscape of the Saccharomyces Cerevisiae Genome by Nanopore Sequencing.” *Genome Biology* 21(1):1–25. doi: 10.1186/s13059-020-02013-3.

Hennion, Magali, Bertrand Theulot, Jean-Michel Arbona, Benjamin Audit, and Olivier Hyrien. 2022. “FORK-Seq: Single-Molecule Profiling of DNA ReplicationDNA Replication.” Pp. 107–28 in *Yeast Functional Genomics: Methods and Protocols*, *Methods in Molecular Biology*, edited by F. Devaux. New York, NY: Springer US.

Herman, Robert K., and Nomi B. Dworkin. 1971. “Effect of Gene Induction on the Rate of Mutagenesis by ICR-191 in Escherichia Coli.” *Journal of Bacteriology* 106(2):543–50. doi: 10.1128/jb.106.2.543-550.1971.

Heyer, Wolf-Dietrich, Kirk T. Ehmsen, and Jie Liu. 2010. “Regulation of Homologous Recombination in Eukaryotes.” *Annual Review of Genetics* 44(1):113–39. doi: 10.1146/annurev-genet-051710-150955.

Hodges, Amelia J., Dalton A. Plummer, and John J. Wyrick. 2019. “NuA4 Acetyltransferase Is Required for Efficient Nucleotide Excision Repair in Yeast.” *DNA Repair* 73:91–98. doi: 10.1016/j.dnarep.2018.11.006.

Hodson, Charlotte, Sylvie Van Twest, Malgorzata Dylewska, Julienne J. O’Rourke, Winnie Tan, Vincent J. Murphy, Mannu Walia, Lara Abbouche, Jadwiga Nieminuszczy, Elyse Dunn, Rohan Bythell-Douglas, Jörg Heierhorst, Wojciech Niedzwiedz, and Andrew J. Deans. 2022. “Branchpoint Translocation by Fork Remodelers as a General Mechanism of R-Loop Removal.” *Cell Reports* 41(10):111749. doi: 10.1016/j.celrep.2022.111749.

Hodson, Jeffrey A., Julie M. Bailis, and Susan L. Forsburg. 2003. “Efficient Labeling of Fission Yeast Schizosaccharomyces Pombe with Thymidine and BUdR.” *Nucleic Acids Research* 31(21):e134. doi: 10.1093/nar/gng134.

Hu, Jiazhi, Lei Sun, Fenfen Shen, Yufei Chen, Yu Hua, Yang Liu, Mian Zhang, Yiren Hu, Qingsong Wang, Wei Xu, Fei Sun, Jianguo Ji, Johanne M. Murray, Antony M. Carr, and Daochun Kong. 2012. "The Intra-S Phase Checkpoint Targets Dna2 to Prevent Stalled Replication Forks from Reversing." *Cell* 149(6):1221–32. doi: 10.1016/j.cell.2012.04.030.

Hu, Y., A. Tareen, Y. J. Sheu, W. T. Ireland, C. Speck, H. Li, L. Joshua-Tor, J. B. Kinney, and B. Stillman. 2020. "Evolution of DNA Replication Origin Specification and Gene Silencing Mechanisms." *Nature Communications* 11(1):5175. doi: 10.1038/s41467-020-18964-x.

Hu, Yixin, and Bruce Stillman. 2023. "Origins of DNA Replication in Eukaryotes." *Molecular Cell* 83(3):352–72. doi: 10.1016/j.molcel.2022.12.024.

Huang, Chuan, Xiaolin Wang, Xu Liu, Shuhuan Cao, and Ge Shan. 2015. "RNAi Pathway Participates in Chromosome Segregation in Mammalian Cells." *Cell Discovery* 1(1):1–15. doi: 10.1038/celldisc.2015.29.

Huertas, Pablo, and Andrés Aguilera. 2003. "Cotranscriptionally Formed DNA:RNA Hybrids Mediate Transcription Elongation Impairment and Transcription-Associated Recombination." *Molecular Cell* 12(3):711–21. doi: 10.1016/j.molcel.2003.08.010.

Hurst, Verena, Kiran Challa, Felix Jonas, Romain Forey, Ragna Sack, Jan Seebacher, Christoph D. Schmid, Naama Barkai, Kenji Shimada, Susan M. Gasser, and Jérôme Poli. 2021. "A Regulatory Phosphorylation Site on Mec1 Controls Chromatin Occupancy of RNA Polymerases during Replication Stress." *The EMBO Journal* 40(21):e108439. doi: 10.15252/embj.2021108439.

Huvet, Maxime, Samuel Nicolay, Marie Touchon, Benjamin Audit, Yves d'Aubenton-Carafa, Alain Arneodo, and Claude Thermes. 2007. "Human Gene Organization Driven by the Coordination of Replication and Transcription." *Genome Research* 17(9):1278–85. doi: 10.1101/gr.6533407.

Hyjek, Malwina, Małgorzata Figiel, and Marcin Nowotny. 2019. "RNases H: Structure and Mechanism." *DNA Repair* 84:102672. doi: 10.1016/j.dnarep.2019.102672.

Ikeda, H., and I. Kobayashi. 1977. "Involvement of DNA-Dependent RNA Polymerase in a recA-Independent Pathway of Genetic Recombination in Escheria Coli." *Proceedings of the National Academy of Sciences* 74(9):3932–36. doi: 10.1073/pnas.74.9.3932.

Iraqui, Ismail, Yasmina Chekkal, Nada Jmari, Violena Pietrobon, Karine Fréon, Audrey Costes, and Sarah A.E. Lambert. 2012. "Recovery of Arrested Replication Forks by Homologous Recombination Is Error-Prone." *PLoS Genetics* 8(10):e1002976. doi: 10.1371/journal.pgen.1002976.

Iraqui, Ismail, Yasmina Chekkal, Nada Jmari, Violena Pietrobon, Karine Fréon, Audrey Costes, and Sarah A. E. Lambert. 2012. "Recovery of Arrested Replication Forks by Homologous Recombination Is Error-Prone." *PLOS Genetics* 8(10):e1002976. doi: 10.1371/journal.pgen.1002976.

Irvine, Danielle V., Mikel Zaratiegui, Niraj H. Tolia, Derek B. Goto, Daniel H. Chitwood, Matthew W. Vaughn, Leemor Joshua-Tor, and Robert A. Martienssen. 2006. "Argonaute Slicing Is Required for Heterochromatic Silencing and Spreading." *Science* 313(5790):1134–37. doi: 10.1126/science.1128813.

Ivessa, Andreas S., Jin-Qiu Zhou, and Virginia A. Zakian. 2000. "The Saccharomyces Pif1p DNA Helicase and the Highly Related Rrm3p Have Opposite Effects on Replication Fork Progression in Ribosomal DNA." *Cell* 100(4):479–89. doi: 10.1016/S0092-8674(00)80683-2.

Iyer, Lakshminarayan M., Eugene V. Koonin, and L. Aravind. 2003. "Evolutionary Connection between the Catalytic Subunits of DNA-Dependent RNA Polymerases and Eukaryotic RNA-Dependent RNA Polymerases and the Origin of RNA Polymerases." *BMC Structural Biology* 3(1):1. doi: 10.1186/1472-6807-3-1.

Jaehning, Judith A. 2010. "The Paf1 Complex: Platform or Player in RNA Polymerase II Transcription?" *Biochimica et Biophysica Acta - Gene Regulatory Mechanisms* 1799(5–6):379–88. doi: 10.1016/j.bbagrm.2010.01.001.

Jinks-Robertson, Sue, and Ashok S. Bhagwat. 2014. "Transcription-Associated Mutagenesis." *Annual Review of Genetics* 48(1):341–59. doi: 10.1146/annurev-genet-120213-092015.

Jolly, Samson M., Ildar Gainetdinov, Karina Jouravleva, Han Zhang, Lara Strittmatter, Shannon M. Bailey, Gregory M. Hendricks, Avantika Dhabaria, Beatrix Ueberheide, and Phillip D. Zamore. 2020. "Thermus

Thermophilus Argonaute Functions in the Completion of DNA Replication." *Cell* 182(6):1545-1559.e18. doi: 10.1016/j.cell.2020.07.036.

Jones, Morgan L., Yasemin Baris, Martin R. G. Taylor, and Joseph T. P. Yeeles. 2021. "Structure of a Human Replisome Shows the Organisation and Interactions of a DNA Replication Machine." *The EMBO Journal* 40(23):e108819. doi: 10.15252/embj.2021108819.

Judd, Julius, Luke A. Wojenski, Lauren M. Wainman, Nathaniel D. Tippens, Edward J. Rice, Alexis Dziubek, Geno J. Villafano, Erin M. Wissink, Philip Versluis, Lina Bagepalli, Sagar R. Shah, Dig B. Mahat, Jacob M. Tome, Charles G. Danko, John T. Lis, and Leighton J. Core. 2020. "A Rapid, Sensitive, Scalable Method for Precision Run-On Sequencing (PRO-Seq)." 2020.05.18.102277.

Kanagaraj, Radhakrishnan, Nurten Saydam, Patrick L. Garcia, Lu Zheng, and Pavel Janscak. 2006. "Human RECQ5β Helicase Promotes Strand Exchange on Synthetic DNA Structures Resembling a Stalled Replication Fork." *Nucleic Acids Research* 34(18):5217–31. doi: 10.1093/nar/gkl677.

Kanno, Tatsuo, M. Florian Mette, David P. Kreil, Werner Aufsatz, Marjori Matzke, and Antonius J. M. Matzke. 2004. "Involvement of Putative SNF2 Chromatin Remodeling Protein DRD1 in RNA-Directed DNA Methylation." *Current Biology* 14(9):801–5. doi: 10.1016/j.cub.2004.04.037.

Kannouche, Patricia L., Jonathan Wing, and Alan R. Lehmann. 2004. "Interaction of Human DNA Polymerase η with Monoubiquitinated PCNA: A Possible Mechanism for the Polymerase Switch in Response to DNA Damage." *Molecular Cell* 14(4):491–500. doi: 10.1016/S1097-2765(04)00259-X.

Kato, Hiroaki. 2005. "RNA Polymerase II Is Required for RNAi-Dependent Heterochromatin Assembly." *Science* 309(5733):467–69. doi: 10.1126/science.1114955.

Katou, Yuki, Yutaka Kanoh, Masashige Bando, Hideki Noguchi, Hirokazu Tanaka, Toshihiko Ashikari, Katsunori Sugimoto, and Katsuhiko Shirahige. 2003. "S-Phase Checkpoint Proteins Tof1 and Mrc1 Form a Stable Replication-Pausing Complex." *Nature* 424(6952):1078–83. doi: 10.1038/nature01900.

Keil, Ralph L., and G. Shirleen Roeder. 1984. "Cis-Acting, Recombination-Stimulating Activity in a Fragment of the Ribosomal DNA of S. Cerevisiae." *Cell* 39(2, Part 1):377–86. doi: 10.1016/0092-8674(84)90016-3.

Keogh, Michael-Christopher, Thomas A. Mennella, Chika Sawa, Sharon Berthelet, Nevan J. Krogan, Adam Wolek, Vladimir Podolny, Laura Rocco Carpenter, Jack F. Greenblatt, Kristin Baetz, and Stephen Buratowski. 2006. "The Saccharomyces Cerevisiae Histone H2A Variant Htz1 Is Acetylated by NuA4." *Genes & Development* 20(6):660–65. doi: 10.1101/gad.1388106.

Ketley, Ruth F., Federica Battistini, Adele Alagia, Clémence Mondielli, Florence Iehl, Esra Balikçi, Kilian V. M. Huber, Modesto Orozco, and Monika Gullerova. 2022. "DNA Double-Strand Break-Derived RNA Drives TIRR/53BP1 Complex Dissociation." *Cell Reports* 41(4):111526. doi: 10.1016/j.celrep.2022.111526.

Kidwell, Mary Anne, Jessica M. Chan, and Jennifer A. Doudna. 2014. "Evolutionarily Conserved Roles of the Dicer Helicase Domain in Regulating RNA Interference Processing." *Journal of Biological Chemistry* 289(41):28352–62. doi: 10.1074/jbc.M114.589051.

Kile, Andrew C., Diana A. Chavez, Julien Bacal, Sherif Eldirany, Dmitry M. Korzhnev, Irina Bezsonova, Brandt F. Eichman, and Karlene A. Cimprich. 2015. "HLTF's Ancient HIRAN Domain Binds 3' DNA Ends to Drive Replication Fork Reversal." *Molecular Cell* 58(6):1090–1100. doi: 10.1016/j.molcel.2015.05.013.

Kim, Hee-Dai, Joonho Choe, and Yeon-Soo Seo. 1999. "The Sen1+ Gene of Schizosaccharomyces Pombe, a Homologue of Budding Yeast SEN1, Encodes an RNA and DNA Helicase." *Biochemistry* 38(44):14697–710. doi: 10.1021/bi991470c.

Kim, Hyun-Soo, Rituparna Mukhopadhyay, Scott B. Rothbart, Andrea C. Silva, Vincent Vanoosthuyse, Ernest Radovani, Thomas Kislinger, Assen Roguev, Colm J. Ryan, Jiewei Xu, Harlizawati Jahari, Kevin G. Hardwick, Jack F. Greenblatt, Nevan J. Krogan, Jeffrey S. Fillingham, Brian D. Strahl, Eric E. Bouhassira, Winfried Edelmann, and Michael-Christopher Keogh. 2014. "Identification of a BET Family Bromodomain/Casein Kinase II/TAF-Containing Complex as a Regulator of Mitotic Condensin Function." *Cell Reports* 6(5):892–905. doi: 10.1016/j.celrep.2014.01.029.

Kim, Nayun, Amy L. Abdulovic, Regan Gealy, Malcolm J. Lippert, and Sue Jinks-Robertson. 2007. "Transcription-Associated Mutagenesis in Yeast Is Directly Proportional to the Level of Gene Expression and Influenced by the Direction of DNA Replication." *DNA Repair* 6(9):1285–96. doi: 10.1016/j.dnarep.2007.02.023.

Kim, Nayun, and Sue Jinks-Robertson. 2012. "Transcription as a Source of Genome Instability." *Nature Reviews Genetics* 13(3):204–14. doi: 10.1038/nrg3152.

Kim, Sangin, Nalae Kang, Su Hyung Park, James Wells, Taejoo Hwang, Eunjin Ryu, Byung-gyu Kim, Sunyoung Hwang, Seong-jung Kim, Sukhyun Kang, Semin Lee, Peter Stirling, Kyungjae Myung, and Kyoo-young Lee. 2020. "ATAD5 Restricts R-Loop Formation through PCNA Unloading and RNA Helicase Maintenance at the Replication Fork." *Nucleic Acids Research* 48(13):7218–38. doi: 10.1093/nar/gkaa501.

Kloc, Anna, Mikel Zaratiegui, Elphege Nora, and Rob Martienssen. 2008. "RNA Interference Guides Histone Modification during the S Phase of Chromosomal Replication." *Current Biology* 18(7):490–95. doi: 10.1016/j.cub.2008.03.016.

Kobayashi, Takehiko. 2003. "The Replication Fork Barrier Site Forms a Unique Structure with Fob1p and Inhibits the Replication Fork." *Molecular and Cellular Biology* 23(24):9178–88. doi: 10.1128/MCB.23.24.9178-9188.2003.

Kobayashi, Takehiko. 2014. "Ribosomal RNA Gene Repeats, Their Stability and Cellular Senescence." *Proceedings of the Japan Academy Series B: Physical and Biological Sciences* 90(4):119–29. doi: 10.2183/pjab.90.119.

Kobayashi, Takehiko, and Austen R. D. Ganley. 2005. "Recombination Regulation by Transcription-Induced Cohesin Dissociation in rDNA Repeats." *Science* 309(5740):1581–84. doi: 10.1126/science.1116102.

Komori, Kayoko, Ryosuke Fujikane, Hideo Shinagawa, and Yoshizumi Ishino. 2002. "Novel Endonuclease in Archaea Cleaving DNA with Various Branched Structure." *Genes & Genetic Systems* 77(4):227–41. doi: 10.1266/ggs.77.227.

Komori, Kayoko, Masumi Hidaka, Takashi Horiuchi, Ryosuke Fujikane, Hideo Shinagawa, and Yoshizumi Ishino. 2004. "Cooperation of the N-Terminal Helicase and C-Terminal Endonuclease Activities of Archaeal Hef Protein in Processing Stalled Replication Forks *." *Journal of Biological Chemistry* 279(51):53175–85. doi: 10.1074/jbc.M409243200.

Kondratick, Christine M., M. Todd Washington, and Maria Spies. 2021. "Making Choices: DNA Replication Fork Recovery Mechanisms." *Seminars in Cell & Developmental Biology* 113:27–37. doi: 10.1016/j.semcdb.2020.10.001.

Koonin, Eugene V. 2017. "Evolution of RNA- and DNA-Guided Antivirus Defense Systems in Prokaryotes and Eukaryotes: Common Ancestry vs Convergence." *Biology Direct* 12(1):5. doi: 10.1186/s13062-017-0177-2.

Koonin, Eugene V., Mart Krupovic, Sonoko Ishino, and Yoshizumi Ishino. 2020. "The Replication Machinery of LUCA: Common Origin of DNA Replication and Transcription." *BMC Biology* 18(1):61. doi: 10.1186/s12915-020-00800-9.

Koopal, Balwina, Sumanth K. Mutte, and Daan C. Swarts. 2023. "A Long Look at Short Prokaryotic Argonautes." *Trends in Cell Biology* 33(7):605–18. doi: 10.1016/j.tcb.2022.10.005.

Kotsantis, Panagiotis, Sandra Segura-Bayona, Pol Margalef, Paulina Marzec, Phil Ruis, Graeme Hewitt, Roberto Bellelli, Harshil Patel, Robert Goldstone, Anna R. Poetsch, and Simon J. Boulton. 2020. "RTEL1 Regulates G4/R-Loops to Avert Replication-Transcription Collisions." *Cell Reports* 33(12):108546. doi: 10.1016/j.celrep.2020.108546.

Kowalik, Katarzyna Maria, Yukiko Shimada, Valentin Flury, Michael Beda Stadler, Julia Batki, and Marc Bühler. 2015. "The Paf1 Complex Represses Small-RNA-Mediated Epigenetic Gene Silencing." *Nature* 520(7546):248–52. doi: 10.1038/nature14337.

Koyanagi, Eri, Yoko Kakimoto, Tamiko Minamisawa, Fumiya Yoshifuji, Toyoaki Natsume, Atsushi Higashitani, Tomoo Ogi, Antony M. Carr, Masato T. Kanemaki, and Yasukazu Daigaku. 2022. "Global Landscape of Replicative DNA Polymerase Usage in the Human Genome." *Nature Communications* 13(1):7221. doi: 10.1038/s41467-022-34929-8.

Kramarz, Karol, Anissia Ait Saada, and Sarah A. E. Lambert. 2021. "The Analysis of Recombination-Dependent Processing of Blocked Replication Forks by Bidimensional Gel Electrophoresis." Pp. 365–81 in *Methods in Molecular Biology*. Vol. 2153. Humana Press Inc.

Krupovic, Mart, Valerian V. Dolja, and Eugene V. Koonin. 2019. "Origin of Viruses: Primordial Replicators Recruiting Capsids from Hosts." *Nature Reviews Microbiology* 17(7):449–58. doi: 10.1038/s41579-019-0205-6.

Kulish, Dmitry, and Kevin Struhl. 2001. "TFIIS Enhances Transcriptional Elongation through an Artificial Arrest Site In Vivo." *Molecular and Cellular Biology* 21(13):4162–68. doi: 10.1128/MCB.21.13.4162-4168.2001.

Kumar, Charanya, Sahil Batra, Jack D. Griffith, and Dirk Remus. 2021. "The Interplay of RNA:DNA Hybrid Structure and G-Quadruplexes Determines the Outcome of R-Loop-Replisome Collisions" edited by B. Stillman, J. K. Tyler, B. Stillman, and P. Pasero. *eLife* 10:e72286. doi: 10.7554/eLife.72286.

Kuzmenko, Anton, Anastasiya Oguienko, Daria Esyunina, Denis Yudin, Mayya Petrova, Alina Kudinova, Olga Maslova, Maria Ninova, Sergei Ryazansky, David Leach, Alexei A. Aravin, and Andrey Kulbachinskiy. 2020. "DNA Targeting and Interference by a Bacterial Argonaute Nuclease." *Nature* 587(7835):632–37. doi: 10.1038/s41586-020-2605-1.

Lam, Fred C., Yi Wen Kong, Qiuying Huang, Tu-Lan Vu Han, Amanda D. Maffa, Ekkehard M. Kasper, and Michael B. Yaffe. 2020. "BRD4 Prevents the Accumulation of R-Loops and Protects against Transcription–Replication Collision Events and DNA Damage." *Nature Communications* 11(1):4083. doi: 10.1038/s41467-020-17503-y.

Lamarche, Brandon J., Nicole I. Orazio, and Matthew D. Weitzman. 2010. "The MRN Complex in Double-Strand Break Repair and Telomere Maintenance." *FEBS Letters* 584(17):3682–95. doi: 10.1016/j.febslet.2010.07.029.

Lambert, Sarah, Ken'ichi Mizuno, Joël Blaisonneau, Sylvain Martineau, Roland Chanet, Karine Fréon, Johanne M. Murray, Antony M. Carr, and Giuseppe Baldacci. 2010. "Homologous Recombination Restarts Blocked Replication Forks at the Expense of Genome Rearrangements by Template Exchange." *Molecular Cell* 39(3):346–59. doi: 10.1016/j.molcel.2010.07.015.

Lambert, Sarah, Adam Watson, Daniel M. Sheedy, Ben Martin, and Antony M. Carr. 2005. "Gross Chromosomal Rearrangements and Elevated Recombination at an Inducible Site-Specific Replication Fork Barrier." *Cell* 121(5):689–702. doi: 10.1016/j.cell.2005.03.022.

Landsverk, Helga B., Lise E. Sandquist, Lilli T. E. Bay, Barbara Steurer, Coen Campsteijn, Ole J. B. Landsverk, Jurgen A. Marteijn, Eva Petermann, Laura Trinkle-Mulcahy, and Randi G. Syljuåsen. 2020. "WDR82/PNUTS-PP1 Prevents Transcription-Replication Conflicts by Promoting RNA Polymerase II Degradation on Chromatin." *Cell Reports* 33(9):108469. doi: 10.1016/j.celrep.2020.108469.

Lang, Kevin S., Ashley N. Hall, Christopher N. Merrikh, Mark Ragheb, Hannah Tabakh, Alex J. Pollock, Joshua J. Woodward, Julia E. Dreifus, and Houra Merrikh. 2017. "Replication-Transcription Conflicts Generate R-Loops That Orchestrate Bacterial Stress Survival and Pathogenesis." *Cell* 170(4):787-799.e18. doi: 10.1016/j.cell.2017.07.044.

Langley, Alexander R., Stefan Gräf, James C. Smith, and Torsten Krude. 2016. "Genome-Wide Identification and Characterisation of Human DNA Replication Origins by Initiation Site Sequencing (Ini-Seq)." *Nucleic Acids Research* 44(21):10230–47. doi: 10.1093/nar/gkw760.

Langmead, Ben, and Steven L. Salzberg. 2012. "Fast Gapped-Read Alignment with Bowtie 2." *Nature Methods* 9(4):357–59. doi: 10.1038/nmeth.1923.

Lantermann, Alexandra B., Tobias Straub, Annelie Strålfors, Guo-Cheng Yuan, Karl Ekwall, and Philipp Korber. 2010. "Schizosaccharomyces Pombe Genome-Wide Nucleosome Mapping Reveals Positioning Mechanisms Distinct from Those of Saccharomyces Cerevisiae." *Nature Structural & Molecular Biology* 17(2):251–57. doi: 10.1038/nsmb.1741.

Larivière, Laurent, Clemens Plaschka, Martin Seizl, Larissa Wenzeck, Fabian Kurth, and Patrick Cramer. 2012. "Structure of the Mediator Head Module." *Nature* 492(7429):448–51. doi: 10.1038/nature11670.

Leão, Pedro, Mary E. Little, Kathryn E. Appler, Daphne Sahaya, Emily Aguilar-Pine, Kathryn Currie, Ilya J. Finkelstein, Valerie De Anda, and Brett J. Baker. 2023. "Asgard Archaea Defense Systems and Their Roles in the Origin of Immunity in Eukaryotes." 2023.09.13.557551.

Lee, Heng Chi, Shwu Shin Chang, Swati Choudhary, Antti P. Aalto, Mekhala Maiti, Dennis H. Bamford, and Yi Liu. 2009. "QiRNA Is a New Type of Small Interfering RNA Induced by DNA Damage." *Nature* 459(7244):274–77. doi: 10.1038/nature08041.

Lee, Heng-Chi, Antti P. Aalto, Qiuying Yang, Shwu-Shin Chang, Guocun Huang, Daniel Fisher, Joonseok Cha, Minna M. Poranen, Dennis H. Bamford, and Yi Liu. 2010. "The DNA/RNA-Dependent RNA Polymerase QDE-1 Generates Aberrant RNA and dsRNA for RNAi in a Process Requiring Replication Protein A and a DNA Helicase." *PLOS Biology* 8(10):e1000496. doi: 10.1371/journal.pbio.1000496.

Lee, Kyoo-young, Haiqing Fu, Mirit I. Aladjem, and Kyungjae Myung. 2012. "ATAD5 Regulates the Lifespan of DNA Replication Factories by Modulating PCNA Level on the Chromatin." *Journal of Cell Biology* 200(1):31–44. doi: 10.1083/jcb.201206084.

Lee, Suzanne R., Daniel A. Pollard, Domenico F. Galati, Megan L. Kelly, Brian Miller, Christina Mong, Megan N. Morris, Kerry Roberts-Nygren, Geoffrey M. Kapler, Matthew Zinkgraf, Hung Q. Dang, Erica Branham, Jason Sasser, Erin Tessier, Courtney Yoshiyama, Maya Matsumoto, and Gaea Turman. 2021. "Disruption of a ~23–24 Nucleotide Small RNA Pathway Elevates DNA Damage Responses in Tetrahymena Thermophila." *Molecular Biology of the Cell* 32(15):1335–46. doi: 10.1091/mbc.E20-10-0631.

Lee, Wei Ting C., Yandong Yin, Michael J. Morten, Peter Tonzi, Pam Pam Gwo, Diana C. Odermatt, Mauro Modesti, Sharon B. Cantor, Kerstin Gari, Tony T. Huang, and Eli Rothenberg. 2021. "Single-Molecule Imaging Reveals Replication Fork Coupled Formation of G-Quadruplex Structures Hinders Local Replication Stress Signaling." *Nature Communications* 12(1):2525. doi: 10.1038/s41467-021-22830-9.

Lee, Yong Woo, Rajika Arora, Harry Wischnewski, and Claus M. Azzalin. 2018. "TRF1 Participates in Chromosome End Protection by Averting TRF2-Dependent Telomeric R Loops." *Nature Structural & Molecular Biology* 25(2):147–53. doi: 10.1038/s41594-017-0021-5.

Lee, Young Sik, Kenji Nakahara, John W. Pham, Kevin Kim, Zhengying He, Erik J. Sontheimer, and Richard W. Carthew. 2004. "Distinct Roles for Drosophila Dicer-1 and Dicer-2 in the siRNA/miRNA Silencing Pathways." *Cell* 117(1):69–81. doi: 10.1016/S0092-8674(04)00261-2.

Lee, Youngsoo, Sachin Katyal, Susanna M. Downing, Jingfeng Zhao, Helen R. Russell, and Peter J. McKinnon. 2012. "Neurogenesis Requires TopBP1 to Prevent Catastrophic Replicative DNA Damage in Early Progenitors." *Nature Neuroscience* 15(6):819–26. doi: 10.1038/nn.3097.

Lee, Youngsoo, Erin RP Shull, Pierre-Olivier Frappart, Sachin Katyal, Vanessa Enriquez-Rios, Jingfeng Zhao, Helen R. Russell, Eric J. Brown, and Peter J. McKinnon. 2012. "ATR Maintains Select Progenitors during Nervous System Development." *The EMBO Journal* 31(5):1177–89. doi: 10.1038/emboj.2011.493.

Legros, Pénélope, Amélie Malapert, Sho Niinuma, Pascal Bernard, and Vincent Vanoosthuyse. 2014. "RNA Processing Factors Swd2.2 and Sen1 Antagonize RNA Pol III-Dependent Transcription and the Localization of Condensin at Pol III Genes." *PLOS Genetics* 10(11):e1004794. doi: 10.1371/journal.pgen.1004794.

Lesnik, Elena A., and Susan M. Freier. 1995. "Relative Thermodynamic Stability of DNA, RNA, and DNA:RNA Hybrid Duplexes: Relationship with Base Composition and Structure." *Biochemistry* 34(34):10807–15. doi: 10.1021/bi00034a013.

Lestini, Roxane, Zhenhong Duan, and Thorsten Allers. 2010. "The Archaeal Xpf/Mus81/FANCM Homolog Hef and the Holliday Junction Resolvase Hjc Define Alternative Pathways That Are Essential for Cell Viability in Haloferax Volcanii." *DNA Repair* 9(9):994–1002. doi: 10.1016/j.dnarep.2010.06.012.

Lewis, Jacob S., Lisanne M. Spenkelink, Grant D. Schauer, Flynn R. Hill, Roxanna E. Georgescu, Michael E. O'Donnell, and Antoine M. van Oijen. 2017. "Single-Molecule Visualization of *Saccharomyces Cerevisiae* Leading-Strand Synthesis Reveals Dynamic Interaction between MTC and the Replisome." *Proceedings of the National Academy of Sciences* 114(40):10630–35. doi: 10.1073/pnas.1711291114.

Li, Fei, Robert A. Martienssen, and W. Zacheus Cande. 2011. “Coordination of DNA Replication and Histone Modification by the Rik1-Dos2 Complex.” *Nature* 475(7355):244–48. doi: 10.1038/nature10161.

Li, Heng, Bob Handsaker, Alec Wysoker, Tim Fennell, Jue Ruan, Nils Homer, Gabor Marth, Goncalo Abecasis, Richard Durbin, and 1000 Genome Project Data Processing Subgroup. 2009. “The Sequence Alignment/Map Format and SAMtools.” *Bioinformatics* 25(16):2078–79. doi: 10.1093/bioinformatics/btp352.

Li, Min, Xiaohua Xu, Chou-Wei Chang, and Yilun Liu. 2020. “TRIM28 Functions as the SUMO E3 Ligase for PCNA in Prevention of Transcription Induced DNA Breaks.” *Proceedings of the National Academy of Sciences* 117(38):23588–96. doi: 10.1073/pnas.2004122117.

Li, Min, Xiaohua Xu, Chou-Wei Chang, Li Zheng, Binghui Shen, and Yilun Liu. 2018. “SUMO2 Conjugation of PCNA Facilitates Chromatin Remodeling to Resolve Transcription-Replication Conflicts.” *Nature Communications* 9(1):2706. doi: 10.1038/s41467-018-05236-y.

Li, Wentao, Kathiresan Selvam, Tengyu Ko, and Shisheng Li. 2014. “Transcription Bypass of DNA Lesions Enhances Cell Survival but Attenuates Transcription Coupled DNA Repair.” *Nucleic Acids Research* 42(21):13242–53. doi: 10.1093/nar/gku1150.

Lin, Yin C., and Jay D. Gralla. 2005. “Stimulation of the XPB ATP-Dependent Helicase by the Beta Subunit of TFIIE.” *Nucleic Acids Research* 33(9):3072–81. doi: 10.1093/nar/gki623.

Lin, Yunfu, Vincent Dion, and John H. Wilson. 2006. “Transcription Promotes Contraction of CAG Repeat Tracts in Human Cells.” *Nature Structural & Molecular Biology* 13(2):179–80. doi: 10.1038/nsmb1042.

Lindahl, Tomas. 1993. “Instability and Decay of the Primary Structure of DNA.” *Nature* 362(6422):709–15. doi: 10.1038/362709a0.

Linder, Tomas, and Claes M. Gustafsson. 2004. “The Soh1/MED31 Protein Is an Ancient Component of Schizosaccharomyces Pombe and Saccharomyces Cerevisiae Mediator*.” *Journal of Biological Chemistry* 279(47):49455–59. doi: 10.1074/jbc.M409046200.

Lippert, Malcolm J., Jennifer A. Freedman, Melissa A. Barber, and Sue Jinks-Robertson. 2004. “Identification of a Distinctive Mutation Spectrum Associated with High Levels of Transcription in Yeast.” *Molecular and Cellular Biology* 24(11):4801–9. doi: 10.1128/MCB.24.11.4801-4809.2004.

Lippert, Malcolm J., Nayun Kim, Jang-Eun Cho, Ryan P. Larson, Nathan E. Schoenly, Shannon H. O’Shea, and Sue Jinks-Robertson. 2011. “Role for Topoisomerase 1 in Transcription-Associated Mutagenesis in Yeast.” *Proceedings of the National Academy of Sciences* 108(2):698–703. doi: 10.1073/pnas.1012363108.

Lisitskaya, Lidiya, Yeonoh Shin, Aleksei Agapov, Anna Olina, Ekaterina Kropocheva, Sergei Ryazansky, Alexei A. Aravin, Daria Esyunina, Katsuhiko S. Murakami, and Andrey Kulbachinskiy. 2022. “Programmable RNA Targeting by Bacterial Argonaute Nucleases with Unconventional Guide Binding and Cleavage Specificity.” *Nature Communications* 13(1):4624. doi: 10.1038/s41467-022-32079-5.

Liu, B., M. L. Wong, and B. Alberts. 1994. “A Transcribing RNA Polymerase Molecule Survives DNA Replication without Aborting Its Growing RNA Chain.” *Proceedings of the National Academy of Sciences* 91(22):10660–64. doi: 10.1073/pnas.91.22.10660.

Liu, Bin, and Bruce M. Alberts. 1995. “Head-on Collision between a DNA Replication Apparatus and RNA Polymerase Transcription Complex.” *Science* 267(5201):1131–37. doi: 10.1126/science.7855590.

Liu, Bin, Mei Lie Wong, Rachel L. Tinker, E. Peter Geiduschek, and Bruce M. Alberts. 1993. “The DNA Replication Fork Can Pass RNA Polymerase without Displacing the Nascent Transcript.” *Nature* 366(6450):33–39. doi: 10.1038/366033a0.

Liu, Chang, Ying Xin, Le Xu, Zhaokui Cai, Yuanchao Xue, Yong Liu, Daoxin Xie, Yule Liu, and Yijun Qi. 2018. “*Arabidopsis* ARGONAUTE 1 Binds Chromatin to Promote Gene Transcription in Response to Hormones and Stresses.” *Developmental Cell* 44(3):348-361.e7. doi: 10.1016/j.devcel.2017.12.002.

Liu, L. F., and J. C. Wang. 1987. “Supercoiling of the DNA Template during Transcription.” *Proceedings of the National Academy of Sciences* 84(20):7024–27. doi: 10.1073/pnas.84.20.7024.

Liu, Leroy F., Shyamal D. Desai, Tsai-Kun Li, Yong Mao, Mei Sun, and Sai-Peng Sim. 2000. “Mechanism of Action of Camptothecin.” *Annals of the New York Academy of Sciences* 922(1):1–10. doi: 10.1111/j.1749-6632.2000.tb07020.x.

Liu, Yang, Kira S. Makarova, Wen-Cong Huang, Yuri I. Wolf, Anastasia N. Nikolskaya, Xinxu Zhang, Mingwei Cai, Cui-Jing Zhang, Wei Xu, Zhuhua Luo, Lei Cheng, Eugene V. Koonin, and Meng Li. 2021. "Expanded Diversity of Asgard Archaea and Their Relationships with Eukaryotes." *Nature* 593(7860):553–57. doi: 10.1038/s41586-021-03494-3.

Lockhart, Arianna, Vanessa Borges Pires, Fabio Bento, Vanessa Kellner, Sarah Luke-Glaser, George Yakoub, Helle D. Ulrich, and Brian Luke. 2019. "RNase H1 and H2 Are Differentially Regulated to Process RNA-DNA Hybrids." *Cell Reports* 29(9):2890-2900.e5. doi: 10.1016/j.celrep.2019.10.108.

Long, Qilin, Zhichao Liu, and Monika Gullerova. 2021. "Sweet Melody or Jazz? Transcription Around DNA Double-Strand Breaks." *Frontiers in Molecular Biosciences* 8.

Lopes, Mariana, Sandra Louzada, Daniela Ferreira, Gabriela Veríssimo, Daniel Eleutério, Margarida Gama-Carvalho, and Raquel Chaves. 2023. "Human Satellite 1A Analysis Provides Evidence of Pericentromeric Transcription." *BMC Biology* 21(1):28. doi: 10.1186/s12915-023-01521-5.

Lopes, Massimo, Cecilia Cotta-Ramusino, Achille Pellicioli, Giordano Liberi, Paolo Plevani, Marco Muzi-Falconi, Carol S. Newlon, and Marco Foiani. 2001. "The DNA Replication Checkpoint Response Stabilizes Stalled Replication Forks." *Nature* 412(6846):557–61. doi: 10.1038/35087613.

Love, Michael I., Wolfgang Huber, and Simon Anders. 2014. "Moderated Estimation of Fold Change and Dispersion for RNA-Seq Data with DESeq2." *Genome Biology* 15(12):550. doi: 10.1186/s13059-014-0550-8.

Lu, Wei Ting, Ben R. Hawley, George L. Skalka, Robert A. Baldock, Ewan M. Smith, Aldo S. Bader, Michal Malewicz, Felicity Z. Watts, Ania Wilczynska, and Martin Bushell. 2018. "Drosha Drives the Formation of DNA:RNA Hybrids around DNA Break Sites to Facilitate DNA Repair." *Nature Communications* 9(1). doi: 10.1038/s41467-018-02893-x.

Lye, Lon-Fye, Katherine Owens, Huafang Shi, Silvane M. F. Murta, Ana Carolina Vieira, Salvatore J. Turco, Christian Tschudi, Elisabetta Ullu, and Stephen M. Beverley. 2010. "Retention and Loss of RNA Interference Pathways in Trypanosomatid Protozoans." *PLOS Pathogens* 6(10):e1001161. doi: 10.1371/journal.ppat.1001161.

Ma, Jin-Biao, Yu-Ren Yuan, Gunter Meister, Yi Pei, Thomas Tuschl, and Dinshaw J. Patel. 2005. "Structural Basis for 5′-End-Specific Recognition of Guide RNA by the A. Fulgidus Piwi Protein." *Nature* 434(7033):666–70. doi: 10.1038/nature03514.

Ma, Xiaolu, Tie-Shan Tang, and Caixia Guo. 2020. "Regulation of Translesion DNA Synthesis in Mammalian Cells." *Environmental and Molecular Mutagenesis* 61(7):680–92. doi: 10.1002/em.22359.

Macheret, Morgane, Rahul Bhowmick, Katarzyna Sobkowiak, Laura Padayachy, Jonathan Mailler, Ian D. Hickson, and Thanos D. Halazonetis. 2020. "High-Resolution Mapping of Mitotic DNA Synthesis Regions and Common Fragile Sites in the Human Genome through Direct Sequencing." *Cell Research* 30(11):997–1008. doi: 10.1038/s41422-020-0358-x.

Macheret, Morgane, and Thanos D. Halazonetis. 2018. "Intragenic Origins Due to Short G1 Phases Underlie Oncogene-Induced DNA Replication Stress." *Nature* 555(7694):112–16. doi: 10.1038/nature25507.

Machour, Feras E., and Nabieh Ayoub. 2020. "Transcriptional Regulation at DSBs: Mechanisms and Consequences." *Trends in Genetics* 36(12):981–97. doi: 10.1016/j.tig.2020.01.001.

Machwe, Amrita, Rajashree Karale, Xioahua Xu, Yilun Liu, and David K. Orren. 2011. "The Werner and Bloom Syndrome Proteins Help Resolve Replication Blockage by Converting (Regressed) Holliday Junctions to Functional Replication Forks." *Biochemistry* 50(32):6774–88. doi: 10.1021/bi2001054.

Machwe, Amrita, Enerlyn Lozada, Marc S. Wold, Guo-Min Li, and David K. Orren. 2011. "Molecular Cooperation between the Werner Syndrome Protein and Replication Protein A in Relation to Replication Fork Blockage *." *Journal of Biological Chemistry* 286(5):3497–3508. doi: 10.1074/jbc.M110.105411.

Machwe, Amrita, Liren Xiao, Joanna Groden, and David K. Orren. 2006. "The Werner and Bloom Syndrome Proteins Catalyze Regression of a Model Replication Fork." *Biochemistry* 45(47):13939–46. doi: 10.1021/bi0615487.

MacRae, I. J., Fei Li, K. Zhou, W. Zacheus Cande, and Jennifer A. Doudna. 2006. “Structure of Dicer and Mechanistic Implications for RNAi.” *Cold Spring Harbor Symposia on Quantitative Biology* 71:73–80. doi: 10.1101/sqb.2006.71.042.

Mahat, Dig Bijay, Hojoong Kwak, Gregory T. Booth, Iris H. Jonkers, Charles G. Danko, Ravi K. Patel, Colin T. Waters, Katie Munson, Leighton J. Core, and John T. Lis. 2016. “Base-Pair-Resolution Genome-Wide Mapping of Active RNA Polymerases Using Precision Nuclear Run-on (PRO-Seq).” *Nature Protocols* 11(8):1455–76. doi: 10.1038/nprot.2016.086.

Makarova, K. S., Y. I. Wolf, J. van der Oost, and E. V. Koonin. 2009. “Prokaryotic Homologs of Argonaute Proteins Are Predicted to Function as Key Components of a Novel System of Defense against Mobile Genetic Elements.” *Biology Direct* 4:29. doi: 10.1186/1745-6150-4-29.

Makarova, K. S., Y. I. Wolf, S. Snir, and E. V. Koonin. 2011. “Defense Islands in Bacterial and Archaeal Genomes and Prediction of Novel Defense Systems.” *Journal of Bacteriology* 193(21):6039–56. doi: 10.1128/JB.05535-11.

Makharashvili, Nodar, Sucheta Arora, Yizhi Yin, Qiong Fu, Xuemei Wen, Ji-Hoon Lee, Chung-Hsuan Kao, Justin WC Leung, Kyle M. Miller, and Tanya T. Paull. 2018. “Sae2/CtIP Prevents R-Loop Accumulation in Eukaryotic Cells” edited by A. Aguilera and J. K. Tyler. *eLife* 7:e42733. doi: 10.7554/eLife.42733.

Malagon, Francisco, Maria L. Kireeva, Brenda K. Shafer, Lucyna Lubkowska, Mikhail Kashlev, and Jeffrey N. Strathern. 2006. “Mutations in the Saccharomyces Cerevisiae RPB1 Gene Conferring Hypersensitivity to 6-Azauracil.” *Genetics* 172(4):2201–9. doi: 10.1534/genetics.105.052415.

Mangiameli, Sarah M., Christopher N. Merrikh, Paul A. Wiggins, and Houra Merrikh. 2017. “Transcription Leads to Pervasive Replisome Instability in Bacteria” edited by A. M. van Oijen. *eLife* 6:e19848. doi: 10.7554/eLife.19848.

Marabitti, Veronica, Giorgia Lillo, Eva Malacaria, Valentina Palermo, Massimo Sanchez, Pietro Pichierri, and Annapaola Franchitto. 2019. “ATM Pathway Activation Limits R-Loop-Associated Genomic Instability in Werner Syndrome Cells.” *Nucleic Acids Research* 47(7):3485–3502. doi: 10.1093/nar/gkz025.

Marasovic, Mirela, Manuel Zocco, and Mario Halic. 2013. “Argonaute and Triman Generate Dicer-Independent Prirnas and Mature siRNAs to Initiate Heterochromatin Formation.” *Molecular Cell* 52(2):173–83. doi: 10.1016/j.molcel.2013.08.046.

Marchal, Claire, Jiao Sima, and David M. Gilbert. 2019. “Control of DNA Replication Timing in the 3D Genome.” *Nature Reviews Molecular Cell Biology* 20(12):721–37. doi: 10.1038/s41580-019-0162-y.

Marlétaz, Ferdinand, Nataliya Timoshevskaya, Vladimir A. Timoshevskiy, Elise Parey, Oleg Simakov, Daria Gavriouchkina, Masakazu Suzuki, Kaoru Kubokawa, Sydney Brenner, Jeramiah J. Smith, and Daniel S. Rokhsar. 2024. “The Hagfish Genome and the Evolution of Vertebrates.” *Nature* 1–3. doi: 10.1038/s41586-024-07070-3.

Martienssen, Robert A., and Danesh Moazed. 2015. “RNAi and Heterochromatin Assembly.” *Cold Spring Harbor Perspectives in Biology* 7(8):a019323. doi: 10.1101/cshperspect.a019323.

Martin, Marcel. 2011. “Cutadapt Removes Adapter Sequences from High-Throughput Sequencing Reads.” *EMBnet.Journal* 17(1):10–12. doi: 10.14806/ej.17.1.200.

Mason, Jennifer M., Yuen Ling Chan, Ralph W. Weichselbaum, and Douglas K. Bishop. 2019. “Non-Enzymatic Roles of Human RAD51 at Stalled Replication Forks.” *Nature Communications* 10(1). doi: 10.1038/s41467-019-12297-0.

Masuda, Koji, Claire Renard-Guillet, Katsuhiko Shirahige, and Takashi Sutani. 2020. “Bioinformatical Dissection of Fission Yeast DNA Replication Origins.” *Open Biology* 10(7):200052. doi: 10.1098/rsob.200052.

Matos, Dominick A., Jia-min Zhang, Jian Ouyang, Hai Dang Nguyen, Marie-michelle Genois, and Lee Zou. 2019. “ATR Protects the Genome against R Loops through a MUS81-Triggered Feedback Loop.” *Molecular Cell* 1–14. doi: 10.1016/j.molcel.2019.10.010.

Matsui, Masayuki, Yongjun Chu, Huiying Zhang, Keith T. Gagnon, Sarfraz Shaikh, Satya Kuchimanchi, Muthiah Manoharan, David R. Corey, and Bethany A. Janowski. 2013. “Promoter RNA Links Transcriptional

Regulation of Inflammatory Pathway Genes." *Nucleic Acids Research* 41(22):10086–109. doi: 10.1093/nar/gkt777.

Mazina, Olga M., Havva Keskin, Kritika Hanamshet, Francesca Storici, and Alexander V. Mazin. 2017. "Rad52 Inverse Strand Exchange Drives RNA-Templated DNA Double-Strand Break Repair." *Molecular Cell* 67(1):19-29.e3. doi: 10.1016/j.molcel.2017.05.019.

McDevitt, Shane, Timur Rusanov, Tatiana Kent, Gurushankar Chandramouly, and Richard T. Pomerantz. 2018. "How RNA Transcripts Coordinate DNA Recombination and Repair." *Nature Communications* 9(1):1–10. doi: 10.1038/s41467-018-03483-7.

McInerney, Peter, and Mike O'Donnell. 2004. "Functional Uncoupling of Twin Polymerases: MECHANISM OF POLYMERASE DISSOCIATION FROM A LAGGING-STRAND BLOCK*." *Journal of Biological Chemistry* 279(20):21543–51. doi: 10.1074/jbc.M401649200.

McLean, Michael J., Kenneth H. Wolfe, and Kevin M. Devine. 1998. "Base Composition Skews, Replication Orientation, and Gene Orientation in 12 Prokaryote Genomes." *Journal of Molecular Evolution* 47(6):691–96. doi: 10.1007/PL00006428.

McStay, Brian, and Ingrid Grummt. 2008. "The Epigenetics of rRNA Genes: From Molecular to Chromosome Biology." *Annual Review of Cell and Developmental Biology* 24(1):131–57. doi: 10.1146/annurev.cellbio.24.110707.175259.

McVey, Mitch, Varandt Y. Khodaverdian, Damon Meyer, Paula Gonçalves Cerqueira, and Wolf-Dietrich Heyer. 2016. "Eukaryotic DNA Polymerases in Homologous Recombination." *Annual Review of Genetics* 50(1):393–421. doi: 10.1146/annurev-genet-120215-035243.

Meers, Chance, Havva Keskin, Gabor Banyai, Olga Mazina, Taehwan Yang, Alli L. Gombolay, Kuntal Mukherjee, Efiyenia I. Kaparos, Gary Newnam, Alexander Mazin, and Francesca Storici. 2020. "Genetic Characterization of Three Distinct Mechanisms Supporting RNA-Driven DNA Repair and Modification Reveals Major Role of DNA Polymerase ζ." *Molecular Cell* 1–14. doi: 10.1016/j.molcel.2020.08.011.

Mellone, Barbara G., and Daniele Fachinetti. 2021. "Diverse Mechanisms of Centromere Specification." *Current Biology* 31(22):R1491–1504. doi: 10.1016/j.cub.2021.09.083.

Merrikh, Christopher N., and Houra Merrikh. 2018. "Gene Inversion Potentiates Bacterial Evolvability and Virulence." *Nature Communications* 9(1):4662. doi: 10.1038/s41467-018-07110-3.

Mersaoui, Sofiane Y., Zhenbao Yu, Yan Coulombe, Martin Karam, Franciele F. Busatto, Jean-Yves Masson, and Stéphane Richard. 2019. "Arginine Methylation of the DDX5 Helicase RGG/RG Motif by PRMT5 Regulates Resolution of RNA:DNA Hybrids." *The EMBO Journal* 38(15):e100986. doi: 10.15252/embj.2018100986.

Meryet-Figuiere, Matthieu, Babak Alaei-Mahabadi, Mohamad Moustafa Ali, Sanhita Mitra, Santhilal Subhash, Gaurav Kumar Pandey, Erik Larsson, and Chandrasekhar Kanduri. 2014. "Temporal Separation of Replication and Transcription during S-Phase Progression." *Cell Cycle* 13(20):3241–48. doi: 10.4161/15384101.2014.953876.

Michalik, Katharina M., Romy Böttcher, and Klaus Förstemann. 2012. "A Small RNA Response at DNA Ends in Drosophila." *Nucleic Acids Research* 40(19):9596–9603. doi: 10.1093/nar/gks711.

Michelini, Flavia, Sethuramasundaram Pitchiaya, Valerio Vitelli, Sheetal Sharma, Ubaldo Gioia, Fabio Pessina, Matteo Cabrini, Yejun Wang, Ilaria Capozzo, Fabio Iannelli, Valentina Matti, Sofia Francia, G. V. Shivashankar, Nils G. Walter, and Fabrizio d'Adda di Fagagna. 2017. "Damage-Induced lncRNAs Control the DNA Damage Response through Interaction with DDRNAs at Individual Double-Strand Breaks." *Nature Cell Biology* 19(12):1400–1411. doi: 10.1038/ncb3643.

Mijic, Sofija, Ralph Zellweger, Nagaraja Chappidi, Matteo Berti, Kurt Jacobs, Karun Mutreja, Sebastian Ursich, Arnab Ray Chaudhuri, Andre Nussenzweig, Pavel Janscak, and Massimo Lopes. 2017. "Replication Fork Reversal Triggers Fork Degradation in BRCA2-Defective Cells." *Nature Communications* 8(1):859. doi: 10.1038/s41467-017-01164-5.

Miki, Daisuke, Peiying Zhu, Wencan Zhang, Yanfei Mao, Zhengyan Feng, Huan Huang, Hui Zhang, Yanqiang Li, Renyi Liu, Huiming Zhang, Yijun Qi, and Jian-Kang Zhu. 2017. "Efficient Generation of diRNAs

Requires Components in the Posttranscriptional Gene Silencing Pathway." *Scientific Reports* 7(1):301. doi: 10.1038/s41598-017-00374-7.

Millán-Zambrano, Gonzalo, Adam Burton, Andrew J. Bannister, and Robert Schneider. 2022. "Histone Post-Translational Modifications — Cause and Consequence of Genome Function." *Nature Reviews Genetics* 23(9):563–80. doi: 10.1038/s41576-022-00468-7.

Mirkin, Ekaterina V., and Sergei M. Mirkin. 2005. "Mechanisms of Transcription-Replication Collisions in Bacteria." *Molecular and Cellular Biology* 25(3):888–95. doi: 10.1128/MCB.25.3.888-895.2005.

Mischo, Hannah E., Belén Gómez-González, Pawel Grzechnik, Ana G. Rondón, Wu Wei, Lars Steinmetz, Andrés Aguilera, and Nick J. Proudfoot. 2011. "Yeast Sen1 Helicase Protects the Genome from Transcription-Associated Instability." *Molecular Cell* 41(1):21–32. doi: 10.1016/j.molcel.2010.12.007.

Mochizuki, Kazufumi, and Martin A. Gorovsky. 2005. "A Dicer-like Protein in Tetrahymena Has Distinct Functions in Genome Rearrangement, Chromosome Segregation, and Meiotic Prophase." *Genes & Development* 19(1):77–89. doi: 10.1101/gad.1265105.

Morales, Julio C., Patricia Richard, Praveen L. Patidar, Edward A. Motea, Tuyen T. Dang, James L. Manley, and David A. Boothman. 2016. "XRN2 Links Transcription Termination to DNA Damage and Replication Stress." *PLOS Genetics* 12(7):e1006107. doi: 10.1371/journal.pgen.1006107.

Motamedi, Mohammad R., André Verdel, Serafin U. Colmenares, Scott A. Gerber, Steven P. Gygi, and Danesh Moazed. 2004. "Two RNAi Complexes, RITS and RDRC, Physically Interact and Localize to Noncoding Centromeric RNAs." *Cell* 119(6):789–802. doi: 10.1016/j.cell.2004.11.034.

Mugal, Carina F., Hans-Hennig von Grünberg, and Martin Peifer. 2009. "Transcription-Induced Mutational Strand Bias and Its Effect on Substitution Rates in Human Genes." *Molecular Biology and Evolution* 26(1):131–42. doi: 10.1093/molbev/msn245.

Mukherjee, Krishanu, Henry Campos, and Bryan Kolaczkowski. 2013. "Evolution of Animal and Plant Dicers: Early Parallel Duplications and Recurrent Adaptation of Antiviral RNA Binding in Plants." *Molecular Biology and Evolution* 30(3):627–41. doi: 10.1093/molbev/mss263.

Müller, Carolin A., Michael A. Boemo, Paolo Spingardi, Benedikt M. Kessler, Skirmantas Kriaucionis, Jared T. Simpson, and Conrad A. Nieduszynski. 2019. "Capturing the Dynamics of Genome Replication on Individual Ultra-Long Nanopore Sequence Reads." *Nature Methods* 16(5):429–36. doi: 10.1038/s41592-019-0394-y.

Muniz, Lisa, Estelle Nicolas, and Didier Trouche. 2021. "RNA Polymerase II Speed: A Key Player in Controlling and Adapting Transcriptome Composition." *The EMBO Journal* 40(15):e105740. doi: 10.15252/embj.2020105740.

Munoz-Galvan, S., C. Tous, M. G. Blanco, E. K. Schwartz, K. T. Ehmsen, S. C. West, W. D. Heyer, and Andrés Aguilera. 2012. "Distinct Roles of Mus81, Yen1, Slx1-Slx4, and Rad1 Nucleases in the Repair of Replication-Born Double-Strand Breaks by Sister Chromatid Exchange." *Molecular and Cellular Biology* 32(9):1592–1603. doi: 10.1128/mcb.00111-12.

Murray, Johanne M., Adam T. Watson, and Antony M. Carr. 2016. "Transformation of Schizosaccharomyces Pombe: Lithium Acetate/ Dimethyl Sulfoxide Procedure." *Cold Spring Harbor Protocols* 2016(4):pdb.prot090969. doi: 10.1101/pdb.prot090969.

Nakamura, Toru M., Li-Lin Du, Christophe Redon, and Paul Russell. 2004. "Histone H2A Phosphorylation Controls Crb2 Recruitment at DNA Breaks, Maintains Checkpoint Arrest, and Influences DNA Repair in Fission Yeast." *Molecular and Cellular Biology* 24(14):6215–30. doi: 10.1128/MCB.24.14.6215-6230.2004.

Nazer, Ezequiel, Ryan K. Dale, Madoka Chinen, Behram Radmanesh, and Elissa P. Lei. 2018. "Argonaute2 and LaminB Modulate Gene Expression by Controlling Chromatin Topology." *PLOS Genetics* 14(3):e1007276. doi: 10.1371/journal.pgen.1007276.

Nazer, Ezequiel, Ryan K. Dale, Cameron Palmer, and Elissa P. Lei. 2018. "Argonaute2 Attenuates Active Transcription by Limiting RNA Polymerase II Elongation in Drosophila Melanogaster." *Scientific Reports* 8(1):15685. doi: 10.1038/s41598-018-34115-1.

Nazer, Ezequiel, Luciana Gómez Acuña, and Alberto R. Kornblihtt. 2022. “Seeking the Truth behind the Myth: Argonaute Tales from ‘Nuclearland.’” *Molecular Cell* 82(3):503–13. doi: 10.1016/j.molcel.2021.11.005.

Neelsen, Kai J., and Massimo Lopes. 2015. “Replication Fork Reversal in Eukaryotes: From Dead End to Dynamic Response.” *Nature Reviews Molecular Cell Biology* 16(4):207–20. doi: 10.1038/nrm3935.

Nelson, Jonathan O., George J. Watase, Natalie Warsinger-Pepe, and Yukiko M. Yamashita. 2019. “Mechanisms of rDNA Copy Number Maintenance.” *Trends in Genetics* 35(10):734–42. doi: 10.1016/j.tig.2019.07.006.

Nicholson, Allen W. 2014. “Ribonuclease III Mechanisms of Double-Stranded RNA Cleavage.” *WIREs RNA* 5(1):31–48. doi: 10.1002/wrna.1195.

Nishino, Tatsuya, Kayoko Komori, Daisuke Tsuchiya, Yoshizumi Ishino, and Kosuke Morikawa. 2005. “Crystal Structure and Functional Implications of Pyrococcus Furiosus Hef Helicase Domain Involved in Branched DNA Processing.” *Structure* 13(1):143–53. doi: 10.1016/j.str.2004.11.008.

Noe Gonzalez, Melvin, Daniel Blears, and Jesper Q. Svejstrup. 2021. “Causes and Consequences of RNA Polymerase II Stalling during Transcript Elongation.” *Nature Reviews Molecular Cell Biology* 22(1):3–21. doi: 10.1038/s41580-020-00308-8.

Nogales, Eva, Robert K. Louder, and Yuan He. 2017. “Structural Insights into the Eukaryotic Transcription Initiation Machinery.” *Annual Review of Biophysics* 46:59–83. doi: 10.1146/annurev-biophys-070816-033751.

Noguchi, Eishi, Chiaki Noguchi, Li-Lin Du, and Paul Russell. 2003. “Swi1 Prevents Replication Fork Collapse and Controls Checkpoint Kinase Cds1.” *Molecular and Cellular Biology* 23(21):7861–74. doi: 10.1128/MCB.23.21.7861-7874.2003.

Noguchi, Eishi, Chiaki Noguchi, W. Hayes McDonald, John R. Yates III, and Paul Russell. 2004. “Swi1 and Swi3 Are Components of a Replication Fork Protection Complex in Fission Yeast.” *Molecular and Cellular Biology* 24(19):8342–55. doi: 10.1128/MCB.24.19.8342-8355.2004.

Noto, Tomoko, and Kazufumi Mochizuki. 2017. “Whats, Hows and Whys of Programmed DNA Elimination in Tetrahymena.” *Open Biology* 7(10):170172. doi: 10.1098/rsob.170172.

Nozawa, Kayo, Thomas R. Schneider, and Patrick Cramer. 2017. “Core Mediator Structure at 3.4 Å Extends Model of Transcription Initiation Complex.” *Nature* 545(7653):248–51. doi: 10.1038/nature22328.

Nudler, Evgeny. 2009. “RNA Polymerase Active Center: The Molecular Engine of Transcription.” *Annual Review of Biochemistry* 78(1):335–61. doi: 10.1146/annurev.biochem.76.052705.164655.

Obado, Samson O., Christopher Bot, Daniel Nilsson, Bjorn Andersson, and John M. Kelly. 2007. “Repetitive DNA Is Associated with Centromeric Domains in Trypanosoma Brucei but Not Trypanosoma Cruzi.” *Genome Biology* 8(3):R37. doi: 10.1186/gb-2007-8-3-r37.

Ohkuni, Kentaro, and Katsumi Kitagawa. 2011. “Endogenous Transcription at the Centromere Facilitates Centromere Activity in Budding Yeast.” *Current Biology* 21(20):1695–1703. doi: 10.1016/j.cub.2011.08.056.

Ohle, Corina, Rafael Tesorero, Géza Schermann, Nikolay Dobrev, Irmgard Sinning, and Tamás Fischer. 2016. “Transient RNA-DNA Hybrids Are Required for Efficient Double-Strand Break Repair.” *Cell* 167(4):1001-1013.e7. doi: 10.1016/j.cell.2016.10.001.

Olovnikov, Ivan, Ken Chan, Ravi Sachidanandam, Dianne K. Newman, and Alexei A. Aravin. 2013. “Bacterial Argonaute Samples the Transcriptome to Identify Foreign DNA.” *Molecular Cell* 51(5):594–605. doi: 10.1016/j.molcel.2013.08.014.

Onaka, Atsushi T., Naoko Toyofuku, Takahiro Inoue, Akiko K. Okita, Minami Sagawa, Jie Su, Takeshi Shitanda, Rei Matsuyama, Faria Zafar, Tatsuro S. Takahashi, Hisao Masukata, and Takuro Nakagawa. 2016. “Rad51 and Rad54 Promote Noncrossover Recombination between Centromere Repeats on the Same Chromatid to Prevent Isochromosome Formation.” *Nucleic Acids Research* 44(22):10744–57. doi: 10.1093/nar/gkw874.

Onishi, Ryo, Soichiro Yamanaka, and Mikiko C. Siomi. 2021. “piRNA- and siRNA-mediated Transcriptional Repression in Drosophila, Mice, and Yeast: New Insights and Biodiversity.” *EMBO Reports* 22(10):e53062. doi: 10.15252/embr.202153062.

Orsi, Guillermo A., Sivakanthan Kasinathan, Gabriel E. Zentner, Steven Henikoff, and Kami Ahmad. 2015. “Mapping Regulatory Factors by Immunoprecipitation from Native Chromatin.” *Current Protocols in Molecular Biology* 2015(April):21.31.1-21.31.25. doi: 10.1002/0471142727.mb2131s110.

Osman, Sara, and Patrick Cramer. 2020. “Structural Biology of RNA Polymerase II Transcription: 20 Years On.” *Annual Review of Cell and Developmental Biology* 36:1–34. doi: 10.1146/annurev-cellbio-042020-021954.

Osmundson, Joseph S., Jayashree Kumar, Rani Yeung, and Duncan J. Smith. 2017. “Pif1-Family Helicases Cooperatively Suppress Widespread Replication-Fork Arrest at tRNA Genes.” *Nature Structural & Molecular Biology* 24(2):162–70. doi: 10.1038/nsmb.3342.

Oya, Eriko, Hiroaki Kato, Yuji Chikashige, Chihiro Tsutsumi, Yasushi Hiraoka, and Yota Murakami. 2013. “Mediator Directs Co-Transcriptional Heterochromatin Assembly by RNA Interference-Dependent and -Independent Pathways.” *PLoS Genetics* 9(8). doi: 10.1371/journal.pgen.1003677.

Ozata, Deniz M., Ildar Gainetdinov, Ansgar Zoch, Dónal O’Carroll, and Phillip D. Zamore. 2019. “PIWI-Interacting RNAs: Small RNAs with Big Functions.” *Nature Reviews Genetics* 20(2):89–108. doi: 10.1038/s41576-018-0073-3.

Papadopoulos, Dimitrios, Daniel Solvie, Apoorva Baluapuri, Theresa Endres, Stefanie Anh Ha, Steffi Herold, Jacqueline Kalb, Celeste Giansanti, Christina Schülein-Völk, Carsten Patrick Ade, Cornelius Schneider, Abdallah Gaballa, Seychelle Vos, Utz Fischer, Matthias Dobbelstein, Elmar Wolf, and Martin Eilers. 2022. “MYCN Recruits the Nuclear Exosome Complex to RNA Polymerase II to Prevent Transcription-Replication Conflicts.” *Molecular Cell* 82(1):159-176.e12. doi: 10.1016/j.molcel.2021.11.002.

Parrilla-Castellar, Edgardo R., and Larry M. Karnitz. 2003. “Cut5 Is Required for the Binding of Atr and DNA Polymerase α to Genotoxin-Damaged Chromatin*.” *Journal of Biological Chemistry* 278(46):45507–11. doi: 10.1074/jbc.C300418200.

Patel, Jinal A., and Hyungjin Kim. 2023. “The TIMELESS Effort for Timely DNA Replication and Protection.” *Cellular and Molecular Life Sciences* 80(4):84. doi: 10.1007/s00018-023-04738-3.

Patro, Rob, Geet Duggal, Michael I. Love, Rafael A. Irizarry, and Carl Kingsford. 2017. “Salmon Provides Fast and Bias-Aware Quantification of Transcript Expression.” *Nature Methods* 14(4):417–19. doi: 10.1038/nmeth.4197.

Paul, Sandip, Samuel Million-Weaver, Sujay Chattopadhyay, Evgeni Sokurenko, and Houra Merrikh. 2013. “Accelerated Gene Evolution through Replication–Transcription Conflicts.” *Nature* 495(7442):512–15. doi: 10.1038/nature11989.

Pek, Jun Wei, and Toshie Kai. 2011. “DEAD-Box RNA Helicase Belle/DDX3 and the RNA Interference Pathway Promote Mitotic Chromosome Segregation.” *Proceedings of the National Academy of Sciences* 108(29):12007–12. doi: 10.1073/pnas.1106245108.

Peng, Jamy C., and Gary H. Karpen. 2007. “H3K9 Methylation and RNA Interference Regulate Nucleolar Organization and Repeated DNA Stability.” *Nature Cell Biology* 9(1):25–35. doi: 10.1038/ncb1514.

Petermann, Eva, Li Lan, and Lee Zou. 2022. “Sources, Resolution and Physiological Relevance of R-Loops and RNA–DNA Hybrids.” *Nature Reviews Molecular Cell Biology*. doi: 10.1038/s41580-022-00474-x.

Petryk, Nataliya, Malik Kahli, Yves d’Aubenton-Carafa, Yan Jaszczyszyn, Yimin Shen, Maud Silvain, Claude Thermes, Chun-Long Chen, and Olivier Hyrien. 2016. “Replication Landscape of the Human Genome.” *Nature Communications* 7(1):10208. doi: 10.1038/ncomms10208.

Picard, Franck, Jean-Charles Cadoret, Benjamin Audit, Alain Arneodo, Adriana Alberti, Christophe Battail, Laurent Duret, and Marie-Noelle Prioleau. 2014. “The Spatiotemporal Program of DNA Replication Is Associated with Specific Combinations of Chromatin Marks in Human Cells.” *PLOS Genetics* 10(5):e1004282. doi: 10.1371/journal.pgen.1004282.

Plaschka, C., M. Hantsche, C. Dienemann, C. Burzinski, J. Plitzko, and P. Cramer. 2016. “Transcription Initiation Complex Structures Elucidate DNA Opening.” *Nature* 533(7603):353–58. doi: 10.1038/nature17990.

Plaschka, C., L. Larivière, L. Wenzeck, M. Seizl, M. Hemann, D. Tegunov, E. V. Petrotchenko, C. H. Borchers, W. Baumeister, F. Herzog, E. Villa, and Patrick Cramer. 2015. “Architecture of the RNA Polymerase II-Mediator Core Initiation Complex.” *Nature* 518(7539):376–80. doi: 10.1038/nature14229.

Poli, Jérôme, Christian Benedikt Gerhold, Alessandro Tosi, Nicole Hustedt, Andrew Seeber, Ragna Sack, Franz Herzog, Philippe Pasero, Kenji Shimada, Karl Peter Hopfner, and Susan M. Gasser. 2016. “Mec1, INO80, and the PAF1 Complex Cooperate to Limit Transcription Replication Conflicts through RNAPII Removal during Replication Stress.” *Genes and Development* 30(3):337–54. doi: 10.1101/gad.273813.115.

Pomerantz, R. T., and Mike O’Donnell. 2010. “Direct Restart of a Replication Fork Stalled by a Head-On RNA Polymerase.” *Science* 327(5965):590–92. doi: 10.1126/science.1179595.

Pomerantz, Richard T., and Mike O’Donnell. 2008. “The Replisome Uses mRNA as a Primer after Colliding with RNA Polymerase.” *Nature* 456(7223):762–67. doi: 10.1038/nature07527.

Porrua, Odil, and Domenico Libri. 2013. “A Bacterial-like Mechanism for Transcription Termination by the Sen1p Helicase in Budding Yeast.” *Nature Structural & Molecular Biology* 20(7):884–91. doi: 10.1038/nsmb.2592.

Pourquier, Philippe, Li-Ming Ueng, Glenda Kohlhagen, Abhijit Mazumder, Malini Gupta, Kurt W. Kohn, and Yves Pommier. 1997. “Effects of Uracil Incorporation, DNA Mismatches, and Abasic Sites on Cleavage and Religation Activities of Mammalian Topoisomerase I*.” *Journal of Biological Chemistry* 272(12):7792–96. doi: 10.1074/jbc.272.12.7792.

Prado, Félix, and Andrés Aguilera. 2005. “Impairment of Replication Fork Progression Mediates RNA polII Transcription-Associated Recombination.” *EMBO Journal* 24(6):1267–76. doi: 10.1038/sj.emboj.7600602.

Prendergast, Lisa, Urszula L. McClurg, Rossitsa Hristova, Rolando Berlinguer-Palmini, Sarah Greener, Katie Veitch, Inmaculada Hernandez, Philippe Pasero, Daniel Rico, Jonathan M. G. Higgins, Anastas Gospodinov, and Manolis Papamichos-Chronakis. 2020. “Resolution of R-Loops by INO80 Promotes DNA Replication and Maintains Cancer Cell Proliferation and Viability.” *Nature Communications* 11(1):4534. doi: 10.1038/s41467-020-18306-x.

Prioleau, Marie-Noëlle, and David M. MacAlpine. 2016. “DNA Replication Origins—Where Do We Begin?” *Genes & Development* 30(15):1683–97. doi: 10.1101/gad.285114.116.

Promonet, Alexy, Ismaël Padioleau, Yaqun Liu, Lionel Sanz, Anna Biernacka, Anne Lyne Schmitz, Magdalena Skrzypczak, Amélie Sarrazin, Clément Mettling, Maga Rowicka, Krzysztof Ginalski, Frédéric Chedin, Chun Long Chen, Yea Lih Lin, and Philippe Pasero. 2020. “Topoisomerase 1 Prevents Replication Stress at R-Loop-Enriched Transcription Termination Sites.” *Nature Communications* 11(1):1–12. doi: 10.1038/s41467-020-17858-2.

Provost, Patrick, Rebecca A. Silverstein, David Dishart, Julian Walfridsson, Ingela Djupedal, Barbara Kniola, Anthony Wright, Bengt Samuelsson, Olof Rådmark, and Karl Ekwall. 2002. “Dicer Is Required for Chromosome Segregation and Gene Silencing in Fission Yeast Cells.” *Proceedings of the National Academy of Sciences of the United States of America* 99(26):16648–53. doi: 10.1073/pnas.212633199.

Pugliese, Giusj Monia, Federico Salaris, Valentina Palermo, Veronica Marabitti, Nicolò Morina, Alessandro Rosa, Annapaola Franchitto, and Pietro Pichierri. 2019. “Inducible SMARCAL1 Knockdown in iPSC Reveals a Link between Replication Stress and Altered Expression of Master Differentiation Genes.” *Disease Models & Mechanisms* 12(10):dmm039487. doi: 10.1242/dmm.039487.

Qiu, Chenxi, Huiyan Jin, Irina Vvedenskaya, Jordi Abante Llenas, Tingting Zhao, Indranil Malik, Alex M. Visbisky, Scott L. Schwartz, Ping Cui, Pavel Čabart, Kang Hoo Han, William K. M. Lai, Richard P. Metz, Charles D. Johnson, Sing-Hoi Sze, B. Franklin Pugh, Bryce E. Nickels, and Craig D. Kaplan. 2020. “Universal Promoter Scanning by Pol II during Transcription Initiation in Saccharomyces Cerevisiae.” *Genome Biology* 21(1):132. doi: 10.1186/s13059-020-02040-0.

Qiu, Shan, Guixing Jiang, Liping Cao, and Jun Huang. 2021. “Replication Fork Reversal and Protection.” *Frontiers in Cell and Developmental Biology* 9:670392. doi: 10.3389/fcell.2021.670392.

Quinlan, Aaron R., and Ira M. Hall. 2010. “BEDTools: A Flexible Suite of Utilities for Comparing Genomic Features.” *Bioinformatics* 26(6):841–42. doi: 10.1093/bioinformatics/btq033.

Ramírez, Fidel, Friederike Dündar, Sarah Diehl, Björn A. Grüning, and Thomas Manke. 2014. “deepTools: A Flexible Platform for Exploring Deep-Sequencing Data.” *Nucleic Acids Research* 42(W1):W187–91. doi: 10.1093/nar/gku365.

Reddy, Bharat D., Yu Wang, Lifang Niu, Emily C. Higuchi, Samuel B. Marguerat, Jürg Bähler, Gerald R. Smith, and Songtao Jia. 2011. “Elimination of a Specific Histone H3K14 Acetyltransferase Complex Bypasses the RNAi Pathway to Regulate Pericentric Heterochromatin Functions.” *Genes and Development* 25(3):214–19. doi: 10.1101/gad.1993611.

Redinbo, Matthew R., Lance Stewart, Peter Kuhn, James J. Champoux, and Wim G. J. Hol. 1998. “Crystal Structures of Human Topoisomerase I in Covalent and Noncovalent Complexes with DNA.” *Science* 279(5356):1504–13. doi: 10.1126/science.279.5356.1504.

Régnier, P., and M. Grunberg-Manago. 1990. “RNase III Cleavages in Non-Coding Leaders of Escherichia Coli Transcriptscontrol mRNA Stability and Genetic Expression.” *Biochimie* 72(11):825–34. doi: 10.1016/0300-9084(90)90192-J.

Remus, Dirk, Fabienne Beuron, Gökhan Tolun, Jack D. Griffith, Edward P. Morris, and John F. X. Diffley. 2009. “Concerted Loading of Mcm2–7 Double Hexamers around DNA during DNA Replication Origin Licensing.” *Cell* 139(4):719–30. doi: 10.1016/j.cell.2009.10.015.

Rengachari, Srinivasan, Sandra Schilbach, Shintaro Aibara, Christian Dienemann, and Patrick Cramer. 2021. “Structure of the Human Mediator–RNA Polymerase II Pre-Initiation Complex.” *Nature* 594(7861):129–33. doi: 10.1038/s41586-021-03555-7.

Reyes-Castro, Raisa A., Shin-Yu Chen, Jacob Seemann, Samrat T. Kundu, Don L. Gibbons, and Swathi Arur. 2023. “Phosphorylated Nuclear DICER1 Promotes Open Chromatin State and Lineage Plasticity of AT2 Tumor Cells in Lung Adenocarcinomas.” *Science Advances* 9(30):eadf6210. doi: 10.1126/sciadv.adf6210.

Reyes-Turcu, Francisca E., Ke Zhang, Martin Zofall, Eesin Chen, and Shiv I. S. Grewal. 2010. “Defects in RNA Quality Control Factors Reveal RNAi-Independent Nucleation of Heterochromatin.” *Nature Structural and Molecular Biology* 18(10):1132–38. doi: 10.1038/nsmb.2122.

Rhind, N., B. Furnari, and P. Russell. 1997. “Cdc2 Tyrosine Phosphorylation Is Required for the DNA Damage Checkpoint in Fission Yeast.” *Genes & Development* 11(4):504–11. doi: 10.1101/gad.11.4.504.

Richter, William F., Shraddha Nayak, Janet Iwasa, and Dylan J. Taatjes. 2022. “The Mediator Complex as a Master Regulator of Transcription by RNA Polymerase II.” *Nature Reviews Molecular Cell Biology* 23(11):732–49. doi: 10.1038/s41580-022-00498-3.

Rivosecchi, Julieta, Marc Larochelle, Camille Teste, Frédéric Grenier, Amélie Malapert, Emiliano P. Ricci, Pascal Bernard, François Bachand, and Vincent Vanoosthuyse. 2019. “Senataxin Homologue Sen1 Is Required for Efficient Termination of RNA Polymerase III Transcription.” *The EMBO Journal* 38(16):e101955. doi: 10.15252/embj.2019101955.

Rocha, Eduardo P. C., and Antoine Danchin. 2003. “Gene Essentiality Determines Chromosome Organisation in Bacteria.” *Nucleic Acids Research* 31(22):6570–77. doi: 10.1093/nar/gkg859.

Roche, Benjamin, Benoit Arcangioli, and Robert A. Martienssen. 2016. “RNA Interference Is Essential for Cellular Quiescence.” *Science* 354(6313). doi: 10.1126/science.aah5651.

Rogakou, Emmy P., Duane R. Pilch, Ann H. Orr, Vessela S. Ivanova, and William M. Bonner. 1998. “DNA Double-Stranded Breaks Induce Histone H2AX Phosphorylation on Serine 139 *.” *Journal of Biological Chemistry* 273(10):5858–68. doi: 10.1074/jbc.273.10.5858.

Roseaulin, Laura, Yoshiki Yamada, Yasuhiro Tsutsui, Paul Russell, Hiroshi Iwasaki, and Benoit Arcangioli. 2008. “Mus81 Is Essential for Sister Chromatid Recombination at Broken Replication Forks.” *The EMBO Journal* 27(9):1378–87. doi: 10.1038/emboj.2008.65.

Rougvie, Ann E., and John T. Lis. 1988. “The RNA Polymerase II Molecule at the 5′ End of the Uninduced Hsp70 Gene of D. Melanogaster Is Transcriptionally Engaged.” *Cell* 54(6):795–804. doi: 10.1016/S0092-8674(88)91087-2.

Ryazansky, Sergei, Andrey Kulbachinskiy, and Alexei A. Aravin. 2018. “The Expanded Universe of Prokaryotic Argonaute Proteins.” *mBio* 9(6):10.1128/mbio.01935-18. doi: 10.1128/mbio.01935-18.

Rzeszutek, Iwona, Xyrus X. Maurer-Alcalá, and Mariusz Nowacki. 2020. “Programmed Genome Rearrangements in Ciliates.” *Cellular and Molecular Life Sciences* 77(22):4615–29. doi: 10.1007/s00018-020-03555-2.

Saldivar, Joshua C., David Cortez, and Karlene A. Cimprich. 2017. “The Essential Kinase ATR: Ensuring Faithful Duplication of a Challenging Genome.” *Nature Reviews Molecular Cell Biology* 18(10):622–36. doi: 10.1038/nrm.2017.67.

Sale, Julian E. 2012. “Competition, Collaboration and Coordination – Determining How Cells Bypass DNA Damage.” *Journal of Cell Science* 125(7):1633–43. doi: 10.1242/jcs.094748.

Salgado, Paula S., Minni R. L. Koivunen, Eugene V. Makeyev, Dennis H. Bamford, David I. Stuart, and Jonathan M. Grimes. 2006. “The Structure of an RNAi Polymerase Links RNA Silencing and Transcription” edited by G. Petsko. *PLoS Biology* 4(12):e434. doi: 10.1371/journal.pbio.0040434.

Sankar, T. Sabari, Brigitta D. Wastuwidyaningtyas, Yuexin Dong, Sarah A. Lewis, and Jue D. Wang. 2016. “The Nature of Mutations Induced by Replication–Transcription Collisions.” *Nature* 535(7610):178–81. doi: 10.1038/nature18316.

Saponaro, Marco, Theodoros Kantidakis, Richard Mitter, Gavin P. Kelly, Mark Heron, Hannah Williams, Johannes Söding, Aengus Stewart, and Jesper Q. Svejstrup. 2014. “RECQL5 Controls Transcript Elongation and Suppresses Genome Instability Associated with Transcription Stress.” *Cell* 157(5):1037–49. doi: 10.1016/j.cell.2014.03.048.

Savić, D. J., and D. T. Kanazir. 1972. “The Effect of a Histidine Operator-Constitutive Mutation on UV-Induced Mutability within the Histidine Operon ofSalmonella Typhimurium.” *Molecular and General Genetics MGG* 118(1):45–50. doi: 10.1007/BF02428331.

Schauer, Grant D., Lisanne M. Spenkelink, Jacob S. Lewis, Olga Yurieva, Stefan H. Mueller, Antoine M. van Oijen, and Michael E. O’Donnell. 2020. “Replisome Bypass of a Protein-Based R-Loop Block by Pif1.” *Proceedings of the National Academy of Sciences* 117(48):30354–61. doi: 10.1073/pnas.2020189117.

Scherr, Matthias J., Syafiq Abd Wahab, Dirk Remus, and Karl E. Duderstadt. 2022. “Mobile Origin-Licensing Factors Confer Resistance to Conflicts with RNA Polymerase.” *Cell Reports* 38(12):110531. doi: 10.1016/j.celrep.2022.110531.

Schilbach, Sandra, Shintaro Aibara, Christian Dienemann, Frauke Grabbe, and Patrick Cramer. 2021. “Structure of RNA Polymerase II Pre-Initiation Complex at 2.9 Å Defines Initial DNA Opening.” *Cell* 184(15):4064-4072.e28. doi: 10.1016/j.cell.2021.05.012.

Schwer, Beate, Susanne Schneider, Yi Pei, Anna Aronova, and Stewart Shuman. 2009. “Characterization of the Schizosaccharomyces Pombe Spt5-Spt4 Complex.” *RNA* 15(7):1241–50. doi: 10.1261/rna.1572709.

Scully, Ralph, Arvind Panday, Rajula Elango, and Nicholas A. Willis. 2019. “DNA Double-Strand Break Repair-Pathway Choice in Somatic Mammalian Cells.” *Nature Reviews Molecular Cell Biology* 20(November). doi: 10.1038/s41580-019-0152-0.

Selby, Christopher P., Laura A. Lindsey-Boltz, Wentao Li, and Aziz Sancar. 2023. “Molecular Mechanisms of Transcription-Coupled Repair.” *Annual Review of Biochemistry* 92(1):115–44. doi: 10.1146/annurev-biochem-041522-034232.

Sessa, Gaetana, Belén Gómez-González, Sonia Silva, Carmen Pérez-Calero, Romane Beaurepere, Sonia Barroso, Sylvain Martineau, Charlotte Martin, Åsa Ehlén, Juan S. Martínez, Bérangère Lombard, Damarys Loew, Stephan Vagner, Andrés Aguilera, and Aura Carreira. 2021. “BRCA2 Promotes DNA-RNA Hybrid Resolution by DDX5 Helicase at DNA Breaks to Facilitate Their Repair‡.” *The EMBO Journal* 40(7):e106018. doi: 10.15252/embj.2020106018.

Shaaban, Salam A., Ekaterina V. Bobkova, David M. Chudzik, and Benjamin D. Hall. 1996. “In Vitro Analysis of Elongation and Termination by Mutant RNA Polymerases with Altered Termination Behavior.” *Molecular and Cellular Biology* 16(11):6468–76. doi: 10.1128/MCB.16.11.6468.

Shaaban, Salam A., Brent M. Krupp, and Benjamin D. Hall. 1995. “Termination-Altering Mutations in the Second-Largest Subunit of Yeast RNA Polymerase III.” *Molecular and Cellular Biology* 15(3):1467–78. doi: 10.1128/MCB.15.3.1467.

Shabalina, Svetlana A., and Eugene V. Koonin. 2008. “Origins and Evolution of Eukaryotic RNA Interference.” *Trends in Ecology and Evolution* 23(10):578–87. doi: 10.1016/j.tree.2008.06.005.

Shandilya, Jayasha, and Stefan G. E. Roberts. 2012. “The Transcription Cycle in Eukaryotes: From Productive Initiation to RNA Polymerase II Recycling.” *Biochimica et Biophysica Acta (BBA) - Gene Regulatory Mechanisms* 1819(5):391–400. doi: 10.1016/j.bbagrm.2012.01.010.

Shang, Wei-Hao, Tetsuya Hori, Atsushi Toyoda, Jun Kato, Kris Popendorf, Yasubumi Sakakibara, Asao Fujiyama, and Tatsuo Fukagawa. 2010. “Chickens Possess Centromeres with Both Extended Tandem Repeats and Short Non-Tandem-Repetitive Sequences.” *Genome Research* 20(9):1219–28. doi: 10.1101/gr.106245.110.

Sharma, Anupma, Thomas K. Wolfgruber, and Gernot G. Presting. 2013. “Tandem Repeats Derived from Centromeric Retrotransposons.” *BMC Genomics* 14(1):142. doi: 10.1186/1471-2164-14-142.

Sharma, Deepti, Amanda F. Say, LeAnna L. Ledford, Ami J. Hughes, Hilarie A. Sehorn, Donard S. Dwyer, and Michael G. Sehorn. 2013. “Role of the Conserved Lysine within the Walker A Motif of Human DMC1.” *DNA Repair* 12(1):53–62. doi: 10.1016/j.dnarep.2012.10.005.

Sheridan, R. M., N. Fong, A. D’Alessandro, and D. L. Bentley. 2019. “Widespread Backtracking by RNA Pol II Is a Major Effector of Gene Activation, 5′ Pause Release, Termination, and Transcription Elongation Rate.” *Molecular Cell* 73(1):107-118.e4. doi: 10.1016/j.molcel.2018.10.031.

Shimada, Atsushi, Jonathan Cahn, Evan Ernst, Jason Lynn, Daniel Grimanelli, Ian Henderson, Tetsuji Kakutani, and Robert A. Martienssen. 2023. *Retrotransposon Addiction Promotes Centromere Function via Epigenetically Activated Small RNAs*. *preprint*. Molecular Biology. doi: 10.1101/2023.08.02.551486.

Shimmoto, Michie, Seiji Matsumoto, Yukari Odagiri, Eishi Noguchi, Paul Russell, and Hisao Masai. 2009. “Interactions between Swi1-Swi3, Mrc1 and S Phase Kinase, Hsk1 May Regulate Cellular Responses to Stalled Replication Forks in Fission Yeast.” *Genes to Cells* 14(6):669–82. doi: 10.1111/j.1365-2443.2009.01300.x.

Shinohara, Akira, Hideyuki Ogawa, and Tomoko Ogawa. 1992. “Rad51 Protein Involved in Repair and Recombination in S. Cerevisiae Is a RecA-like Protein.” *Cell* 69(3):457–70. doi: 10.1016/0092-8674(92)90447-K.

Singh, Amanpreet, and Yong-Jie Xu. 2016. “The Cell Killing Mechanisms of Hydroxyurea.” *Genes* 7(11):99. doi: 10.3390/genes7110099.

Singh, Raushan K., McKenzie Jonely, Evan Leslie, Nick A. Rejali, Rodrigo Noriega, and Brenda L. Bass. 2021. “Transient Kinetic Studies of the Antiviral Drosophila Dicer-2 Reveal Roles of ATP in Self•nonself Discrimination.” *eLife* 10:1–24. doi: 10.7554/eLife.65810.

Sinha, Niladri K., Janet Iwasa, Peter S. Shen, and Brenda L. Bass. 2018. “Dicer Uses Distinct Modules for Recognizing dsRNA Termini.” *Science* 359(6373):329–34. doi: 10.1126/science.aaq0921.

Siow, Cheuk C., Sian R. Nieduszynska, Carolin A. Müller, and Conrad A. Nieduszynski. 2012. “OriDB, the DNA Replication Origin Database Updated and Extended.” *Nucleic Acids Research* 40(D1):D682–86. doi: 10.1093/nar/gkr1091.

Skourti-Stathaki, Konstantina, Nicholas J. Proudfoot, and Natalia Gromak. 2011. “Human Senataxin Resolves RNA/DNA Hybrids Formed at Transcriptional Pause Sites to Promote Xrn2-Dependent Termination.” *Molecular Cell* 42(6):794–805. doi: 10.1016/j.molcel.2011.04.026.

Smith, Jeramiah J., Vladimir A. Timoshevskiy, and Cody Saraceno. 2021. “Programmed DNA Elimination in Vertebrates.” *Annual Review of Animal Biosciences* 9(1):173–201. doi: 10.1146/annurev-animal-061220-023220.

Smits, Wiep Klaas, Houra Merrikh, Carla Yaneth Bonilla, and Alan D. Grossman. 2011. “Primosomal Proteins DnaD and DnaB Are Recruited to Chromosomal Regions Bound by DnaA in Bacillus Subtilis.” *Journal of Bacteriology* 193(3):640–48. doi: 10.1128/jb.01253-10.

Sollier, Julie, Caroline Townsend Stork, María L. García-Rubio, Renee D. Paulsen, Andrés Aguilera, and Karlene A. Cimprich. 2014. "Transcription-Coupled Nucleotide Excision Repair Factors Promote R-Loop-Induced Genome Instability." *Molecular Cell* 56(6):777–85. doi: 10.1016/j.molcel.2014.10.020.

Song, Chenlin, Agnes Hotz-Wagenblatt, Renate Voit, and Ingrid Grummt. 2017. "SIRT7 and the DEAD-Box Helicase DDX21 Cooperate to Resolve Genomic R Loops and Safeguard Genome Stability." *Genes & Development* 31(13):1370–81. doi: 10.1101/gad.300624.117.

Song, Ji-Joon, Stephanie K. Smith, Gregory J. Hannon, and Leemor Joshua-Tor. 2004. "Crystal Structure of Argonaute and Its Implications for RISC Slicer Activity." *Science* 305(5689):1434–37. doi: 10.1126/science.1102514.

Soutourina, Julie. 2018. "Transcription Regulation by the Mediator Complex." *Nature Reviews Molecular Cell Biology* 19(4):262–74. doi: 10.1038/nrm.2017.115.

Sparks, Justin L., Gheorghe Chistol, Alan O. Gao, Markus Räschle, Nicolai B. Larsen, Matthias Mann, Julien P. Duxin, and Johannes C. Walter. 2019. "The CMG Helicase Bypasses DNA-Protein Cross-Links to Facilitate Their Repair." *Cell* 176(1–2):167-181.e21. doi: 10.1016/j.cell.2018.10.053.

Sriramachandran, Annie M., Giuseppe Petrosino, María Méndez-Lago, Axel J. Schäfer, Liliana S. Batista-Nascimento, Nicola Zilio, and Helle D. Ulrich. 2020. "Genome-Wide Nucleotide-Resolution Mapping of DNA Replication Patterns, Single-Strand Breaks, and Lesions by GLOE-Seq." *Molecular Cell* 78(5):975-985.e7. doi: 10.1016/j.molcel.2020.03.027.

Srivastava, Rakesh, Rashmi Srivastava, and Seong Hoon Ahn. 2016. "The Epigenetic Pathways to Ribosomal DNA Silencing." *Microbiology and Molecular Biology Reviews* 80(3):545–63. doi: 10.1128/mmbr.00005-16.

Stein, Chad B., Andrew R. Field, Claudia A. Mimoso, ChenCheng Zhao, Kai-Lieh Huang, Eric J. Wagner, and Karen Adelman. 2022. "Integrator Endonuclease Drives Promoter-Proximal Termination at All RNA Polymerase II-Transcribed Loci." *Molecular Cell* 82(22):4232-4245.e11. doi: 10.1016/j.molcel.2022.10.004.

Stork, Caroline Townsend, Michael Bocek, Madzia P. Crossley, Julie Sollier, Lionel A. Sanz, Frédéric Chédin, Tomek Swigut, and Karlene A. Cimprich. 2016. "Co-Transcriptional R-Loops Are the Main Cause of Estrogen-Induced DNA Damage." *eLife* 5(AUGUST):1–21. doi: 10.7554/eLife.17548.

Sugiyama, Tomoyasu, Hugh P. Cam, Rie Sugiyama, Ken-ichi Noma, Martin Zofall, Ryuji Kobayashi, and Shiv I. S. Grewal. 2007. "SHREC, an Effector Complex for Heterochromatic Transcriptional Silencing." *Cell* 128(3):491–504. doi: 10.1016/j.cell.2006.12.035.

Sun, Cheng, Grace Wyngaard, D. Brian Walton, Holly A. Wichman, and Rachel Lockridge Mueller. 2014. "Billions of Basepairs of Recently Expanded, Repetitive Sequences Are Eliminated from the Somatic Genome during Copepod Development." *BMC Genomics* 15(1):186. doi: 10.1186/1471-2164-15-186.

Sung, Patrick. 1997. "Function of Yeast Rad52 Protein as a Mediator between Replication Protein A and the Rad51 Recombinase *." *Journal of Biological Chemistry* 272(45):28194–97. doi: 10.1074/jbc.272.45.28194.

Šviković, Saša, Alastair Crisp, Sue Mei Tan-Wong, Thomas A. Guilliam, Aidan J. Doherty, Nicholas J. Proudfoot, Guillaume Guilbaud, and Julian E. Sale. 2019. "R-loop Formation during S Phase Is Restricted by PrimPol-mediated Repriming." *The EMBO Journal* 38(3):e99793. doi: 10.15252/embj.201899793.

Swahari, Vijay, Ayumi Nakamura, Jeanette Baran-Gale, Idoia Garcia, Andrew J. Crowther, Robert Sons, Timothy R. Gershon, Scott Hammond, Praveen Sethupathy, and Mohanish Deshmukh. 2016. "Essential Function of Dicer in Resolving DNA Damage in the Rapidly Dividing Cells of the Developing and Malignant Cerebellum." *Cell Reports* 14(2):216–24. doi: 10.1016/j.celrep.2015.12.037.

Swahari, Vijay, Ayumi Nakamura, and Mohanish Deshmukh. 2016. "The Paradox of Dicer in Cancer." *Molecular & Cellular Oncology* 3(3):e1155006. doi: 10.1080/23723556.2016.1155006.

Swarts, Daan C., Matthijs M. Jore, Edze R. Westra, Yifan Zhu, Jorijn H. Janssen, Ambrosius P. Snijders, Yanli Wang, Dinshaw J. Patel, José Berenguer, Stan J. J. Brouns, and John van der Oost. 2014. "DNA-Guided DNA Interference by a Prokaryotic Argonaute." *Nature* 507(7491):258–61. doi: 10.1038/nature12971.

Swarts, Daan C., Kira Makarova, Yanli Wang, Kotaro Nakanishi, René F. Ketting, Eugene V. Koonin, Dinshaw J. Patel, and John van der Oost. 2014. "The Evolutionary Journey of Argonaute Proteins." *Nature Structural & Molecular Biology* 21(9):743–53. doi: 10.1038/nsmb.2879.

Takahashi, Diane T., Guenaelle Burguiere-Slezak, Patricia Auffret Van der Kemp, and Serge Boiteux. 2011. "Topoisomerase 1 Provokes the Formation of Short Deletions in Repeated Sequences upon High Transcription in Saccharomyces Cerevisiae." *Proceedings of the National Academy of Sciences* 108(2):692–97. doi: 10.1073/pnas.1012582108.

Talbert, Paul B., and Steven Henikoff. 2018. "Transcribing Centromeres: Noncoding RNAs and Kinetochore Assembly." *Trends in Genetics* 34(8):587–99. doi: 10.1016/j.tig.2018.05.001.

Talbert, Paul B., and Steven Henikoff. 2020. "What Makes a Centromere?" *Experimental Cell Research* 389(2):111895. doi: 10.1016/j.yexcr.2020.111895.

Tan, Jun, Xiangyu Wang, Laiyee Phoon, Haibo Yang, and Li Lan. 2020. "Resolution of ROS-Induced G-Quadruplexes and R-Loops at Transcriptionally Active Sites Is Dependent on BLM Helicase." *FEBS Letters* 594(9):1359–67. doi: 10.1002/1873-3468.13738.

Tang, Kai-Fu, Hong Ren, Jia Cao, Gui-Li Zeng, Jing Xie, Min Chen, Lu Wang, and Cai-Xia He. 2008. "Decreased Dicer Expression Elicits DNA Damage and Up-Regulation of MICA and MICB." *Journal of Cell Biology* 182(2):233–39. doi: 10.1083/jcb.200801169.

Tang, Wei, Margaret Dominska, Patricia W. Greenwell, Zachary Harvanek, Kirill S. Lobachev, Hyun-Min Kim, Vidhya Narayanan, Sergei M. Mirkin, and Thomas D. Petes. 2011. "Friedreich's Ataxia (GAA)N•(TTC)n Repeats Strongly Stimulate Mitotic Crossovers in Saccharomyces Cerevisae." *PLOS Genetics* 7(1):e1001270. doi: 10.1371/journal.pgen.1001270.

Taylor, Martin R. G., and Joseph T. P. Yeeles. 2018. "The Initial Response of a Eukaryotic Replisome to DNA Damage." *Molecular Cell* 70(6):1067-1080.e12. doi: 10.1016/j.molcel.2018.04.022.

Taylor, Martin R. G., and Joseph T. P. Yeeles. 2019. "Dynamics of Replication Fork Progression Following Helicase–Polymerase Uncoupling in Eukaryotes." *Journal of Molecular Biology* 431(10):2040–49. doi: 10.1016/j.jmb.2019.03.011.

Técher, Hervé, Stéphane Koundrioukoff, Dana Azar, Therese Wilhelm, Sandra Carignon, Olivier Brison, Michelle Debatisse, and Benoît Le Tallec. 2013. "Replication Dynamics: Biases and Robustness of DNA Fiber Analysis." *Journal of Molecular Biology* 425(23):4845–55. doi: 10.1016/j.jmb.2013.03.040.

Tehranchi, Ashley K., Matthew D. Blankschien, Yan Zhang, Jennifer A. Halliday, Anjana Srivatsan, Jia Peng, Christophe Herman, and Jue D. Wang. 2010. "The Transcription Factor DksA Prevents Conflicts between DNA Replication and Transcription Machinery." *Cell* 141(4):595–605. doi: 10.1016/j.cell.2010.03.036.

Teixeira-Silva, Ana, Anissia Ait Saada, Julien Hardy, Ismail Iraqui, Marina Charlotte Nocente, Karine Fréon, and Sarah A. E. Lambert. 2017. "The End-Joining Factor Ku Acts in the End-Resection of Double Strand Break-Free Arrested Replication Forks." *Nature Communications* 8(1). doi: 10.1038/s41467-017-02144-5.

Tercero, José Antonio, and John F. X. Diffley. 2001. "Regulation of DNA Replication Fork Progression through Damaged DNA by the Mec1/Rad53 Checkpoint." *Nature* 412(6846):553–57. doi: 10.1038/35087607.

Thakar, Tanay, and George-Lucian Moldovan. 2021. "The Emerging Determinants of Replication Fork Stability." *Nucleic Acids Research* 49(13):7224–38. doi: 10.1093/nar/gkab344.

Thangavel, Saravanabhavan, Matteo Berti, Maryna Levikova, Cosimo Pinto, Shivasankari Gomathinayagam, Marko Vujanovic, Ralph Zellweger, Hayley Moore, Eu Han Lee, Eric A. Hendrickson, Petr Cejka, Sheila Stewart, Massimo Lopes, and Alessandro Vindigni. 2015. "DNA2 Drives Processing and Restart of Reversed Replication Forks in Human Cells." *Journal of Cell Biology* 208(5):545–62. doi: 10.1083/jcb.201406100.

Theulot, Bertrand, Laurent Lacroix, Jean-Michel Arbona, Gael A. Millot, Etienne Jean, Corinne Cruaud, Jade Pellet, Florence Proux, Magali Hennion, Stefan Engelen, Arnaud Lemainque, Benjamin Audit, Olivier Hyrien, and Benoît Le Tallec. 2022. "Genome-Wide Mapping of Individual Replication Fork Velocities Using Nanopore Sequencing." *Nature Communications* 13(1):3295. doi: 10.1038/s41467-022-31012-0.

Thorsen, Michael, Heidi Hansen, Michela Venturi, Steen Holmberg, and Genevieve Thon. 2012. "Mediator Regulates Non-Coding RNA Transcription at Fission Yeast Centromeres." *Epigenetics and Chromatin* 5(1):1–10. doi: 10.1186/1756-8935-5-19.

Timoshevskiy, Vladimir A., Joseph R. Herdy, Melissa C. Keinath, and Jeramiah J. Smith. 2016. "Cellular and Molecular Features of Developmentally Programmed Genome Rearrangement in a Vertebrate (Sea Lamprey: Petromyzon Marinus)." *PLOS Genetics* 12(6):e1006103. doi: 10.1371/journal.pgen.1006103.

Tirman, Stephanie, Emily Cybulla, Annabel Quinet, Alice Meroni, and Alessandro Vindigni. 2021. "PRIMPOL Ready, Set, Reprime!" *Critical Reviews in Biochemistry and Molecular Biology* 56(1):17–30. doi: 10.1080/10409238.2020.1841089.

Torres, Jorge Z., Jessica B. Bessler, and Virginia A. Zakian. 2004. "Local Chromatin Structure at the Ribosomal DNA Causes Replication Fork Pausing and Genome Instability in the Absence of the S. Cerevisiae DNA Helicase Rrm3p." *Genes & Development* 18(5):498–503. doi: 10.1101/gad.1154704.

Torri, Alessandro, Johannes Jaeger, Thomas Pradeu, and Maria-Carla Saleh. 2022. "The Origin of RNA Interference: Adaptive or Neutral Evolution?" *PLOS Biology* 20(6):e3001715. doi: 10.1371/journal.pbio.3001715.

Toubiana, Shir, and Sara Selig. 2018. "DNA:RNA Hybrids at Telomeres – When It Is Better to Be out of the (R) Loop." *The FEBS Journal* 285(14):2552–66. doi: 10.1111/febs.14464.

Tourrière, Hélène, Gwennaëlle Versini, Violeta Cordón-Preciado, Constance Alabert, and Philippe Pasero. 2005. "Mrc1 and Tof1 Promote Replication Fork Progression and Recovery Independently of Rad53." *Molecular Cell* 19(5):699–706. doi: 10.1016/j.molcel.2005.07.028.

Tuduri, Sandie, Laure Crabbé, Chiara Conti, Hélène Tourrière, Heidi Holtgreve-Grez, Anna Jauch, Véronique Pantesco, John De Vos, Aubin Thomas, Charles Theillet, Yves Pommier, Jamal Tazi, Arnaud Coquelle, and Philippe Pasero. 2009. "Topoisomerase I Suppresses Genomic Instability by Preventing Interference between Replication and Transcription." *Nature Cell Biology* 11(11):1315–24. doi: 10.1038/ncb1984.

Uchino, Satoshi, Yuma Ito, Yuko Sato, Tetsuya Handa, Yasuyuki Ohkawa, Makio Tokunaga, and Hiroshi Kimura. 2021. "Live Imaging of Transcription Sites Using an Elongating RNA Polymerase II–Specific Probe." *Journal of Cell Biology* 221(2):e202104134. doi: 10.1083/jcb.202104134.

Uhlmann, Frank. 2016. "SMC Complexes: From DNA to Chromosomes." *Nature Reviews Molecular Cell Biology* 17(7):399–412. doi: 10.1038/nrm.2016.30.

Ünsal-Kaçmaz, Keziban, Paul D. Chastain, Ping-Ping Qu, Parviz Minoo, Marila Cordeiro-Stone, Aziz Sancar, and William K. Kaufmann. 2007. "The Human Tim/Tipin Complex Coordinates an Intra-S Checkpoint Response to UV That Slows Replication Fork Displacement." *Molecular and Cellular Biology* 27(8):3131–42. doi: 10.1128/MCB.02190-06.

Urban, Vaclav, Jana Dobrovolna, Daniela Hühn, Jana Fryzelkova, Jiri Bartek, and Pavel Janscak. 2016. "RECQ5 Helicase Promotes Resolution of Conflicts between Replication and Transcription in Human Cells." *Journal of Cell Biology* 214(4):401–15. doi: 10.1083/jcb.201507099.

Van, Christopher, Shan Yan, W. Matthew Michael, Shou Waga, and Karlene A. Cimprich. 2010. "Continued Primer Synthesis at Stalled Replication Forks Contributes to Checkpoint Activation." *Journal of Cell Biology* 189(2):233–46. doi: 10.1083/jcb.200909105.

Van Hooser, Aaron A., Ilia I. Ouspenski, Heather C. Gregson, Daniel A. Starr, Tim J. Yen, Michael L. Goldberg, Kyoko Yokomori, William C. Earnshaw, Kevin F. Sullivan, and B. R. Brinkley. 2001. "Specification of Kinetochore-Forming Chromatin by the Histone H3 Variant CENP-A." *Journal of Cell Science* 114(19):3529–42. doi: 10.1242/jcs.114.19.3529.

Varon, Mor, Daniel Dovrat, Jonathan Heuzé, Ioannis Tsirkas, Saurabh P. Singh, Philippe Pasero, Roberto Galletto, and Amir Aharoni. 2023. "Rrm3 and Pif1 Division of Labor during Replication through Leading and Lagging Strand G-Quadruplex." *Nucleic Acids Research* gkad1205. doi: 10.1093/nar/gkad1205.

Verdel, André, Songtao Jia, Scott Gerber, Tomoyasu Sugiyama, Steven Gygi, Shiv I. S. Grewal, and Danesh Moazed. 2004. "RNAi-Mediated Targeting of Heterochromatin by the RITS Complex." *Science* 303(5658):672–76. doi: 10.1126/science.1093686.

Voelkel-Meiman, Karen, Ralph L. Keil, and G. Shirleen Roeder. 1987. “Recombination-Stimulating Sequences in Yeast Ribosomal DNA Correspond to Sequences Regulating Transcription by RNA Polymerase I.” *Cell* 48(6):1071–79. doi: 10.1016/0092-8674(87)90714-8.

Volpe, Thomas A., Catherine Kidner, Ira M. Hall, Grace Teng, Shiv I. S. Grewal, and Robert A. Martienssen. 2002. “Regulation of Heterochromatic Silencing and Histone H3 Lysine-9 Methylation by RNAi.” *Science* 297(5588):1833–37. doi: 10.1126/science.1074973.

Volpe, Tom, Vera Schramke, Georgina L. Hamilton, Sharon A. White, Grace Teng, Robert A. Martienssen, and Robin C. Allshire. 2003. “RNA Interference Is Required for Normal Centromere Function Infission Yeast.” *Chromosome Research* 11(2):137–46. doi: 10.1023/A:1022815931524.

Vujanovic, Marko, Jana Krietsch, Maria Chiara Raso, Nastassja Terraneo, Ralph Zellweger, Jonas A. Schmid, Angelo Taglialatela, Jen Wei Huang, Cory L. Holland, Katharina Zwicky, Raquel Herrador, Heinz Jacobs, David Cortez, Alberto Ciccia, Lorenza Penengo, and Massimo Lopes. 2017. “Replication Fork Slowing and Reversal upon DNA Damage Require PCNA Polyubiquitination and ZRANB3 DNA Translocase Activity.” *Molecular Cell* 67(5):882-890.e5. doi: 10.1016/j.molcel.2017.08.010.

Wahba, Lamia, Loren Hansen, and Andrew Z. Fire. 2021. “An Essential Role for the piRNA Pathway in Regulating the Ribosomal RNA Pool in C. Elegans.” *Developmental Cell* 56(16):2295-2312.e6. doi: 10.1016/j.devcel.2021.07.014.

Wang, Dong, David A. Bushnell, Xuhui Huang, Kenneth D. Westover, Michael Levitt, and Roger D. Kornberg. 2009. “Structural Basis of Transcription: Backtracked RNA Polymerase II at 3.4 Angstrom Resolution.” *Science* 324(5931):1203–6. doi: 10.1126/science.1168729.

Wansink, Derick G., Erik E. M. Manders, Ineke van der Kraan, Jacob A. Aten, Roel van Driel, and Luitzen de Jong. 1994. “RNA Polymerase II Transcription Is Concentrated Outside Replication Domains throughout S-Phase.” *Journal of Cell Science* 107(6):1449–56. doi: 10.1242/jcs.107.6.1449.

Washburn, Robert S., and Max E. Gottesman. 2011. “Transcription Termination Maintains Chromosome Integrity.” *Proceedings of the National Academy of Sciences of the United States of America* 108(2):792–97. doi: 10.1073/pnas.1009564108.

Watanabe, Tomomichi, Kazuhiro Hayashi, Aki Tanaka, Tadashi Furumoto, Fumio Hanaoka, and Yoshiaki Ohkuma. 2003. “The Carboxy Terminus of the Small Subunit of TFIIE Regulates the Transition from Transcription Initiation to Elongation by RNA Polymerase II.” *Molecular and Cellular Biology* 23(8):2914–26. doi: 10.1128/MCB.23.8.2914-2926.2003.

Watase, George J., and Yukiko M. Yamashita. 2024. “RNA Polymerase II-Mediated rDNA Transcription Mediates rDNA Copy Number Expansion in Drosophila.” 2024.01.11.575146.

Wei, Wei, Zhaoqing Ba, Min Gao, Yang Wu, Yanting Ma, Simon Amiard, Charles I. White, Jannie Michaela Rendtlew Danielsen, Yun Gui Yang, and Yijun Qi. 2012. “A Role for Small RNAs in DNA Double-Strand Break Repair.” *Cell* 149(1):101–12. doi: 10.1016/j.cell.2012.03.002.

Wei, Xiangyun, Jagath Samarabandu, Rakendu S. Devdhar, Alan J. Siegel, Raj Acharya, and Ronald Berezney. 1998. “Segregation of Transcription and Replication Sites Into Higher Order Domains.” *Science* 281(5382):1502–5. doi: 10.1126/science.281.5382.1502.

Welsh, Sarah A., and Alessandro Gardini. 2023. “Genomic Regulation of Transcription and RNA Processing by the Multitasking Integrator Complex.” *Nature Reviews Molecular Cell Biology* 24(3):204–20. doi: 10.1038/s41580-022-00534-2.

Wendte, Jered M., and Craig S. Pikaard. 2017. “The RNAs of RNA-Directed DNA Methylation.” *Biochimica et Biophysica Acta (BBA) - Gene Regulatory Mechanisms* 1860(1):140–48. doi: 10.1016/j.bbagrm.2016.08.004.

Werner, Marcel, and Stephan Hamperl. 2024. “A Quick Restart: RNA Polymerase Jumping onto Post-Replicative Chromatin.” *Molecular Cell* 84(2):186–88. doi: 10.1016/j.molcel.2023.12.029.

Whitby, Matthew C. 2010. “The FANCM Family of DNA Helicases/Translocases.” *DNA Repair* 9(3):224–36. doi: 10.1016/j.dnarep.2009.12.012.

White, Eleanor, Margarita Schlackow, Kinga Kamieniarz-Gdula, Nicholas J. Proudfoot, and Monika Gullerova. 2014. “Human Nuclear Dicer Restricts the Deleterious Accumulation of Endogenous Double-Stranded RNA.” *Nature Structural and Molecular Biology* 21(6):552–59. doi: 10.1038/nsmb.2827.

White, Malcolm F., and Thorsten Allers. 2018. “DNA Repair in the Archaea—an Emerging Picture.” *FEMS Microbiology Reviews* 42(4):514–26. doi: 10.1093/femsre/fuy020.

Williams, Jessica S., Scott A. Lujan, and Thomas A. Kunkel. 2016. “Processing Ribonucleotides Incorporated during Eukaryotic DNA Replication.” *Nature Reviews Molecular Cell Biology* 17(6):350–63. doi: 10.1038/nrm.2016.37.

Williams, Tom A., Peter G. Foster, Cymon J. Cox, and T. Martin Embley. 2013. “An Archaeal Origin of Eukaryotes Supports Only Two Primary Domains of Life.” *Nature* 504(7479):231–36. doi: 10.1038/nature12779.

Wilson, Thomas E., Martin F. Arlt, So Hae Park, Sountharia Rajendran, Michelle Paulsen, Mats Ljungman, and Thomas W. Glover. 2015. “Large Transcription Units Unify Copy Number Variants and Common Fragile Sites Arising under Replication Stress.” *Genome Research* 25(2):189–200. doi: 10.1101/gr.177121.114.

Winston, Fred. 2008. “EMS and UV Mutagenesis in Yeast.” *Current Protocols in Molecular Biology* 82(1):13.3B.1-13.3B.5. doi: 10.1002/0471142727.mb1303bs82.

Wu, Yuliang, Kazuo Shin-ya, and Robert M. Brosh Jr. 2008. “FANCJ Helicase Defective in Fanconia Anemia and Breast Cancer Unwinds G-Quadruplex DNA To Defend Genomic Stability.” *Molecular and Cellular Biology* 28(12):4116–28. doi: 10.1128/MCB.02210-07.

Wyatt, Haley D. M., and Stephen C. West. 2014. “Holliday Junction Resolvases.” *Cold Spring Harbor Perspectives in Biology* 6(9):a023192–a023192. doi: 10.1101/cshperspect.a023192.

Xie, Ying, Minying Zheng, Xinlei Chu, Yue Chen, Huisha Xu, Jiawei Wang, Hao Zhou, and Jiafu Long. 2018. “Paf1 and Ctr9 Subcomplex Formation Is Essential for Paf1 Complex Assembly and Functional Regulation.” *Nature Communications* 9(1). doi: 10.1038/s41467-018-06237-7.

Xu, Congling, Chengyu Li, Jiwei Chen, Yan Xiong, Zhibin Qiao, Pengyu Fan, Conghui Li, Shuangyu Ma, Jin Liu, Aixia Song, Bolin Tao, Tao Xu, Wei Xu, Yayun Chi, Jingyan Xue, Pu Wang, Dan Ye, Hongzhou Gu, Peng Zhang, Qiong Wang, Ruijing Xiao, Jingdong Cheng, Hai Zheng, Xiaoli Yu, Zhen Zhang, Jiong Wu, Kaiwei Liang, Yan-Jun Liu, Huasong Lu, and Fei Xavier Chen. 2023. “R-Loop Dependent Promoter-Proximal Termination Ensures Genome Stability.” *Nature* 1–3. doi: 10.1038/s41586-023-06515-5.

Xu, Peng, Chengmin Li, Zhihong Chen, Shuanying Jiang, Shilong Fan, Jiawei Wang, Junbiao Dai, Ping Zhu, and Zhucheng Chen. 2016. “The NuA4 Core Complex Acetylates Nucleosomal Histone H4 through a Double Recognition Mechanism.” *Molecular Cell* 63(6):965–75. doi: 10.1016/j.molcel.2016.07.024.

Yadav, Vikas, Sheng Sun, R. Blake Billmyre, Bhagya C. Thimmappa, Terrance Shea, Robert Lintner, Guus Bakkeren, Christina A. Cuomo, Joseph Heitman, and Kaustuv Sanyal. 2018. “RNAi Is a Critical Determinant of Centromere Evolution in Closely Related Fungi.” *Proceedings of the National Academy of Sciences* 115(12):3108–13. doi: 10.1073/pnas.1713725115.

Yan, Qingqing, and Kavitha Sarma. 2020. “MapR: A Method for Identifying Native R-Loops Genome Wide.” *Current Protocols in Molecular Biology* 130(1):1–12. doi: 10.1002/cpmb.113.

Yan, Qingqing, Emily J. Shields, Roberto Bonasio, and Kavitha Sarma. 2019. “Mapping Native R-Loops Genome-Wide Using a Targeted Nuclease Approach.” *Cell Reports* 29(5):1369-1380.e5. doi: 10.1016/j.celrep.2019.09.052.

Yang, Chen, and Alfred S. Ponticelli. 2012. “Evidence That RNA Polymerase II and Not TFIIB Is Responsible for the Difference in Transcription Initiation Patterns between Saccharomyces Cerevisiae and Schizosaccharomyces Pombe.” *Nucleic Acids Research* 40(14):6495–6507. doi: 10.1093/nar/gks323.

Yang, Qiuying, Qiaohong Anne Ye, and Yi Liu. 2015. “Mechanism of siRNA Production from Repetitive DNA.” *Genes and Development* 29(5):526–37. doi: 10.1101/gad.255828.114.

Yang, Shizhuo, Lacey Winstone, Sohaumn Mondal, and Yuliang Wu. 2023. “Helicases in R-Loop Formation and Resolution.” *Journal of Biological Chemistry* 299(11):105307. doi: 10.1016/j.jbc.2023.105307.

Yeeles, Joseph T. P., and K. J. Marians. 2011. “The Escherichia Coli Replisome Is Inherently DNA Damage Tolerant.” *Science* 334(6053):235–38. doi: 10.1126/science.1209111.

Yeeles, Joseph T. P., and Kenneth J. Marians. 2013. “Dynamics of Leading-Strand Lesion Skipping by the Replisome.” *Molecular Cell* 52(6):855–65. doi: 10.1016/j.molcel.2013.10.020.

Yeung, Rani, and Duncan J. Smith. 2020. “Determinants of Replication-Fork Pausing at tRNA Genes in Saccharomyces Cerevisiae.” *Genetics* 214(4):825–38. doi: 10.1534/genetics.120.303092.

Yu, Yang, Jing Yi Ren, Jia-min Zhang, Fang Suo, Xiao Feng Fang, Fan Wu, and Li Lin Du. 2013. “A Proteome-Wide Visual Screen Identifies Fission Yeast Proteins Localizing to DNA Double-Strand Breaks.” *DNA Repair* 12(6):433–43. doi: 10.1016/j.dnarep.2013.04.001.

Zapletal, David, Eliska Taborska, Josef Pasulka, Radek Malik, Karel Kubicek, Martina Zanova, Christian Much, Marek Sebesta, Valeria Buccheri, Filip Horvat, Irena Jenickova, Michaela Prochazkova, Jan Prochazka, Matyas Pinkas, Jiri Novacek, Diego F. Joseph, Radislav Sedlacek, Carrie Bernecky, Dónal O’Carroll, Richard Stefl, and Petr Svoboda. 2022. “Structural and Functional Basis of Mammalian microRNA Biogenesis by Dicer.” *Molecular Cell* 82(21):4064-4079.e13. doi: 10.1016/j.molcel.2022.10.010.

Zaratiegui, Mikel, Stephane E. Castel, Danielle V. Irvine, Anna Kloc, Jie Ren, Fei Li, Elisa De Castro, Laura Marín, An Yun Chang, Derek Goto, W. Zacheus Cande, Francisco Antequera, Benoit Arcangioli, and Robert A. Martienssen. 2011. “RNAi Promotes Heterochromatic Silencing through Replication-Coupled Release of RNA Pol II.” *Nature* 479(7371):135–38. doi: 10.1038/nature10501.

Zaremba, Mindaugas, Donata Dakineviciene, Edvardas Golovinas, Evelina Zagorskaitė, Edvinas Stankunas, Anna Lopatina, Rotem Sorek, Elena Manakova, Audrone Ruksenaite, Arunas Silanskas, Simonas Asmontas, Algirdas Grybauskas, Ugne Tylenyte, Edvinas Jurgelaitis, Rokas Grigaitis, Kęstutis Timinskas, Česlovas Venclovas, and Virginijus Siksnys. 2022. “Short Prokaryotic Argonautes Provide Defence against Incoming Mobile Genetic Elements through NAD+ Depletion.” *Nature Microbiology* 7(11):1857–69. doi: 10.1038/s41564-022-01239-0.

Zaremba-Niedzwiedzka, Katarzyna, Eva F. Caceres, Jimmy H. Saw, Disa Bäckström, Lina Juzokaite, Emmelien Vancaester, Kiley W. Seitz, Karthik Anantharaman, Piotr Starnawski, Kasper U. Kjeldsen, Matthew B. Stott, Takuro Nunoura, Jillian F. Banfield, Andreas Schramm, Brett J. Baker, Anja Spang, and Thijs J. G. Ettema. 2017. “Asgard Archaea Illuminate the Origin of Eukaryotic Cellular Complexity.” *Nature* 541(7637):353–58. doi: 10.1038/nature21031.

Zatreanu, Diana, Zhong Han, Richard Mitter, Emanuela Tumini, Hannah Williams, Lea Gregersen, A. Barbara Dirac-Svejstrup, Stefania Roma, Aengus Stewart, Andres Aguilera, and Jesper Q. Svejstrup. 2019. “Elongation Factor TFIIS Prevents Transcription Stress and R-Loop Accumulation to Maintain Genome Stability.” *Molecular Cell* 76(1):57-69.e9. doi: 10.1016/j.molcel.2019.07.037.

Zaytseva, Olga, Naomi C. Mitchell, Linna Guo, Owen J. Marshall, Linda M. Parsons, Ross D. Hannan, David L. Levens, and Leonie M. Quinn. 2020. “Transcriptional Repression of Myc Underlies the Tumour Suppressor Function of AGO1 in Drosophila.” *Development* 147(11):dev190231. doi: 10.1242/dev.190231.

Zellweger, Ralph, Damian Dalcher, Karun Mutreja, Matteo Berti, Jonas A. Schmid, Raquel Herrador, Alessandro Vindigni, and Massimo Lopes. 2015. “Rad51-Mediated Replication Fork Reversal Is a Global Response to Genotoxic Treatments in Human Cells.” *Journal of Cell Biology* 208(5):563–79. doi: 10.1083/jcb.201406099.

Zeng, Zhifeng, Yu Chen, Rafael Pinilla-Redondo, Shiraz A. Shah, Fen Zhao, Chen Wang, Zeyu Hu, Chang Wu, Changyi Zhang, Rachel J. Whitaker, Qunxin She, and Wenyuan Han. 2022. “A Short Prokaryotic Argonaute Activates Membrane Effector to Confer Antiviral Defense.” *Cell Host & Microbe* 30(7):930-943.e6. doi: 10.1016/j.chom.2022.04.015.

Zhan, Yumeng, Frauke Grabbe, Elisa Oberbeckmann, Christian Dienemann, and Patrick Cramer. 2023. *Three-Step Mechanism of Promoter Escape by RNA Polymerase II*. *preprint*. Biochemistry. doi: 10.1101/2023.12.22.572998.

Zhang, Zhenyu, Shwu Shin Chang, Zhenying Zhang, Zhihong Xue, Hanxing Zhang, Shaojie Li, and Yi Liu. 2013. “Homologous Recombination as a Mechanism to Recognize Repetitive DNA Sequences in an RNAi Pathway.” *Genes and Development* 27(2):145–50. doi: 10.1101/gad.209494.112.

Zhao, Hongchang, Min Zhu, Oliver Limbo, and Paul Russell. 2018. “RNase H Eliminates R-loops That Disrupt DNA Replication but Is Nonessential for Efficient DSB Repair.” *EMBO Reports* 19(5):1–10. doi: 10.15252/embr.201745335.

Zheng, Wen-Xin, Cheng-Si Luo, Yan-Yan Deng, and Feng-Biao Guo. 2015. “Essentiality Drives the Orientation Bias of Bacterial Genes in a Continuous Manner.” *Scientific Reports* 5(1):16431. doi: 10.1038/srep16431.